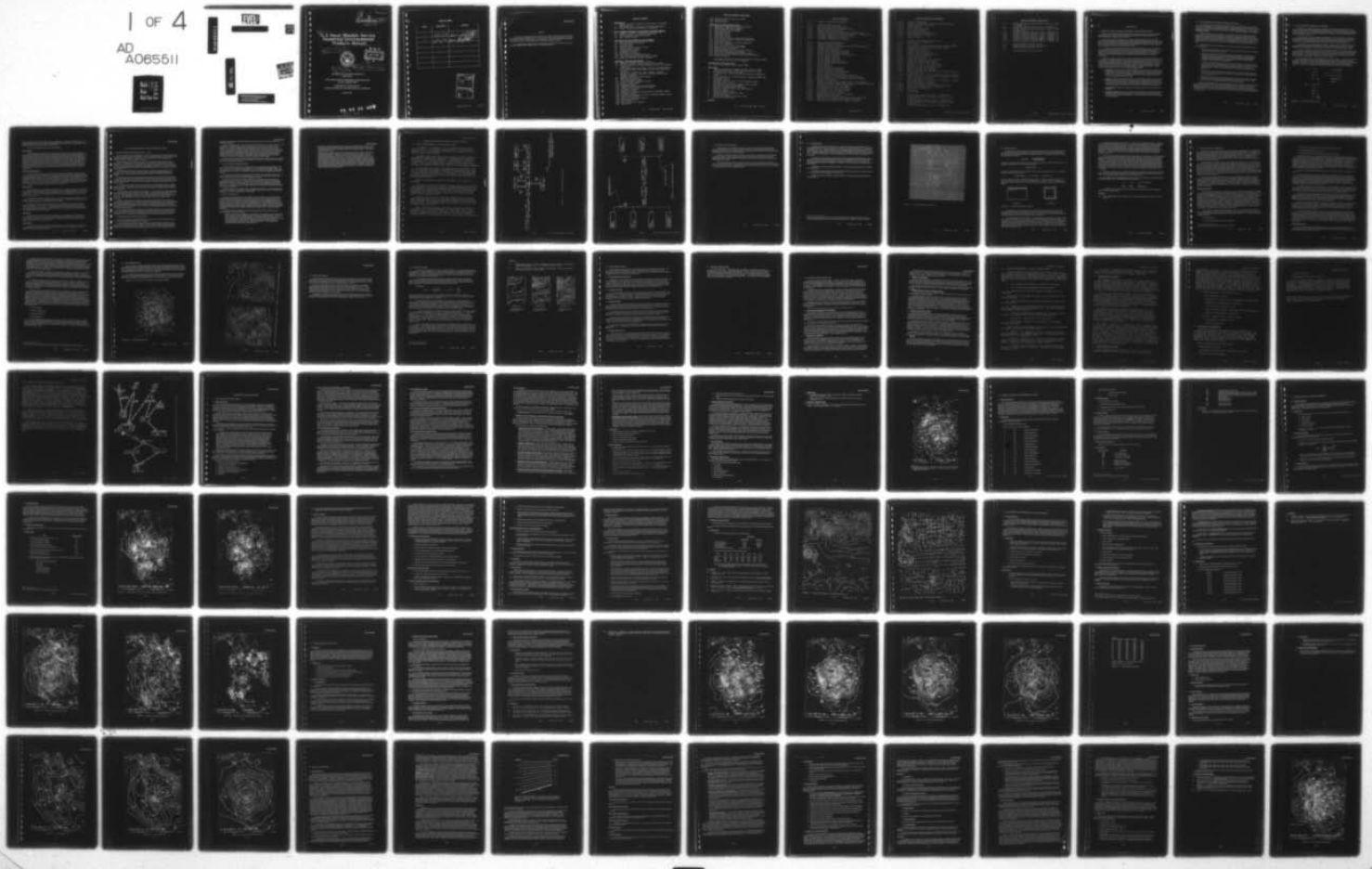
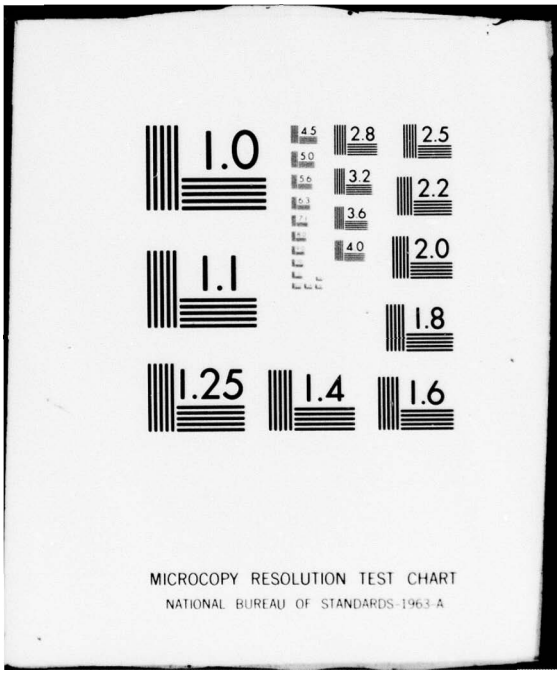
AD-A065 511 NAVAL WEATHER SERVICE COMMAND WASHINGTON D C F/G 4/2
U.S. NAVAL WEATHER SERVICE NUMERICAL ENVIRONMENTAL PRODUCTS MAN--ETC(U)
FEB 79 E T HARDING

UNCLASSIFIED NAVAIR-50-1G-522-REV NL

1 OF 4
AD A065511




1.0
1.1
1.25
1.4
1.6
1.8
2.0
2.2
2.5
2.8
3.2
3.6
4.0
4.5
5.0
5.6
MICROCOPY RESOLUTION TEST CHART
NATIONAL BUREAU OF STANDARDS-1963-A

(2) Revision

(19)

(18) NAVAIR 50-1G-522 - REV

A024702

(16)

U. S. Naval Weather Service Numerical Environmental Products Manual,

(11) 22 Feb 79

DDC
RECEIVED
MAR 8 1979
C



(12) 322 p.

(10) Edwin T. Harding

DISTRIBUTION OF THIS DOCUMENT IS
UNLIMITED

THIS PUBLICATION SUPERCEDES NAVAIR 50-1G-522
DATED 1 MARCH 1967

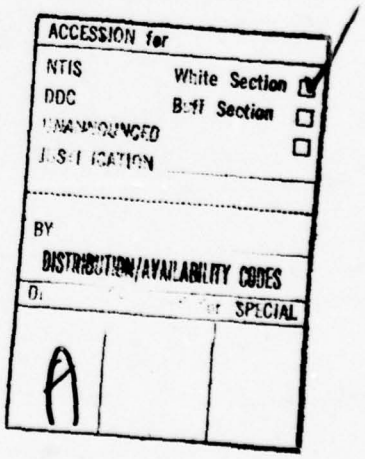
PUBLISHED BY DIRECTION OF
COMMANDER NAVAL WEATHER SERVICE COMMAND

1 JUNE 1975

79 03 02 028
253 350

RECORD OF CHANGES

Change	Date Entered	Signature
1	2/22/79	Kevin L Ringstad
2	2/22/79	Kevin L Ringstad



FORWARD

The numerical environmental products available from the Naval Weather Service require adequate documentation if their full potential is to be realized. These products consist of a variety of analyses and predictions of the air-sea environment. This publication is issued for the information and guidance of users of the products. The loose-leaf format is designed to facilitate up-dating.

This publication was largely the work of Captain Edwin T. Harding USN (Retired) after technical briefings by cognizant Naval Weather Service and Contractor Scientists.

TABLE OF CONTENTS

1. Introduction
- 1.1 History and Role of Numerical Forecasting in the Naval Weather Service
- 1.2 FNWC Operational Philosophy and Program Development.
- 1.3 A Basic Functional Description of Computers

2. Use of Computer Products in the Synoptic Forecast Routine
- 2.1 History of Synoptic Forecasting in the U.S. Navy
- 2.2 Computer Products in Synoptic Forecasting
- 2.3 Use of Numerical Computer Analyses
- 2.4 Use of FNWC Products

3. Techniques and Tools Common to Navy Products
- 3.1 Naval Environmental Data Network (NEDN)
- 3.2 Data Sources and Processing
- 3.3 The FNWC Grids
- 3.4 Program Outputs
- 3.5 Quality Control and Verification
- 3.6 Field Expansion (ZOOM)
- 3.7 Expanded Area Analysis
- 3.8 GG Operator Analysis
- 3.9 FNWC Objective Analysis
- 3.10 FIB Objective Analysis Methodology
- 3.11 Naval Environmental Display Station (NEDS)
- 3.12 Satellite Data Sources and Processing

4. Atmospheric Program Descriptions
- 4.1 Sea-Level Pressure Analysis (SLPFIB)
- 4.2 Planetary Boundary Layer Parameterization Scheme
- 4.3 Surface Pressure and 500-mb Forecast Changes and Prognosis Diagnostics
- 4.4 Global Band/Spherical Analysis Model for Surface Pressure and Wind and Global Band Upper Air Wind and Temperature Analyses
- 4.5 Surface Air Temperature, Vapor Pressure, Dewpoint Depression Analysis, Surface to 300-mb, Northern and Southern Hemisphere
- 4.6 Upper-Air Analysis, 1000 to 100 mb
- 4.7 Stratosphere Analysis
- 4.8 Primitive Equation Model
- 4.9 Scale and Pattern Separation Model
- 4.10 Analog Forecast Model
- 4.11 Unassigned Section
- 4.12 Tropopause Height Analysis and Prognosis
- 4.13 Freezing Level Analysis and Prognosis
- 4.14 Turbulence Forecasts
- 4.15 Atmospheric Fronts
- 4.16 Tropical Cyclone Steering Trajectories (HATRACK, MOHATT)
- 4.17 Unassigned Section
- 4.18 Convective Instability Analysis and Severe Weather Threat
- 4.19 Flight Winds Forecast
- 4.20 Contrail Probability Forecast
- 4.21 Radiological Fallout
- 4.22 Ditch Headings
- 4.23 Marine Layer Wind Prognosis
- 4.24 Cloud Cover

4.25 Horizontal Weather Depiction (HWD)
4.26 Advection Fog
4.27 Wind Extraction

5. Oceanographic Program Descriptions
5.1 Sea-Surface Temperature Analysis (SSTFIB)
5.2 Sea-Surface Temperature Anomalies
5.3 Bathythermograph Error Summary
5.4 Ocean Thermal Structure Model
5.5 Unassigned Section
5.6 Unassigned Section
5.7 Unassigned Section
5.8 Unassigned Section
5.9 Ocean Surface Current Analyses and Prognoses
5.10 Heat Exchange Analysis Transient Thermoclines
5.11 Unassigned Section
5.12 Subsurface Temperature Structure Analysis
5.13 Ocean Front Analysis
5.14 Search and Rescue Planning Program
5.15 Hydrodynamical Numerical Model (HN)
5.16 Spectral Wave Forecasting
5.17 Bathythermograph and Sound Velocity Extracts
5.18 Operational Propagation Loss Model
5.19 Synoptic Bathythermograph Extraction (KRILL)
5.20 Hydroclimatological Data Retrieval Program (HYDAT)
5.21 Unassigned Section

The classification of other enviro-acoustic products places them beyond the scope of this document.

6. Products From Other Activities
6.1 Naval Environmental Watch System (NEWS)

7. Appendices
A General Environmental Computer Product Catalog (issued under separate cover as FNWC Tech. Note 11) (Revised)
B Carstensen FNWC Objective Analysis
C An Application of the 500-mb Scale and Pattern Separation Charts
D Basic Equations for the Hydrodynamical Numerical Model (HN)
E Unassigned Section
F Unassigned Section
G Systematic Errors in FNWC Primitive Equation Model Prognoses (April 1973)
H Wave Analysis and Prognosis (Global Band Singular Advective Wind-Wave/Swell Model)
I Sea-Level Pressure Analysis (SLPFIB)
J Spherical Surface Pressure and Wind Analysis
K Upper-Air Analysis
L Primitive Equation Model
M Scale and Pattern Separation Model
N Unassigned Section
O Sea-Surface Temperature Analysis (FIB)
P Singular Sea/Swell Model

8. Glossary

LIST OF FIGURES

1.3.1	Binary to Decimal Conversion
3.1.1	NEDN Mainline Circuitry
3.1.2	East and West Coast Tie Lines
3.3.1	The 63x63 Northern Hemisphere Grid
3.6.1	Surface Pressure Analysis
3.6.2	Expansion of Surface Analysis in Figure 3.6.1
3.6.3	Further Expansion of Surface Analysis in Figure 3.6.1
3.8.1	Potential Temperature Analysis Field
3.8.2	Potential Temperature Gradient
3.8.3	Potential Temperature GG Field
4.1.1	Sea Level Pressure Analysis
4.3.1	Surface Pressure Change
4.3.2	Surface Pressure Forecast Minus Verifying Analysis
4.4.1	Surface Pressure Analysis
4.4.2	Surface Wind Analysis
4.5.1	Surface Air Temperature Analysis
4.5.2	Surface Vapor Pressure Analysis
4.5.3	850-mb Dew Point Depression Analysis
4.6.1	850-mb Height Analysis
4.6.2	500-mb Height Analysis
4.6.3	300-mb Height Analysis
4.6.4	700-mb Temperature Analysis
4.6.5	700-mb Height Analysis Message
4.7.1	50-mb Analysis
4.7.2	10-mb Analysis
4.7.3	50-mb Temperature Analysis
4.8.1	Surface Pressure Prognosis
4.8.2	500-mb Pressure Height Prognosis
4.8.3	500-mb Temperature Prognosis
4.9.1	500-mb Small-Scale Disturbance Analysis
4.9.2	500-mb Residual Disturbance 48-Hour Forecast
4.9.3	500-mb Large-Scale Disturbance 48-Hour Forecast
4.10.1	Analog Date Message
4.10.2	Surface Pressure Analog Model Seven Day Prognosis
4.10.3	500-mb Long-Wave Height Analog Model Seven Day Prognosis
4.12.1	Tropopause Height 36-Hour Porgnosis
4.13.1	Freezing Level 36-Hour Prognosis
4.14.1	CAT Analysis for 400-300-mb Layer
4.14.2	CAT Analysis for 300-200-mb Layer
4.15.1	Atmospheric Fronts Analysis
4.15.2	Atmospheric Fronts 48-Hour Prognosis
4.16.1	Sample HATRACK Forecast
4.16.2	Worksheet for Computing MOHATT Forecast Positions
4.16.3	Error Ratios of NHC-67 and TYRACK to MOHATT
4.16.4	Comparison of Official and MOHATT Forecasts

LIST OF FIGURES (Continued)

4.19.1	Flight Wind Message
4.20.1	Contrail Probability 36-Hour Prognosis Message
4.21.1	RADFO Pre-Burst Prediction
4.21.2	RADFO Warning
4.22.1	Ditch Heading Message
4.23.1	Wind Speed Analysis
4.23.2	Wind Direction Analysis
4.23.3	Surface Marine Layer Wind GEM
4.24.1	Total Cloud Cover Chart
4.26.1	Advection Fog
5.1.1	Northern Hemisphere SST Analysis
5.1.2	Gulf Stream SST Analysis
5.2.1	SST Anomaly
5.3.1	The Monthly Bathythermograph Error Summary Report
5.4.1	Temperature Gradient at the Primary Layer
5.4.2	Temperature at 200 Feet
5.4.3	Primary Layer Depth
5.9.1	Surface Current Transport
5.9.2	Surface Current Stream Function
5.9.3	Ocean Current Direction
5.10.1	Total Heat Exchange
5.10.2	Latent and Sensible Heat Exchange
5.10.3	Transient Thermoclines (day)
5.10.4	Transient Thermoclines (depth)
5.13.1	Gradient of SST in the Gulf Stream
5.13.2	Gradient of SST in the Gulf Stream
5.14.1	Sample Incoming NSAR Message
5.14.2	Sample Outgoing NSAR Message
5.15.1	Example Printout of Current Speed and Direction at a Specified Time
5.15.2	Example Printout of Water Level at a Specified Time
5.15.3	Tidal Currents in the Straits of Gibralter 3 Hours after Low Water at Tarifa
5.15.4	Tidal Currents in the Straits of Gibralter 3 Hours after High Water at Tarifa
5.16.1	Zig-Zag Propagation Sequence
5.16.2	Compacted Spectra of Periods and Directions
5.18.1	Source Level Signal from a Submarine
5.18.2	Point Source Radiations
5.18.3	Refraction
5.18.4	Ray Tracing
C.1	500-mb Height Analysis 1200Z 1 JANUARY '66
C.2	500-mb Small-Scale Disturbance Analysis 1200Z 1 JANUARY '66
C.3	500-mb Residual Analysis 1200Z 1 JANUARY '66
C.4	500-mb Large-Scale Disturbance Analysis 1200Z 1 JANUARY '66
C.5	500-mb Height Analysis 1200Z 3 JANUARY '66

LIST OF FIGURES (Continued)

C.6	500-mb Small-Scale Disturbance Analysis 1200Z 3 JANUARY '66
C.7	500-mb Residual Analysis 1200Z 3 JANUARY '66
C.8	500-mb Large-Scale Disturbance Analysis 1200Z 3 JANUARY '66
C.9	Surface Pressure Analysis 0000Z 1 JANUARY '66
C.10	Surface Pressure Analysis 0000Z 2 JANUARY '66
C.11	Surface Pressure Analysis 0000Z 3 JANUARY '66
C.12	Surface Pressure Analysis 0000Z 4 JANUARY '66
C.13	Surface Pressure Analysis 0600Z 4 JANUARY '66
C.14	Surface Pressure Analysis 0000Z 5 JANUARY '66
1.1	The Arbitrary l,m Area Module
1.2	Computational Sub-Area for A* l,m
1.3	Subset Labeling in the A* l,m
0.1	The Arbitrary l,m Area Module

1. INTRODUCTION

1.1 HISTORY AND ROLE OF NUMERICAL FORECASTING IN THE NAVAL WEATHER SERVICE

During the past decade, numerical forecasting has assumed a dominant role in Naval Weather Service operations. Numerical objective analyses and prognoses have largely replaced the old ponderously-produced, subjective manual products.

The decision to explore the feasibility of adopting numerical forecasting in the Navy was motivated by the growing evidence that the huge volume of available hemispheric data had outrun man's ability to digest it efficiently. Computers offered an exciting prospect of being able to do a much better job. A strong consideration for computers was the growing demand in the Navy for a wider range of high-quality products, particularly oceanographic products.

The decision to explore the Navy potential in numerical forecasting was not one to be taken lightly, since this would ultimately involve a large allocation of Naval Weather Service assets in men and money with no assurance that these assets could be provided by drawing from existing field activities. Numerical forecasting was still a struggling infant as a scientific tool, and many were convinced that numerical forecasting would remain forever in the R&D stage, never to appear operationally.

The founding fathers of today's Fleet Numerical Weather Central (FNWC) were aggressive and knowledgeable. In a surprisingly short time, programs were developed, rapid communications methods were devised, and computer products were receiving favorable evaluations in the field. This early success encouraged further support for an expansion of the numerical development group. The goal was to build toward a Naval Weather Service system around FNWC. Numerical forecasting in the Navy evolved toward its present dominant role--dominant because the decision to use numerical methods involved a major upheaval in the old system. The key changes included:

1. Philosophy--The change from man to a man-machine mix caused field users to change their forecasting practices and office routines. Machine products had to be accepted and used, subject only to a critical local evaluation. More time had to be devoted to thinking through a forecast, and the time was now available because the old plot, analyze, and forecast routine was replaced by the computer output.

2. Education--Courses at the Naval Postgraduate School and NATTC Lakehurst, and on-the-job training at FNWC accomplished the instruction of Naval Weather Service personnel in the numerical methods being adopted. The Products Manual is intended as an instructional aid, and is a basic guide to the products available through the computer network, the numerical techniques employed in their production, and their use in the synoptic forecast routine.

3. Communications--Computer-to-computer communications networks had to be devised and activated.

4. Allocation of Resources--A greater percentage of Naval Weather Service resources had to be allocated to support the numerical system. This involved changes in the Naval Weather Service personnel structure and management, and major changes of emphasis in procurement and program support.

1.2 FNWC OPERATIONAL PHILOSOPHY AND PROGRAM DEVELOPMENT

The FNWC operational philosophy was laid down when the Naval Weather Service decided to adopt the use of computers. The original principles, to a surprising extent, are still in effect, and have done much to shape the unique character of FNWC as a centralized weather activity. There are two areas under which FNWC's operating principles can be grouped--customer orientation and an applied engineering approach.

FNWC is oriented to just one customer, the U. S. Navy. The relationship dictates that the operating Navy initiates product requirements. All of FNWC's operational procedures and program development are designed around the specialized operational requirements of the fleet. Since most of the Navy's operations involve the environment at the interface between the air and the ocean, FNWC's pioneering efforts have been mostly in this area. The atmosphere and the oceans are treated as a coupled medium, so that the interactions of the two are reflected in the FNWC products that go to the fleet.

The FNWC applied engineering approach favors both the operations and development areas. Some examples are:

1. Programs are designed along engineering lines; the quality of the program logic is critically examined to ensure a decisive program.

2. FNWC does not abandon the time-tested methods of hand analysis and prognosis; these methods are still sound. Most efforts are engineering applications using computers to imitate successful manual operations. The philosophy is that operations and program development should simulate the actions and thought processes of a highly skilled synoptician with unlimited time at his disposal.

3. At FNWC, the data processing, analysis, and prognostic routines are all fully automated. This eliminates manual plotting and analysis, and takes advantage of the computer's speed. By being automated, human fallibility and intuition are not allowed to intervene in the objective computer process; the same analysis will always be reproduced with the same input data.

4. Quality control of FNWC products is an important part of the operational and development routine. Every product is thoroughly evaluated by the FNWC Quality Control section before it is declared operational.

5. FNWC's goal is always a usable operational product. Accordingly, the output is designed for the field forecaster dealing with the particular operational problem at hand. In many cases, the product is specifically tailored to the customer's problem.

FNWC program development has always been characterized by its practicality. In large measure, this is probably because the bulk of the program development has been done by (or supervised by) experienced Navy meteorologists. They know what the problem is at sea, forecast for a variety of operational conditions, and appreciate the need for things that work, as contrasted with the interesting but academic class of product. Navy meteorologists are not at all opposed to the empirical approach--if it will do the job.

1.3 A BASIC FUNCTIONAL DESCRIPTION OF COMPUTERS

The heart of any computer operation is the program, the listing of each individual step the computer must perform. Programming follows when the problem is defined, the mathematics is complete and the solution is defined. The FORTRAN programming language, used almost exclusively at FNWC, is a compiler language. That is, there is a program called the compiler, which translates FORTRAN statements into machine instructions.

The discussion to follow is intended to provide familiarity with the capabilities, limitations, terminology, and operating characteristics of digital computers as they are used in the Naval Weather Service System. This knowledge will be useful in following descriptions of the FNWC products, in which there are many references to what the computer does during the production process.

To the uninitiated, computers are rather mysterious creatures, falsely endowed with all sorts of magical ability--super brainpower in particular. Even the initiated have some tendency to think of computers as having personality. FNWC's three big computers are called Bonnie, Clyde, and Hal.

In reality, the computer is just a device for manipulating numbers, like an adding machine. The computer is a cold, obedient slave to man, doing whatever it is told to do with complete accuracy and at incredible speed. But, all the computer can do is add, subtract, multiply, and divide. The computer has no initiative. It must be told every step of the way just which operation to perform, when to do it, where to get the working numbers, and what to do with the answers.

The distinguishing feature of digital machinery is its binary character. Computers are composed of electronic and magnetic devices. These characteristically have a two state information carrying capability: circuits are on or off and small regions of magnetic films are magnetized in one pole direction or the other. This "yes-no" configuration supports the binary number system used by computers. Figure 1.3.1 illustrates a comparison of the binary number system with the decimal number system.

$7_{10} = 00111_2$

$1 \times 2^0 = 1$

$1 \times 2^1 = 2$

$1 \times 2^2 = \underline{4}$

7_{10}

$89_{10} = 1011001_2$

$1 \times 2^0 = 1$

$1 \times 2^3 = 8$

$1 \times 2^4 = 16$

$1 \times 2^6 = \underline{64}$

89_{10}

BIT POSITIONS

0 0 0 0 0 0 0 0

2^7 2^6 2^5 2^4 2^3 2^2 2^1 2^0

POSITION VALUES

(BINARY)

FIGURE 1.3.1 Binary to Decimal Conversion

The one and zero positions in the binary notation are called BITS, a contraction of Binary Digits. All computer operations are done with BITS. The CDC 6500 has the capacity of storing 60-BIT words; smaller computers might be of the 30-BIT, 18-BIT or 6-BIT variety.

There are five functional sections of a digital computer.

Control Section

The Control Section controls and supervises the operation of all other computer sections and works within the guidelines of the program. The program can be thought of as a detailed Operation Plan. The first step is for Control to go to where the program is stored and bring back the first instruction. Control reads and executes this first instruction; generally it has something to do with pulling data from storage and moving it to some register where it can be operated upon. The program gives Control an "address" where the information is stored. After instruction 1 is executed, Control reads and executes instruction 2. This process goes on step by step until action on all instructions is completed. By following this prescribed routine, the control section sets up the sequence of operations, determines where computations will be done, provides input data at the right time and place, stores intermediate answers and, finally, executes the instructions that tell the output section where and how to put out the answers.

Arithmetic and Logic Section

This is the workhorse section, where the arithmetic operations of addition, subtraction, multiplication, and division are accomplished. This section can also perform certain logical operations such as comparing numbers or symbols, and testing numbers for zero or negative. This capability is important, as there are usually many steps in a program where direction of future action hinges on a decision. Statements such as, "If cos A $\geq$ cos B, go to instruction 40", are common. The "40" will be some other computation. If cos A $<$ cos B in this case, the arithmetic section keeps working right where it was in the program unless told otherwise. Note that the computer's "thinking" is strictly guided. It is not told, "Do whatever you think best after you compare cos A and cos B".

Memory Section

The Memory Section is the computer's storehouse for data, program instructions, intermediate and final answers. Memory is made up of groups of magnetic cores, tiny pieces of material. Each core of a group can store one digit of a binary number by being magnetized in one direction for a 0 or in the other direction for a 1. The cores are arranged in groups that vary in size with different computers. Each group is called a word.

The large FNWC computers use 60-bit words, and in central memory these are stored in 32 banks of 4096 words each. Each word in memory has to have an address. The address specifies which bank contains the word and where the word is located within the bank.

The handling involved in the memory section is a big logistics problem. Each CDC 6500 at FNWC has a capabity of 131,000 words in Central Memory, 500,000 words in Extended Core Storage, and 15 million words on disc storage. A small program might need only 3000 words in memory, while the largest programs, such as the Primitive Equation Model, may saturate Central Memory and Extended Core storage of both big FNWC computers.

Input Section

The function of this section is to bring in information to the computer from the outside world. The information is transmitted to memory in coded binary form. The mainelements of information are main programs, subroutines, and the working data. The information may be taken from disc storage, cards, magnetic tape, or a console typewriter.

Output Section

The output section is just the reverse of the input section. When information is to be passed to the outside world, the output section arranges for the transfer to one of the various output devices: printer, microfiche recorder, card punch, etc.

2. USE OF COMPUTER PRODUCTS IN THE SYNOPTIC FORECAST ROUTINE

2.1 HISTORY OF SYNOPTIC FORECASTING IN THE U. S. NAVY

Prior to World War II, the general belief was that the significant weather producing processes were confined to the lowest levels of the atmosphere. The surface pressure analysis was the primary tool used in producing synoptic forecasts. Needless to say, luck, artistic talent, and salesmanship were essential attributes of the successful fleet forecaster.

During and subsequent to World War II, the world-wide upper-air observation network was established. This was heralded by many authorities as the turning point in the science of synoptic forecasting. From this time on, it was reasoned, the forecaster would be able to take into account the full three dimensional state of the atmosphere in the preparation of his forecasts. Luck, artistic talent, and salesmanship would take a back seat to scientific forecasting methods. Unfortunately, this was not entirely the case.

Individual forecast units were barely able to handle all the upper-air data that had been made available. The forecaster was forced to spend a majority of his time constructing analysis and prognostic charts. The time available for preparation of required local and regional forecasts was minimal.

Recognizing this, the Naval Weather Service established a system of regional centers which were to produce the large-scale working charts required in the local forecast routine. These products were communicated to the forecaster in the field who then converted them into the forecasts required in support of specific fleet operations. This total system, though sound in principle, demonstrated some major flaws in practice.

Conventional communications as well as hand techniques of data processing, analysis and prognosis were too slow. The regional centers were not able to increase sufficiently the tools available to the fleet forecaster. Application of scientific methods in preparation of forecasts was still limited by a lack of basic tools.

Even more serious was the problem of product quality. A wide variation in techniques employed by those who produced the large scale analyses and prognoses was too often apparent. Prognostic methods were crude. Simple atmospheric interactions were difficult to handle; complex interactions almost impossible. Three dimensional and time continuity, though sought after, were rarely attained. Hydrostatic and inertial instability were common to the hand product, though rarely observed in the atmosphere.

Probably, the most disconcerting problem to the fleet forecaster was the extreme subjectivity represented in the hand product. It is well known that in sparse data regions, such as the oceanic areas in which fleet operations take place, a group of analysts given identical data will generally produce as many different analyses as there are analysts. Validity of the hand product depends as much on the individual drawing it as upon the data. For that matter, a particular individual's mood or health might be represented in the end product.

The fleet forecaster responsible for providing an operational commander with environmental information was generally reluctant to rely completely on the products available from the regional centers. His primary forecast tool remained the hand plotted and analyzed surface pressure analysis produced in his own shop. Luck, artistic talent, and salesmanship were still important qualities for success.

2.2 COMPUTER PRODUCTS IN SYNOPTIC FORECASTING

Against the background of the preceding history, the areas of potential improvement to synoptic forecasting by using computer products are very apparent.

First, the operational forecaster is relieved of the time-consuming burden of preparing his own working charts and processing his data. He now has a wide variety of working charts at his disposal--many more than he would have by local preparation. The extra charts can often contribute that little added piece of information that makes the final forecast more accurate. The most important effect here

is that the forecaster has time for analytical thinking and for application of scientific methods in the preparation of forecasts.

Second, the forecaster can do his work with assurance that the maximum accuracy attainable will be reflected in the computer product. Given correct data in sufficient density the computer performs analyses with an accuracy exceeding that of the instruments used to measure the elements being analyzed. (The forecaster's confidence in computer products is not innate; it is built by observing the level and consistency of the day-to-day quality and by knowledge of the techniques and procedures used in preparing the products.) Prognostic charts are produced by precise solution of the theoretical and empirical mathematical relationships that govern the evolution of atmospheric and oceanic systems. Complex interactions are easily handled. Unreasonable noise and stability values are prevented. Continuity in time and space is maintained beyond the capability of hand methods.

Third, the forecaster need no longer be concerned with who draws his working charts. The computer always has the watch, and is always completely objective to the point of: same data--always the same answer. The only variable is the data.

2.3 USE OF NUMERICAL COMPUTER ANALYSES

The role of numerical analysis is to provide the forecaster an anchor point in his thinking. The analysis, based on data, is the nearest thing there is to a true picture of the atmospheric state. From this firm platform, the forecaster can move forward in time in his thinking, evaluating his working tools, the prognostic charts, as he goes. The prognostic charts must be logical developments from the basic analyses.

If errors exist in an analysis, the prognosis derived therefrom will be at least equally in error. In addition, certain initial states may be handled poorly by the model. The initial state problem areas must be recognized before there can be effective synoptic forecasting.

By eliminating all subjective influences, FNWC operational methods make the recognition of analysis problems relatively simple. The forecaster can have absolute confidence that the analyses transmitted from FNWC are completely objective. They will reflect only what the actual data portray. Analysis errors, if they occur, will be due almost without exception to insufficient or erroneous data. These errors, if significant to accuracy of derived forecasts, will usually be quite obvious and can thus be corrected by the forecaster.

A numerical analysis is not recommended as an operational briefing aid. Few are the operations that require a knowledge of past weather. Present weather briefings should normally be performed with a prognostic chart verifying at briefing time or close thereto.

2.4 USE OF FNWC PRODUCTS

The use of FNWC products involves the question of the man-machine mix. The Naval Weather Service position, generally speaking, is to centralize production of basic numerical products (mostly at FNWC) and deliver them to the man at the end of the line for such manual massage and use as he desires. Only a very few products go directly to the operational user. The reasoning for keeping man so prominent in the mix is that he can make valuable additions to the quality of the machine product by use of local terrain knowledge and on-scene parameter information, and that he can tailor the forecast to the particular operational problem at hand. Another reason is that the forecaster adds the personal touch in presenting the forecasts, thus avoiding the rather sterile computer image. A little salesmanship doesn't hurt.

The following general procedure for using computer-produced analyses and prognoses in the synoptic forecast routine is recommended:

1. Evaluate the accuracy of the analyses in and upstream of the operational area of concern. The surface pressure and 500-mb height analyses should receive particular attention since they are anchor levels for many other FNWC analyses. The evaluation should make use of: (1) on-scene information such as pilot reports, radar data, satellite data, and the often-forgotten look out the window; (2) the warning given by abrupt continuity breaks between analyses; (3) unrealistic patterns in the analyses; (4) vertical inconsistency. The principles of good analysis should be evident in the computer products.

2. If necessary, modify the prognoses that will be used in preparing required forecasts. This should never be done by intuition, only by correcting for any errors detected in the analysis evaluation above or for known weaknesses inherent in the prognostic model. (The Products Manual discusses these.)

3. Interpret the hand-massaged analyses and prognoses to obtain the required meteorological/oceanographic forecasts. Correct for known local effects, always keeping in mind that computer products (because of the large-scale analysis grid) are necessarily insensitive to critical parameter values that may exist on a given day. Assuming about an equal grasp of theoretical principles among the forecasters, those forecasters with the greatest experience will generally do a better job at this third stage. They have more built-in weather statistics and, from practice, are better able to predict operationally significant mesoscale phenomena from interactions within the synoptic or large-scale processes. The beginner is prone to fall back on the time-honored but not-always-to-be-trusted system of assuming a "perfect prog" and then pulling his weather from the frontal-cyclone model. A great deal of the significant weather is independent of frontal activity.

3. TECHNIQUES AND TOOLS COMMON TO NAVY PRODUCTS

3.1 NAVAL ENVIRONMENTAL DATA NETWORK (NEDN)

The NEDN is a component of the Integrated Fleet Weather Central System. Its two-part configuration is illustrated in Figure 3.1.1, the High-Speed Trunk Line; and Figure 3.1.2, the East and West Coast tielines.

The NEDN high-speed trunk line is used to transmit FNWC's hemispheric analyses and forecasts of environmental elements to the network Fleet Weather Centrals. Transmission is computer-to-computer at a rate equivalent to 7700 teletype words per minute. This rapid communication capability is a potent factor in providing good and "real time" service to operational customers.

At the Weather Centrals, the FNWC products are either tailored as necessary for specific operational requirements or used just as they come from FNWC. The final product is disseminated to fleet users by radioteletype or facsimile. The messages are all machine produced, which is a great improvement over the old hand-processing system.

Backup of computer operations throughout the network is provided.

The NEDS-1 (Naval Environmental Display Station), a land-based communications and display device, is being integrated into the Fleet Weather Centrals and FLEWEAFAC Suitland with communications provided by the NEDN network. This device gives these units a rapid display of weather charts and data for improved quality control and customer services.

The East and West Coast tielines (Figure 3.1.2) are high-speed communication links serving smaller Naval Weather Service units and other governmental agencies throughout the continental United States. Data transmission between units is at about 4000 teletype words per minute.

Naval activities at Adak, Keflavik, Bermuda, and London receive their tailored FNWC products on drops from an Air Force teletype circuit keyed from Carswell. Most other Naval Weather Service overseas activities have drops on Air Force teletype circuits and could be provided with the same service upon request.

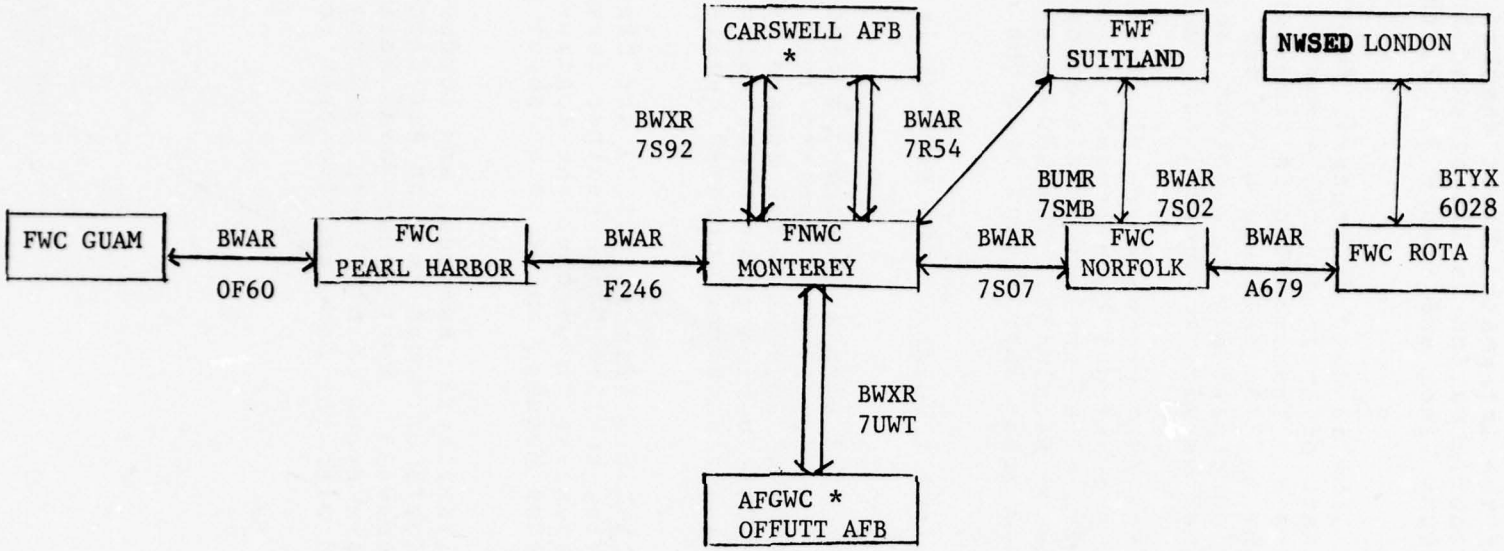


FIGURE 3.1.1 NEDN MAINLINE CIRCUITRY

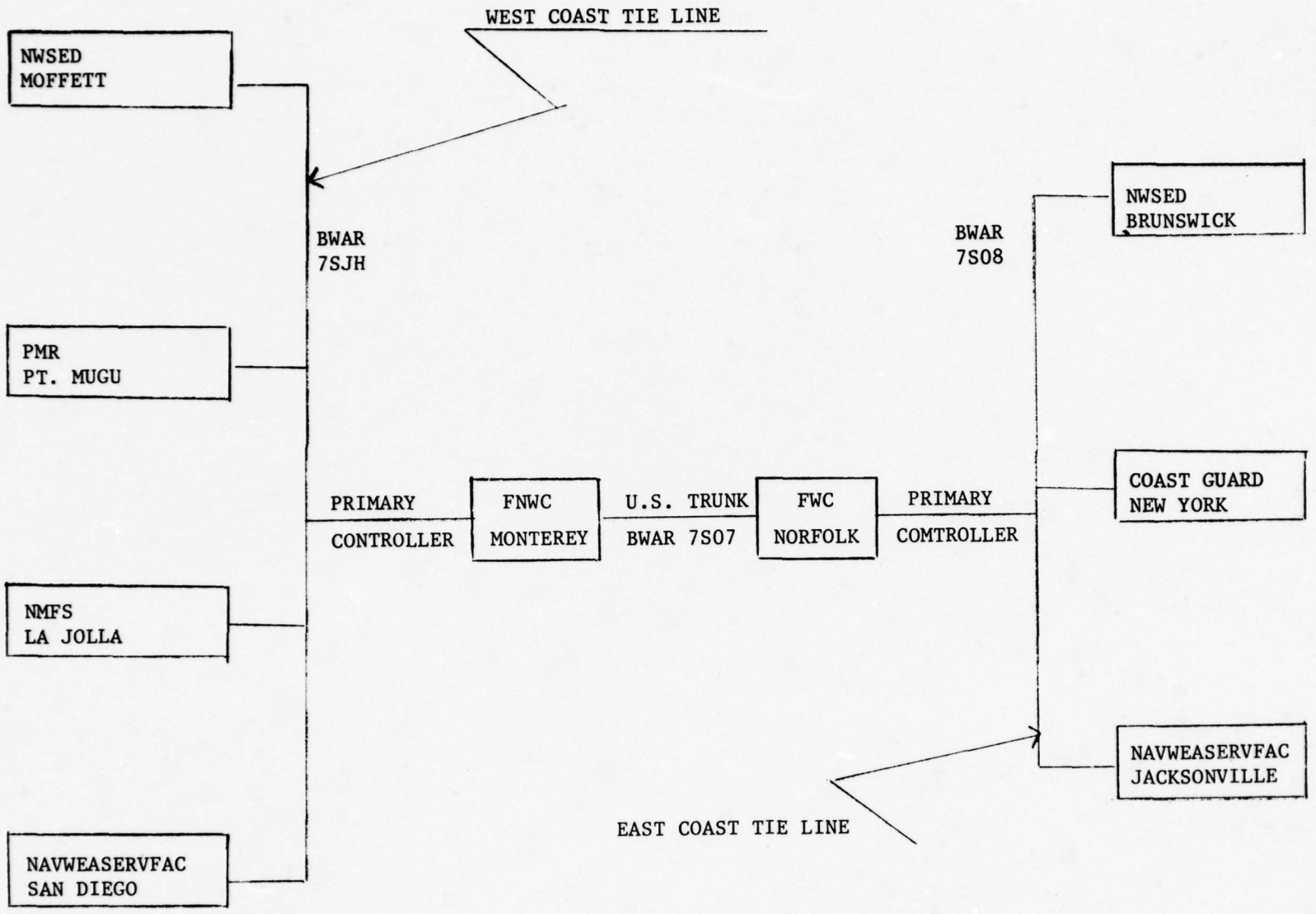


FIGURE 3.1.2 EAST AND WEST COAST TIELINES

3.2 DATA SOURCES AND PROCESSING

A further data source is Offut AFB, Nebraska, by way of the high-speed data exchange link between Offut and FNWC. Data from this source are primarily fields with observational information available primarily as backup. An additional source of backup for observational data is from the National Meteorological Center via FWF Suitland, Maryland.

Navy ships, wherever the area of operation, include FNWC as an addressee on all weather and oceanographic reports. Satellite-derived sea-surface temperature data are received from National Environmental Satellite Service (NESS) via FWF Suitland. Various other satellite-derived products from NESS are received via AWN.

Most data received at FNWC are unedited, and must be processed initially by the Automatic Data Processing (ADP) programs. These programs sort the data by area and type and eliminate duplicates. All correctly coded data are then arranged in data lists in packed binary format and stored in the computer on disc, ready for use in the various FNWC models.

3.3 THE FNWC GRIDS

The FNWC operational* grid (Figure 3.3.1) is a square containing 63 columns and 63 rows of equally spaced points. Each point is identified by a letter (i for column values and j for row values) and by a number from 0 to 62. Superimposed on a polar stereographic projection of the earth (true at 60° N) with the pole at its center, the grid encloses the entire northern hemisphere with the equator an inscribed circle. The distance between points on the grid is related to distance on the map by the map scale factor [(1 + sin 60°)/(1 + sin (latitude))]. At 60° N this distance is 236.7 miles (381 km); at the equator it is 126.9 miles.

The smaller the grid spacing, the better the definition of the parameter being analyzed. But this is realized at the cost of more computer time. For two of the fundamental and most important FNWC products, Sea-Level Pressure and Sea-Surface Temperature, a 125x125 grid is used. This adds grid points midway between points on the 63x63 grid. Computation time is almost four times greater than on the 63x63 grid.

An 89x89 grid is used for all upper-air analyses, but the products are transmitted via the NEDN on the 63x63 grid.

The Mercator (global band) grid is 145x49 on a Mercator secant projection, with a mesh distance of 2.5° longitude (150 nm at the equator, 75 nm at 60° N).

Section 2 of the FNWC Computer User Guide contains a more detailed description of the grids discussed above.

---

*NOTE: There are grid depictions of the Northern Hemisphere 89x89, Northern Hemisphere 125x125, Southern Hemisphere 63x63, Mercator and Spherical in Section 2 of the FNWC Computer User Guide.

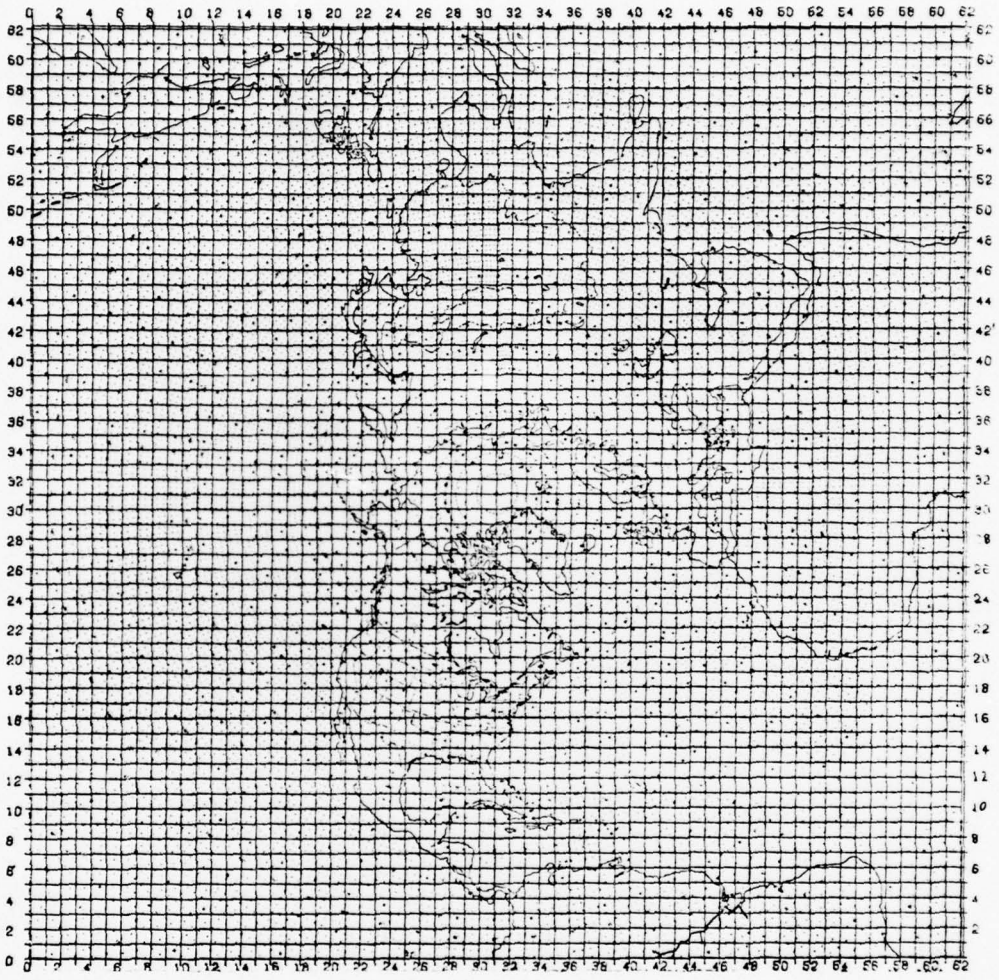


FIGURE 3.3.1 The 63x63 Northern Hemisphere Grid

3.4 PROGRAM OUTPUTS

Output from all hemispheric analyses and prognoses includes fields of discrete parameter values. The grids used are discussed in Section 3.3. For rapid transmission over high-speed communication links, the basic data fields are abbreviated into band index values, and compacted. Band index values are computed from the formula

$$\text{Band Index} = \frac{\text{Data-Contour Origin}}{\text{Contour Interval}}$$

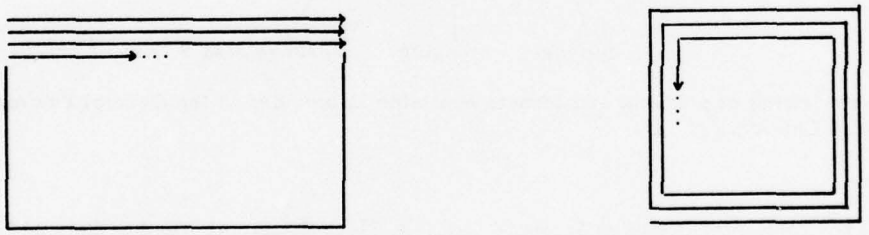
For example, the surface pressure contour origin is chosen to be 1000 mb and the contour interval, 4 mb. Therefore, a parameter value of 1004 mb is abbreviated as

$$\frac{1004 - 1000}{4} = 1$$

Compaction is accomplished by creating smaller values to represent the band index values. Compaction values are computed from the formula

$$\text{Compaction Value}\,|_i = \text{Band Index}\,|_i - \text{Band Index}\,|_{i-1}$$

where the i subscript refers to the element being processed, i-1 refers to the previous element. The first value processed, though, remains as a band index value. The order in which the elements are processed is shown in Figure 3.4.1. Further discussion on this material is found in the NEDN Software Manual.



a. *Mercator* b. *Hemispheric*

FIGURE 3.4.1 Order of Processing for Compaction

To obtain charts, program output fields are converted to plotter commands and routed to the appropriate plotting device. The NWS uses two methods for plotting charts, the Calcomp electromechanical plotter and the Varian electrostatic printer. The Varian at FNWC is assuming a growing load of plotting demands over the Calcomp; both are described as follows.

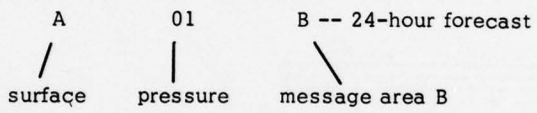
In the electromechanical plotter system, a chart is obtained by interpolating in the data field for each isoline to be plotted. Isoline coordinates are converted into digital map plotter commands. These commands direct the movements of the pen and drum of an electromechanical map plotter to reproduce the converted isolines on a map projection. Each command initiates a .01" movement of the plotter drum and/or the plotter pen producing a line segment along one of eight directions. Thus each isoline drawn by the plotter consists of a series of small line segments. Pen up and pen down commands establish the end points of a plotted isoline.

The standard hemispheric plotter map is a 1:60 million polar stereographic projection. This map when plotted at a remote location requires only 3 to 5 minutes of transmission time. The time depends on the total length of all isolines to be drawn. Resolution is of such superior quality that the small scale is readily usable in the forecast routine. The map size allows the forecaster to study large numbers of hemispheric parameter distributions without the need for handling bulky and clumsy larger-scale charts. 1:30 million strip charts for the Pacific and Atlantic Ocean regions are also routinely available. In addition, a map of any desired scale can be specially obtained (See Field Expansion program, Section 3.6).

The Varian digital plotter operates by an electrostatic process. The chart paper is electrostatically charged. A comb crosses the full width of the paper. Each metal tooth of the comb is 0.01 inch apart (1400 teeth), and each tooth can be charged individually at the direction of the controlling computer program. The comb scans one line at a time; each charged tooth affects the paper so that a black mark will appear later at that point. After the paper has run past the comb for the full length of the chart, the chart is chemically toned and all the isolines, numbers, symbols, and geographical background appear. The process is controlled by a computer that uses a previously stored geographic background and the band index field from FNWC as input. The desired scale is preset and can be anything from 1:60 million, 1:30 million, 1:20 million, 1:15 million on down to 1:1 million. A Varian chart can be printed in about 10 seconds.

Messages are produced for most hemispheric analyses and prognoses by interpolating in the data field to desired latitude-longitude intersections. Standard areas for which messages can be derived are listed in the General Environmental Computer Products Catalog (Ref. 1).

The first line of each message contains a catalog number which identifies the contents by LEVEL, PARAMETER, FORMAT, AREA, and FORECAST HOUR. For example:



A complete listing of products and formats available is provided in the General Environmental Computer Products Catalog (Ref. 1).

References

[1] General Environmental Computer Products Catalog, Fleet Numerical Weather Central Technical Note No. 11.

3.5 QUALITY CONTROL AND VERIFICATION

Quality Control is an organized effort to monitor a product for maintenance of consistent quality. Field activities play a limited part in the extensive quality control of FNWC products, but suggestions from these outlying activities are likely to be based on experience, familiarity with, and careful study of the pertinent local area; they are a source of reliable diagnostic information. Large-scale quality control procedures are confined, mostly to FNWC, though, because of the centralized resourses available. A strong quality control program at FNWC is required to satisfy the demand for high quality environmental products by the Navy.

The present form of the FNWC Quality Control Program was initiated in 1971 by the formation of the Quality Control Group, consisting of several experienced Navy meteorologists. The Quality Control Group made a thorough assessment of Quality Control at FNWC to determine the methods which would produce the most effective results with the available manpower. The conclusions were, then, that effort should be concentrated on three basic analyses (sea-level pressure, sea-surface temperature, and 500mb-pressure-surface height) rather than be expended upon the huge task of covering the whole line of products on a real-time basis. These three products have had great influence on the initialization step of many other FNWC products. The importance of the initialization step in the generation of many FNWC products cannot be over emphasized.

The verification program at FNWC is primarily for the improvement of the various prognostic models in use and under development. In some cases, software separate from the model is used to supply statistics about the output prognoses, and in other cases, statistics packages are contained within the model. Most often used are RMSE (root-mean-square-error) values which are categorized as to geographic areas, latitude-longitude bands, or land and sea stations. Knowledge of systematic errors aids in the development of improved models and in the correction of defects related to geographic features or other areas.

Meteorological Products

The sea-level pressure analysis is considered the most important of the meteorological analyses because it contains the most physically significant variability; it is used in the initialization of so many atmospheric and oceanographic models. The northern hemisphere (Section 4.1) and the Global Band (Section 4.4) [SLP analyses] are both quality controlled. The process begins by examining a preliminary analysis for gross errors. This analysis is based on data received within 1 hour 30 minutes after observation time. At +2 hours,* the analysis is sent to all the FWC's for study with respect to their particular areas of responsibility. Within one hour, the FWC's may respond by submitting modifications as bogus reports which reflect the FWC's requirements for alteration of the analysis--perhaps deepening or moving a low pressure system or adjusting the position of some contours. The Centrals have lists of ship reports used in the analysis, and those rejected by the model. The FWC's will inform FNWC of any rejected reports which are good and which should be included in the +3 analysis; and supply FNWC with reports which are missing from the data lists.

The +3 analysis, consisting of all data received prior to 2 hours 30 minutes after observation time, is now subjected to critical examination at FNWC. This analysis includes zoomed charts of the northern hemisphere which provide greater detail and facilitate close study. It is judged against these information sources:

1. Satellite pictures.

2. Weather Central warnings and bogus information.

---

*Two hours after observation time is referred to as +2 hours.

3. A data evaluation taken from a plot of all used and rejected reports.

4. The NMC preliminary Pacific strip charts.

5. Preceeding analysis charts for meteorological continuity in time.

After using all the sources to make appropriate changes, the final operational analysis is run between +3·30 and +4. This run is examined for accuracy and sent to the field by +4·30. This operational run is the one used as input to other FNWC models. The Upper-Air (particularly 500 mb) analyses are subjected to a similar but less elaborate treatment by the Quality Control section. The routine of Weather Central feedback is omitted, but all the other data checks, cross-checks, continuity checks, and the strict subjective evaluation are applied. Modifications, through bogusing, are made as warranted. The upper-air analyses rarely require Quality Control action, as they are based on high quality data from professional observers. Further, the analysis model has shown over a long period that it is one of FNWC's strongest and most reliable.

Once the basic analyses have had the Quality Control treatment, attention is directed to other products.

The Primitive Equation model (Section 4.8) receives specific attention. The P.E. surface pressure and 500-mb prognostic charts are monitored at each 12-hour step out to 48 hours and again at 72 hours. The charts are evaluated subjectively. Precise positioning and intensities are not required; the objective is to have the patterns mateorologically reasonable and chronologically consistent. If any stage is reached where the analysis seems to be breaking down--such as the case where the integration appears to have become unstable for mathematical/physical reasons--the program run is stopped and restarted at the previous six-hour point.

The smoothing attendant to the reinitialization is usually sufficient to remove instabilities which could cause model breakdown. If, after the restart, the prognoses continue to show discrepancies, the only recourse is to obtain aid from the responsible programmer. At this stage, products are distributed with a message relating the problems that occurred and the areas of the prognoses affected.

Prognostic discussion sheets returned to FNWC from the FWC's are helpful critiques of the P.E. prognoses. These discussions include appraisal of the forecast movements of weather systems, and added information as to details of recent weather history and expected meteorological developments in the area of responsibility of the FWC's. These discussion sheets are received up to twice daily at FNWC, providing further quality control and verification information.

After the P.E. products are transmitted, the Quality Control section examines all the remaining FNWC products that are plotted for display. As with monitoring of the P.E., this is a subjective evaluation to answer the question of whether the analysis or prognosis is reasonable. If an obvious discrepancy is found, this is brought to the attention of the FNWC programmer in charge of this particular program for corrective measures.

Part of the quality control program is to insure that all the available reports are used in each analysis. This is done by making an hourly check of all incoming data against a standardized list of data normally received during the hour being checked. If the check shows that the data count is low or not properly distributed, a tracking procedure through AWS communication channels is initiated to find missing data and determine the cause of the fault. A data comparison can be made with AFGWC Offutt to see if they are missing the same data. If recovery of the missing data is not possible through normal channels and the loss is a serious one, action is promptly initiated to acquire the data from NMC, via FWF Suitland.

Oceanographic Products

The sea-surface temperature (SST) analysis and the ocean thermal structure analyses are key oceanographic analysis products. The SST analysis serves as input to the thermal model which, in turn, provides fields used by the acoustic models.

Quality control of these analyses includes emphasis on maximizing the number and quality of the bathythermograph (BT) reports used as data in the production of SST and thermal structure analyses. Real-time BT reports are the source of data for the ocean thermal structure model; the BT surface temperatures comprise a portion of the input to the SST model. BT reports are received from United States and foreign ships, from institutional organizations, government agencies, private organizations, and environmental data buoys. At FNWC, 200-250 reports are received daily, but these tend to be clustered in naval operations areas, shipping lanes, and ocean stations. Considering the expanse of the world oceans, this is sparse coverage indeed.

Upon receipt at FNWC, BT reports are first checked by computer for coding errors. Rejected BT's are then examined by personnel to detect coding errors that can be manually corrected. Because an average of 30% of incoming reports contain coding errors, a significant effort is made to notify reporting activities of their repeated errors immediately, or at some later time by means of the Bathy Error Summary Program.

The Bathy Error Summary Program maintains a record of BT error conditions arranged by reporting activity,* and compiles summaries for any single activity or group of activities. Each summary indicates the number of BT reports received during some time period, and the number and percentage of correct and unusable reports. To identify the types of errors committed, specific error diagnostics are also listed. Naval Weather Service activities and Fleet commanders are encouraged to use the program to improve BT accuracy.

The SST analysis is closely monitored because of its significance as input to the ocean thermal structure and primitive equation models. Input data consists of synoptic ship reports, BT surface temperature, airborne radiation thermometer data and isolated sea-surface temperature reports. Quality control of the SST analysis involves an examination of data counts to ensure that they are within the expected range, and a look for patterns of rejected data which would show possible unreliability of the analysis in certain areas. The analysis is compared with the long term mean and with climatological charts to ascertain that the analysis is of the appropriate character; it is also expected to match satellite coverage information Graphic features such as steep gradients, isoline kinks and concentric features, when they occur, are used to trace other error possibilities. Customers are encouraged to submit bogus reports (real time feed back) to improve the analysis. Fine resolution charts are available for study for the following areas:

1. Gulf Stream area
2. Kuroshio Current system
3. Labrador Current area
4. Mediterranean Sea

The ocean thermal-structure analyses are checked similarly to the SST for inconsistent graphic features or inconsistent agreement with means, climatology, sources of other data, and for unexpected data count values. Additionally, analyses are compared with their 24-hour-old counterpart analyses. Changes of unusually large magnitude, in consideration of the depth, are examined as possible indicators of unreliable analysis areas.

*The reporting activity is identified by the International Call Sign terminator on the BT message.

3.6 FIELD EXPANSION (ZOOM)

The field expansion subroutines (ZOOM, ZOOMX1, XM, XMS) provide field scale and rotation transformation capability. Standard FNWC products are mapped on the hemispheric 63x63 grid, global band 49x144 grid, and the spherical 73x144 grid. Outlying activities frequently want portions of these grids, representative of their areas of responsibility, extracted and enlarged. These zoomed charts are better than the large area charts for local briefing and analysis.

The field expansion subroutines extract any arbitrary rectangular portion of the basic field and expand it to a 63x63 (or other dimension) grid field at any desired scale. A double interior quadratic interpolation is performed from the original grid points to the location of the array in the new field.

Figures 3.6.1, 3.6.2, and 3.6.3 illustrate surface analysis ZOOMS.

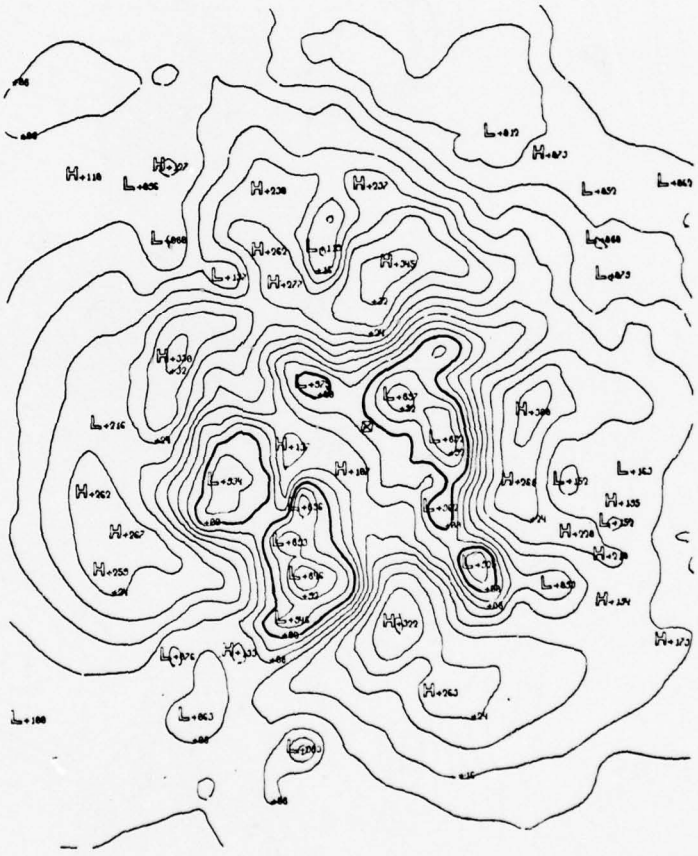


FIGURE 3.6.1 Surface Pressure Analysis

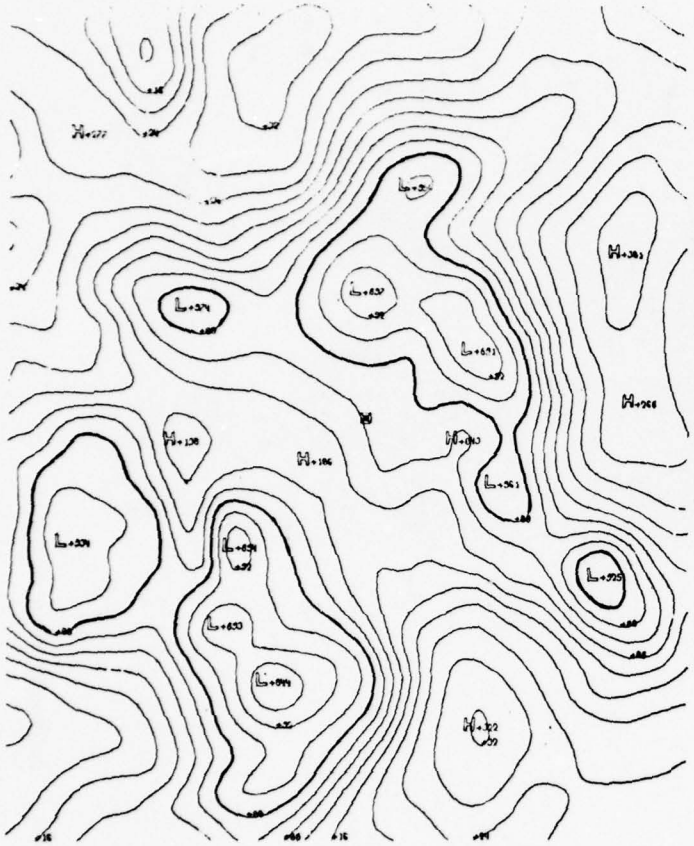


FIGURE 3.6.2 Expansion of Surface Analysis in Figure 3.6.1

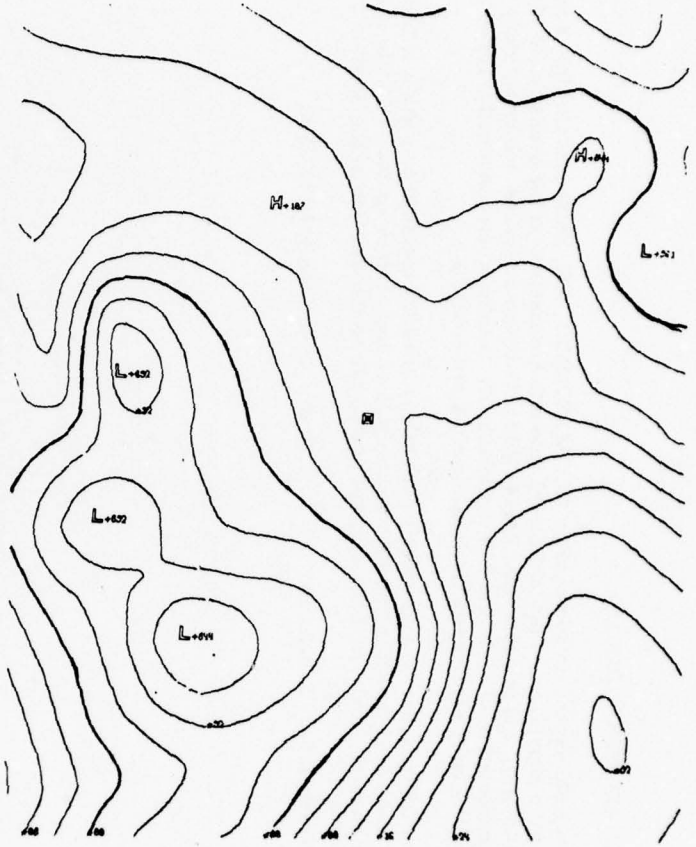


FIGURE 3.6.3 Further Expansion of Surface Analysis in Figure 3.6.1

3.7 EXPANDED AREA ANALYSIS

In dense data areas, significant detail may be lost from an analysis performed on the basic 63x63 FNWC grid where, for instance, the distance between grid points at 40°N is about 180 miles. In general, features with a wave length of less than two grid lengths will not be represented, and those with a wave length less than six grid lengths may lose a significant amount of definition.

To reduce the grid length over which an analysis is performed, the first step is to expand the desired portion of the hemispheric analysis using the Field Expansion Program (Section 3.6). This program effectively adds grid points in proportion to the size of the expanded area. Then, using the original raw data, a reanalysis is performed. The analysis program is the same as that used in the hemispheric analysis except that it must be modified for the new grid length. The original hemispheric analysis is used as the first guess in the reanalysis.

Operationally, the expanded area analyses are most useful when the operating area is restricted in size and has plenty of data. The Mediterranean is a good case. Another favorable situation would be in an area of very strong gradients, such as an SST analysis along the edges of the Gulf Stream.

3.8 GG OPERATOR ANALYSIS

GGζ stands for gradient of the gradient of a dummy variable, ζ; it is the second derivative of the parameter, ζ, along the gradient of ζ. This mathematical operator can be applied to the analysis of any scalar with the object of locating discontinuities in the scalar field, so the operator is general, in application to a wide variety of meteorological problems. At FNWC, the GGζ operator is used in the analysis of both atmospheric and ocean fronts.

The GG operator was designed and introduced by Renard and Clarke (Ref. 1) during their development of an objective analysis method for locating atmospheric fronts. Their frontal parameter, GGθ,* is simple, easily computed, and reassuring to the user in the sense that frontal location is an objective simulation of the subjective procedure followed by a meteorologist.

Symbolically,

$$GG\zeta = -\frac{\nabla\zeta \cdot \nabla|\nabla\zeta|}{|\nabla\zeta|} = -n_\zeta \cdot \nabla|\nabla\zeta| = \frac{\partial^2\zeta}{\partial n_\zeta^2}$$

where n_ζ is a unit vector in the direction of the gradient of the dummy variable ζ. GGζ is the directional derivative of the gradient of ζ along the gradient of ζ. It is from the expression "gradient of the gradient", that the acronym, GG, is derived.

The GG operator picks out discontinuities in any scalar field. Of the meteorological applications, front finding is the most obvious; although, GG could be used to delineate the boundaries of any air masses of different characteristics. GG has enough sensitivity to uncover an upper air sounding in error which somehow passed the gross error check. The response to such an error will be to draw a tiny "ring" front around the offending sounding. Another useful capability of a GGζ analysis is to show the strength of the discontinuity in ζ by the closeness of the GGζ isolines.

Using potential temperature, θ, (Figure 3.8.1) as an example of operator application, location of a frontal zone will be discussed. In the figures, GGθ troughs are indicated by - - - - - and GGθ ridges, by + + + + +. The first step is to analyze temperature in the usual way; this gives an isothermal pattern. GG is then applied to the isotherm field; first it derives a temperature gradient analysis (Figure 3.8.2). The gradient is the rate of change of θ, written $\nabla\theta$, with distance along a line normal to the isotherms, n_θ. The axes of maximum and minimum $|\nabla\theta|$ nearly coincide with GGθ = 0. Maximum $|\nabla\theta|$ defines the centrum of the baroclinic zone; minimum $|\nabla\theta|$ locates the barotropic zone.

Next, the GG operator derives the rate of change of the gradient along n_θ (Figure 3.8.3). In the GGθ analysis, ridges locate the warm air boundaries of the frontal zone, and troughs locate the cold air boundaries. A line of maximum GGθ represents a front. The larger the transverse width of the frontal zone from maximum GGθ to minimum GGθ, the stronger a frontal zone indicated. Additionally, a stronger zone is indicated by a larger $|\nabla\theta|$ within the zone. The high correlation between maximum $|\nabla\theta|$ in the zone and maximum GGθ at the adjacent frontal boundary allows use of maximum GGθ as an additional strength factor.

---

*θ = potential temperature.

References

[1] Renard, Robert J. and Leo C. Clarke, "Experiments in Numerical Objective Frontal Analysis", Monthly Weather Review, Vol. 93, No. 9, September 1965, pp. 547-556.

[2] Clark, Leo C. and Robert J. Renard, "Objective Frontal Analysis", Fleet Numerical Weather Central Technical Note No. 24, August 1966.

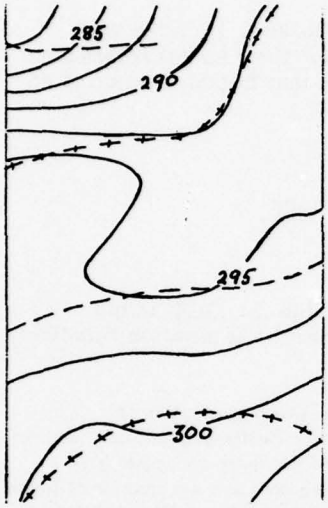


FIGURE 3.8.1

Potential Temperature
Analysis Field

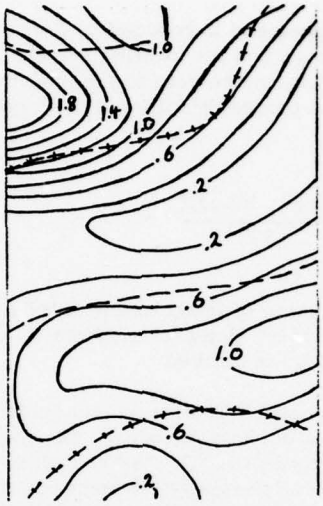


FIGURE 3.8.2

Potential Temperature
Gradient Field

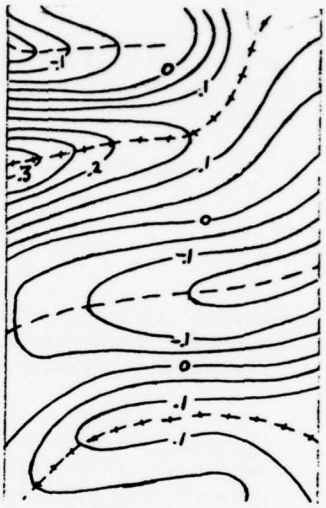


FIGURE 3.8.3

Potential Temperature
GG Field

3.9 FNWC OBJECTIVE ANALYSIS

Basic to many numerical analyses is an objective analysis scheme developed at FNWC. The routine is designed to analyze exactly to isolated observations and to a weighted mean of the observations in regions of dense data coverage. In sparse data areas, the influence of an observation is extended farther than in regions of high data density.

A. The First Approximation (First Guess)

Essentially the routine corrects a first approximation to the analysis for actual observations. The first approximation is a best estimate of the analysis without considering current data. (It is thus commonly referred to as the first guess.) The accuracy of the first guess has a direct bearing on the accuracy of the analysis in sparse data areas. A well-constructed first guess will provide continuity with the preceding analysis and prognoses derived therefrom. For most analyses at FNWC, the first guess is a modified previous analysis or prognosis verifying at the present analysis time.

B. The Gross-Error Check

Prior to constructing the analysis, a gross-error check is performed on all reported data. The procedure consists of comparing each report to the interpolated value at its location in the guess field for the analysis. If the difference between the reported data and the guess field value exceeds a prescribed tolerance, the report is rejected. Tolerance values are based on the characteristic variability of the field being analyzed as determined from climatology.

C. The Analysis Scheme

For each reported observation which passes the gross-error check, the analysis interpolates in the guess field to the location of the observation and obtains the guess value at that point. The difference between the guess value and the reported data is computed. This difference is weighted by the distance of the observation from each of the four surrounding grid points.

The weighted difference is then applied as a correction to the guess value at each grid point within one mesh length of the observation. Where more than one observation influences a particular grid point, the weighted mean of the corrections computed for that grid point is applied.

After all guess values influenced by observed data have been corrected, the adjusted field is combined with the original guess field by a relaxation process which holds the corrected values constant. This spreads the influence of isolated observations while at the same time exactly fits each observation that is consistent with surrounding reports.

Portions of the analysis process are repeated, depending upon the assumed accuracy of the original guess field. A mathematical description of the objective analysis scheme is contained in Appendix B.

D. The Lateral Fitting Check

A lateral fitting check is normally performed during each analysis pass except the initial one. The purpose of this check is to reevaluate each report which passed the gross-error check, taking into account the other observations in the immediate area. Each report is compared to the interpolated value at the report location resulting from the previous analysis scan, using tolerances smaller than those used in the gross-error check. In this way, a report which does not agree with other reports in the immediate area is rejected.

E. Vorticity Limiting Check

In the literature, it has been shown that negative absolute vorticity in atmospheric flow is rare. This criterion is used as a final check on the validity of most pressure and pressure-height analyses. A pass is made through the analyzed field to reveal any region in which the value of absolute vorticity is less than a suitable fraction of the coriolis parameter. In these regions the absolute vorticity is adjusted to an adopted minimum value. This limiter is also referred to as the "Ellipticity Criterion".

3.10 FIB OBJECTIVE ANALYSIS METHODOLOGY

The Fields by Information Blending (FIB) is a powerful, new analysis technique, applicable to virtually any two-dimensional physical variable. As of this writing, the Sea Surface Temperature and Sea Level Pressure disbtributions are being analyzed operationally at FNWC by FIB programs. Sections 4.1 and 5.1 and their appendices can be examined for specific details and mathematical formulations of the technique. A FIB adaptation for wind analysis (u,v) has been formulated and other applications are under development.

The FIB technique analyzes the distribution of a variable by blending measurements of the variable and its gradients, which come from different sources and locations. The program uses reports from various observation stations, with estimates of reliability, and it accepts regional or whole field estimates of the parameter and its derivatives (gradient, Laplacian, etc.). It checks all input data, rejects gross errors, and assembles the data. From this, it blends or analyzes to produce the optimum analysis which best fits all the information at hand. The technique also produces grid-point reliabilities of the final product. All input data are reevaluated individually by comparison with the blended analysis, which includes the interacting effects of all information that went into the analysis.

Reliability or weight is a measure of the worth of a piece of information. In every step of the FIB process, information exercises only that degree of influence specified by its reliability value at that particular stage of the analysis. The ability to compute information reliability is the key to the power of the FIB technique.

FIB has six component operations, to be discussed in the following sections.

A. First-Guess Field Preparation of Initialization

The first guess is an estimate of what the analysis will be without considering current data. It provides continuity into data-sparse areas and gives an estimate of the shape (gradients, curvature, etc.) of the field. In sparse-data areas, accuracy of the final analysis must depend partly upon first-guess accuracy. The first guess is also useful for keeping "impossible" data from entering the analysis by indicating the approximate values expected in an area. Information is thus tested for credibility against the first guess.

The first guess in objective analysis methods is either a previous analysis, extrapolated to analysis time, or a prognostic chart verifying at analysis time.

FIB has the unique capability of accepting several first-guess fields, each weighted by its proportionate value. Later in the program, FIB can reevaluate individually the worth of each first-guess field. If a previous analysis is to be one of the first-guess fields, the FIB program has a special steering subroutine to bring the old analysis up to analysis time. In the sea-level pressure application, the 500-mb SR (residual) height field steers the previous analyses the appropriate distance and direction. This process, called kinematical extrapolation, gives a conservative first guess and is very useful when used in conjunction with a more sophisticated, primitive-equation forecast.

B. Assembly of New Information

Reports of the parameter being analyzed are placed at their proper geographical positions. The first-guess field value is interpolated at the report location, and the values are compared. In some analysis systems, just an arbitrarily assigned difference is allowed. If the allowed difference is exceeded, the report is thrown out. In the FIB method, the difference varies with the magnitude of the gradients near the report and, for some parameters, with latitude.

If the report passes the gross-error check, it is assigned a reliability or weight. This is based on the standard deviation of the errors associated with that type of report--the larger the standard deviation, the smaller the reliability. Other factors involved in determining the reliability vary with the parameter; examples include magnitude of the gradients near the report, age of the report, and station elevation.

The difference between the interpolated first-guess value and the report value is applied at the nearest grid point as a correction to the grid-point guess value. The total assembled value of the parameter at a grid point is a weighted mean of all the data referred to the grid point, with each value contributing to the mean in accordance with its reliability.

C. Blending for the Parameter

Blending is the analysis stage, corresponding to the drawing of isolines by a hand analyst. The assembly step combined reports at their nearest grid points. The grid-point information is now spread to surrounding grid points through gradient knowledge and higher order fields such as the Laplacian. The degree of spreading is increased with higher reliability in the gradient and other spreading fields.

After blending, each grid point will have a new parameter value, reflecting surrounding information as well as information at the grid point itself. This is an optimum compromise of all the weighted information.

D. Computing Reliability Field of the Blended Parameter

A reliability field for the blended parameter is computed at this point. This is needed for the next step of reevaluation and error checking.

The blending process results in new parameter values at each grid point, and these values will have a different reliability or weight. For example, if one grid point had nothing but first-guess information before blending, its reliability would be much lower than surrounding grid points that have information from several observations. Blending spreads the information from the high reliability grid points to the ones that have lower reliability. Blending increases reliability at all grid points, reflecting the additional information flowing in from surrounding grid points. Even the low reliability points can add information to surrounding areas. The interaction between the grid points is greatest over one grid interval and diminishes with distance. The strength of interaction is limited by the gradient weight, i.e., if the gradient is known only slightly (low weight), even adjacent grid points will have little effect on each other.

E. Reevaluation and Lateral Rejection

FIB uses the blended parameter field and grid-point reliabilities to reevaluate each piece of information that entered into the analysis. The reevaluation provides a quality measure for each observation and a quality measure for each first-guess field. The analysis cycle will be repeated using the reweighted information. The reevaluation stage is a vital and integral part of the FIB technique. This allows a second or even third analysis pass with ever-improving weights.

To reevaluate reports of any parameter, a statistical parameter is computed for each report. This parameter measures how accurate a report really is as compared to its expected accuracy as given by its assigned reliability. Each report, with its weight, is removed individually from its grid point and compared with what remains, or the "background". If the report is within its expected error, no change is made in its reliability. If the error is greater than expected but within some upper limit, the report's reliability is reduced. If the error limit is exceeded, the report is rejected (i.e., its weight becomes zero) and it will have no effect when the next assembly and blending is made.

The reliability of the first-guess fields can be similarly evaluated. Where new information disagrees with the first guess, its weight is reduced. In some applications where fast changes occur, such as sea-level pressure, the first-guess weight is so small that reevaluation is really not necessary.

F. Reanalysis

The reanalysis begins by returning to the assembly stage. The new assembly starts with the first-guess fields, which may be reweighted, and the reports are assembled with their reevaluated weights. The whole cycle is repeated exactly as before. In the final pass (second or third analysis), the program skips the reevaluation and proceeds to the output section. The final analysis is stored in the computer for transmission and for input to other programs.

3.11 NAVAL ENVIRONMENTAL DISPLAY STATION (NEDS)

The NEDS concept was initiated in the early 1970's with the ultimate objective of improved services to the Fleet through the provision of more and improved forecasting aids to the environmentalist. Evolution of the NEDS devices have been predicated upon the following design constraints for maximum cost-effectiveness:

a. No increase in personnel to operate or maintain.

b. Use of existing telecommunications systems.

c. Replacement of existing computer equipment at the FLEWEACENs.

Development of the NEDS has also evolved around the following criteria:

a. Rapid dissemination of Navy environmental products to all Fleet users.

b. Capability of exchanging products with other agencies which are developing similar systems (e.g., the AFOS system of the National Weather Service).

c. Automated communications permitting the orderly flow of data at a wide variety of data transmission rates.

d. Modularity, commonality, and flexibility.

e. Man/machine interface, including man's functional working environment.

Varying Fleet requirements have resulted in the development of several components of the NEDS family:

a. NEDS-1: Full capability for use at major NEDN sites (four FLEWEACENs plus FLEWEAFAC Suitland). Minicomputer-based. Deployment will be completed in 1978.

b. NEDS-1A: Smaller, less complex microprocessor-based version designed primarily for use by the Naval Aviation community. Deployment is scheduled to begin in 1979.

c. NEDS-1R: Remote terminal device for display of data stored in a nearby NEDS-1 or NEDS-1A. Deployment is scheduled to begin in 1979.

d. NEDS-2: Ruggedized shipboard version of the NEDS-1A. This version is still in the definition phase, and is not expected to be deployed before the 1982-83 time-frame.

A. DESCRIPTION OF NEDS-1

The equipment is "state-of-the-art" for transmitting, receiving, storing, and displaying digital environmental graphics data as well as conventional alphanumeric (a/n) data. Computer produced graphical information such as weather charts can be encrypted and transmitted over the NEDN or over 100 wpm TTY circuitry. The graphic encryption will result in increased accuracy and timeliness resulting in increased combat effectiveness.

At each of the four Fleet Weather Centrals (FLEWEACENs), plus Fleet Weather Facility Suitland, the AN/FMC-1 will replace obsolete and inefficient computer equipment, thereby enhancing overall Naval Environmental Data Network (NEDN) operations. Graphics information will be prepared on the FNWC computing system and forwarded to each AN/FMC-1 installation where it will be automatically processed and made available to the environmentalist (meteorologist/oceanographer).

The NEDS-1 will allow computer produced graphics to be transmitted over almost any kind of existing data link, from 100 words per minute (100 wpm TTY) to 9600 bits per second (bps) computer lines. NEDS a/n data will pass through AUTODIN switching with the standard message heading with full encryption. It will receive graphics and alphanumeric weather data on input communications lines, then index, store and display data as selected by an operator.

The AN/FMC-1 consists of a minicomputer which controls operations of the overall system. Two multiplexors, synchronous and asynchronous, provide input/output interfacing with various communications lines, the minicomputer, and other AN/FMC-1 assemblies. The disc controller and storage module drive are used to store incoming data. The graphics CFT (color) and keyboard combine with interfacing circuits to display selected overlays and map data. The system console CRT (black and white) and associated keyboard are used to display alphanumeric weather data, tables of stored data, and AN/FMC-1 operational status data. The graph pen allows graphics to be modified. The electrostatic printer/plotter generates copies of displayed data.

B. DESCRIPTION OF NEDS-1A

The microprocessor-based NEDS-1A is mounted in and on a cabinet of typewriter desk height on a data equipment table

approximately 5½'x3'x2'. The 17 inch black and white CRT and graphics and alphanumeric keyboards are mounted on the top working surface of the cabinet. Two optional components, if used, are also mounted on the top working surface: (1) the color CRT is mounted on the right hand side of the cabinet; and (2) the graph pen and its pad are mounted in front of the color CRT. All printed circuit boards and power supplies are mounted in the left side pedestal. The power and isolation transformers are mounted in the central cavity. The right hand pedestal is empty and may be used for storage. The B/W CRT and the color CRT, if installed, are yoke mounted to permit tilting for operator comfort and are equipped with anti-glare screens to improve visibility.

1. Major components of the NEDS-1A are:

   - Data equipment cabinet.
   - B/W graphics terminal with alphanumerics capabilities.
   - Graphics and alphanumerics keyboards.
   - Electrostatic printer/plotter.
   - Mass storage, Magnetic Cartridge Tape Device (MCTD).
   - NEDS-1A microprocessor subsystem.

2. Optional components for selected sites:

   - Color graphics terminal (CRT).
   - Graph pen and pad.

C. Description of NEDS-1R

NEDS-1R is mounted on and under a data equipment table measuring approximately 49" long by 26" high by 30" deep. The 17 inch black and white CRT and the graphics and alphanumerics keyboards are mounted on the top working surface of the data equipment table. Power isolation and line voltage regulation transformers and the electronic enclosure are rail-mounted beneath the table working surface.

Major components of the NEDS-1R are:

- Electronics enclosure.
- B/W graphics terminal with A/N capability (CRT).
- Graphics and A/N keyboards.

- Acoustic coupler.

- Electrostatic plotter (optional).

The CRT is yoke mounted to permit tilting for operator comfort and is equipped with an antiglare screen to improve display visibility. The display processor (D/P) in NEDS-1R provides the capability of displaying A/N messages on the CRT instead of requiring a separate A/N CRT as does the AN/FMC-1. The keyboards on the NEDS-1R do not have all the edit functions and some other capabilities that the AN/FMC-1 keyboards have.

Additional information may be found in the NEDS Planning Document dated July 1976, which has been distributed by the Director, Naval Oceanography and Meteorology.

3.12 SATELLITE DATA SOURCE AND PROCESSING

The Fleet Numerical Weather Central will, beginning in the Summer of 1978, expand its operations to include the processing of selected satellite telementry. This capability is referred to as the FLENUMWEACEN Satellite Processing Center or simply the FLENUMWEACEN SPC. At the outset of satellite processing by the SPC, telemetry from the Defense Meteorological Satellite System (DMSP) and the NASA sponsored SEASAT-A satellite will be processed. Figure 3.12.1 illustrates the expected transmit paths for the satellite telemetry. For both satellite systems, data recorded aboard the satellites on tape recorders is dumped to selected sites, and these sites subsequently relay the data via communications satellites to FLENUMWEACEN for processing. No real-time data read out capability will exist at FLENUMWEACEN.

At the SPC initial operational capability, the DMSP data will be processed into a mapped image base for use by DOD activities; primarily the Fleet Weather Centrals. In addition, the special sensor "H" (SSH) aboard the DMSP satellites will be used to determine a vertical temperature profile with total moisture which will provide an input to the FLENUMWEACEN upper air products.

The SEASAT data will not generate an image base but will provide geophysical measurements of various surface environmental parameters which will be inputs to respective analyses programs, along with conventional data. These satellite observations will also be made available to selected military and civil organizations.

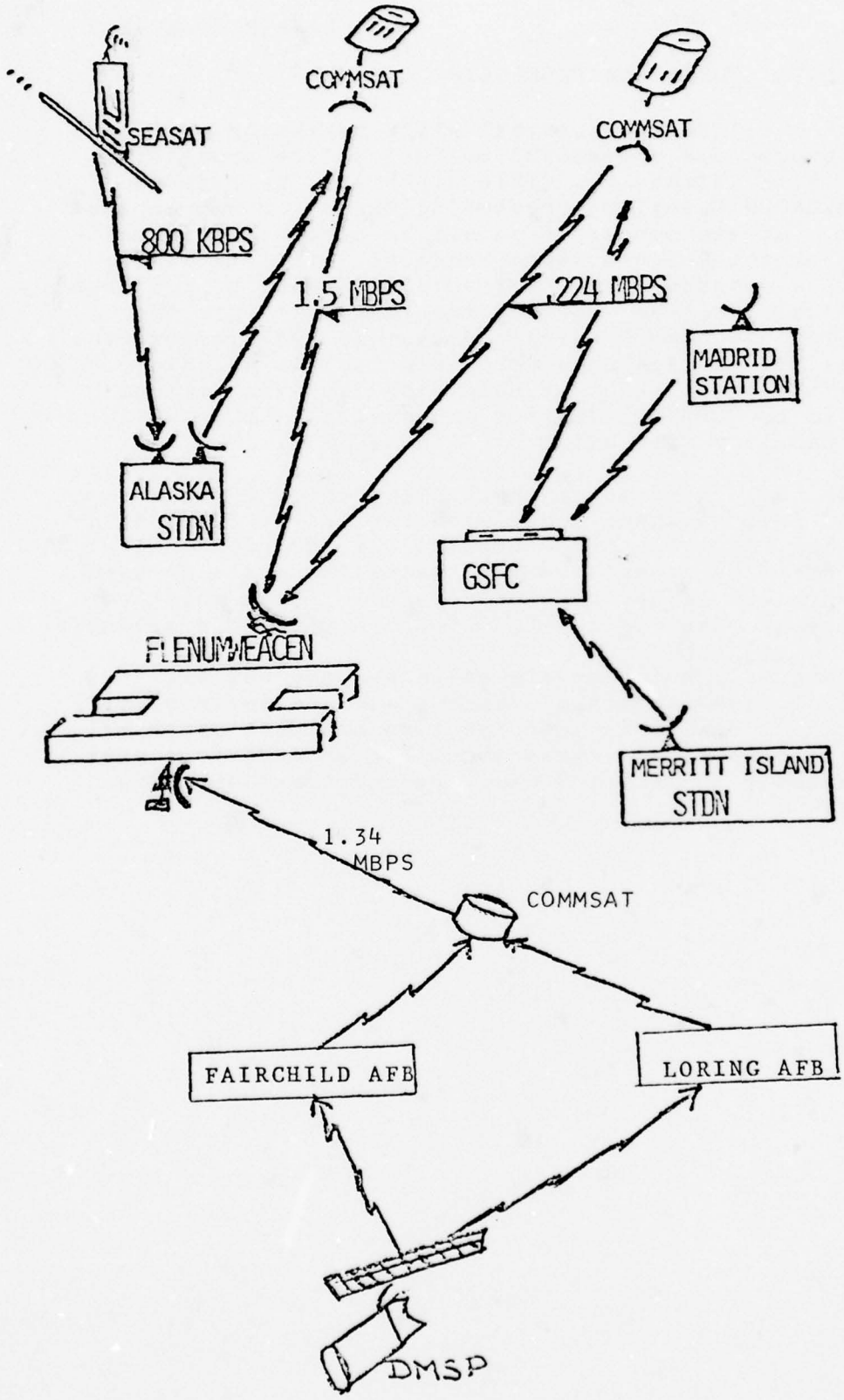


FIGURE 3.12.1 Expected Transmit Paths for the Satellite Telemetry

4. ATMOSPHERIC PROGRAM DESCRIPTIONS

4.1 SEA-LEVEL PRESSURE ANALYSIS (FIBSLP)

A. Model Development

The sea-level pressure analysis (Fig. 4.1.1) has always been a key chart in any forecasting method. It has more input data than any other level in the atmosphere, which leads to confidence in the analysis and its use as a base for building fields at higher levels. However, even at the surface level there are large areas with no data. FNWC has to have the very best possible surface analysis because this analysis directly influences the quality of so many important FNWC products--P.E. prognoses, sea and swell analyses and prognoses, tropical analyses, and many others.

The old FNWC objective surface analysis method was quite successful. The products were operationally useful and were generally equal or better in quality than those from other computer centers. But, with the advent of the P.E. model at FNWC, consistent high quality in the surface analysis became a matter of greater concern because of the importance of this level of input in initialization. During development of the P.E. model, it appeared that the surface analysis was sometimes lacking in accuracy. The P.E. model--ever at the mercy of initialization--would perform poorly. A better analysis was needed.

At about this time, development of a new objective analysis technique was nearing completion--Fields by Information Blending (FIB), described in Section 3.10. The sea-level pressure version (Ref. 1) replaced the older FNWC surface analysis program in March 1972.

The following is a formal description of what FIB does; the details will be explained in the subsequent discussion:

> FIB analyzes a scalar distribution by weighting and blending information in the value, in the gradient, and in the Laplacian of the field. It accepts spot (e.g., station) values of these properties with purported individual or class estimates of reliability. It also accepts regional and whole field estimates of these properties, such as derived from first-guess fields, climatology, satellite data, etc.--preprocessed as individual grid-point values, each with an associated reliability estimate. It checks all pieces of information (spot or grid point), rejects gross errors in observations and estimations, and reevaluates the reliability of each information piece in the total resolution afforded by all available information. It reassembles and blends to produce the "best" analysis in accordance with how "best" is defined as to the utility of properties. The resultant field is the optimum compromise, in the desired properties and object scale-range of resolution, of all weighted information components.

FIB/SLP will be described in order of component operations. In this way, the concepts upon which the methodology is based will be shown, as will the means of obtaining the maximum use from each piece of information. The mathematical formulations for FIBSLP are given in Appendix I.

There are many similarities between the computerized and hand analysis approach, but no hand analyst (even genius caliber) could possibly carry out all the operations performed by the program in less than a week. By considering the similarities of the FIB computations to the hand analysis process, the abstract computer operation can be related to actual physical concepts.

FIB/SLP has six component operations:

1. First-Guess Field Preparation, or Initialization
2. Assembly of New Information
3. Blending or analyzing for pressure
4. Computing the reliability field for the analysis
5. Reevaluation and Lateral Rejection
6. Recycling

Step 1--First-Guess Field Preparation, or Initialization

The first-guess field is the best possible estimate, before considering the current observations, of what the forthcoming analysis will be. The first-guess field plays an important role in the analysis process. It provides guidance and exercises restraints on the analysis; it prevents radical changes in pattern and abnormal movements of atmospheric features. Restraints are invoked by comparing observation values with first-guess values. The observations must be within certain limits, or they won't be believed. The first guess to the computer serves the same function as the history analysis does to the hand analyst. The FIB technique has the valuable capability of accepting several first-guess fields, each weighted by its proportionate value and, later in the program, of reevaluating individually the worth of each first-guess field.

The first guess for FIB/SLP is a combination of the applicable prognosis field and the previous hemispheric and tropical analyses. This combination provides an outstanding first guess, that often turns out to be very close to the final analysis. The hemispheric and tropical analyses are separate programs at FNWC. The two analyses are merged by weighting grid-point values by a system where the tropical analysis counts for zero at 60°N and gradually increases in weight toward the equator and the edges of the grid.

The six-hour-old combined analysis is not used directly, but is extrapolated forward for the intervening time. This is not the old distance-type extrapolation, but a steering process. The residual 500-mb height analysis (SR500)--500-mb analysis with the disturbance field removed--is used as a steering field. Geostrophic winds from this chart determine direction and speed of the six-hour movement. The optimum speed has been determined, on the average, to be 58% of the SR500 geostrophic flow.

The FNWC P.E. sea-level pressure forecast is used as the prognostic portion of the first guess. This field is combined with the extrapolated field discussed above. The prognostic portion is weighted as a function of latitude, so that in southern latitudes the extrapolated field carries relatively more weight. The first guess is completed at this stage. It should be close to the true pressure pattern at analysis time unless new or undetected developments have occurred.

Step 2--Assembly of New Information

New pressure and wind data are assembled from ship, synoptic land, and hourly land reports. The hourly reports (North America only) are used if there are no synoptic reports available at the same location. When current pressure data are missing, the plus 3-hour reports are converted to the synoptic time by using pressure tendency (and ship movement if applicable).

Pressure reports are now extrapolated along the gradients to the nearest grid point. This process involves calculating the guess-field value at the station by interpolation. The difference between the interpolated first guess and station value is added to the first guess at the nearest grid point. This value and its reliability (see below) are then combined with the pressure and reliability information already accrued at the nearest grid point.

The maximum allowable difference between the report and first guess increases with the magnitude of the gradients in the vicinity of the report and with latitude. A formula with latitude, gradient, and some constants is used to determine the allowable difference. If this is exceeded, the report is considered a gross error and is rejected. About 1% of the reports are rejected at this stage.

The report is assigned a reliability if it passes the gross-error check. In FIB, every piece of information used in the analysis has an assigned reliability or weight, and this reliability is not arbitrary but based on measurable things. Reliability is a statistical term involving the standard deviation of the errors associated with measurement of an unknown quantity. Reliability defines the worth of a measurement; a report with high reliability is more likely to be near the true value than a report with low reliability. In the case of pressure reports, reliability is determined by a formula that considers magnitude of the gradients near the report, age of the report, station deviation, and class of the report (viz., a weather ship report gets more weight than a merchant ship report).

The assembled value of pressure at a grid point is a weighted mean of all the data referred to the grid point, with each value contributing to the mean in accordance with its reliability.

Reported surface winds are converted to grid-point pressure differences (gradients) using a balance approximation formula. This formula considers frictional and curvature effects as well as the pressure and coriolis forces. The reliability of the gradient information is derived in a manner similar to the pressure report reliability. The gradient component values and reliabilities are assembled into their own special fields.

Step 3--Blending for Pressure

When all data have been assembled into their respective fields, the program can blend the information into a best-fit pressure field. This stage would correspond to the hand analyst drawing isobars, but the blending process is much more complicated, considering many more factors than could be handled manually, and performed at very high speed with absolute consistency. The blending equation has no less than 61 terms, which include grid-point values for pressure, gradient, second-differences, cross-differences, Laplacians, and reliability values for each one of these. All this to come out with a surface pressure analysis!

In the blending process, grid-point information is spread to surrounding grid points through the gradient and higher derivative fields. The degree of spreading increases with the reliability at the grid points and reliability of the surrounding gradients. After blending, each grid point will have a new pressure value, reflecting surrounding information as well as information at the grid point itself.

Step 4--Computing the Reliability Field for Blended Pressure

After the Step 3 blending process, each new grid-point pressure value will have a different weight or reliability than it did before blending. To illustrate, suppose that a certain grid point had nothing but first-guess information, but surrounding grid points had the help of many reports. After blending, the deserted grid point would have had a helping of information from the rich neighbors, and thereby would have an increased reliability.

For the reevaluation, Step 5, the blended pressure field reliability is needed. In Step 5, reports and fields are evaluated against the blended field. To do this the total reliability of the blended field must be found at grid points. This is done by a special procedure which tests the "firmness" of the analysis grid-point values. The procedure involves making a small change (perturbation) in the assembled pressure value at a grid point and then reblending in the immediate vicinity. If the new blended value is hardly changed, it indicates the analysis at that grid point was very firm because a lot of information was already near or at the point and the pressure change hardly affected it. In this case the grid point reliability is large. The formula used to get this total reliability simply says that the less the analysis is changed by the perturbation, the larger the reliability is.

Step 5--Reevaluation and Lateral Rejection

Knowledge of the blended pressure and the resulting grid-point reliability enables the program to reevaluate, individually, any piece of information that entered the analysis. The purpose of the first analysis cycle is only to get an accurate evaluation of all data and first-guess fields for use in the final analysis. The reevaluation provides a quality measure for each first-guess field and a quality measure for each observation. This reevaluation capability is one of the most valuable features of the FIB technique.

To reevaluate pressure reports, a statistical parameter, λ^2, is computed for each report. This parameter is a measure of how accurate a report really is as compared to its expected accuracy given by its assigned reliability. Each report, and its reliability, is removed from its grid point and compared with what remains (i.e., the blended analysis with the information under examination removed). If $\lambda^2 \leq 1$, the report is within its expected error and no change is made in its reliability. If λ^2 lies between 1 and the upper limit for a pressure report, the report is reevaluated and assigned a new reliability or weight. This case would apply in a situation where, say, three reports surrounded a grid point. Two reported very similar pressures; the third was a few millibars off. The value of λ^2 for the third report would be larger than for the other two that corroborated each other. The two similar reports would keep their original weights while the third would be down graded and have less influence in the next cycle. If a report is so bad that λ^2 exceeds the upper limit, it is completely rejected and will not affect the assembly in the next cycle. This is called lateral rejection. About 2% of the reports are rejected.

Wind reports are subjected to a reevaluation process similar to that for pressure reports. The tests are more severe in low wind speed cases. High elevation and valley reports tend to be nonrepresentative of the sea-level pressure gradient and are frequently rejected.

The relative merit of the separate first-guess fields and their derivatives is also evaluated in this section. Each first-guess field is reweighted before forming the new first guess.

Step 6--Recycling

The next cycle begins by returning to Step 2, the assembly stage. The new assembly starts with the reweighted first-guess fields, and the reports are reassembled with their reevaluated weights. The program then proceeds just the same as in the first cycle. The reevaluation will be more precise, since the doubtful reports were downgraded in the first cycle and had less or no effect in the second cycle. The reevaluation is now more meaningful because it is based only on the good reports. It is possible in the first cycle that some good reports were thrown out. This usually occurs when only one good report is found at an isolated grid point along with a bad one. The reevaluation had insufficient information from surrounding areas to determine which report is actually good. The result is that both were rejected. In the second reevaluation the good report will match the analysis fairly well and will be allowed to enter the analysis again. Because of this type of problem, and to gain further accuracy, a third analysis cycle is made.

In the final analysis, no reevaluation is necessary. Instead, the analysis field is stored in the computer in various forms for transmission and use by other programs.

The three-cycle sea-level pressure analysis program requires 5 minutes of computer time.

A southern hemisphere surface pressure analysis, using the FIB technique, is also produced.

B. Adaptation of the FIB Technique to Sea-Level Pressure Analysis of Small Areas

The FIB sea-level pressure analysis technique described above is designed for hemispheric analysis--for the synoptic scale. Refinements in the technique are required to deal successfully with the sub-synoptic scale ($\leq$ 300 miles) that involves atmospheric and topographic peculiarities of a region. The Mediterranean is well endowed with these peculiarities and, because it is such an important operating area for the U. S. Navy, it was chosen for the first small-area FIB analysis adaptation.

The main features of the small-area adaptation are:

1. Refinement in the first-guess generation. In the hemispheric model, the kinematical extrapolation is reduced to zero at the edge of the grid, so there is no extrapolation of information from outside the grid. This limitation won't work for the Mediterranean grid, where strong systems near the analysis boundaries are common. To allow extrapolation from outside the grid, the 6-hour-old 125x125 hemispheric analysis is zoomed to extend at least 300nm beyond the present object grid (in this case, 6 grid lengths in the object scale). The expanded field and the 6-hour-old object field are then combined with 100% hemispheric weight outside the border and 20% object-field weight at the border, increasing to 100% 4 grid lengths and more inside. In this way, extrapolation may be performed right up to the border, with information also being brought in from surrounding hemispheric grid points.

2. Analysis on smaller scale. Unusual small-scale atmospheric features, characteristic of a complex area like the Mediterranean, will often be lost in an analysis on a large-scale grid. Therefore, the grid size used in the Mediterranean model is one quarter of the normal 63x63 grid, which gives sixteen times the usual number of grid points in the same area. The program allows the grid to be rotated as desired. In the Mediterranean version the approximate corner-point locations (clockwise from upper left) are 57N 38W, 52N 65E, 16N 32E, and 18N 7W.

3. Increased spreading in tropical regions. More spreading (passing information from grid point to grid point) is desirable in tropical regions of the analysis because of the generally smooth character of the field and wide spacing of reports. The desired degree of spreading is achieved by varying the weight of one of the spreading parameters, the Laplacian. A field of zero Laplacian is added, with increasing weight toward the Equator. In the Mediterranean model, the additional weight of the spreading field varies from zero north of 40°N to 0.5 south of 20°N.

4. Exploitation of winds at the sub-synoptic scale. In the hemispheric model, winds are transformed into two pressure-gradient components according to large-scale dynamics. In the sub-synoptic scale, the winds may not perform in accordance with the large-scale balance equations. Topography, also, has a distorting effect. Equations were formulated to account for the small-scale and topographic effects, thus to get full value from the wind reports.

5. Treatment of pressure and wind reports in relation to elevation and terrain. The weights of above-sea-level pressure reports are treated individually or considered constant in most objective analysis systems. Variances (possible errors) may be assigned for: (1) measurement

error, (2) reduction to sea level, and (3) extrapolation to nearest grid point. When reports are added, the accrued weights are limited only by the number of reports in the area. Such a large weight is unrealistic in a high elevation area.

The proper method, and the one used in the Mediterranean model, is to assemble the reports at the mean height of the module. This collective value is then applied at sea level in the analysis by adding the variance involved. This variance reflects the uncertainty in reducing pressure from station elevations to sea level and places a bound on the total weight at the grid point.

An elevation field was developed to implement the above scheme. This was done in 10-minute lat/long squares over the whole analysis area, a resolution considerably finer than the analysis grid mesh. The height range or terrain roughness along the grid lines is derived from the high resolution elevation field. The ranges are used to reduce wind weights for the effect of uneven terrain. Thus, across a mountain barrier, pressure gradient field weights are cut almost to zero, allowing the true strength of an air mass boundary to be analyzed. The pressure gradient can, therefore, be tightly packed behind the mountains rather than spilling over into the sea. This feature of the analysis is especially useful in the Mediterranean for the bora and mistral situations.

6. Interpretation scheme for specific stations. The experienced hand analyst routinely adjusts for known peculiarities of individual reporting stations. Some station may always report a millibar higher than his neighbors. Another station may be located in such a way as to force his winds 20-30 degrees away from the direction called for by the pressure gradient. A computer analysis program should have a capability for dealing with these individualistic station cases, using a library of station characteristics. The Mediterranean model can utilize such specific station information. However, considerable effort would be required to complete the necessary detailed climatological study for more than a few stations.

C. Program Input

1. Primitive Equation Model Surface Prognosis verifying at analysis time.
2. SR500mb Prognosis verifying at analysis time.
3. Previous 6-hourly FIBSLP analysis.
4. Previous 6-hourly Global Band analysis.
5. Surface Wind Reports for analysis time.
6. 6-hourly, 3-hourly, and hourly surface pressure reports.

D. Program Computation

1. Combine the six-hour-old FNWC SLP and Tropical analyses, weighting the fields according to the FIBSLP formulas.
2. Extrapolate the combined analysis six hours forward, using the 500-mb SR kinematical technique.
3. Combine the appropriate P.E. SLP prognostic chart with the kinematically extrapolated analysis. Weight the prognostic portion as a function of the sine of latitude so that in southern latitudes the extrapolated field carries more weight.
4. From the first-guess pressure field computed above, calculate the higher derivative fields--the first-guess finite difference, Laplacian, second difference, and cross difference.
5. Read in and sort new pressure and wind data.
6. Extrapolate pressure reports to nearest grid point. Perform gross error check, and reject failing reports. Adjust first-guess grid-point value on basis of extrapolated report value.
7. Convert wind reports to pressure finite differences along the grid coordinates and compute wind report reliabilities. Assemble wind values at grid points in the same manner as pressure reports.
8. Blend or analyze for pressure.
9. Compute reliability field for blended pressure field.

10. Reevaluate all reports and first-guess fields.
11. Return to assembly stage, using reweighted first-guess fields and reports. Recycle through all stages.
12. Recycle through blending stage, then output the final analysis.

E. Program Limitations and Verification

The only important limitation on the FIBSLP is lack of data. FIB makes the most from whatever data is provided, with its advanced spreading techniques and its reliability measures, but there are bound to be some analysis weaknesses in the data-sparse areas. There are about 5000 reports accepted for each analysis, but the spacing of these is poor. Only 10% are ship reports, and the land reports have high concentrations over European and U. S. areas. Of the 15,625 grid points used in the program, fewer than 3000 have reports within half a grid length for any one analysis.

The only characteristic bias or weakness in the FIBSLP that has been detected during the first few months of operation is the case of forming low pressure systems. FIBSLP tends to analyze these newly discovered (usually by satellite) lows with slightly higher than actual pressure, on the order of 1-2mb. Corrections are usually made by insertion of bogus reports sent in from Weather Centrals. The customary procedure at FNWC is to send a preliminary SLP analysis to Weather Centrals. The Centrals examine this for accuracy in the light of local knowledge--perhaps some late ship reports or late satellite pictures. If there is evidence of faulty analysis or of a forming low pressure system, the Central will send FNWC bogus reports to correct the situation. These bogus reports are included with the regular data in the final analysis, with the effect of forcing the program into the correct analysis.

No formal verification program has been run on FIBSLP, primarily because the reevaluation feature of FIB essentially amounts to self-verification or self-calibration. FIB is forced to draw well to the reports. Further, the output section of FIBSLP includes a frequency distribution of a report-vs-analysis comparison. This shows how well the analysis fits the data. The mean error of grid values versus interpolated values is 1/3 mb, which says that FIBSLP draws, on the average, to within 1/3 mb to reported values.

The Quality Control team at FNWC reports that there is considerably less bogusing necessary with FIBSLP than with earlier analysis models. This is indicative of good decision making in the program with a resulting analysis that is smooth and yet fits the data closely.

F. Uses of the Product

The surface pressure analysis is the starting point or basis for the thought processes to be followed in making a forecast. It is at this level that the forecaster develops an organized picture of the pressure patterns and weather distribution, and the history of the changes in each. From here, the forecaster can bring in analyses of other parameters at varying levels and relate them to what is happening at surface level. Prognoses develop from this basis.

If pertinent FNWC analyses and prognoses are not available, the FIBSLP analysis would be used to derive surface winds and movement values to develop prognostic charts, sea and swell forecasts, and weather advection patterns.

G. Relationship to Other Products

The FIBSLP analysis is very important input to many of the FNWC programs. It is, in a sense, the foundation on which the other programs are built.

The following FNWC programs use FIBSLP input:

1. P.E. Model
2. Global Band
3. Sea and Swell
4. SAR and Ditch Headings
5. Upper Air Analysis
6. Precipitation and Moisture Model
7. Ocean Currents

H. Program Output

1. Surface Pressure Analysis for 0000, 0600, 1200, and 1800Z, for Northern and Southern Hemispheres. (Catalog No. A-01)
2. Surface Pressure Analysis of the Mediterranean area for 0000, 0600, 1200, and 1800Z. (Catalog No. A-04)

I. References or Suggested Reading

[1] Holl, M. M. and B. R. Mendenhall, 1971; "Fields by Information Blending, Sea-Level Pressure Version", FNWC Technical Note No. 72-2, March 1972.

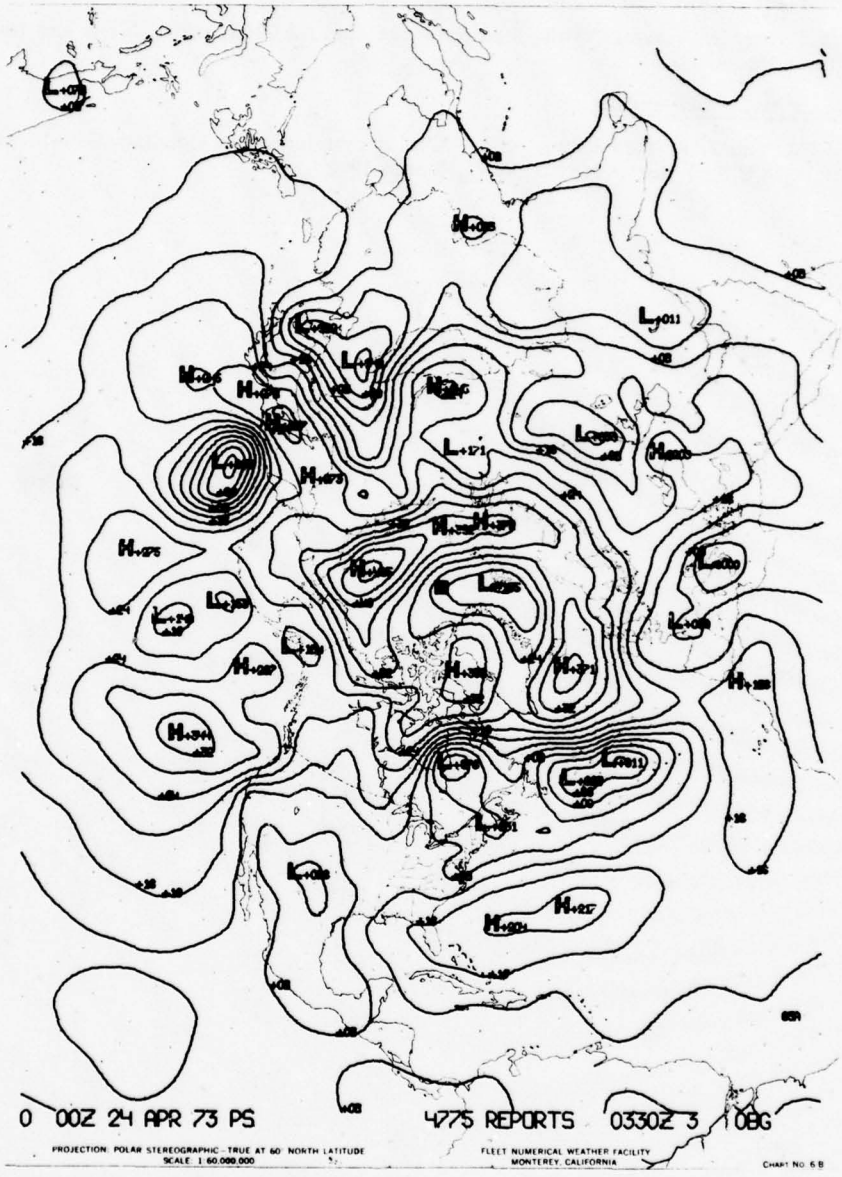


Figure 4.1.1
Sea Level Pressure Analysis For 0000Z 24 APR 1973. Contour Interval 4-MBS. 4775 Reports were used in the Analysis. The Analysis was made at 0330Z. No Bogus Reports were used.

4.2 PLANETARY BOUNDARY LAYER PARAMETERIZATION SCHEME

A. Program Development

The planetary boundary layer (PBL) is the transition zone between the earth's surface and the atmosphere, and is created by the effects of both. Indication of the importance of the PBL is that in this zone, most terrestrial life forms occur, surface weather happens, and Naval surface operations are performed. The PBL parameterization scheme, in use at FNWC since October 1975, is designed to represent the relevant scales of motion and average properties of this important layer. From this, profiles of wind, temperature and moisture can be calculated and such specific characteristics as optical and electromagnetic properties. These boundary layer products are computed from synoptic-hemispheric data fields. Emphasis is placed on the parameterization of the marine PBL since the sea state is of prime importance and appropriate wind fields can be produced to drive the spectral ocean wave model.

B. Program Input

Northern hemisphere polar stereographic projection analyses and forecasts and permanent climatology are used as input fields.

Current analyses and prognoses used:

Tau = 0 to 72 hours, by 6-hour increments

1.	C00	1000mb height anomaly
2.	C10	1000mb temperature
3.	D00	850mb height anomaly
4.	D10	850mb temperature
5.	E00	700mb height anomaly
6.	E10	700mb temperature
7.	F00	500mb height anomaly
8.	F10	500mb temperature
9.	H00	300mb height anomaly
10.	H10	300mb temperature
11.	A13	surface temperature
12.	A07	surface air temperature
13.	A15	surface air vapor pressure
14.	A01	surface pressure
15.	A29	marine wind U component
16.	A30	marine wind V component

Permanent climatology used:

1. Roughness length (seasonal)

2. Terrain height

C. Program Computation

1. Read in synoptic scale data.

2. Calculate PBL external parameter fields.

3. Calculate sub-grid scale steady state parameters and vertical structure.

4. Calculate output fields.

D. Program Limitations

The PBL is parameterized from synoptic-hemispheric data fields, and the parameters, therefore, represent an interpretation of the PBL processes on a comparable scale and are not intended to be explicit descriptions of small-scale processes. But, estimates of the magnitude of small-scale processes may be made. The coarse resolution of the data fields, for example, does not contain the information to parameterize the small-scale wind fluctuations. The gustiness, however, may be estimated by calculating the expected maximum gust (i.e., the maximum wind speed expected over, say, any 2-minute interval).

The parameterization of the PBL height is not representative in low latitudes where it may become unrealistically large. Thus, the PBL products must be used with caution in the tropics.

E. Uses of the Products

The primary products are the SOWM winds (see Section 4.2, reference [1]) and the maximum horizontal gust. Other wind products are the 19.5 meter winds--speed, direction, U component, and V component. Other products are related to the velocity, temperature, and moisture scales in the PBL, the radar evaporative duct, and heat fluxes.

F. Relationship to Other Products

Special wind fields are produced especially to couple to the SOWM.

G. Program Output

Catalog Number	Description
A27*	19.5m wind speed
A28*	19.5m wind direction
A29*	19.5m wind, U component
A30*	19.5m wind, V component
A35	SOWM wind speed
A36	SOWM wind direction
A20	SOWM wind, U component
A21	SOWM wind, V component
A53	19.5m wind gust

*19.5 meter winds are produced only in the forecast mode.

A90	surface based radar duct height
A92	difference between radar refractive index in duct and at surface
A93	height at which refractive index profile slope becomes sharp
A94	difference between radar refractive index at sharp slope (A93) and at surface
A95	PBL velocity scale
A96	PBL temperature scale
A97	PBL moisture scale
A98	PBL sensible heat flux
A99	PBL latent heat flux

H. Reference

[1] Kaitala, J. E., "A Brief Description and Preliminary Evaluation of an Operational Planetary Boundary Layer Parameterization Scheme", FNWC.

4.3 FORECAST CHANGES AND PROGNOSIS DIAGNOSTICS

A. Program Development

This program was developed to provide a comparison of fields to show the actual change between successive analysis and forecast fields, and to show the differences between prognoses and corresponding analyses, or forecast error. Of particular interest are surface pressure, 500-mb height, 300-mb height, significant wave height, and marine wind speed.

B. Program Input

1. The present analysis and the 12, 24, 36, 48, 60, and 72 hour previous analyses for:
   a. Surface Pressure
   b. 500-mb height
   c. 300-mb height
   d. significant wave height
   e. marine wind speed.
2. The 12, 24, 36, 48, 60, and 72 hour prognoses verifying at present analysis time for parameters a-e above.

C. Program Computations

For each selected environmental parameter, algebraic and root-mean-square differences are computed between the present analysis and:

1. The 12, 24, 36, 48, 60, and 72 hour previous analyses.
2. The 12, 24, 36, 48, 60, and 72 hour verifying prognoses, where the root-mean-square (RMS) difference is computed from:

$$RMS = \left\{ \sum_{i=1}^{n} \frac{(P-A)^2}{n} \right\}^{1/2}$$

   where P is the prognostic or previous analysis value at a grid point, A is the verifying analysis value and n is the number of grid points over which the differences are computed.

3. The 12, 24, 36, 48, 60, and 72 hour old analyses are subtracted from the corresponding prognoses to obtain the prognostic surface change.

D. Program Limitations

Charts derived from these products portray only grid-point differences between two fields. They do not represent any dynamical or physical processes, but they have value primarily as diagnostic tools, and are helpful in verification studies.

E. Uses of the Products

The actual change charts show what changes have been and are occurring. These changes indicate areas of important weather development. The forecast change charts continue this into the near future, thus aiding in weather prognostication and providing a basis of comparison of model performance with the forthcoming actual change charts. If forecast changes seem unreasonable, the forecaster must search for dynamic weather processes which might contribute to poor model performance--subtle variations of flow patterns or moisture transfer, short wave effects, etc. Such a search might help diagnose troubles with the model; and the forecaster develops a firmer basis for his forecast efforts.

The root-mean-square (RMS) difference computations are used mostly by the program developers, and are calculated in various geographic areas. Verification data show the programmer the patterns of systematic errors and thus aid in determining which geographic or environmental conditions produce program errors.

F. Relationship to Other Products

These diagnostic products are not used as direct input to other FNWC programs for the creation of FNWC products.

G. Program Output

	Field	Catalog Number
1.	48-hour Surface-Pressure Change (Fig. 4.3.1)	A17
	48-hour 500-mb Height Change	F17
	48-hour 300-mb Height Change	H17
	48-hour Marine Wind Speed Change	M70
	48-hour Significant Wave Height Change	M71
2.	48-hour Surface Pressure Prognosis Error (Fig. 4.3.2)	A19
	48-hour 500-mb Prognosis Error	F19
	48-hour 300-mb Prognosis Error	H19

3. *Root-mean-square error and change for 12, 24, 36 hours for surface-pressure, 500-mb Height, and 300-mb Height for:

   Northern or Southern Hemisphere
   Land points
   Sea points
   Various Latitude Bands
   Specific Land Regions
   Specific Sea Regions

*NOTE: RMS error and change are available upon request.

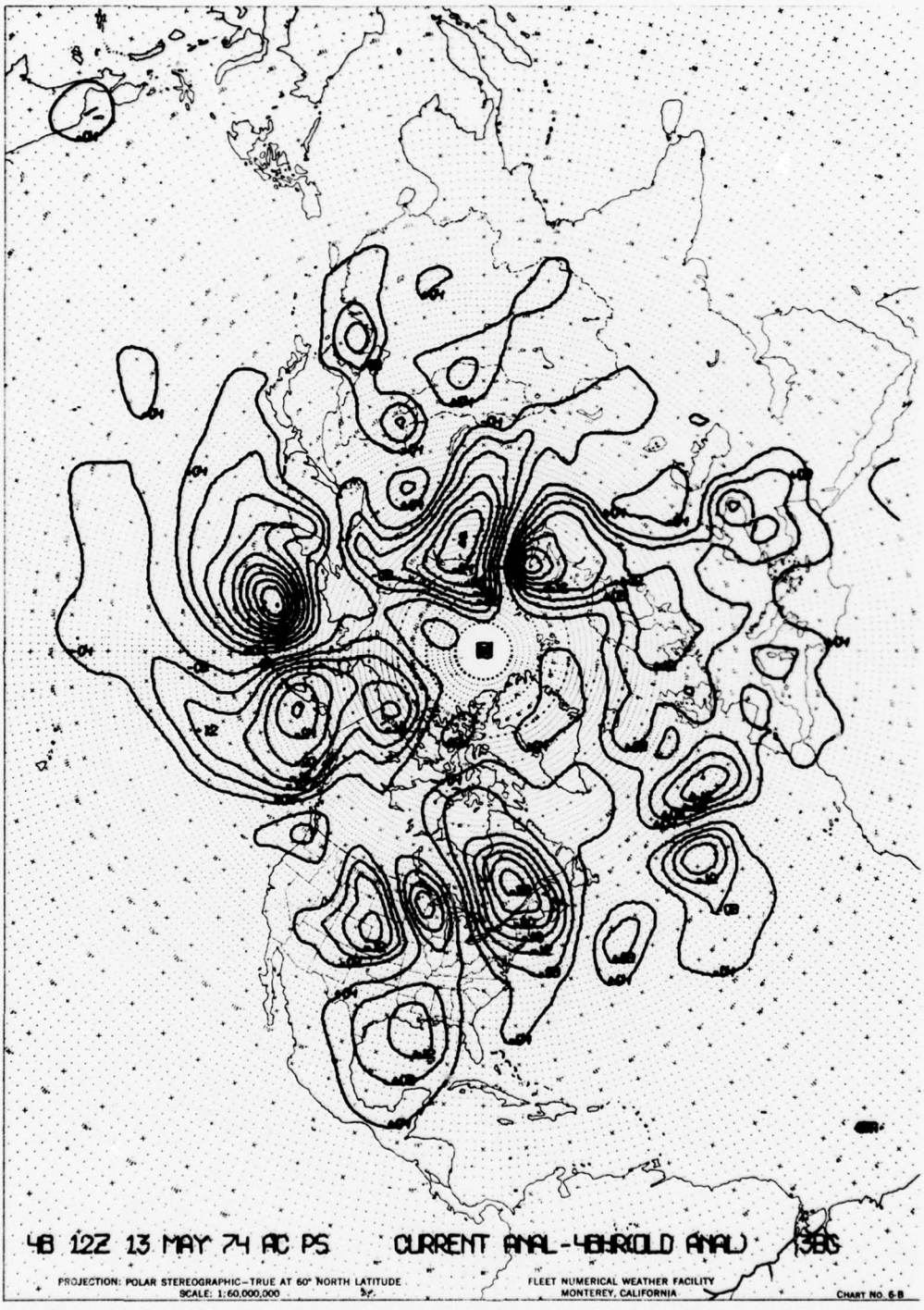


FIGURE 4.3.1 Surface Pressure Change Current Analysis minus old analysis (A17)

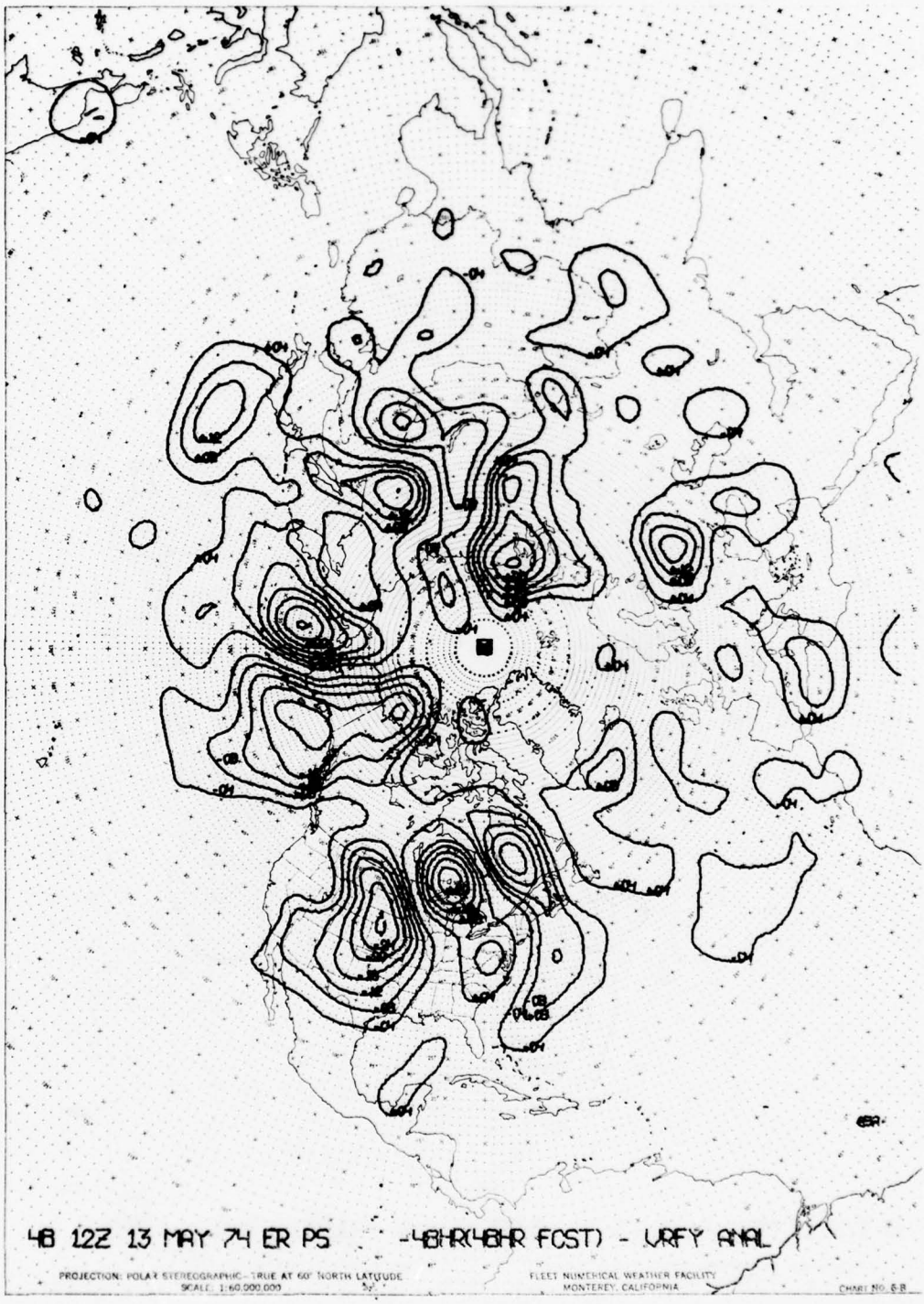


FIGURE 4.3.2 Surface Pressure Forecast minus verifying analysis (A19)

4.4 GLOBAL BAND/SPHERICAL ANALYSIS MODEL FOR SURFACE PRESSURE AND MARINE WIND AND GLOBAL BAND UPPER-AIR WIND AND TEMPERATURE ANALYSIS

A. Model Development

The FNWC global band sea-level pressure and marine wind model was developed to (1) provide an initial surface wind field for the FNWC sea/swell program in the tropics, (2) provide support over an expanded area for OTSR, and (3) provide a surface analysis for future incorporation into a multi-level wind analysis program. The global band upper-air analysis program was designed primarily to improve support of flight operations in the 400-mb turboprop level, in particular. Methods of the upper-air analysis are very similar to surface analysis methods; only the latter will be described in detail.

The general coverage of this analysis model invites several problems. Only in the northern hemisphere is the data coverage adequate. Lack of data in the tropics, southern hemisphere, and, globally, in the upper air constitutes a frustration for analysis schemes. In the tropics, the character of weather is difficult to analyze due to the masking of synoptic weather effects by diurnal fluctuations and the effect of orographic features. The standard grids have not seemed adequate for the capture of mesoscale convection. And the pressure-wind relationship is not well defined. Choice of analysis technique is in consideration of the wide range of weather encountered--the global band grid covers the area 41°S to 60°N; the spherical grid (to which the analysis has been converted) covers the entire globe.

The analysis procedure chosen is one of the earliest methods developed in numerical analysis (Cressman, 1959), the successive corrections method (SCM). Still, there were problems of inconsistency between the wind fields and the pressure fields; for example, the occurrence of 90° angles between wind direction and isobars. These problems were solvable by coupling these fields. In late 1971, numerical variational analysis (NVA) was introduced to the model; (1) to relieve the problem of coupling the wind and pressure fields; (2) to extrapolate dynamically, from data-rich areas to data-poor areas; (3) to retrieve, from the surface pressure fields, information of the winds; and (4) to subject the accomplishment of (1), (2), and (3) to a sound wind-pressure formulation.

The first-guess field used for the surface pressure analysis is composed of three fields; the northern hemisphere FIB surface pressure analysis, north of 25°N; the 6-hour-old spherical surface pressure analysis, between 15°S and 15°N; and the southern hemisphere FIB surface pressure analysis south of 25°S. The two blend zones--15° to 25° north and south--are linearly weighted combinations of the two fields adjacent to the zones.

The first-guess field used for the marine wind analysis is also a blend of fields with a linearly weighted combination of two fields in the blend zones. A modified geostrophic wind from the surface pressure analysis, poleward of 20° north and south and the 6-hour-old marine wind analysis in the band 15°S to 15°N, comprise the first-guess field.

The analysis model was developed on the global band grid, a Mercator secant projection. Grid mesh size is 145x49 with 2.5° longitude per grid distance. This grid is now used for transmission only, the analysis is carried out on the spherical grid. Grid size is 145x73, with 2.5° longitude and latitude per grid distance. The basic procedure in these analysis techniques is to assemble the best estimate of the field to be analyzed--the first guess--and then to modify it as required to fit the acceptable observational data.

The surface pressure analysis technique restricts observational data to the band 20°S to 20°N. Therefore, poleward of 20° latitude, north and south, the FIB hemispheric analyses used as the first guess are left unchanged.

The marine wind analysis, though, must accept global wind reports, since there is no FIB analysis covering winds. Reports consist of ship reports up to 6-hours old, current island reports, and low level satellite winds (converted to surface by using 80% of reported speed). Wind reports must pass a gross error check (GEC). Reliability weights are then assigned to each report according to type: island, weather ship, regular ship measured wind, regular ship estimated wind, 1-2-hour-old offtime ship winds, and 3-5-hour-old offtime ship winds, for example. A weight factor is assigned to each report according to distance between report and grid point under consideration, report density in the area, latitude, scan cycle number, and wind direction (if wind speed is greater than 13 knots). A correction to a first-guess grid point value is applied, subject to the reliability weight and the weighting factor of surrounding reports. Scan radius (radius of report influence) is a function of report density and latitude and decreases with each additional cycle in rich-data areas, resulting in increasing detail with higher scan numbers. Lateral checking for observational discrepancies occurs in all but the first scan. Scan radii are limited to 300 nm in cycle 1, 200 nm in cycle 2, and 100 miles in the last two cycles. To aid in the definition of tropical cyclones, eight pseudo-wind reports (speeds derived from storm warnings) are inserted symmetrically at a 50-mile radius around the storm.

The NVA couples the surface pressure and wind analyses using the dynamic constraint of the primitive momentum equations. Inputs for this phase of the surface analysis are (1) pressure analysis, (2) wind analysis, and (3) data density field (produced by the SCM). This analysis phase is conducted on the spherical grid. Analysis adjustment begins in dense-data areas where data reports predominate over dynamics. In rare-data areas, dynamic extrapolation from dense-data areas predominates.

B. Program Input for Surface Model

1. Reported surface pressure observations (approximately 1000 to 1500 reports). No pressure observations poleward of 20° latitude are included. Values for pressure are extracted from the FIB/SLP analysis for the area north of 20°N.

2. Reported surface wind observations.

3. Current northern and southern hemispheric surface pressure analysis.

4. Current northern hemispheric sea-surface temperature analysis.

5. 6-hour-old spherical surface pressure analysis.

6. 6-hour-old spherical surface wind analysis (u and v component fields).

7. Spherical surface pressure climatology field for the current month.

8. Spherical surface wind climatology (u and v component fields for the current month).

9. Spherical surface pressure and wind analyses for use in the NVA.

Program Input for Upper-Air Model

1. 12-hour-old global band upper-air wind and temperature analyses south of 22 1/2°N.

2. Current FNWC upper-air analyses north of 22 1/2°N.

3. Upper-air observational data from: rasondes, aireps, pibals, satellites (250- and 200-mb winds, and temperatures from SIRS).

C. Program Computation Order for Surface Analysis

1. Read in input fields.

2. Construct first guess of surface pressure as described in Section A. The combination is an average of the two fields weighted linearly so that at 15°, Spherical is 100%, SLP is 0%; at 25°, the percentages are reversed.

3. Extract surface pressure and winds from each observation, and apply GEC.

4. Analyze surface pressure in four scans over entire grid by SCM.

5. Construct surface wind first guess by calculating a modified geostrophic wind field for use north of 20°N and south of 20°S, and in combination with the spherical 6-hour-old wind analysis between 15° and 20° north and south. From 15°N to 15°S use spherical 6-hour-old winds.

6. Analyze surface wind in three cycles and compute u and v component fields.

7. Adjust pressure and wind analyses using the NVA Model.

8. Compute 12- and 24-hr surface pressure changes.

Program Computation Order for Upper-Air Analysis

1. Read in current Global Band surface pressure and wind analyses.

2. Analyze (by SCM) the temperatures at 850, 500, 300, and 200 mb and the winds at 700, 400, 250, and 200 mb.

3. Couple the wind and temperature fields in the vertical by the NVA process to obtain adjusted values of temperature at 850, 500, and 300 mb and wind at 700 and 400 mb. Recycle to obtain final analyses.

4. Interpolate between levels to obtain analyses of temperature at 700 and 400 mb and winds at 850, 500, and 300 mb.

D. Program Limitations

The surface pressure analysis makes use of reported pressure and wind only. No attempt is made to model the pressure distribution using other elements of the reports.

Analysis flaws are usually the result of one or all of the following problems:

1. Lack of Data

In regions of no reported data, the final analysis is a combination of the first guess and climatology. Initially, the contribution made by climatological values is small but increases with the number of synoptic periods in which no reports are received in the area.

2. Erroneous Data

Surface observations reported in error may be used in the analysis. No internal consistency checking of reports is presently attempted. A datum will either pass the error checks, resulting in an incorrect analysis, or it will be rejected with the possible loss of some significant information.

Surface pressure and wind observations reported in error will normally be rejected in the GEC. If the erroneous report should pass the GEC tolerances, it will contaminate the analysis.

If the bad report, accepted in the GEC, is located in a high data density region (e.g., over land), it will probably be rejected when compared with its neighbors in the lateral fitting check. It may, however, have already had a slight adverse influence on the final analysis. If the bad report is located in a sparse data region (e.g., over oceans), it may pass the lateral fitting check as well as the GEC. In this case the analysis will depict the pressure distribution represented by the erroneous report.

3. Extreme Atmospheric Change

Occasionally extreme atmospheric change will manifest itself as an error in the analysis. In this case, strong development results in valid data failing the GEC. GEC tolerances are predicated on a

reasonable forecast being used in construction of the first approximation. If the forecast is abnormally poor and off-time and late reports do not correct it sufficiently, this type of error may occur. This represents a serious flaw.

4. Detection of Errors

Errors of the types previously discussed can easily be discerned at major network centers. Data density upon which the analysis is based is provided by the Hemispheric Surface Coverage and Gross-Error-Check Reject Coverage charts. Data lists, including all ship reports used in the analysis as well as those rejected by the gross-error and lateral-fitting checks, are available. Major network centers should use this information to determine validity of the surface pressure analysis in their areas of responsibility. Corrections, if necessary, will be initiated or notices of error will be disseminated to fleet users, by these centers.

Errors may be detected by the operational forecaster who receives the analysis directly. The total number of reports used, a simple indicator of analysis quality, appears in the title of all surface pressure analyses. The 24-hour surface pressure change chart or message (Catalog No. A47) can be used to determine areas of abnormal surface development. Non-meteorological or new disturbances should be cross checked with available observations.

E. Uses of the Product

Uses of the global band/spherical products in the field is concentrated in the tropics; the hemispheres are already covered by the FIB/SLP surface analysis and the P.E. prognoses.

The analyses provide the forecaster with an accurate pattern description--location and intensity of highs, lows, fronts, etc. Comparison with the previous analysis shows how the pattern is changing, and forms a basis for extrapolation of features on the current analysis.

In the tropics, the forecaster uses the surface pressure and wind analyses, and the upper-air wind analyses to:

1. Locate the Equatorial Trough (Intertropical Front), and make a rough estimate of its intensity by noting areas of convergence in the wind field. Weather in the Equatorial Trough is produced principally by convergence.

2. Locate Easterly Waves, or inverted troughs. Easterly Waves, when well defined, have characteristic weather patterns which can be used as a forecast basis when the Easterly Wave is moving toward a point of forecast interest. The 24-hr pressure-change chart will help in detection.

3. Locate shear lines. These are cold front remnants, and can be located by an abrupt change in the horizontal wind component parallel to the shear line. A typical case would be E25-30 knots on one side of the line, and E15-20 on the other. Shear lines are usually marked by a pronounced line of convection at the leading edge, and there may be a few convection lines behind the shear line. Low ceilings and rainfall occur along the shear line.

4. Locate and provide tracking history of subtropical and tropical cyclones. The subtropical cyclones are the Kona-type storm. The others are hurricanes and typhoons.

5. Calculate sea/swell fields, using standard techniques such as outlined in H.O. 603. Surf forecasts are derived from the sea/swell.

6. Locate areas of convergence and divergence by wind field examination. Convergence is in areas where winds tend to blow inward toward some central line, or where fast winds are blowing along the same line into areas of slower winds. Convergence of either type tends to increase cloud cover and precipitation.

7. Provide flight level winds for aircraft clearances.

8. Provide WEAX forecasts for ships.

In the southern hemisphere midlatitudes, sea-level pressure analyses (global band, spherical, or FIB/SLP) would be used in the traditional sense, because no prognostic charts are available. Further, the analyses will tend to be inaccurate over wide areas--because of data sparsity. In forecasting, almost complete reliance will have to be placed on historical-type extrapolation of systems. Lows which have been moving along at, say, a steady 20 knots will be permitted to continue this rate of movement for the forecast period. This type of prognostication can lead to serious error because it misses dynamical changes which might be just starting. Development and implementation of the global primitive equation model promises relief in the future with its dynamic prognostic fields.

F. Relationship to Other Products

The spherical marine wind analysis is the principal input to the FNWC spectral wave analyses.

The global band/spherical surface products are used routinely in the Optimum Track Ship Routing Program.

G. Program Output

1. Global band surface level products for 0000/1200 hours:

	Catalog No.	
	Global Band	Spherical
Pressure analysis	A40	A01$
u,v wind components	A41,A42	A29$,A30$
Isogon analysis	A43	A28$
Isotach analysis	A44	A27$
12- and 24-hr pressure change	A47 Tau = 12, 24	

2. Global band upper-air products for 0000/1200 hours:

(mb)	850	700	500	400	300	250	200
Winds (u,v)	D41,42	E41,43	F41,42	G41,42	H41,42	T41,42	I41,42
Isogon	D43	E43	F43	G43	H43	T43	I43
Isotach	D44	E44	F44	G44	H44	T44	I44
Temperature	D45	E45	F45	G45	H45	T45	I45

Note: Wind fields at 850, 500 and 300 mb and temperature fields at 700 and 400 mb are interpolated from balanced fields. The 250 and 200 mb fields are analyzed but are not NVA balances.

H. References

[1] Grayson, T. H., 1971; "FNWC Global Band Surface Pressure and Wind Analyses", FNWC Technical Note 71-3.

[2] Cressman, G. P., 1959; "An Operational Objective Analysis System", Monthly Weather Review, Vol. 87, No. 10.

[3] Hubert, W. E. and B. R. Mendenhall, 1970; "The FNWC Singular Sea Swell Model", FNWC Technical Note 59.

[4] Lewis, J. M. and T. H. Grayson, 1972; "The Adjustment of Surface Wind and Pressure by Sasaki's Variational Matching Technique", Journal of Applied Meteorology, Vol. 11, No. 4.

[5] Lewis, J. M., 1972; "An Operational Upper Air Analysis Using the Variational Method", Tellus, Vol. 24, No. 6.

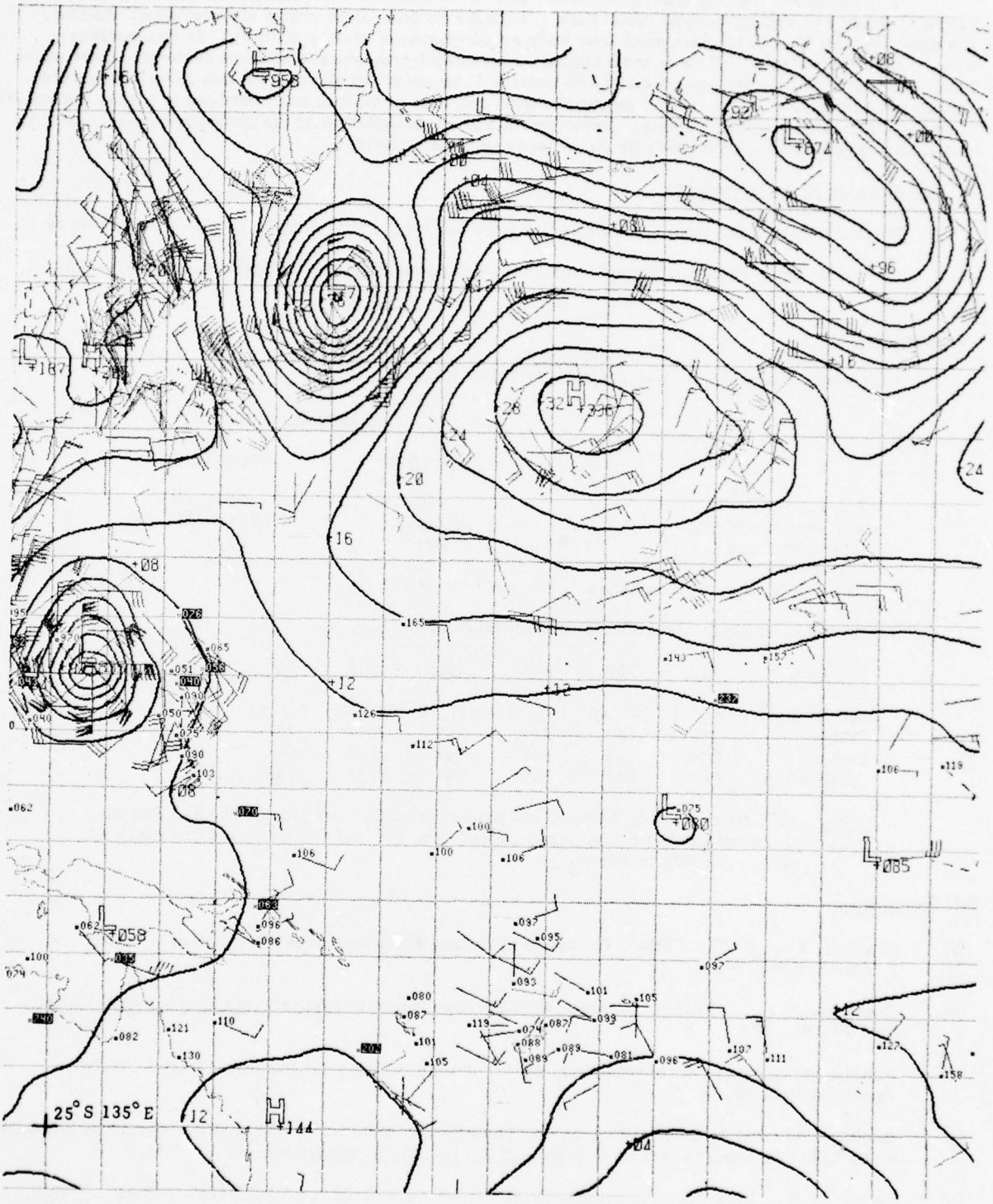


FIGURE 4.4.1 Surface Pressure Analysis. Global band grid interval, 5°.

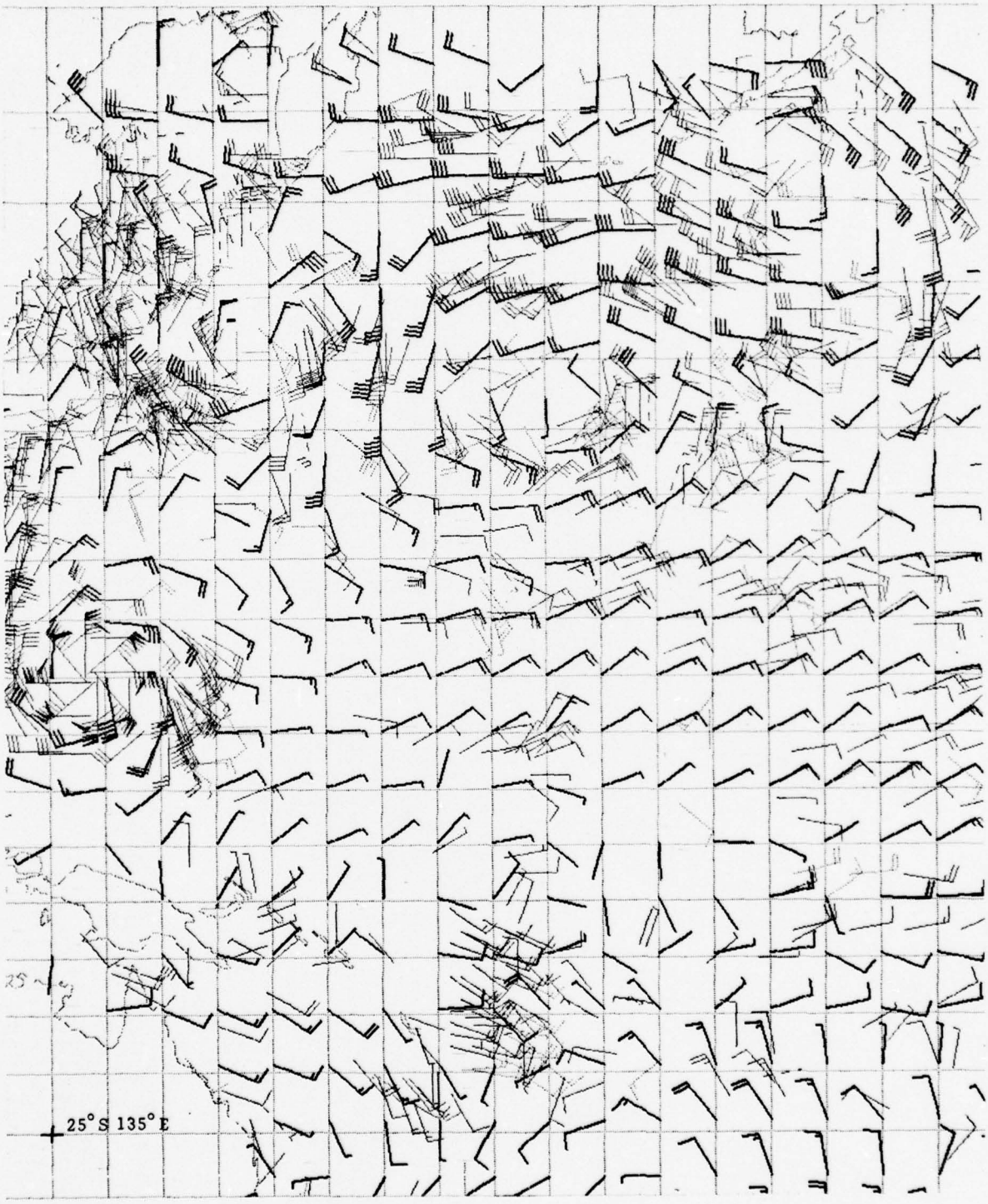


FIGURE 4.4.2 Marine Wind Analysis. Global band grid interval, 5°.

4.5 AIR TEMPERATURE, VAPOR PRESSURE, AND DEW-POINT ANALYSES

A. Model Development

The two-dimensional scalar analysis problem at hand requires the model to encompass (1) an accurate first guess, which provides continuity and has a direct bearing on the accuracy of the analysis in sparse data areas, (2) a maximum number of carefully screened reports of the parameters to be analyzed, (3) capability for the entry of pseudo data, over no-data areas, and (4) a competent objective analysis scheme.

The first-guess fields were supplied by the P.E. Model, when it became operational; the 12-hour moisture and temperature prognoses are of good quality. The reports used by the model are screened several times by empirically developed relations. Bogus dew-point depression reports at 850, 700, 500, and 400 mb may be entered over data sparse ocean areas. These reports are derived from reported weather at the surface station. The analysis is performed by the FNWC objective analysis technique (Section 3.9).

B. Program Input

1. Northern hemisphere 12-hour-old 12-hour P.E. prognoses and southern hemisphere 12-hour-old analyses for air temperature at the surface, 1000 mb, 925 mb, 850 mb, 700 mb, 500 mb, 400 mb, and 300 mb levels.

2. Northern hemisphere 12-hour-old 12-hour P.E. prognoses for vapor pressure, and southern hemisphere 12-hour-old dew-point depression analyses for the same levels as in 1.

3. Climatological fields corresponding to 1 and 2 above.

4. Ship reports from three hours before analysis time.

5. Synoptic upper-air reports.

6. Synoptic surface reports.

7. Current sea-surface temperature analysis.

In cases where previous analyses and 12-hour P.E. prognoses are unavailable, climatological fields are used instead.

Data Handling

1. All surface and upper-air reports used have been edited by the FNWC ADP program. Upper-air reports, additionally, have been processed as described in Section 4.6, C, "Data Preparation".

2. Surface air temperatures must pass two tests:

   a. Ship reports must be within 8C° of the P.E. prognosis used as a first guess, island reports must be within 25C°.

   b. The difference between report air temperature and sea-surface temperature is also restricted as a function of sea-surface temperature.

c. The difference between reported air vapor pressure and the vapor pressure at sea-surface temperature is restricted, also, as a function of sea-surface temperature.

4. The difference between upper-air dew-point reports and the 12-hour P.E. prognosis is restricted as a function of level and whether the area is land or sea. The whole sounding is not rejected if one level fails the test--only the questionable level.

5. Bogus dew-point depression reports are created at the 850-, 700-, 500-, and 400-mb levels only in sparse data regions; then, surface reports of clouds and present and past weather are used to assign dew-point depressions at the four upper levels. For example, some low clouds reported from the surface would cause a 2C° dew-point depression to be assigned at the 850-mb level.

C. Program Computation

Northern Hemisphere

1. Read in the previous P.E. 12-hour prognosis for surface air temperature.

2. Read in hemispheric air temperature reports.

3. Check reports*.

4. Analyze surface air temperatures**.

5. Read in the previous P.E. 12-hour prognosis for surface, 1000-, 925-, 850-, 700-, 500-, 400-, and 300-mb vapor pressure and temperature.

6. Check reports*.

7. Enter pseudo upper-air reports in no-data regions.

8. Analyze dew-point fields at prescribed levels**.

Southern Hemisphere

The steps are the same as for the northern hemisphere except: for "previous 12-hour P.E. prognosis", read "previous analysis".

D. Program Limitations and Verification

Temperature errors will sometimes develop in unusual circumstances such as: in the lee of the Rocky Mountains during a severe cold outbreak, or in a small area with very high temperatures. In such cases, the gross error check will reject good reports because the first-guess field is not a good approximation in the circumstance.

A sequence of report rejections over a small space-time range is an indication of possible model malfunction. A systematic geographical report reject distribution may be an indication of model weakness.

E. Uses of the Products

The primary use of the model products is as input to other FNWC models. However, there are several potential applications for use in the field.

---

*Data checking is described under "Data Handling", part B, this section.

**The analysis program used is the FNWC objective analysis technique, described in Section 3.9.

In precipitation forecasting, empirical rules involving dew point and dew-point depressions are followed to screen for the moisture patterns necessary for precipitation to occur. The critical minimum dew-point values which provide a possibility of precipitation are: -5°C at 850 mb, -10°C at 700 mb, and -25°C at 500 mb. Moisture tongues are readily determined from the dew-point depression analyses at 850, 700, and 500 mb. The dew-point spread must be 5°C or less for rainfall to occur. After the precipitation possibility is determined from the above guide lines, other factors such as trough location and vertical motion must be considered.

For fog forecasting, the surface temperature and dew-point depression can be used as input to fog prediction diagrams to obtain a forecast of whether or not fog will occur and, if so, time of occurrence. Fog forecasting diagrams must be developed to fit the local station characteristics. They are generally available as part of the station forecasting manual.

To obtain height of the lifting condensation level, the surface dew-point depression analysis can be used in the formula H = 222 x dew-point depression.

A broad screening for thunderstorm possibility can be made from the 850-mb and 700-mb dew-point depression charts. A depression of 13°C or more at either level signals a no-thunderstorm condition.

Cloudiness may be anticipated at any upper level whenever the dew-point depression is 5°C or less.

F. Relationship to Other Products

The products from this model are important inputs to the following FNWC models:

1. P.E. Model--The P.E. model uses surface vapor pressure and dew-point depression analyses aloft for input to the thermodynamic equation to ultimately forecast rain. Actually, the surface temperature/vapor pressure/dew-point depression model is just a part of the P.E. Model.

2. Cloud/Precipitation Model--All of the products are used in the initialization of the Cloud/Precipitation Model.

G. Program Output

1. Surface Field Air Temperature Analysis (Catalog Number A10+, A10-)

2. Surface Vapor Pressure Analysis (Catalog Number A12+, A12-)

3. Dew-Point Depression Analysis for

Surface	(Catalog Number A50+, A50-)
1000 mb	(Catalog Number C50+, C50-)
925 mb	(Catalog Number R50+, R50-)
850 mb	(Catalog Number D50+, D50-)
700 mb	(Catalog Number E50+, E50-)
500 mb	(Catalog Number F50+, F50-)
400 mb	(Catalog Number G50+, G50-)
300 mb	(Catalog Number H50+, H50-)

H. References

[1] Chisholm, Donald A., John T. Ball, Keith W. Veigas and Paul V. Luty, 1968; "The Diagnosis of Upper-Level Humidity", Journal of Applied Meteorology, Vol. 7, No. 4, August 1968.

[2] Ball, John T. and Keith W. Veigas, 1968; "The Analysis of Upper-Level Humidity", Journal of Applied Meteorology, Vol. 7, No. 4, August 1968.

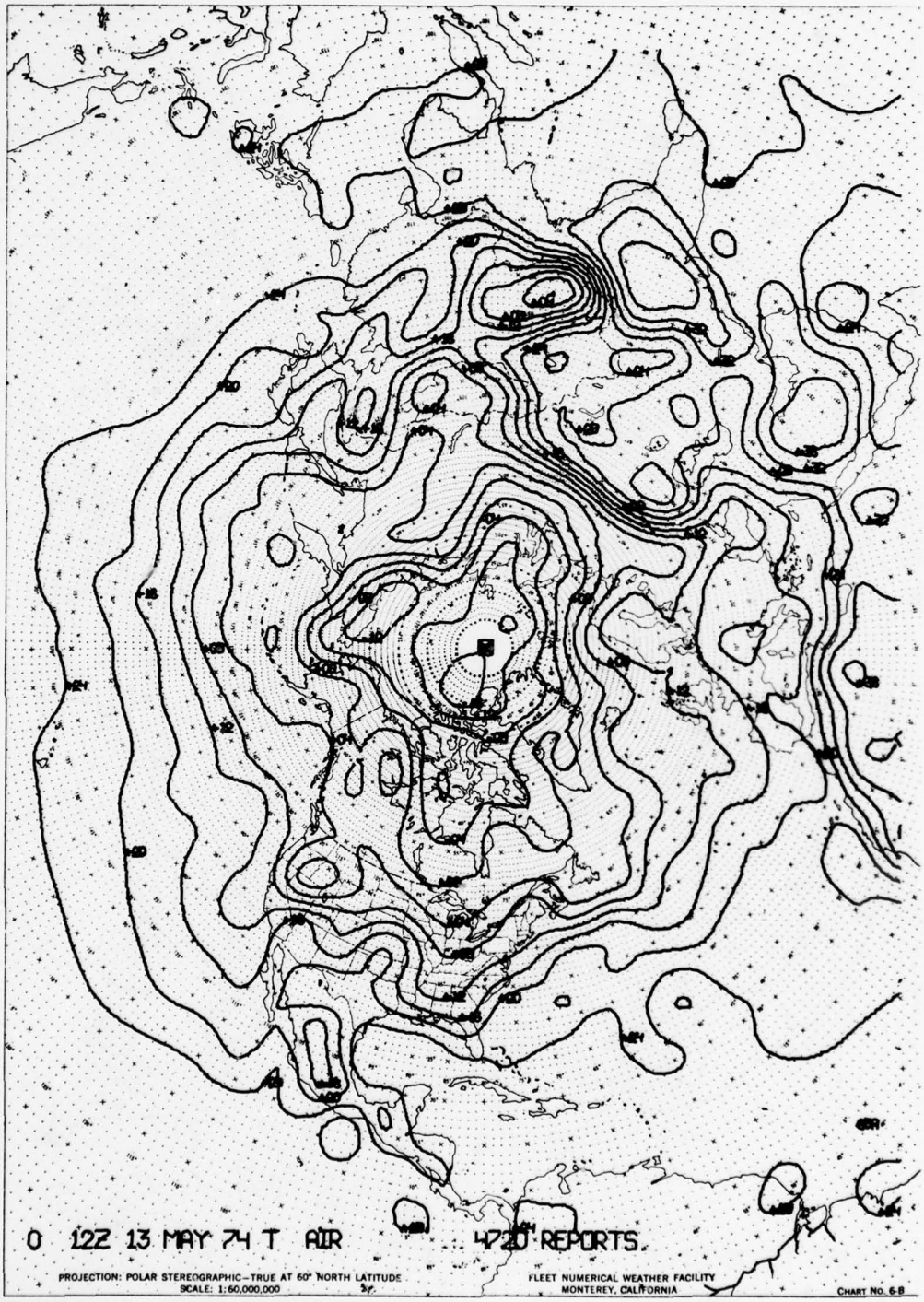


FIGURE 4.5.1 Surface Air Temperature Analysis (A10)

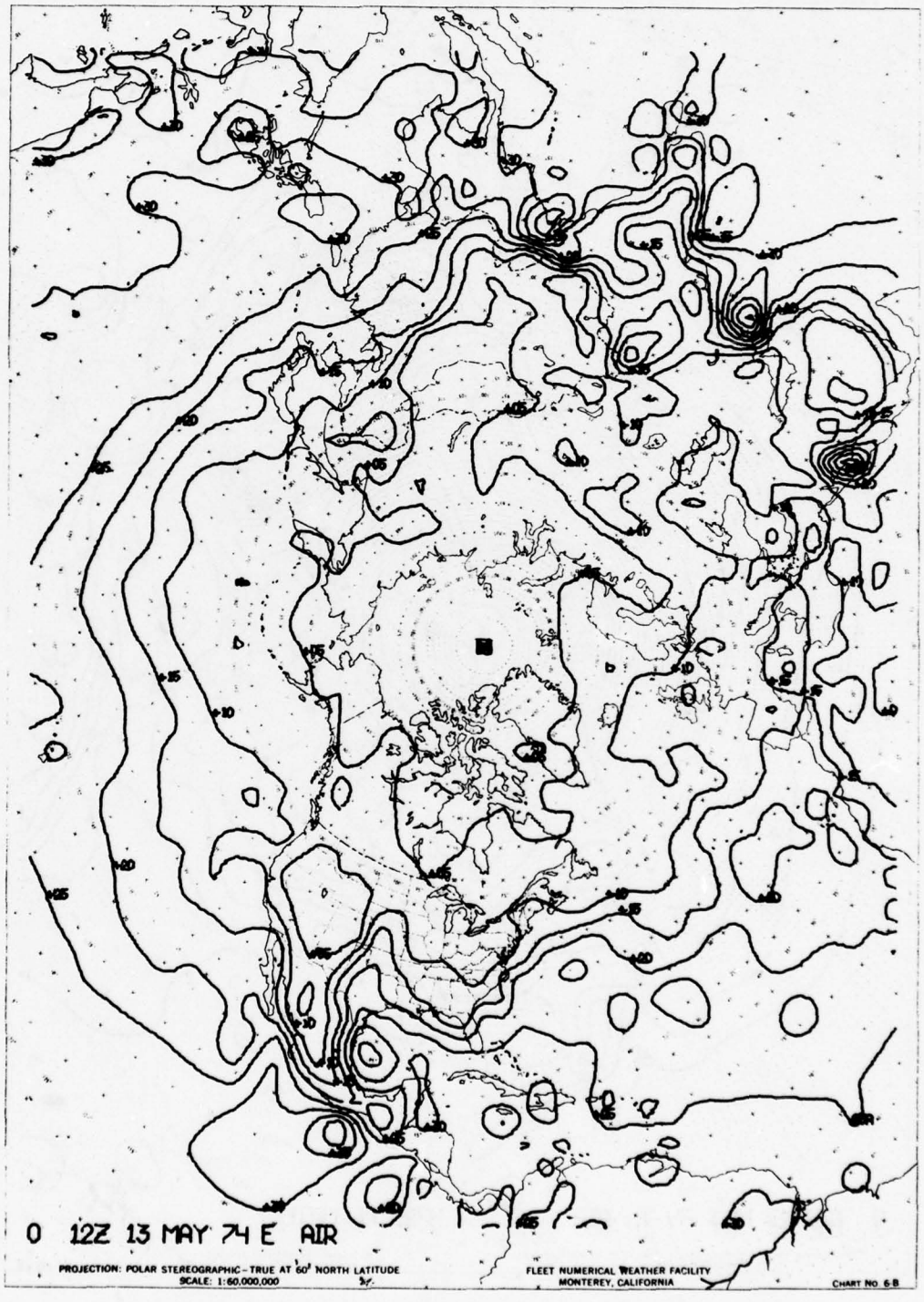


FIGURE 4.5.2 Surface Vapor Pressure Analysis (A12)

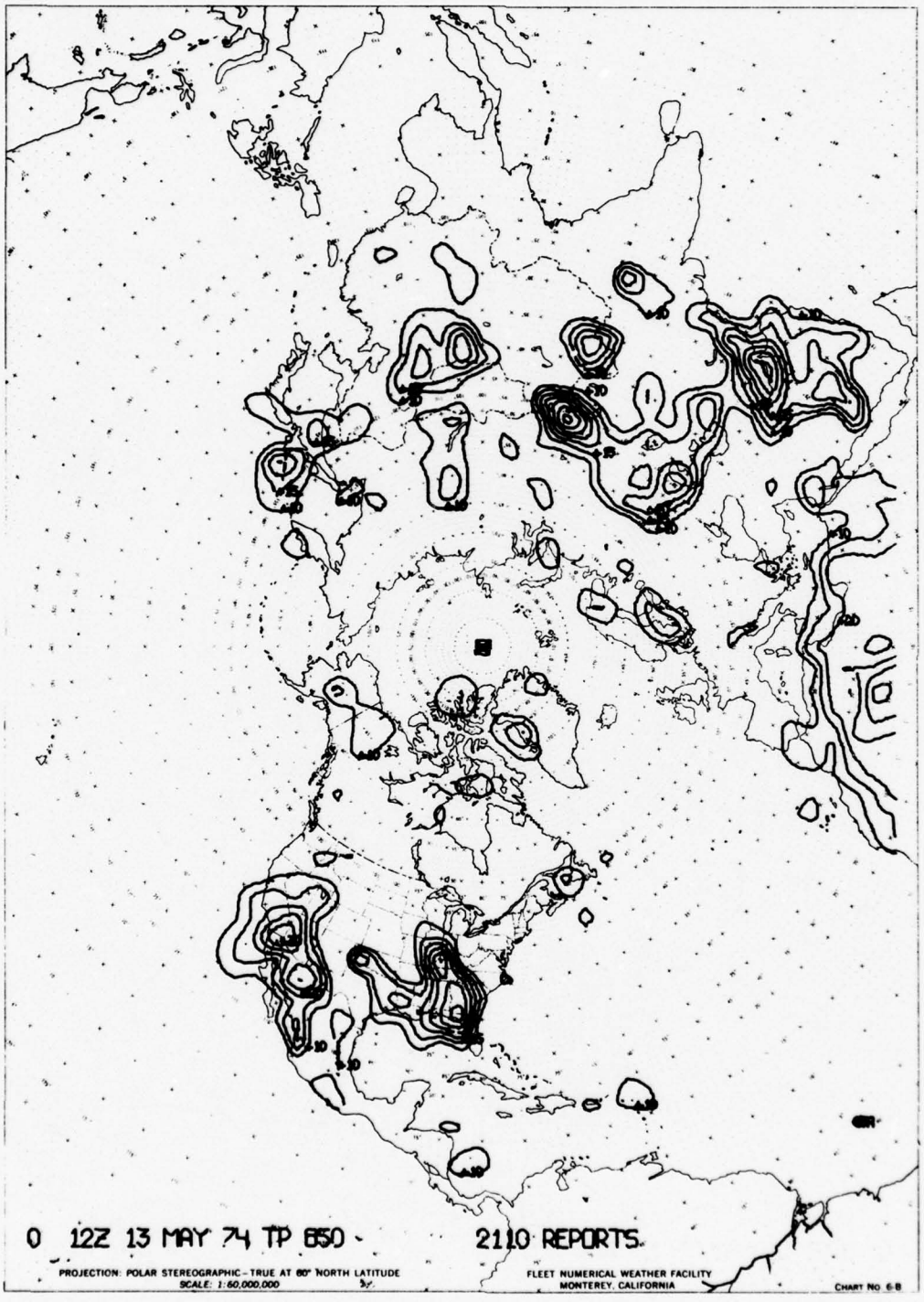


FIGURE 4.5.3 850-mb Dew-Point Depression Analysis (D50)

4.6 UPPER-AIR ANALYSIS, 1000 TO 100 MB

A. Background

The three-dimensional structure of the atmosphere up to 100-mb is modeled such that it can be defined in terms of the 1000-mb height, the 500-1000-mb (or the 300-1000-mb) thickness and the static stability (essentially a measure of virtual temperature lapse rate) in 8 selected layers (1000-775, 775-600, 600-450, 450-350, 350-275, 275-225, 225-175, and 175-100 mb). The model provides pressure-height values and temperatures consistent with all reasonable reported data for any level from 1000 to 100-mb, accurate to within the limits of known instrumental errors. The modeled atmosphere is everywhere statically stable and is therefore suitable for integrations required in the numerical forecast process.

B. Program Input

1. Reported radiosonde and aircraft observations to 100 mb.
2. Surface pressure analysis.
3. Twelve-hour 500-mb prognosis from the previous update analysis.
4. 1000-300 mb thicknesses derived from satellite data (SIRS, overwater only).
5. 300 mb tropical wind fields from the Global Band analysis.
6. Twelve-hour surface prognosis from previous analysis.

C. Program Computations

1. Data Preparation

The preparation of the data for analysis is accomplished by a separate program called the Upper Air Pre-analysis.

(a) Each sounding is checked for vertical consistency of pressure and temperature at the mandatory levels. Where possible, missing or incorrect values in reported data are computed hydrostatically from correctly reported significant-level and mandatory-level elements. Reported winds which imply unreasonable vertical shear are discarded.

(b) Often several differing reports are received from the same station. All such reports are examined for consistency and combined where necessary to produce a single most complete and consistent sounding for that station.

(c) Reported 1000-mb heights are compared with a 1000-mb height field obtained by a hydrostatic conversion of the surface pressure analysis. Differences in excess of prescribed tolerances are interpreted to indicate that the data cannot reasonably be located at the reported position and the entire sounding is rejected.

(d) Reported 500-mb heights are compared with the twelve-hour 500-mb prognosis verifying at map time. Again, the complete sounding is rejected if the difference is in excess of a computed tolerance. The tolerance is based on the 500-mb standard deviation for the month, and geographical location and a confidence factor based on the report type.

2. Analysis of the Structure Model Variables

(a) Stability analyses

For each sounding satisfying the pre-analysis error checks, static stabilities in the 8 selected layers are computed from reported mandatory level pressure-heights. The objective analysis (Section 3.9) routine is then used to perform a horizontal analysis of stability for each layer. The first guess for each stability analysis is derived by correlations with latitude and the 1000-500-mb thickness. The analysis is performed with the constraint that hydrostatic instability is not allowed at any grid point.

(b) Pressure-height analyses; 1000, 500 and 300 mb

Analyses of height at each pressure level subsequently described is performed in the following manner: (1) the first guess is adjusted to reported heights using the objective analysis routine (two passes); then (2), adjusted to fit the gradient as specified by reported winds; then (3), two more passes using heights; then finally (4), two more passes using winds. Varying weights are assigned to different report types; for example, winds from radiosonde reports have a stronger influence on the analysis than do winds from aircraft reports. Lateral checking is performed during each height and wind pass, wherein reports not agreeing with neighboring reports are discarded. Lateral tolerances are modified for each scan, with the tightest tolerance applied during the last scan. A light smoother is applied after each scan except the last.

(1) 1000-mb height analysis. The first guess is the current surface analysis hydrostatically converted to 1000 mb.

(2) Preliminary 500-mb height analysis. The first guess is a 500-mb height field constructed by adding the 12-hour forecast 1000-500-mb thickness for the previous analysis to the 1000-mb analysis performed in (1) above.

(3) 300-mb height analysis. The first guess is obtained by entering a system of matrix equations (Appendix K) with the analyzed 1000- and 500-mb heights and the analyzed stabilities. Data at 300 mb is augmented by wind reports in the vicinity of 300 mb (up to as high as 250 mb, so long as the tropopause is not below 250 mb).

1000-300-mb thicknesses derived from satellite data (SIRS) are used in the following manner: (1) 300-mb heights are computed by adding the 1000-300-mb thicknesses to the already-analyzed 1000-mb field; (2) the resulting 300-mb heights are used, with lesser weights than conventional data, in analyzing the 300-mb height field except in the last analysis pass. This has the effect of analyzing to the satellite data where there are no conventional data, and honors conventional data where there is a conflict. Conflicts may arise due to the asynoptic nature of the satellite data (data from $\pm$6 hours of synoptic time are used) and the still experimental nature of the satellite data retrievals.

The tropical area, including the grid boundary, is controlled by forcing the heights to conform to the 300-mb tropical wind fields from the Global Band analysis.

The 300-mb height analysis and the 1000-mb height analysis now become the "control" levels in the model. The rationale for first analyzing the 500-mb level is that this is the level at which the prognosis, and therefore the first guess, is superior, thereby improving the first guess for 300 mb. Then, by shifting the control level to 300 mb, one takes advantage of the fact that a preponderance of the better aircraft reports are at the higher tropospheric levels, and ultimately provides a mechanism for "feedback" of this information to the lower tropospheric levels.

3. Temperature Analyses

All mandatory levels, plus 925 mb, are analyzed to reported temperatures using the objective analysis technique. The first guess for each level is obtained by entering a system of matrix equations with the analyzed 1000-mb and 300-mb heights and the analyzed stabilities. This provides a first guess which is essentially the virtual temperature at each level.

4. Height Analyses, 925 to 100 mb

The analyzed 1000- and 300-mb heights, plus the analyzed stabilities for the eight layers, define hydrostatically consistent heights at any level to 100 mb. A system of matrix equations is entered with these analyzed fields which produce values of height at all mandatory levels (plus the 925-mb level) at each grid point. In order to introduce additional detail into the final analyses, the

levels 250, 200, 150, 100 and 925 are re-analyzed to reported heights and winds (heights only for 925 mb) in the manner described in 2.b. above. Reported heights at mandatory levels are used, and reported winds are applied at the nearest mandatory level.

5. Insuring Final Hydrostatic Consistency

The re-analysis of heights at mandatory levels described in 4. above may introduce areas of vertical hydrostatic inconsistency. The matrix equations are entered with the analyzed heights to produce new stabilities for the eight layers at each grid point (the process of computing stabilities from mandatory heights is reversible). The resultant stabilities are examined for hydrostatic consistency and adjusted where necessary. The adjusted stabilities and the 1000-300-mb thickness then are used to produce the final height analyses, thus assuring hydrostatic consistency everywhere.

D. Program Output

1. Pressure-height analyses for the 1000- (Catalog No. C00), 925- (J50), 850- (D00, Figure Figure 4.6.1), 700- (E00), 500- (F00, Figure 4.6.2), 400- (G00), 300- (H00, Figure 4.6.3), 250- (I50), 200- (I00), 150- (J00) and 100-mb (K00) levels.

2. Temperature analyses for the 925- (Catalog No. J60), 850- (D10), 700- (E10, Figure 4.6.4), 500- (F10, 400- (G10), 300- (H10), 250- (I60), 200- (I10), 150- (J10) and 100-mb (K10) levels.

3. Static stability analyses for layers from 1000-775 mb (Catalog No. X01), 775-600 mb (X02), 600-450 mb (X03), 450-350 mb (X04), 350-275 mb (X05), 275-225 mb (X06), 225-175 mb (X07) and 175-100 mb (X08).

4. Radiosonde coverage (Catalog No. X00).

E. The "Update"Analysis

Collection of raw data continues after the operational analysis has been completed and distributed. Prior to the next 12-hour analysis cycle, the entire analysis package is run again, using all data collected up to that time. The purpose of this is to prepare an analysis with the most data available for archival purposes, and also to produce a 12-hour prognosis from this better data base to improve the given fields for the next 12-hour analysis cycle.

F. Southern Hemisphere Upper-Air Analysis

An objective upper-air analysis program for the Southern Hemisphere became operational in late 1974. The Southern Hemisphere model, because of meager conventional radiosonde data, must rely heavily upon SIRS reports over large areas. This dependence necessitated two major changes in the Northern Hemisphere model. First, satellite data are used in analyzing the static stability parameter; this is not the case in the Northern Hemisphere model. Second, SIRS data are used in the 500-mb analysis to create the first guess for this level. The method used is exactly the same as that used for deriving the 1000- to 300-mb thickness from satellite data, described in 2.b. above.

A program has been designed to merge the Northern and Southern Hemisphere output across the equator.

G. References

[1] Holl, M. M., J. P. Bibbo and J. R. Clark, 1962; "Linear Transforms for State Parameter Structure", Technical Memorandum No. 1, Meteorology International, Monterey, California.

[2] Holl, M. M. and J. P. Bibbo, 1963; "The Use of Winds in the Analysis of State Parameter Distribution", Technical Memorandum No. 2, Meteorology International, Monterey, California.

[3] Holl, M. M., 1967; "The Assimilation of Wind Observations in the Analysis of the Atmospheric Mass Structures", Project M-129, Meteorology International, Monterey, California.

[4] Holl, M. M., C. Riegel and J. R. Clark, 1964; "The Analysis Cycle for the Mass Structure of the Atmosphere, The Assembly of Component Techniques", Project M-117, Meteorology International, Monterey, California.

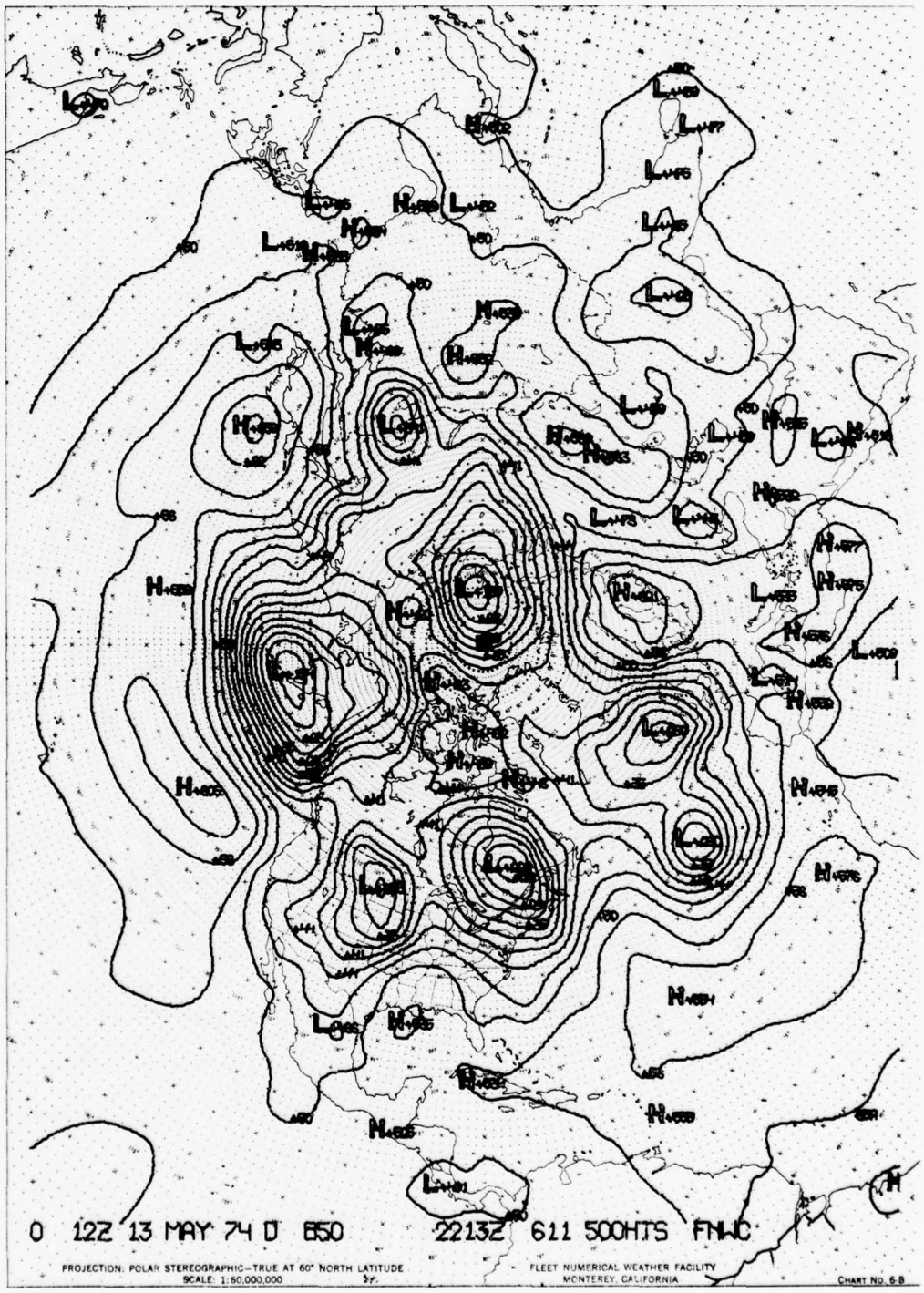


FIGURE 4.6.1 850-mb Height Analysis (D00)

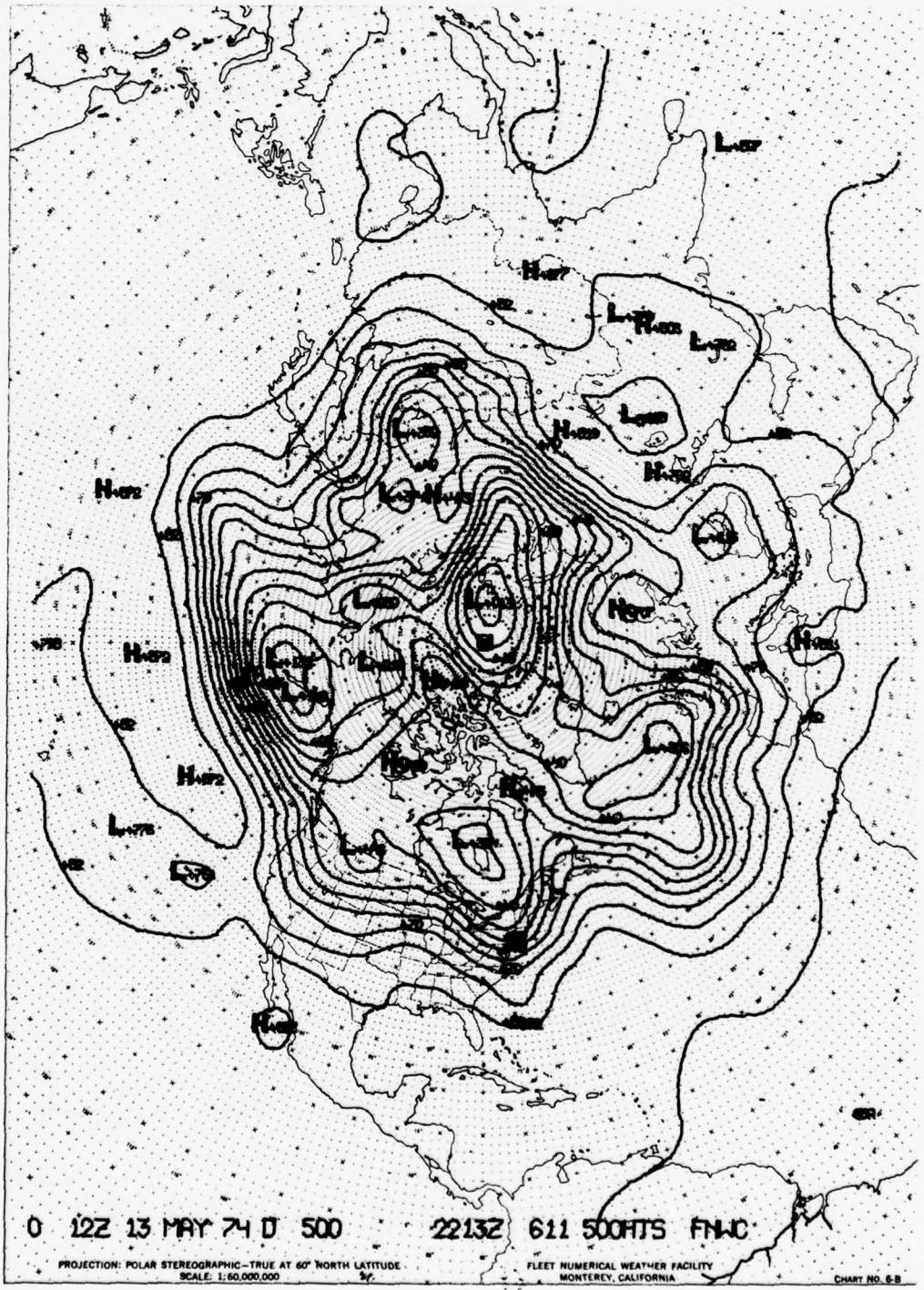


FIGURE 4.6.2 500-mb Height Analysis (F00)

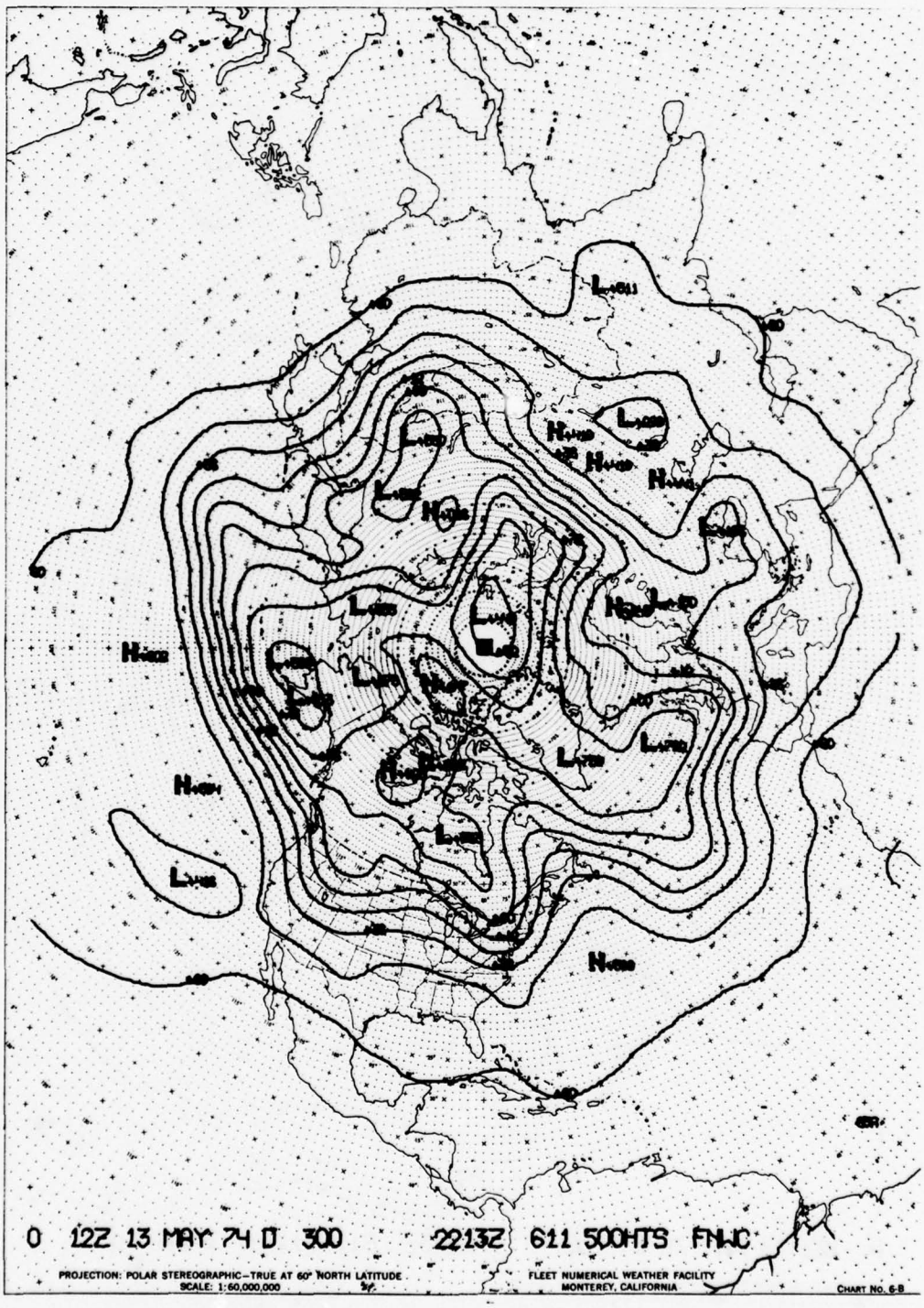


FIGURE 4.6.3 300-mb Height Analysis (H00)

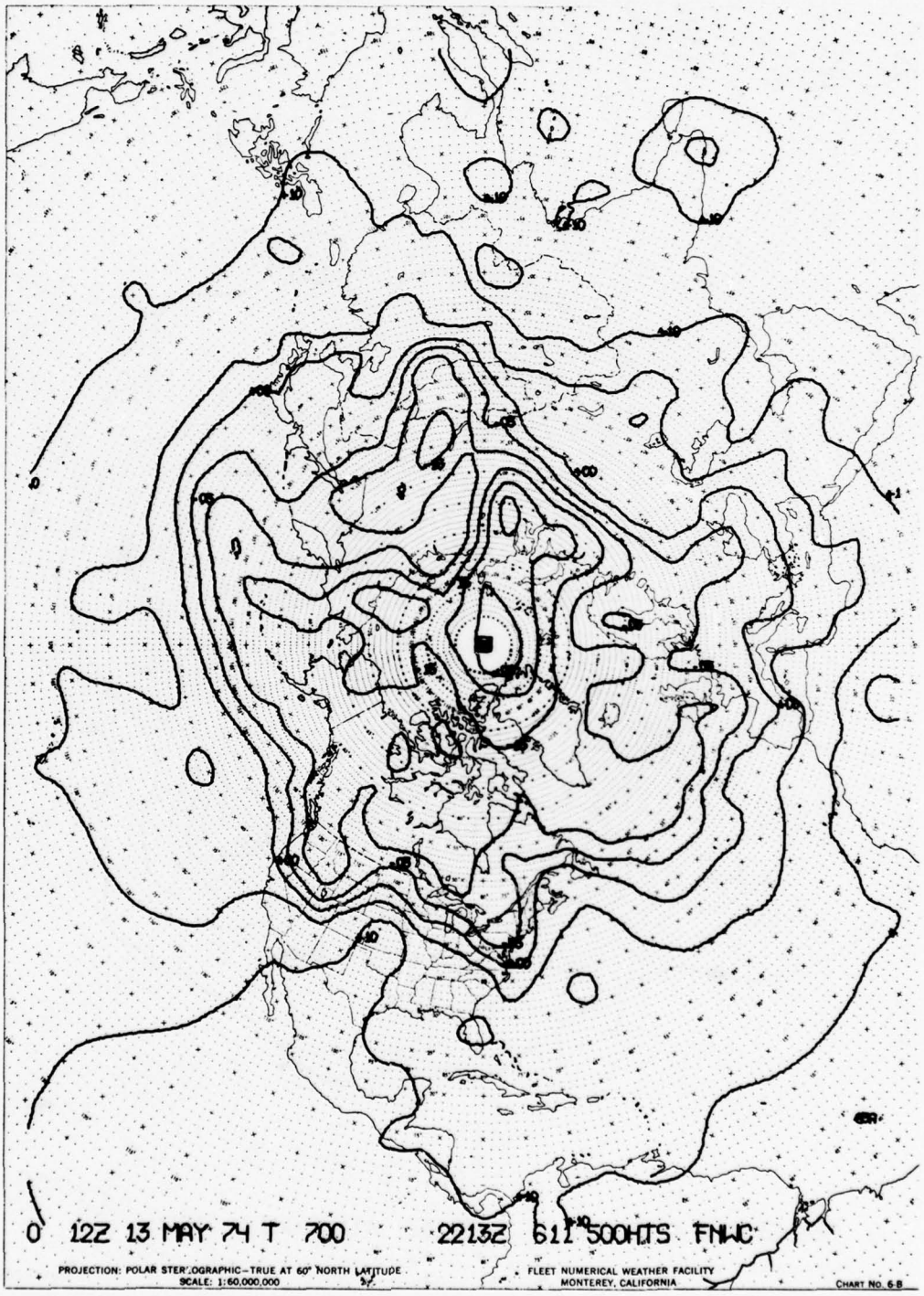


FIGURE 4.6.4 700-mb Temperature Analysis (E10)

FDEC 01
700 HT ANAL 12Z 13 AUG 72 METERS

N	160E	165E	170E	175E
70	2990	2991	2995	2998
65	2960	2955	2968	2984
60	3016	3006	3003	2999
55	3037	3020	3008	2999
50	3021	3013	3005	2998
45	3071	3071	3064	3065
40	3126	3133	3128	3134
35	3166	3174	3165	3158
30	3167	3169	3179	3183
25	3155	3167	3172	3175
20	3145	3144	3153	3154
15	3144	3140	3143	3147
10	3142	3146	3144	3143

FORMAT: HHHHH_ _ _ _ _Pressure-Height in meters

EXAMPLE: 50N 165E__3013 meters

FIGURE 4.6.5 700-MB HEIGHT ANALYSIS GEM

4.7 STRATOSPHERE ANALYSIS

A. Program Development

The possibility of successful synoptic analysis in the stratosphere is severely limited by lack of data. Most radiosonde ascents terminate below the stratospheric analysis levels. Rocketsonde reports are widely scattered and occur irregularly. Some reports are lost because of a predetermined cutoff time for acceptance of reports from communication circuits feeding the computer. The 100-mb level is the highest level where there are enough data to provide a consistently respectable synoptic analysis.

The erratic data situation led FNWC into adopting an analysis program of using the 100-mb level as an anchor and building to higher levels by means of statistical regression equations. The latter were developed by the U. S. Navy and the National Weather Records Center (Ref. 1) with this purpose in mind. The coefficients were computed from historical data, and were stratified by month and by seven latitude bands. The equations have produced excellent results most of the time but, since they necessarily have much built-in smoothing, extreme situations in the stratosphere will not be properly reflected. For example, at 30 mb and 10 mb, there might be a large cold anticyclone and a warm cyclone, diametrically opposite, dominating the Northern Hemisphere. In such cases, the regression equations, with their latitudinal stratification, will fail to specify the true height and temperature patterns over large areas typical of the extremes of the range.

B. Program Input

1. 100-mb height analysis.
2. 100-mb temperature analysis.

C. Program Computation

1. Compute heights and temperatures for 50-mb, 30-mb, and 10-mb levels using regression equations and the 100-mb height and temperature analyses.

D. Program Limitations

The key limitation is that no observed data are used in the analysis except for those which went into the anchor 100-mb analysis. Changes in the pressure/temperature patterns may occur and not be reflected at 100-mb. One case, for example, is when stratospheric warming builds downward from the highest levels. Until it reached the 100-mb level, no one would be the wiser. Spotting a few current observations on the stratospheric analyses would be one way of being warned that changes were underway.

E. Uses of the Products

Stratospheric analyses are not used directly as a forecasting tool. The interactions between stratosphere and troposphere have not yet been firmly enough established for forecasting rules to evolve. The main use of the analyses is in ballistic computations for missiles such as POLARIS and POSEIDON.

The stratospheric charts can be used in a standard way in flight briefings for those few aircraft that fly in the stratosphere. This use will increase with time, as more supersonic aircraft go into operation.

F. Relationship to Other Products

The 50-mb temperature analysis is used as input to the P.E. model.

G. Program Output

1. Pressure-Height analyses for the 50- (Catalog No. L00, Figure 4.7.1), 30- (Catalog No. M00) and 10-mb (Catalog No. N00, Figure 4.7.2).

2. Temperature analyses for the 50- (Catalog No. L10, Figure 4.7.3), 30- (Catalog No. M10), and 10-mb (Catalog No. N10) levels.

H. References or Suggested Reading

[1] Lea, Duane, A., 1961; "Regression Equations for Vertical Extrapolation of Constant-Pressure-Surface Heights and Temperature between 200-mb and 300-mb", 191st Meeting of the AMS, Chicago, Illinois, March 1961.

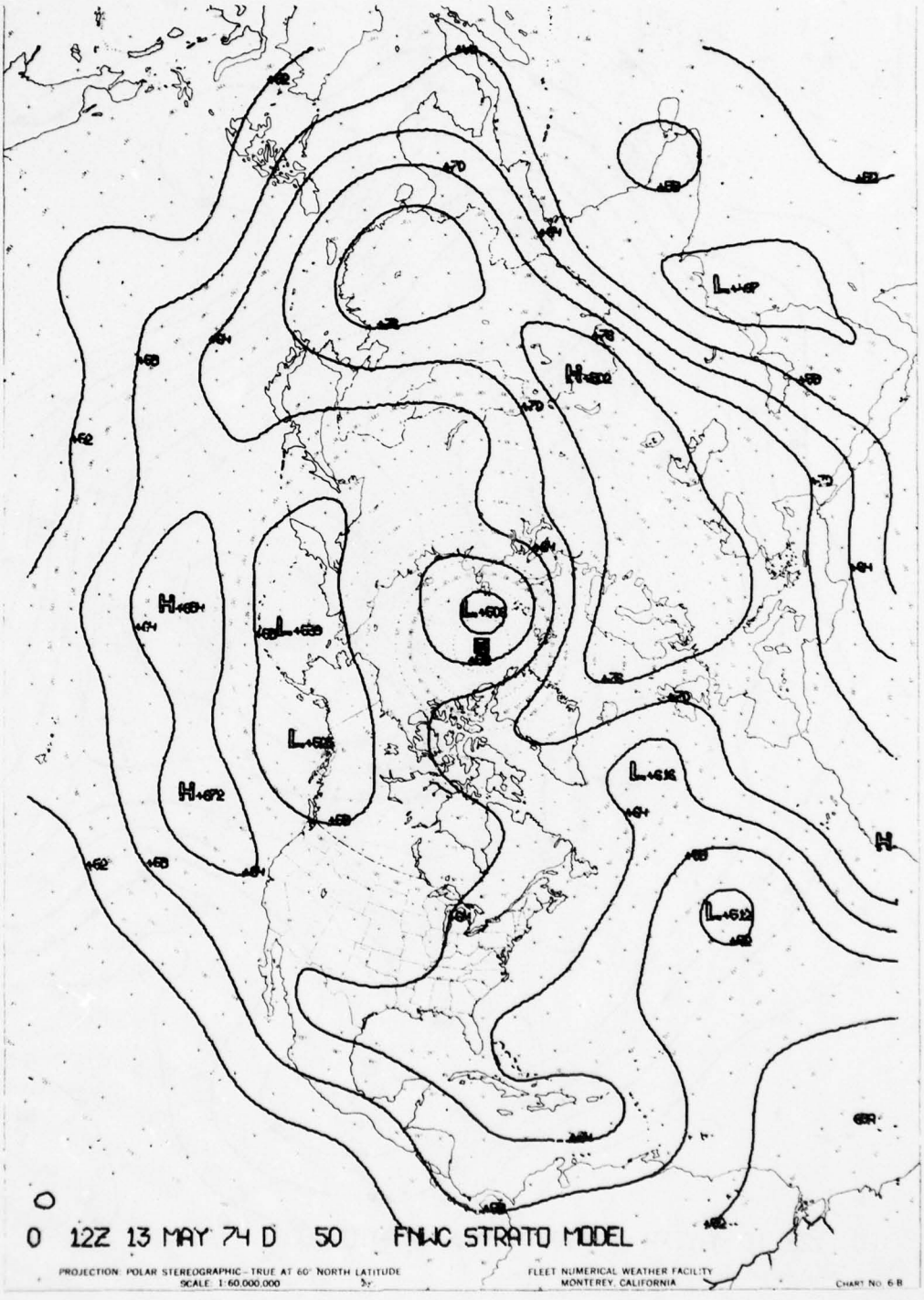


FIGURE 4.7.1 50-mb Analysis (L00)

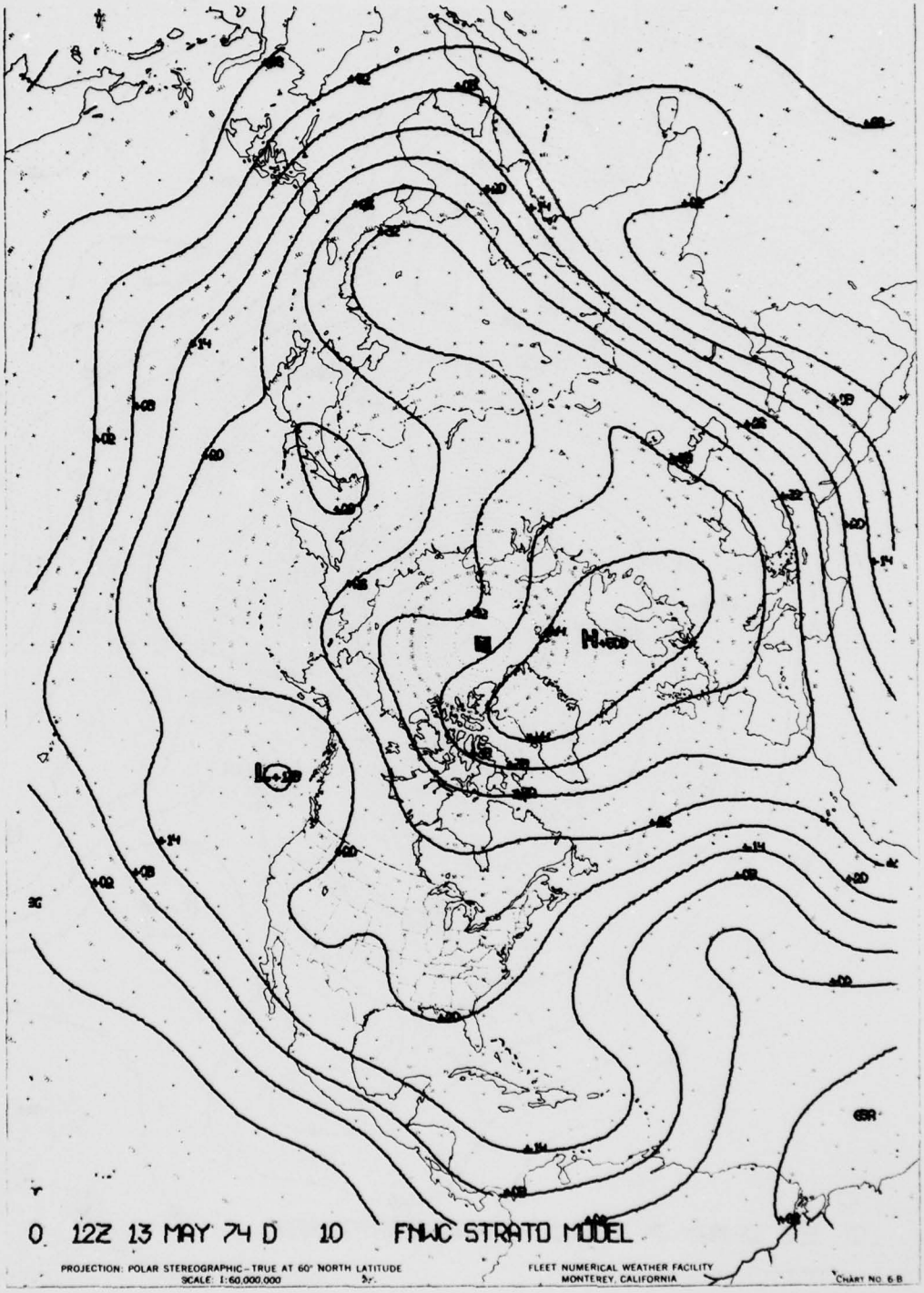


FIGURE 4.7.2 10-mb Analysis (N00)

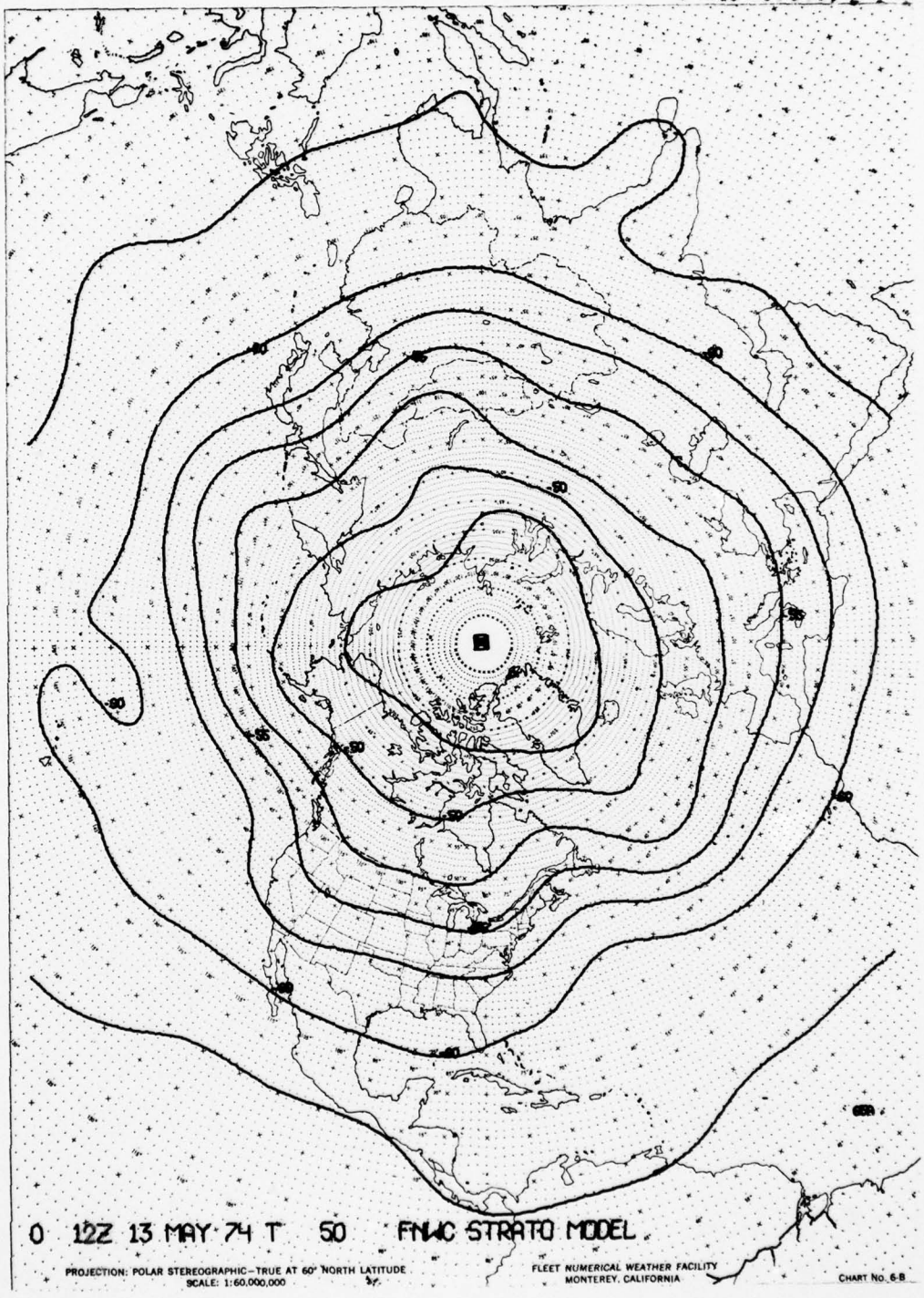


FIGURE 4.7.3 50-mb Temperature Analysis (L10)

4.8 PRIMITIVE EQUATION MODEL

A. Model Development

Numerical or dynamic forecasting is based on the assumption that certain physical laws govern the behavior of the atmosphere and that these laws can be expressed mathematically. Solving the set of governing equations in relation to some initial state, then, will provide the desired forecasts as to the future state of the atmosphere. A Primitive Equation Model (P.E.), while based on this seemingly simple concept, is incredibly complex in operation. It represents the scientists' most advanced effort--a great leap, actually--in the slow forward progress man has made in meteorological forecasting.

Although P.E. models are new, the equations and concepts of how to use them have a history older than the science of meteorology. The equations date back to such old-timers as Newton, Boyle-Charles, Euler, and von Helmholtz. Unfortunately, the basic equations in their general form can't be solved explicitly. It was not until after 1910 that Richardson (a British mathematician/meteorologist) realized that the equations could be solved by brute force, using a purely numerical finite-difference method. Over a period of several months, he computed one set of forecasts (which turned out to be way off), and estimated that the computation process would require 64,000 human computers just to predict weather as fast as it happened, let alone gaining any ground. This chilling statistic and the poor forecast results smothered interest in this style of dynamical forecasting, and there was little further development until the 1940's.

During World War II there was a great expansion of the meteorological observational network, both surface and upper air. For the first time, theoreticians had enough data to make descriptive studies and compare any theories they developed with actual events. These studies showed that some elements of the equations governing fluid behavior were not necessary in describing the atmosphere, so that the equations could be specialized or simplified, and Richardson's 64,000 human computers could be cut to a number somewhat more reasonable--even if still impractical. Help appeared about this time in the shape of newly-developed, high-speed electronic computers, 10,000 times as fast as a man on a desk calculator or abacus. The theoretical meteorologists promptly started a research effort to see if the modified primitive equations could be married to the powerful, new computers, with hope that the union would produce offspring of forecasts far superior to any hand-produced products. The research project was started at the Institute for Advanced Study at Princeton, and spread to other academic institutions later. The Navy got into the program actively at the Joint Numerical Weather Prediction Unit in Washington, and continued the work at Monterey after 1959.

Computers at that time were not powerful enough to handle a full baroclinic P.E. model. Instead, a barotropic model was developed, in which just one level of information (near 500 mb) is used to describe the entire depth of the atmosphere. The model works very well for height description, but is weak at forecasting cyclogenesis or large pressure changes. The barotropic model was used operationally until the P.E. model took over in 1970.

The FNWC P.E. model development was started in late 1968 by LCDR Philip G. Kesel as an M.S. thesis project, under the sponsorship of Professors G. J. Haltiner and R. T. Williams of the USNPGS, and has been continued as an FNWC project from 1969 to the present. Dr. F. J. Winninghoff worked with Kesel for over a year during the development stage, and contributed a good part of the heat package.

Before exploring the intricacies of the P.E. model, a thumbnail sketch of a generalized model will be presented, just as a place on which to hang later thoughts.

What is the goal of the P.E. modeller? What is he trying to do? What tools from physics and mathematics can he use to solve his problem?

The model deals with a huge body of air, such as would be the case if the atmosphere of the Northern Hemisphere were encased in a gigantic glass frame. Air cannot escape into the earth, out of the top of the atmosphere, nor (in the Northern Hemisphere model) into the Southern Hemisphere.

Radiation, in or out, is permitted. Otherwise, everything takes place inside the imaginary glass box. The modeller deals with some arbitrary point within the atmosphere. First, he inquires as to the state of this bit of atmosphere. The questions asked are: How hot are you? How fast are you moving toward the East, the North, and up or down? What is your pressure? What is your weight or density? How is your moisture situation? The answers to all these questions are recorded for that point and for that time.

The modeller, with a complete description in hand, now wants to figure out what his parcel of air will be like at some time in the future. He turns to the body of knowledge embodied in the general equations of hydrodynamics, equations developed over the years and verified (as to quality and ability to represent atmospheric phenomena) by experimentation and by application in many fields. These are the Newtonian equations of motion, which state that the acceleration in any direction is proportional to the resultant of all forces (pressure, coriolis, friction, etc.) acting in that direction; the continuity equation, that says any change of density calls for a balanced import or export of mass at the point; the thermodynamic equation, based on the law that any heat energy added to a system must be equal to the change in its internal energy plus whatever work is done in expanding against pressure forces; the Boyle-Charles equation of state, that relates temperature, pressure, and volume of a system in thermodynamic equilibrium. This gives a solvable combination of six independent equations and six unknowns (density, pressure, temperature, and the three velocity components). If moisture in some form is desired as a seventh unknown, a seventh equation will have to be added.

The next step in the modelling is that of finding a solution to the equations, using the initial state description as input. The equations are formulated to calculate the rate of change of a property and from this to determine the predicted amount of change over a prescribed time period. For example, over the standard ten-minute calculation period, the temperature equation would determine the rate of temperature change--say it's 0.6°C per hour. For the ten-minute integration time step, this would be +0.1°C. This value is applied as a correction at the grid point. New values for other parameters are determined in similar fashion. All the new values for all parameters are collected at the starting grid point. The calculation process is performed at every grid point at all levels around the whole hemisphere. The process then starts all over again, using the predicted values at each grid point for the next integration time step. The process is repeated for enough times to cover any desired forecast period.

There are three main steps in any P.E. model--initialization, integration of equations, and outputting the products. Each step will now be discussed in relation to the FNWC P.E. model. Features and techniques unique to the FNWC model will be pointed out. It is the embellishments on a basic model--the special and new ways of treating things--that make or break the final prediction model in competition, and give it personality.

Initialization

Initialization in the P.E. model amounts to setting the stage for the forecasting computations. It means providing the computer with the best possible estimate, at grid points, of the current state of the atmosphere. The importance of proper initialization is obvious from the standpoint that false information fed to the computer means you are asking for a forecast based on something that doesn't really exist. This demands powers bordering on the supernatural. The P.E. model is particularly vulnerable to initialization errors because of the sensitivity of the equations used. Trying to achieve dynamic balance between areas of good and bad information can cause such distress in the model that it could even give up and refuse to run.

The computational grid used in a model is dictated by computer power, availability of data, and scale of the atmospheric motions involved. The P.E. model uses a 63x63 grid-point array, with variables carried at 5 levels. This gives approximately 20,000 calculation points for each of the 6 variables. The levels where initialization values are carried and where the integrations are performed are sigma (σ) surfaces, that have pressure normalized (sigma takes on values from 0 to 1) with underlying terrain pressure. The sigma surfaces go from 1.0 (terrain pressure) to 0.9, 0.8 and on up to a sigma of 0.0. A sigma of 0.9 in this system, means that the pressure at that level is 90% of the terrain pressure, 0.8 = 80%, etc.

The reason for using sigma surfaces, rather than something more conventional like constant pressure or height is because of the mathematics involved in the boundary layer. The constantly-varying terrain over land causes changes in vertical motion which can only be approximated, and this with mathematical difficulty. The 1.0 sigma surface flows smoothly along the terrain; the upper sigma surfaces adjust to every change of the 1.0 surface just as the top of a snake crawling over rough ground

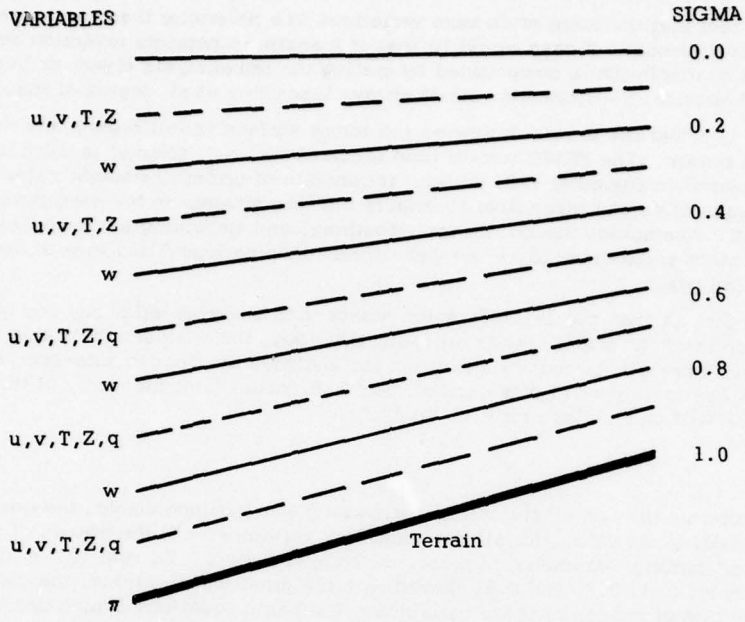


DIAGRAM OF LEVELS AND VARIABLES. The terrain pressure (pi) is carried at sigma = 1.0. The vertical velocity (w) vanishes at the top and bottom of the column. Horizontally, we use a 63x63 array in which the equator is an inscribed circle.

adjusts to changes at belly level. Use of sigma surfaces simplifies the mathematics and improves final accuracy of the P.E. products.

The P.E. model initialization uses values for horizontal wind components (u,v), temperature (T), vertical velocity (w), height (Z), and moisture (q). The values are obtained from regular FNWC operational analyses--virtual temperature at 12 constant-pressure levels from 1000 mbs to 50 mbs, height analyses at seven of these levels, moisture analyses at four levels from surface to 500 mbs. Additionally, sea-level pressure analysis, sea-surface temperature analysis, a terrain field and a seasonal mean albedo field are used.

Getting initialization values is not simply a problem of picking off values from the analyses. The values must be derived in one way or another (viz., wind), and/or interpolated vertically in nearly every case, and errors may be introduced by the process.

Horizontal wind components are obtained by applying a modified non-linear balance equation to pressure surfaces. This gives good results, generally speaking, but long experience has shown that there are really no perfect wind laws--laws which will transform heights into winds that match perfectly with winds as they exist. Errors in the wind initialization values can have a serious effect on the P.E. prognoses, since the wind terms in the primitive equations are used to advect other parameters.

Temperature values must be converted from virtual to dry, and interpolated from twelve pressure surfaces to five sigma surfaces. The interpolation process is a potential source of error.

Moisture analyses are notoriously noisy. Their accuracy is always open to question. Some parameters that go into the heating package (evaporation, radiation, etc.) are based on rather gross estimates. Cloud cover, which is based on an estimate of relative humidity, is a good example.

Other pitfalls in the initialization arise from:

1. The fact that there are often more variations in a parameter than can be resolved in a ten-layer analysis model. A case would be that of a sharp temperature inversion between levels. This lack of resolution is compounded by cutting the ten analysis layers to five model layers. The mathematical transformation itself always leads to a small degree of inaccuracy.
2. The fact that the terrain-following 1.0 sigma surface is following a modelled rather than the real terrain. The FNWC terrain field (devised by L. C. Clarke) is much more refined than that used in any other P.E. model. It consists of grid-point height values derived from an average of values taken from 10-minute lat/long squares in the area surrounding the grid point. Averaging, though, means smoothing, and smoothing a terrain field means that mountain spikes tend to be leveled off and deep valleys filled in with the granite that comes off the peaks.
3. The fact is that the initialization starts with analyses which may not contain all the truth. Since the P.E. model results are generally good, the analyses must also be good in general. Still, there will be those times when the analyses are poor in data-sparse areas. Initialization has to be poor in these areas. The P.E. model is at the mercy of the initialization, and these will be bad days for P.E. products.

Integration

After suffering through all the initialization problems outlined above, the grid points on sigma surfaces are finally given values for all the necessary variables, and the wheels of the integration process can start turning. At each grid point, we know u, v, T, Z, and w. q is known only at three lower sigma levels, 0.5, 0.7, and 0.9. Armed with the primitive equations, the computer will attempt to calculate the rate of change of these variables. The basic equations (which can be seen in basic and in finite difference forms in Appendix L) and what they attempt to forecast are:

East-West Momentum Equation

This will calculate the rate of change with time, the acceleration, of the East-West component of the wind.

North-South Momentum Equation

This will calculate the rate of change with time, the acceleration, of the North-South component of the wind.

Thermodynamic Energy Equation

This equation determines the rate of change of temperature from all possible causes, such as evaporation, advection, vertical motion, condensation, etc.

Moisture Conservation Equation

This equation calculates moisture changes. It is based on the principle that the total moisture content must be conserved.

Continuity Equation

This equation is used to determine change in terrain pressure and to calculate the vertical velocity component.

Hydrostatic Equation

After all the above equations have been solved, the hydrostatic equation uses the answers to compute the new geopotential heights.

The primitive equations above will provide a satisfactory forecast, but two important effects have been ignored in formulation of the equations. These are friction and heating. The FNWC P.E. model incorporates both effects in a relatively sophisticated way.

A friction term is included in both momentum equations. Friction effect is concentrated in the layer of air next to the ground and represents the horizontal stress exerted on a layer of air by the layer of air immediately under it. Friction changes momentum. The friction term is used only in the lowest sigma layer.

The heating package in the P.E. model is quite complicated and, from test results, seems to be very efficient. The heating package attempts to account for the following:

1. Amount of incoming solar radiation. The amount of radiation coming into the top of the model atmosphere is a function of the time of day, latitude, and season. What happens to this radiation is dependent on the vertical distribution of moisture above each grid point. The total amount of precipitable water, the amount of cloudiness, and the surface albedo must be calculated and used to determine how heat from the sun is distributed through the troposphere.

2. Terrestrial radiation (infrared). This calculation determines what happens to the long-wave radiation emitted from the earth's surface and from clouds. The amount of water vapor in the atmosphere is used in the calculation.

3. Sensible heat and evaporation. Sensible heating is determined as a function of air temperature-surface temperature difference. Cool air is heated by a warmer surface. Evaporation over the oceans is computed as a function of the saturation moisture at the surface and the moisture near the surface. Over land the computation is in terms of sensible heat.

4. Condensation and moist convective adjustment. If advection processes cause supersaturation at any computational level, the excess moisture is precipitated. In the lowest layer, it comes out as rain. The temperature in this layer will rise. At higher levels the process is to check the possibility of evaporating precipitated water into the next lower layer and letting rain fall into the layer below this or to the ground only if that next lower level either was or became saturated.

   The Moist Convective Adjustment attempts to incorporate the effects of convection upon precipitation and heat distribution. In effect, the adjustment would correspond to working up a sounding at each grid point, and assessing the possibility of convection based upon stability conditions. Three types of convection are considered: high cumulus (sigma = 0.5 and 0.7), deep penetrating convection (sigma 0.9, 0.7, 0.5), and low cumulus (sigma 0.9, 0.7). Precipitation can occur from the first two types and is included in the precipitation forecast. Equations are used to effect a redistribution of heat and moisture in the lower three layers.

5. Dry convective adjustment. A dry convective adjustment is made as a last step in the heating package computations. This involves a check of the vertical lapse rate of potential temperature. If the lapse rate becomes superadiabatic in any layer, it is adjusted so that the mean potential temperature in the vertical is conserved. This may lead to some redistribution of heat in the vertical, usually at lower levels during daylight hours over land areas. The dry convective adjustment precludes hydrostatic instability.

The integration process proceeds in ten-minute steps. This short time step is necessary to avoid computational instability. Length of the time step is calculated by a formula that relates grid size to the speed of the fastest wave. The time step has to be less than the time required for the wave to traverse the grid distance. If computational instability is allowed, or happens, small random errors will be amplified indefinitely and the solutions to the equations will get further and further from the truth. A typical time step is described in Section C. These time steps are repeated enough times to cover any desired forecast period.

The output section of the program is activated every six hours. Accumulated values from the 6-hour integration period are extracted at sigma surface grid points and converted by standard interpolation techniques to values at constant pressure surface grid points. There are 58 output fields.

B. Program Input

1. Current Virtual Temperature analyses for Northern Hemisphere at 1000-, 925-, 850-, 700-, 500-, 400-, 300-, 250-, 200-, 150-, 100-, and 50-mb levels.
2. Current Pressure Height analyses for Northern Hemisphere for 925-, 700-, 500-, 300-, 250-, 150-, and 100-mb levels.
3. Current Moisture analyses for Northern Hemisphere for 1000-, 850-, 700-, and 500-mb levels.
4. Current Sea-Level Pressure analysis.
5. Current Sea-Surface Temperature analysis.
6. Seasonal Mean Albedo fields.
7. Terrain field.

C. Program Computation

The P.E. model computations are designed around the four CDC 6500 processors so that each processor does all the computations for one quarter of the Northern Hemisphere. The quarter-part results are merged during the output process to give full hemispheric depiction. The order of computation follows:

1. Read in input fields of virtual temperature at 12 constant pressure levels, height analyses at 7 levels, moisture analyses at 4 levels, terrain, sea-level pressure, sea-surface temperature, and monthly mean surface temperature.
2. Solve the non-linear balance equation on pressure surfaces from 925 mb to 100 mb to obtain the initial wind components. Place values at grid points on sigma surfaces.
3. Place initial values of temperature, moisture, and height at sigma surface grid points.
4. Integrate the continuity equation to obtain the local change in terrain pressure, and the vertical velocity fields at the four layer interfaces.
5. Integrate the momentum equation at five levels to obtain the new E-W wind components.
6. Integrate the momentum equation at five levels to obtain the new N-S wind component.
7. Integrate the thermodynamic energy equation at five levels to obtain new temperatures.
8. Integrate the moisture continuity equation to obtain three new levels of moisture.
9. Make the moist convective adjustment.
10. Make the dry convective adjustment.
11. Integrate the hydrostatic equation to obtain new geopotential fields.
12. Repeat steps four through eleven 35 times using newly calculated parameter values at beginning of each time step. This accounts for a six-hour forecast.
13. Output the 54 fields (mostly on sigma surfaces) required to restart the model.
14. Postprocess the output fields (transformation of coordinates, filter, fill in values under terrain) and output data fields. (See Section G.)

D. Program Limitations and Verifications

Building a space ship that will give near-perfect performance is probably easier from the technical standpoint than building a P.E. model that will give near-perfect forecasts. The difference lies mostly in input limitations. In the space ship, all hardware is designed to engineering specifications. Every bolt used has a known tensile strength, and is used in a carefully calculated stress condition that will never exceed the bolt's resistance. All hardware strength and performance characteristics are accurately known from precise mathematical manipulations. The P.E. model, by contrast, has unavoidable limitations that keep it from perfection. The nuts and bolts that go into the P.E. machine are not of even quality, and there is no way to tell with any assurance which part is

causing trouble with the product. In the P.E., it may be something like putting in too much cloud cover; it may be feeding in false parameter values over a no-data area. Any one of dozens of things can contribute to a touch of shabbiness in parts of the P.E. products. The man in the field has no way of determining the cause; all he can do is be alerted in cases where the P.E. heads toward something completely non-meteorological.

The list below includes the most important limitations on the P.E. model. Some of these can be made less stringent, and the FNWC P.E. modellers are doing everything possible, where possible, to make improvements.

Limitations

1. Initialization

The input analyses may be in error, particularly in sparse-data areas. Also, there is always some degree of smoothing or filtering in numerical products, and during the process there is some loss of meteorological detail. Small errors like this are important to the P.E. model.

2. Grid Size and Vertical Resolution

Small-scale details can be hidden between grid points in the 63x63 grid. This is particularly so in areas like the Mediterranean Sea, characterized by a great variety of small-scale weather phenomena. In the vertical, the resolution is in such large steps that inversions might not be accounted for.

3. Truncation and Transformation Errors

Truncation errors are mathematical and arise from using the finite difference method of solving equations involving differentials. The solution to a differential is approximated by using discrete, straight-line differences between two points on a curve rather than solving for the actual curve. As the two points get closer and closer, the true solution is approached. Hence, the smaller the mesh size, the smaller the truncation error.

Transformation errors are those which occur in interpolating and extrapolating from one surface to another, say from 500 mb to 300 mb.

4. Wind Conversion

The wind laws used to derive winds from pressure analyses tend to give inaccurate results.

5. Terrain

The terrain field incorporates a considerable degree of smoothing.

6. Barometry Problem

There has never been a completely satisfactory way of reducing pressure to sea level.

7. Heat Package Input

Only gross estimates are possible for input parameters such as cloud cover, convection, and radiation. These parameters are not observed in the necessary detail. Statistical formulations are necessary.

With all the limitations, one might wonder how the P.E. model can ever get off the ground. The verification discussion to follow will show that, despite all obstacles, the P.E. does its job well.

Verification

Verification on key P.E. products is run daily and monthly at FNWC. Most field activities verify the surface and 500-mb P.E. forecasts. The generally good and well-defined verification results serve two most useful purposes of building confidence in P.E. products at the user level and, secondly of showing the P.E. modellers any persistent weaknesses or biases in the model. The modellers can use

this information diagnostically to tune the model or, as was the case in the early days of the model, to make major additions or changes.

Certain systematic biases remain in the P.E. model, and these should be considered by forecasters using the products in the field.

1. Lows tend to be overdeveloped in the principal cyclone track in the North Pacific.
2. Continental highs tend to be overdeveloped, particularly over Asia.
3. There is a tendency to move small-scale systems too slowly. (This is a characteristic weakness of all numerical models, arising from grid size and the mathematics involved.) This tendency will cause such things as lagging fronts.
4. The model tends to be--it's forced to be, really--insensitive to local effects. This is because of the grid size, and resulting poor treatment of mesoscale events. A temperature forecast, for example, could not be expected to be too precise for two locations between grid points when one might be near water, and the other not.
5. The P.E. forecasts for areas of meager data will tend to be overly smoothed. This is the natural result of the P.E. model using initialization values taken from analyses which had to be heavily smoothed because of lack of data.

The verification results for the P.E. model are encouraging. Pressure prognoses at all levels exhibit considerable skill. Particularly noteworthy is the model's ability to forecast generation of new storms; the older barotropic models were poor at this.

The general conclusion to be drawn from inspection of verification figures for the past two years can only be that the P.E. model products are consistently superior to any other comparable and available numerical or hand-produced products. Further, the P.E. products are improving steadily, reflecting the dozens and dozens of small changes that are regularly made by the modellers.

E. Uses of the Products

The regular availability of a broad span of high-quality P.E. prognostic charts has changed the role of the Navy forecaster from that of a line-drawer and mechanical-style forecaster to that of an evaluator of machine-drawn lines, an interpreter, and a dynamic forecaster. The following discussion will assess this new role in relation to the P.E. products.

Before the day of the computer, the routine in a large forecasting office followed three main steps. First came analysis at surface and an appropriate number of upper levels. Next came the prognostic chart construction, based on the analyses. Here, the constant hope was for perfect progs, thinking that near-perfect forecasts could be made in the third step. During the analysis and prognosis stages, the forecasters were expected to develop a mental picture of the changing three-dimensional structure of the atmosphere and, from this, to reach sound forecasting conclusions. Inevitably, the time squeeze got tighter and tighter with each step, and when it came time to forecast, there was none left for meditation or interpretation.

The P.E. prognostic charts now fill the important middle slot in the routine; the forecaster has been relieved of all the forecasting decisions involved in creating prognoses. Now he has enough time to devote to interpretation and judgment, going beyond the usual quick application of synoptic models (viz., frontal-cyclone) to the prognostic charts to get his forecast. Now he has time to develop a clear picture of the three-dimensional atmospheric structure, structure changes expected with time, and scales of the systems involved. From all this, the forecaster can decide on what interaction between systems of different scale might evolve. This is what forecasting is all about, anyway--figuring interaction between the well-predicted large-scale patterns and the mesoscale processes and, from this, what sort of weather will be produced as a result.

The P.E. products should not be accepted in blind faith. They should always be subjected to local checking. This should follow the order of inspecting first in what could be called a gross-error check. These errors would be evidenced by abnormal changes, changes which would lead to meteorologically unbelievable systems. A low, for instance, that is deepening at a rate of 5 mb per hour is hard to accept. All major systems should get this credibility test, using pertinent analyses as a starting point. The next check is to use local area observations to see if the analyses and prognoses make sense. If either check above reveals obvious errors in the progs, there is no recourse but to make hand modifications before starting the forecasts.

The primary purpose and use of P.E. prognoses is to provide guidance to the forecaster in the field, not to do his forecasting. It is at this stage that the man/machine mix is introduced. The P.E. products arrive just as they came out of the computer, untouched and unmodified by human hand during or after preparation. Except for the subjective, gross-error type check already discussed, the forecaster should use the P.E. output just as it comes. In this way he will learn about and how to adjust for any biases in the model insofar as they relate to the area of forecast interest. Further, regular use of the unmodified products will build up confidence in their quality. If the forecaster sees that time after time, the P.E. progs pick up developing lows southwest of his station, deepen them at about the right rate, and then (because of a persistent model bias) move the lows too slowly, the forecaster will correct for the slow movement and issue his forecast with great confidence.

Users of the P.E. progs must provide all the local knowledge. The model can't account for every little local effect such as small bodies of water that might change the moisture pattern enough to influence a fog forecast, or perhaps an insignificant range of hills that causes weak fronts to hang up.

To summarize, these are the ground rules for using P.E. products:

1. Give them a gross-error check, and modify as necessary.
2. If no modifications are suggested in Step 1, use the progs just as they come from the machine.
3. By repeated use, learn and catalog any persistent biases or idiosyncrasies in the model which affect your forecast area. Account for the biases in your forecasts.
4. Apply local knowledge within the framework of what you know about P.E. model performance.
5. Concentrate heavily on relating large- and small-scale system interaction and the weather it produces in your forecast area. Lean heavily on the large-scale P.E. forecasts; they approach the "perfect prog". Consider all of the latest local-area observations in your thinking. These observations might be from radar, aircraft and, for sure, the look out the window.

F. Relationship of Products to Other FNWC Products

The P.E. products are the backbone of the whole FNWC forecasting effort. All but one or two of the atmospheric programs use P.E. products for input as first-guess fields or for direct derivation of forecast parameters. About half of FNWC's oceanographic programs use P.E. products either directly or indirectly. For example, the Sea-Swell model uses P.E. progs, and the Sea-Swell program products are then used in other oceanographic programs such as Sound Ray Tracing and Mixed Layer Depth. There is hardly an FNWC product that has not been influenced by one or more P.E. prognostic products. If the P.E. model has a bad day, the whole FNWC output for that day will be substandard.

G. Program Output

The P.E. model prognoses below are produced at 6-hour intervals from 6 to 72 hours. Only a small portion of these products is sent to field activities, but all are available on request. Catalog numbers are shown in parentheses.

1. Surface pressure. (A01)
2. Terrain pressure. (A04)
3. Temperature at observation level. (A07)
4. Vapor pressure at observation level. (A15)
5. Surface precipitation analysis. (A62)
6. Vapor pressure at 1000 mb (C12), 850 mb (D12), 700 mb (E12), 500 mb (F12), 400 mb (G12), 925 mb (R12)
7. Pressure height at 1000 mb (C00), 850 mb (D00), 700 mb (E00), 500 mb (F00), 400 mb (G00), 300 mb (H00), 200 mb (I00), 150 mb (J00), 100 mb (K00), 925 mb (R00), 250 mb (T00)
8. Temperature at 1000 mb (C10), 850 mb (D10), 700 mb (E10), 500 mb (F10), 400 mb (G10), 300 mb (H10), 200 mb (I10), 150 mb (J10), 100 mb (K10), 925 mb (R10), 250 mb (T10)

9. U wind component at 1000 mb (C20), 850 mb (D20), 700 mb (E20), 500 mb (F20), 400 mb (G20), 300 mb (H20), 200 mb (I20), 150 mb (J20), 100 mb (K20), 925 mb (R20), 950 mb (T20)

10. V wind component at 1000 mb (C21), 850 mb (D21), 700 mb (E21), 500 mb (F21), 400 mb (G21), 300 mb (H21), 200 mb (I21), 150 mb (J21), 100 mb (K21), 925 mb (R21), 250 mb (T21)

There are other products from the P.E. model but they are not listed here since they are used only within the P.E. model itself.

H. References or Suggested Reading

[1] Kesel, Philip G. and F. J. Winninghoff, 1972; "The Fleet Numerical Weather Central Operational Primitive Equation Model", Monthly Weather Review, Vol. 100, No. 5, pp. 360-373, May 1972.

[2] Kesel, Philip G. and F. J. Winninghoff, 1971; "Fleet Numerical Weather Central's Four-Processor Primitive Equation Model", Proceedings of the 6th AWS Technical Exchange Conference, U. S. Naval Academy, September 1970.

[3] Morenoff, E., W. Beckett, P. G. Kesel, F. J. Winninghoff, and P. M. Wolff, 1971; "4-Way Parallel Processor Partitioning of an Atmospheric Primitive Equation Prediction Model" AFIPS Conference Proceedings, Vol. 38.

[4] Haltiner, G. J., 1971; "Numerical Weather Prediction", John Wiley and Sons, Inc., 317 pp.

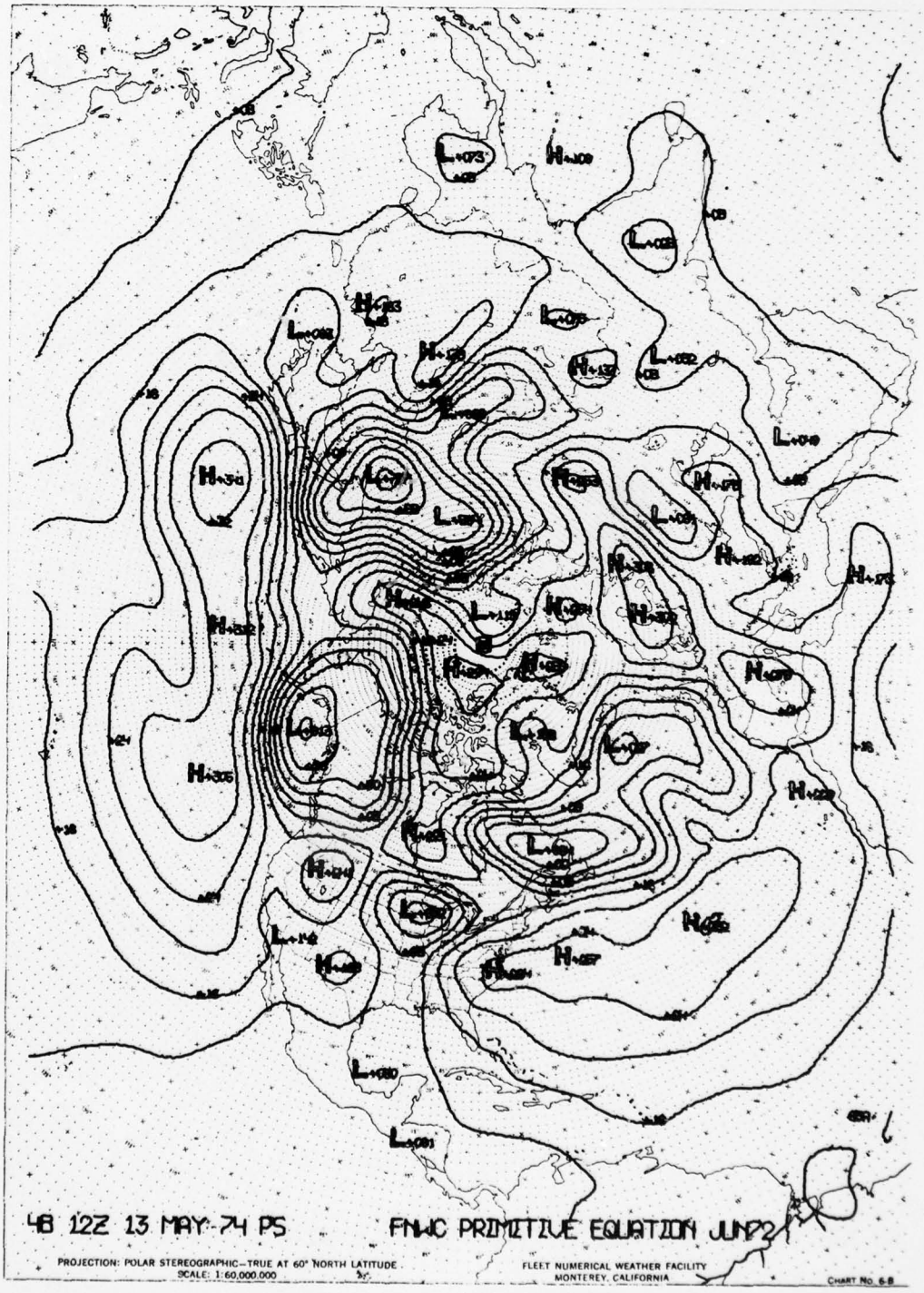


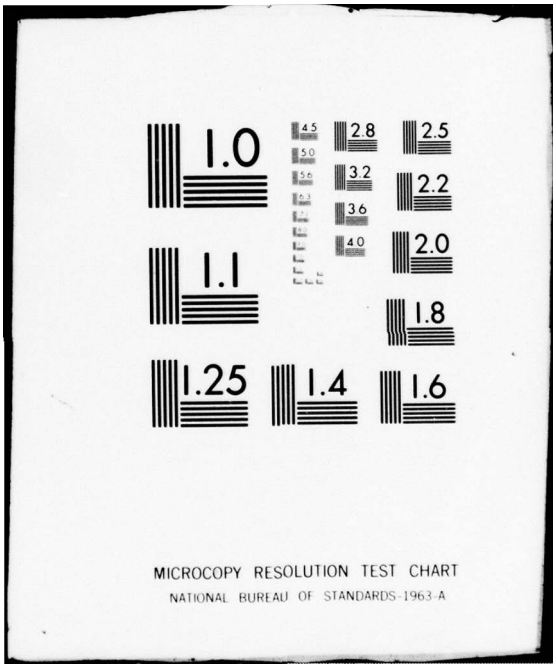
FIGURE 4.8.1 Surface Pressure Prognosis (A01)

AD-A065 511 NAVAL WEATHER SERVICE COMMAND WASHINGTON D C F/G 4/2
U.S. NAVAL WEATHER SERVICE NUMERICAL ENVIRONMENTAL PRODUCTS MAN--ETC(U)
FEB 79 E T HARDING

UNCLASSIFIED NAVAIR-50-1G-522-REV NL

2 OF 4
AD A065511




1.0
1.1
1.25
1.4
1.6
1.8
2.0
2.2
2.5
2.8
3.2
3.6
4.0
4.5
5.0
5.6
6.3
MICROCOPY RESOLUTION TEST CHART
NATIONAL BUREAU OF STANDARDS-1963-A

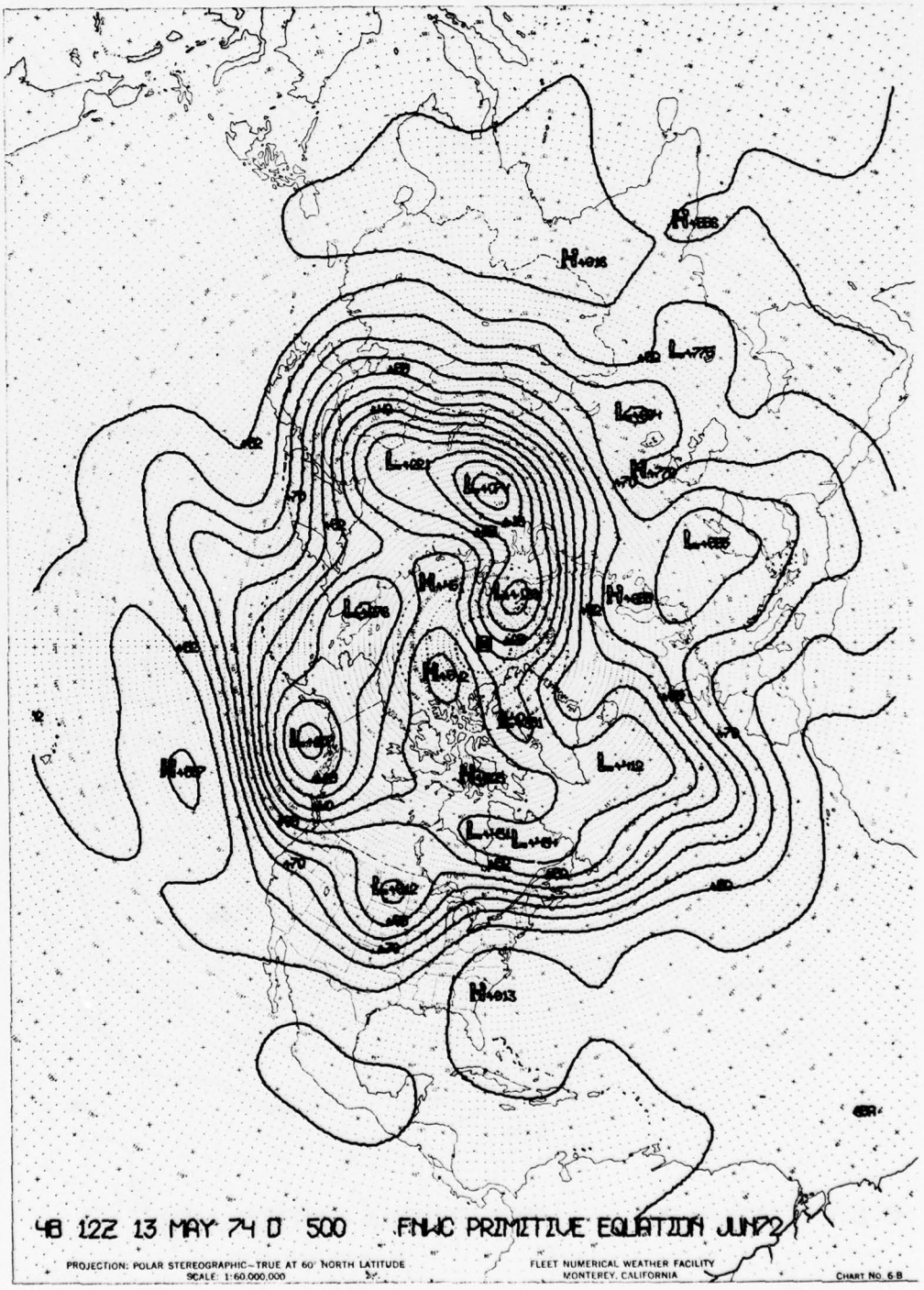


FIGURE 4.8.2 500-mb Pressure Height Prognosis (F00, Tau 48's)



FIGURE 4.8.3 500-mb Temperature Prognosis (F10)

4.9 SCALE AND PATTERN SEPARATION MODEL

A. Model Development

The atmospheric circulation at any level shows features of a wide variety of scale and pattern. At the surface, there are micro-lows, troughs, ridges, migratory cyclones and anticyclones--and there are large-scale features such as the semi-permanent pressure systems. Aloft, there are troughs, ridges, highs, and lows with varying wavelengths and amplitudes, all part of a still larger-scale system--the planetary vortex.

Two fundamental concepts involved in the subjective interpretation of geophysical fields are those of pattern and scale. The interpreter must recognize characteristic patterns and take into account their size. The synoptic forecaster must be able to relate the effects of features at one level with those at another, as well as to determine cross-effects of vari-scaled features upon each other at the same level. Sea level cyclogenesis, for example, is highly dependent upon the upper-air pattern over the cyclogenetical area, but the forecaster is not able to make an objective determination of exact location, intensity, and dimensions of significant upper-level disturbances. Small-scale and large-scale features are too interwoven in a pattern distorted by the reciprocal influence of these features. The classic example of this is the distortion of long waves by short waves making subjective determination of long-wave positions difficult and usually inaccurate.

The scale and pattern separation model was developed to meet the need for an objective and quantitative representation of the contribution of variously scaled pattern features to the total pattern of the scalar distribution. In other words, there existed a need to separate, into several parts, the features of various size. Several techniques for filtering or pattern separation have been available for some time. These include space means, time means, change center histories, and Fourier analyses, among others. The objection surmounted by the FNWC model is the failure of other methods to provide an objective measure of scale while retaining characteristic recognizable patterns.

Field decomposition is essentially a smoothing process in one or more of the independent variables. Separation of the field is accomplished by subtracting from the original field, a smoothed version. The smoothed version will be lacking in the details of the scale to be isolated, and the difference field will represent the isolated scale. This procedure is repeated for each pattern scale to be separated. The end result of this procedure will be a smoothed field representing the planetary vortex.

Decomposition of fields into additive components can be done on any continuous scalar distribution of a parameter--pressure, temperature, thickness, etc. A 500-mb height field will be used here as an example. A field is smoothed by repeated application of a smoothing operator. At first, this reduces the amplitudes of the shortest wavelengths, and gradually affects the longer and longer wavelengths. Thus, there is a constantly increasing wavelength which is contributing most to the smoothing at any time in the process. A wavelength is finally reached where the residual or smoothed field is changing most rapidly. This wavelength gives a measure of a characteristic, stable scale of the field being processed. To separate this scale of the original field from its residual, the smoothing process is continued for a predetermined number of applications. The smoothed field is then subtracted from the original field to yield the small-scale disturbance pattern (SD) (Fig. 4.9.1). This field at the 500-mb level, includes such features as short waves, cut-off lows, cyclones, and ridges.

After the small-scale features are extracted, the smoothed (Fig. 4.9.2), or residual (SR), field is left. It contains the large-scale disturbance features and the planetary vortex, and is an ideal tool for locating long-wave troughs.

A more massive smoothing process continues on the residual field (SR) until the amount of change created by each scan is less than some arbitrarily small amount. At this point, only the planetary vortex remains. This planetary vortex (SV) is centered on the hemispheric center of circulation. The large-scale

(Fig. 4.9.3) disturbance pattern (SL) is obtained by subtracting the planetary vortex field from the residual field (SR).

The field decomposition is now complete. The relationships, in the order given above, are:

$$Z - SD = SR \quad (Z = \text{total field})$$

$$SR - SV = SL$$

Thus,

$$SV = SR - SL = Z - SL - SD$$

$$SL = SR - SV = Z - SV - SD$$

$$SD = Z - SR = Z - SV - SL$$

B. Program Input

Any continuous scalar environmental field produced by FNWC. The program is currently being applied to the following fields:

1. 1000-mb analysis and prognoses
2. 500-mb analysis and prognoses
3. 200-mb aralysis
4. 500-1000-mb thickness analysis
5. Analog 1000-mb and 500-mb analyses.

C. Program Computation

1. Apply the smoothing operator to the field to be decomposed. Repeated applications first reduce the amplitudes of the shortest wavelengths, and gradually smooth out longer and longer wavelengths until one wavelength value is reached. The smoothing process continues for a predetermined number of applications, after which the residual (SR) or smoothed field is subtracted from the original field. The remainder is the small-scale disturbance pattern (SD).
2. A more powerful smoothing operator is applied to the residual field (SR) until a single vortex remains. This is the planetary vortex (SV), centered on the hemispheric center of circulation. Subtracting SV from SR yields the large-scale disturbance pattern (SL).

D. Program Limitations and Verification

The Scale and Pattern Separation program is based on some rather elegant mathematical methods which were formulated specifically to solve the problem of scalar field decomposition. If the equations are properly applied to a field, the component parts just have to come out properly scaled and patterned. Of course, there is always the possibility that the starting field will be a poor analysis, in which case the Separation program can only come up with comparably poor separation fields. Hence, the separation fields cannot be evaluated for accuracy by inspection; evaluation of the analysis of the fields being decomposed is the only clue to the accuracy of the separation fields.

There is one persistent weakness in the separation program which arises from a "convenience" choice of one constant. The inherent scales of the mass structure have a seasonal cycle, which is true of both the small- and the large-scale patterns. The point at which to stop the smoothing process in

order to remove any one scale will vary somewhat with time of year, but changing the cut number periodically represents a considerable stepwise change and disrupts component continuity. For operational use, a year-round cut number, the October value, was adopted. The result is that in summer the SL components are somewhat weaker than they should be, while the SD components are stronger. The reverse is true in winter.

E. Uses of the Products

The Scale and Pattern Separation products are valuable as a base for organizing synoptic forecast thinking. The forecaster can build a coherent picture in his mind as to why systems have evolved as they did. From this he can get a feel for where they are going. The prognostic charts can be viewed with a critical eye. The forecaster's confidence in the prognostic charts is much greater if the progs agree with what has been thought out from the separation charts. The final forecasts will be better.

Specific uses of the Scale and Pattern Separation charts are discussed below, by separation-chart category.

500-mb SR--Residual Charts

1. Location, continuity, and movement of long-waves. Long-waves define areas of storminess along their leading edge.
2. Location of ridges at 500-mb level.
3. Location of blocks at 500-mb level. (SL charts are better.)
4. One input in screening 1000-mb historical charts to obtain analogs for the FNWC Analog Program (Section 4.10).
5. Steering for Tropical Cyclone trajectories (Section 4.16).

500-mb SL--Large-Scale Charts

1. Precise center location and intensities of large-scale disturbances. These large-scale features are often masked or distorted on the 500-mb chart; here, they are clear and precise. Generally speaking, any center with an absolute value of 100 meters or more can be considered significant. Values may exceed 300 meters. The SL charts can be used to determine trends of large-scale features, movement and changes in intensity. The growth of one feature at the expense of another represents a quantitative energy transfer between these features. A general increase or decrease in energy among several adjacent features could be interpreted in several ways: it could represent a cascade of energy to or from the SD range of scale; it could represent a transfer of energy between levels; or it could represent a shift from potential to kinetic energy (or vice-versa).
2. Stability of large-scale features. The atmosphere, under stable conditions, will normally support five long-waves in the Northern Hemisphere, that would show as five SL low centers (or SR troughs). The existence of fewer, or more, often indicates a tendency for readjustment of large-scale features. With fewer than five troughs, there is a tendency for a fifth to develop in the area of the longest wavelength. Existence of more than five usually indicates a tendency for elimination of one or more troughs. Evenly-spaced circular features normally indicate a stable quasi-stationary pattern, while elongated or unusually shaped features signify an unstable pattern with some readjustment taking place or about to take place. If there is one large circular center that dominates the hemisphere (anchor feature), the other weaker features will tend to rotate around it.
3. Location and intensity of blocks. Blocks steer storms along tracks north and south of the block. At the surface beneath the block, a cold anticyclone will be found, with the characteristic weather associated with this feature.
4. Quantitative evaluation of energy transfer, as discussed in 1 above.
5. One input in screening 500-mb charts to obtain analogs for the FNWC Analog Program (Section 4.10).
6. To steer surface low pressure systems. Trace the 24-hr 500-mb SL prognosis on the current sea level pressure analysis. Straight-line flow over the surface low will give the most accurate movement. With curved flow aloft, the surface low will move toward lower height

values. If there is a closed low center aloft over the surface low, the surface low will normally remain stationary or have a slight poleward drift.

500-mb SD--Small-Scale Disturbances

This chart represents the small-scale disturbance field or those features that, by definition, translate through the quasi-stationary large-scale features and account for the movement of storms. The following guidelines and forecast rules are applicable in gleaning maximum synoptic information from this chart:

1. The precise centers of small-scale disturbances are represented on the SD chart. These centers may also be thought of as small-scale kinetic energy centers. Energy may shift here similar to that on the 500-mb SL chart. The positions of the lows are analogous to short-wave positions.
2. Significant features normally have an absolute value in excess of 50 meters, and are generally in excess of 100 meters. Values may be as high as 300 meters.
3. SD centers are analogous to centers of relative vorticity. Advection of SD centers is analogous to positive vorticity advection (PVA). Vorticity affects the genesis of cyclones and anticyclones, and is related to cloudiness, precipitation, and pressure and height changes. Rule 1. When relative vorticity decreases downstream, convergence occurs at lower levels. Cloudiness and precipitation occur if sufficient moisture is present. Rule 2. When an upper-level trough with positive vorticity advection ahead of it overtakes a frontal system, cyclone development at surface level occurs, or deepening of any existing system occurs. Rule 3. Surface pressure falls where relative vorticity decreases downstream in the upper troposphere, or where advection of more cyclonic vorticity takes place aloft. Surface pressure rises in the reverse case. Rule 4. If there are several waves along a front, the one with the most intense cyclonic vorticity aloft will deepen at the expense of the others.
4. Tracking SD centers as they translate through SR troughs is analogous to tracking short-waves through long-wave positions on the 500-mb chart. However, the features tend to be masked using the latter method, making use of the SD/SR charts much more accurate and definitive.
5. As an SD center moves through the related SR trough, surface cyclogenesis or deepening can be expected, other factors being favorable.
6. As an SD center moves ahead of the related SR trough and toward an SR ridge, filling can be expected in the associated surface cyclone.
7. A surface low which moves out well ahead of its associated 500-mb SD center can be expected to fill. In this case, redevelopment at the surface is possible nearer the location of the 500-mb SD center.
8. A rapidly intensifying SD center will tend to slow in movement, even to the point of becoming quasi-stationary. This is almost always the case when a cut-off low forms on the 500-mb chart. Associated energy in such a cut-off low is almost entirely in the SD range of scale.
9. A surface feature which has drifted under its associated 500-mb SD center will tend to fill. Its future movement will be governed by the movement of that SD center. This often happens with a large mature storm.

500-mb SV--Planetary Vortex

1. Strength of zonal winds (westerlies and easterlies).
2. Eccentricity of polar vortex, which relates to the latitudinal position of the westerlies for all longitudes.

1000-mb SR--Residual Charts

Since the planetary vortex is negligible at 1000 mb, the SR and SL fields are nearly synonomous. It is more convenient to use the SR. Smoothed relative centers of high and low surface pressure around the hemisphere are evident from this chart. Synoptic information ascertainable includes:

a. Relative position and strength of Siberian and Canadian Highs in winter, and oceanic highs in summer.
b. General areas of surface storminess (storm tracks).

1000-mb SD--Small-Scale

This chart gives the precise center of the small-scale disturbance of surface features. Often, a fast-moving surface development is almost totally in this range of scale.

H 500-1000 mb SL Thickness Disturbances

This chart depicts the precise center and relative intensities of the large-scale thickness disturbances, or the large-scale areas of cold and warm air. It can be used in much the same way as the 500-mb SL.

F. Product Relationship

The Scale and Pattern Separation products are used primarily as interpretive tools. They are input to these FNWC programs:

1. The Analog program, for screening and selection.

2. Tropical Cyclone Steering Trajectories.

3. Sea-Surface Temperature Anomaly.

G. Program Output

Catalog numbers are listed for levels and output fields indicated; the tau (forecast period) is indicated as a subscript. The "*" indicates tau 0, 12, 24, 36, 48, and 72 except for catalog number C05 for which tau 72 is not produced.

		OUTPUT FIELD			
		SR	SD	SL	SV
LEVEL	1000 mb	$C06_{*}$	$C05_{*}$	$C07_{0}$	$C09_{0}$
	500 mb	$F06_{*}$	$F05_{*}$	$F07_{*}$	$F09_{0}$
	200 mb	$I06_{0}$	X	X	X
	500-1000 mb	X	X	X	$Y09_{0}$

H. References

[1] Thormeyer, C. D. Lt., 1970; "Scale and Pattern Decomposition at Fleet Numerical Weather Central" (*FNWC Working Paper*).

[2] Holl, Manfred M., 1967; "A New Version of the Beta-Program for an 89x89 Grid", Technical Note One, Contract N00228-67-C-2759, Meteorology International Incorporated, Monterey, California.

[3] Holl, Manfred M., 1963; "A Diagnostic-Cycle Routine", Final Report, Contract Cwb-10314, Meteorology International Incorporated, Monterey, California.

[4] Holl, Manfred M., 1963; "Scale-and-Pattern Spectra and Decompositions", Technical Memorandum No. 3, Contract N228-(62271) 60550, Meteorology International Incorporated, Monterey, California.

[5] Holl, Manfred M., 1964; "The Decomposition of the Residual Component", part of Quarterly Report 3, Project M-113, Contract N228-(62271) 62178, Meteorology International Incorporated, Monterey, California.

[6] Holl, Manfred M., 1964; "Variable-Resolution Scale-Separation", part of Quarterly Report 2, Project M-117, Contract N228-(62271) 63686, Meteorology International Incorporated, Monterey, California.

[7] Holl, Manfred M., 1964; "Scale Separation of Third-Degree Steepness", part of Quarterly Report 3 (and Terminal Report), Meteorology International Incorporated, Monterey, California.

[8] Wolff, P. M., Capt., USN, T. Laevastu and W. E. Hubert, Cdr. USN, 1965; "Numerical Scale and Pattern Separation of Sea Surface Temperature for the Northern Hemisphere".

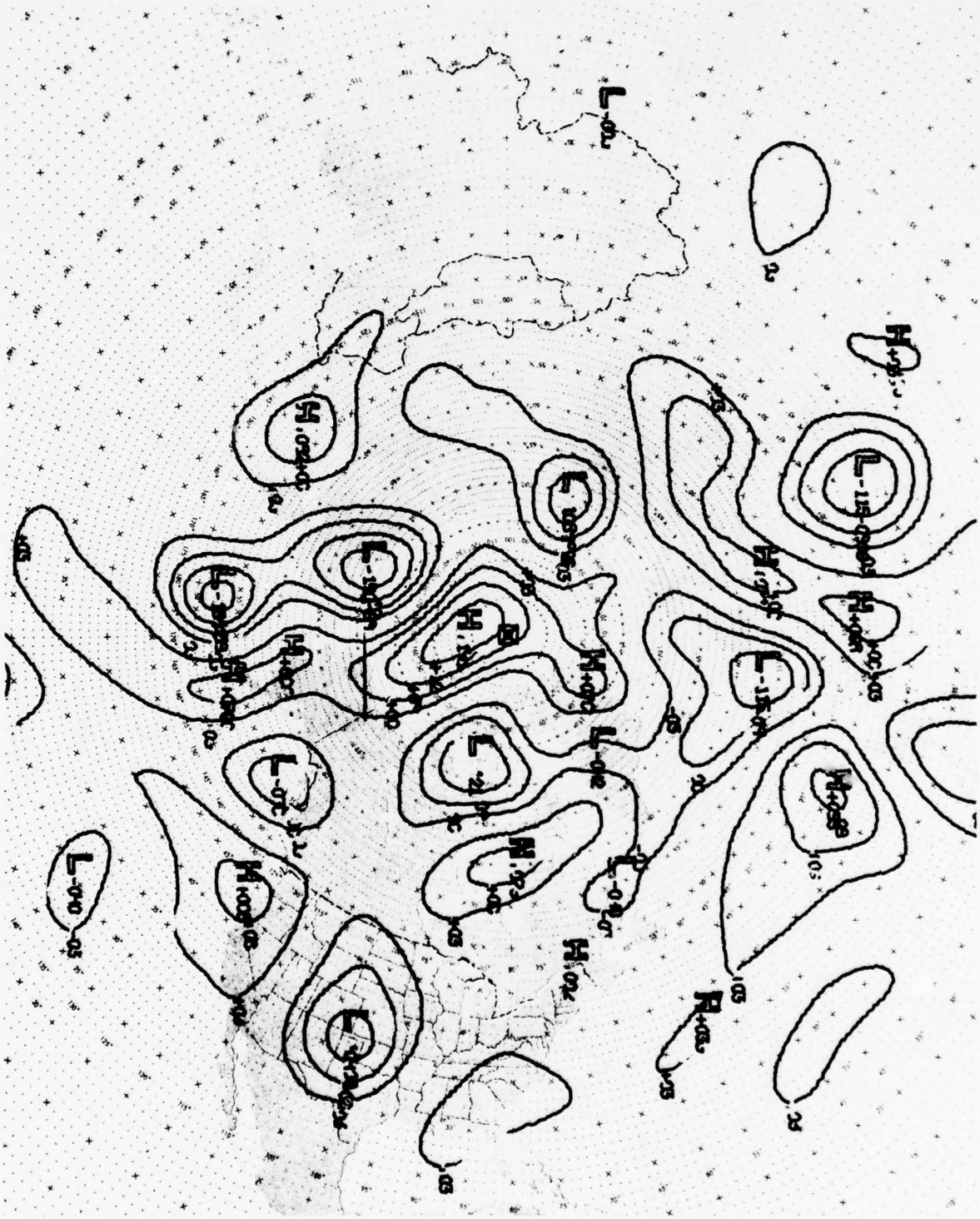


FIGURE 4.9.1 500-mb Small-Scale Disturbance 48-Hour Forecast. SD 500

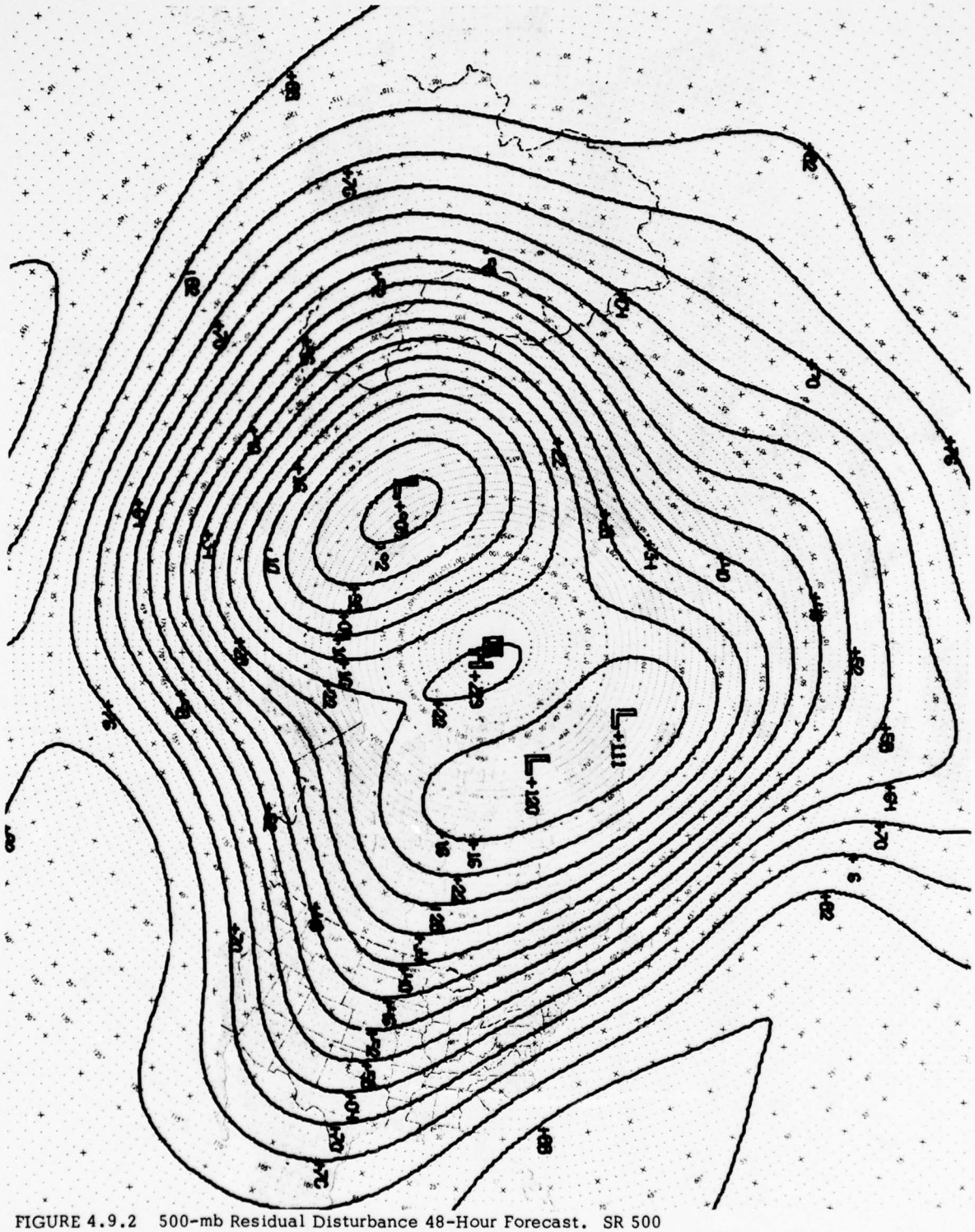


FIGURE 4.9.2 500-mb Residual Disturbance 48-Hour Forecast. SR 500

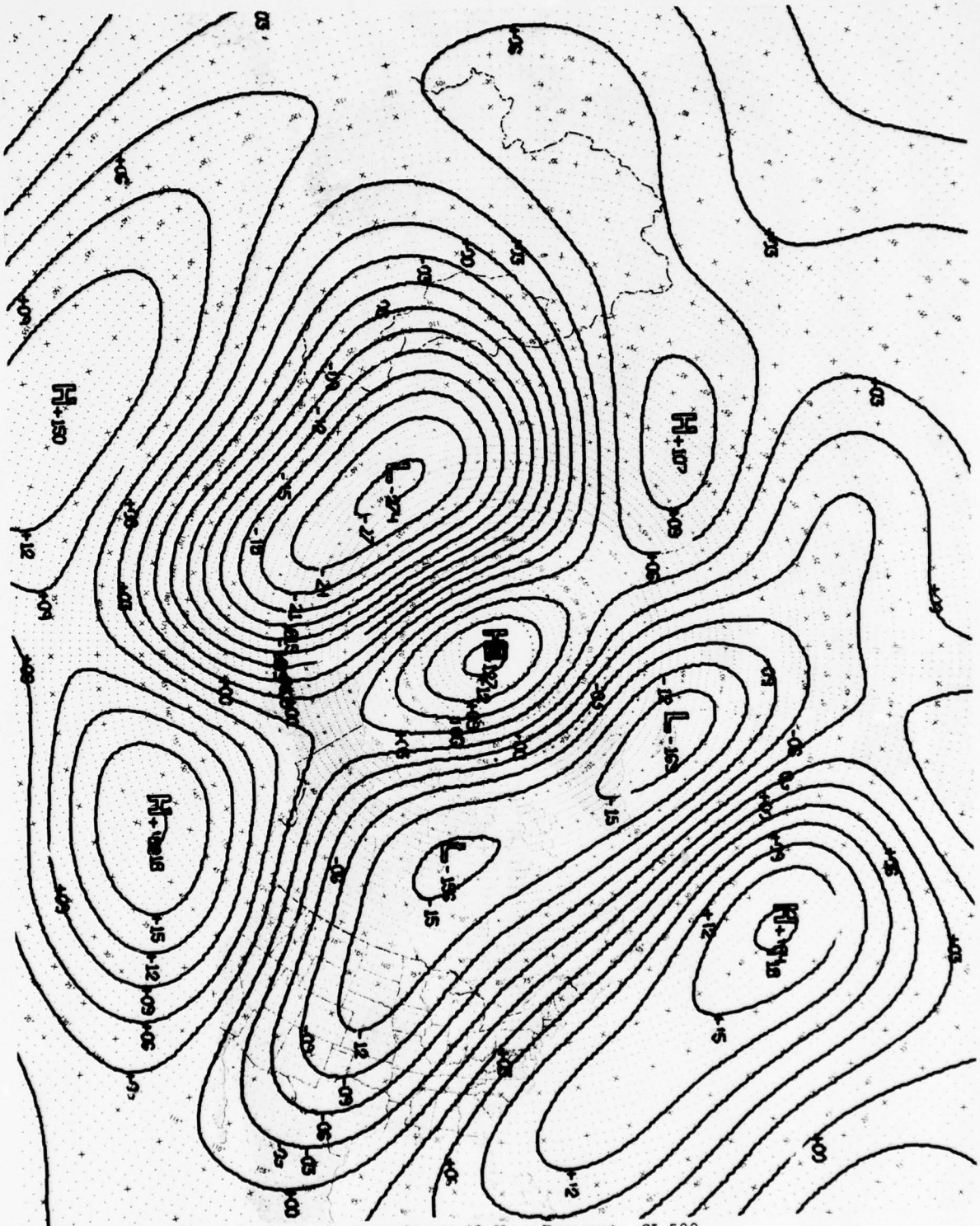


FIGURE 4.9.3 500-mb Large-Scale Disturbance 48-Hour Forecast. SL 500

4.10 ANALOG FORECAST MODEL

A. Model Development

Environmental conditions are a major factor in the success or failure of nearly any military operation. In long-range military planning, detailed long-range forecasts of weather and oceanographic parameters play an important and necessary role.

While purely climatological and statistical approaches are useful in long-range military planning beyond 15 days or so, these methods cannot anticipate the well-defined trends and meso-scale circulation features important to more detailed shorter range planning. Dynamical forecast models show the required detail but have not performed well beyond about three days. Thus neither dynamic nor climatological/statistical approaches provide for the critical 3 to 15 day forecast period. The FNWC Analog Forecast Model has been developed to fill this gap.

The analog model is based on the assumption that if a historical weather case can be found which closely matches the present weather, then the dynamics are similar in both cases, and, therefore, both cases evolve similarly. Thus the development of the present weather is expected to match the development of the historical weather case. This philosophy is applied subjectively by experienced forecasters when making manual prognoses.

FNWC has developed and tested several analog models. The most successful model, developed by Hanna [1], described in further detail in FNWC TECH NOTE 74-1 [2], has been utilized operationally since July 1970. The FNWC effort differs from older methods, such as Elliot's [3] weather typing method, in the following ways:

1. The selection of analogs is totally automated; no human judgment enters into the process.
2. The availability of advanced high-speed digital computers allows a rapid and comprehensive search of a large data base.
3. Use of two levels (surface and 500 mbs) considers the thermal structure, thus sharpening the selection process.
4. The synoptic data base (1946 to present) is more extensive than any previously used and encompasses possible cyclic effects through a double sunspot (22-year) cycle.
5. Use of a pattern separation technique (Holl [4]) improves the selection procedure by separating large- and small-scale disturbances.

The Single Best Analog Approach

Prior to July 1970 the analog forecast model was based on the concept of isolating the one best historical analog. It was found that a good match over the entire hemisphere was a relatively rare event. Hemispheric correlations of 500-mb large-scale history features and current features averaged from 0.70 to 0.75 and rarely exceeded 0.85 (perfect correlation is 1.0). With such poor initial specification, it was not surprising that the single analog model showed only occasional skill over climatology and persistence forecasts, regardless of the selection method used.

The Composite Analog Approach (current model)

It was found that when ten hemispheric analog fields are averaged together grid point by grid point, the correlation of the resulting composite analog with current weather is always higher than that of any of the ten individual components. Further, the composite looked more like the current chart than

did any of the individual charts. Composite correlations have routinely been 0.10 to 0.20 greater than the highest individual correlation included in the composite. In a large number of test cases, the composite chart derived from the ten best candidates consistently outscored the best single analog for a 0 to 10 day forecast period.

It was also found that the method showing the most skill used correlations of heights at all grid points from analyses of four fields: 1000-mb height, 1000-mb SR, 500-mb height and 500-mb SL. The four correlations are performed separately, then normalized to give a correlation value for the one chart. The 40 candidates with the highest correlations are retained for further screening.

B. Program Input (63x63 grid)

1. 500-mb and 1000-mb analyses for current date. (Catalog No. F00, C00)
2. 500-mb SL for current date. (Catalog No. F07)
3. 1000-mb SR for current date. (Catalog No. C06)
4. Historical charts at 1200Z from 1946 to present for:
   (a) 1000-mb analysis.
   (b) 1000-mb SR.
   (c) 500-mb analysis.
   (d) 500-mb SL.

C. Program Computation

1. All years in the data base are searched ±30 days from the current calendar date (ignoring out-of-season months) for the following four parameters:

SL 500	Large-scale disturbance field at 500 mb
SR 1000	Residual disturbance field at 1000 mb
D 500	500-mb height field
D 1000	1000-mb height field

Hemispheric correlations between the historical charts and current charts are computed using all grid points north of 20N (approximately 1500) according to the standard equation

$$r = \frac{\sum(x - \bar{x})\ (y - \bar{y})}{\sqrt{\sum(x - \bar{x})^2\ (y - \bar{y})^2}} \qquad (1)$$

where r is the correlation coefficient, and x and y are corresponding grid points on the current and historical data fields being correlated. Note that since the 500- and 1000-mb height fields include both large- and small-scale disturbances, the large-scale features are weighted about three to one over the small-scale in the selection procedure. Some 1680 individual correlations for each of the four parameters are available at this point; these are normalized (Equation 2) and averaged over the four parameters for each historical date

$$N = \frac{r - \bar{r}}{\sigma} \qquad (2)$$

In this equation, r is the correlation value of a specific chart with the current data, $\bar{r}$ is the mean of all 1680 correlations for that parameter, and σ is the standard deviation of the 1680 correlations for that parameter. The principal function of normalizing is to place the

correlations of all four parameters on an equal basis. The normalized values for all four parameters from the same historical date are averaged together, yielding one correlation (N) for each date. These 1680 normalized and averaged correlations are then ranked, with the best 40 selected as candidates. A typical range in the value of N is from about 2.30 for the highest candidate to about 1.50 for the 40th. A perfect match is near 4.00.

2. The 40 highest values are ranked in order from high to low.

3. The 10 best analog candidates are averaged point by point at surface and 500 mb for each day out to 10 days to derive the surface and 500-mb composite analog charts.

4. The 1000-mb height and SR charts are computed from the surface analogs for the 10-day forecast period. See Holl [4].

5. The 500-mb SL and SR charts are computed from the 500-mb composite D_0 to D_{10} charts. See Holl [4].

D. Program Limitations and Verification

The limitations of the analog model stem from the basic assumption that the dynamic development of two similar patterns from different times will follow similar paths with time. This implies a perfect match, not only of the new screening parameters, but of many more such as height parameters at all levels, sea-surface temperatures, and snow cover, among others. The primary limitation, then, is the looseness of the analog match. The only clue to this is the correlation value tabulation by hemisphere and by sectors, which is sent in the Analog Long-Range Forecast and Analog Dates messages. From this, strength and weakness can be evaluated both hemispherically and by sectors. A low correlation (a poor match with today's chart) is a signal of potential weakness in the analog products. It should be noted that correlation values are generally lower in the transition seasons, higher in summer and winter.

Selection of the analogs is limited by the available historical data. The correlation values will reflect this situation.

Small-scale features tend to be missed or smoothed out by the analog selection process and by use of the composite approach. This limitation means that the forecaster should place his emphasis on the large-scale patterns, associating expected small-scale features to this large-scale forecast so that dynamic continuity is maintained. Any small-scale analog features should be ignored if they do not fit with the large-scale. A further problem in the small-scale is the phase problem. Phase errors are bound to be present in the imperfect initial match of current and past charts. These phase errors often cause the more detailed forecasts based on the analogs to move in and out of phase in space and time with the actual weather which eventually develops. Sometimes this causes the analog to deteriorate or vary in skill with time.

The strong point of the analog system lies in forecasting the large-scale features--blocks, long-wave troughs, ridges, etc. The system can do this with a considerable degree of skill, particularly in the winter. The attempt to forecast change is what makes the analog system superior to climatology or persistence forecasts where change is not considered.

Development of the analog model necessarily involved continuous statistical verification to indicate improvements in model development. The verification comparisons are Composite against: Persistence (a no-change forecast), Mean (climatology) and Best Hindsight (the single best correlated candidate for the Day 0+1 to Day 0+15).

For the years 1973-1974, the Composite was superior to Persistence and Best Hindsight for all time periods, the Composite was superior to the Mean for the <u>average</u> D_0+1 to D_0+10, and comparable to the Mean for the period D_0+6 to D_0+10. In addition, the Composite was superior to the Mean for the <u>average</u> D_0+1 to D_0+15 over the year.

E. Uses of the Products

The image of long-range forecasts, regardless of how they are produced, has always suffered because users tend to demand more than the forecasts are capable of producing. To expect perfect phasing of small-scale features goes beyond what the long-range forecasts promise. The FNWC analog forecasts should be used only to interpret the general structure. Don't expect migratory fronts, lows or highs to be on schedule--or even exist as shown on the analog charts. The large-scale features should receive most attention.

The surface analogs are best used for locating storm tracks and estimating gradients. Storm track information can be applied to OTSR, selection of areas for operations, and forecasts of operating conditions in and near the storm track area. Gradient information is useful for determining the fluctuation in size and intensity of major features such as the Asian High, the Asian thermal low, the monsoon in the China Sea, and the large subtropical, oceanic high-pressure cells. From a knowledge of these major features, forecasts can be made of the strength of the monsoonal flow, the probable location of frontal zones, probable weather and wind conditions within and along the leading edges of the major features. An example might be the tendency of storms to move around subtropical highs, so if the center is abnormally strong or displaced abnormally far to the north, storm tracks lie farther north than usual and encounter the continents at higher than usual latitudes.

The SR and SL analogs depict and forecast the large-scale flow. This is the part of the analog program that shows most skill. Analog users, then, should look for location of long-waves, cut-off lows, blocks, and become familiar with the overall flow pattern. In forecasting, surface lows are steered by the 500-mb flow. Long-waves warn the forecaster to expect storminess near but east of the long-wave location, and that storm movement will parallel the southwest flow ahead of the trough. Cut-off lows will pinpoint stormy areas; the tips of deep occlusions very often are located directly under the low aloft. Blocks do just what the name implies; they block or shunt off surface disturbances.

Keep in mind at all times that the analogs are a smoothed version. Forecasts, thus, should be broad in treatment. Detailed forecasts should never be attempted.

F. Relationship to Other Products

The only use of analog forecasts in other FNWC products is in Optimum Track Ship Routing (OTSR).

The historical series has been processed by the Sea/Swell program to give a Sea/Swell history tape. The OTSR program makes a daily selection of the "ten best analog candidates", using the method described in the Analog Forecast Model. The ten candidates are then matched with the Sea/Swell history, and 21-day Sea/Swell forecasts are extracted. The combined heights and directions from the 10 forecasts are merged and used to issue probability forecasts for the North Atlantic and North Pacific Oceans.

G. Program Output - on Mondays and Thursdays

1. Surface Pressure analysis and prognosis, 0 to 10 days. (Catalog No. A03)

2. 500-mb Height analysis and prognosis, 0 to 10 days. (Catalog No. F01)

3. 500-mb Residual Analog (SR) analysis and prognosis, 0 to 10 days. (Catalog No. F11)

4. 500-mb Large-Scale Disturbance Analog (SL) analysis and prognosis, 0 to 10 days. (Catalog No. F13)

5. 1000-mb Residual Analog (SR) analysis and prognosis, 0 to 10 days. (Catalog No. C03)

6. Analog Dates Message, issued twice weekly, lists the 40 best analog dates and indicates dates used for the composite analog, including hemispheric and sector correlations for each date. (Catalog No. A-66)

H. References

[1] Hanna, P., 21 July 1971; "Composite Analog Statistics 1970-1971, internal unpublished manuscript, FNWC.

[2] McConathy, D. R. and C. D. Thormeyer, December 1974; FNWC Technical Note No. 74-1.

[3] Elliot, R. D., 1951; "Extended-Range Forecasting by Weather Types", Compendium of Meteorology, American Meteorological Society, Boston, Massachusetts.

[4] Holl, M. M., November 1963; "Scale and Pattern Spectra and Decompositions", Technical Memorandum #3, Meteorology International Incorporated, Monterey, California.

MESSAGES PRODUCED FOR CARSWELL, FROM 3200 TAPE DTG = 75032000

ABXN KNWC NR01 200000Z A66 0
ANALOG DATES MESSAGE - FOR METEOROLOGIST ONLY

1. ANALOGS LISTED BELOW MATCH CURRENT DTG OF 75031912

2. QUALITY OF BEST ANALOGS VS. INITIAL MATCH---
(AVERAGE OF SL 500 AND SR 1000, RANGE CAN BE FROM -1.000 TO +1.000). LAST COLUMN INDICATES THOSE DATES ACCEPTED (YES) FOR COMPOSITE ANALOG.

BEST DATES YYMMDDHH	HEMIS 360 DEG	N. AMER. +04-130W	PACIFIC 130W-160E	WESTPAC 160E-60E	ELANT/MED 60E-40W	ACCP COMP
56022512	.5554	.6518	.5784	.4325	.4886	NO
64022812	.6181	.7364	.7224	.4647	.4515	YES
64022912	.6307	.6632	.7871	.5261	.5134	NO
46032512	.5764	.7789	.7478	.4354	.1321	NO
46032612	.6486	.8023	.8000	.5058	.3264	YES
46032712	.6919	.7607	.8857	.5249	.3971	YES
46032812	.6016	.6687	.8426	.4720	.2143	NO
50032112	.5935	.6485	.8269	.5021	.4927	NO
50032212	.6371	.7649	.8010	.5477	.4957	YES
50032712	.5457	.5119	.7573	.4516	.4785	NO
53031712	.6081	.5118	.8254	.6332	.5541	NO
53031812	.6188	.5890	.8311	.5651	.5625	NO
53031912	.6052	.5937	.7794	.5584	.5447	NO
54030912	.5947	.5808	.8042	.5393	.5156	NO
54031012	.5939	.3283	.8181	.6041	.5902	NO
56032912	.6139	.5573	.6303	.6401	.6113	NO
59031912	.5600	.6907	.5348	.5249	.5707	NO
59032112	.5889	.5875	.8199	.5555	.5551	NO
64030112	.6080	.7461	.5497	.5134	.4883	NO
64030912	.5833	.7335	.5765	.4732	.4973	NO
64031012	.6016	.7424	.7362	.4988	.3570	NO
64031212	.5813	.6593	.7353	.4799	.5320	NO
73031112	.5992	.5303	.7151	.4921	.6492	YES
73031212	.6609	.6243	.7051	.5324	.7853	YES
73031312	.6027	.4653	.5849	.5263	.6587	NO
73031512	.6026	.6415	.5499	.4689	.6590	NO
73031612	.6083	.6207	.7288	.5119	.5614	NO
73031712	.5719	.4380	.7758	.5155	.4517	NO
74030412	.5994	.7466	.6028	.4234	.5945	NO
74033012	.5927	.8407	.5428	.5385	.6590	NO
59040212	.5881	.6464	.7645	.5639	.2605	NO
60041612	.6051	.7566	.7011	.5112	.4118	NO
60041712	.6322	.7372	.8045	.5764	.4543	YES
60041812	.6477	.6348	.8069	.7421	.4806	YES
68040912	.5819	.5926	.5048	.6301	.4950	NO
69041812	.6047	.6903	.8026	.4049	.4050	NO
73041612	.6108	.7012	.8143	.7085	.2827	YES
74040612	.5860	.5910	.7386	.5697	.5843	NO
74041712	.5732	.6441	.7356	.4239	.5746	NO
74041812	.6043	.6753	.7961	.4626	.5351	YES

BT

FIGURE 4.10.1 Analog Dates Message

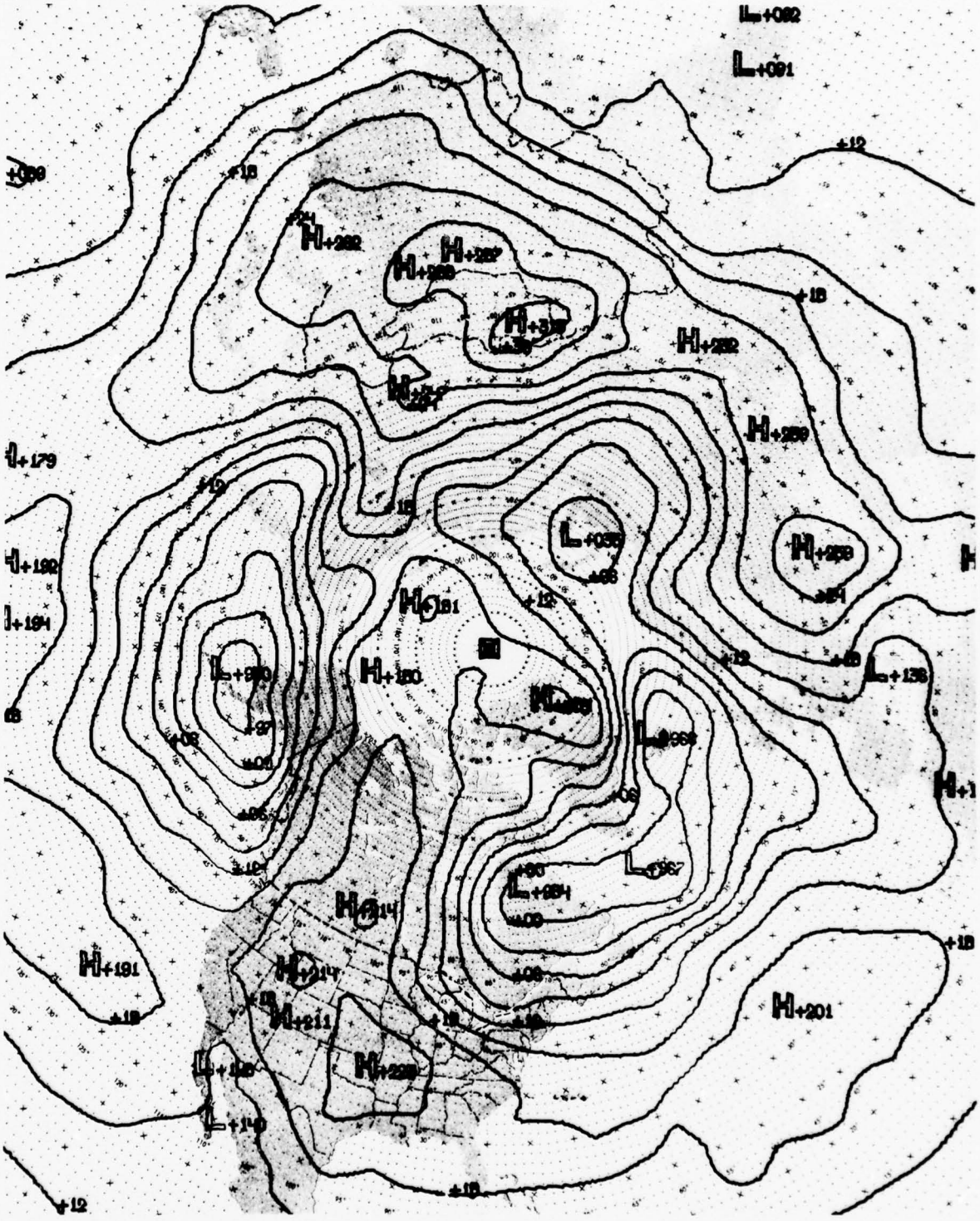


FIGURE 4.10.2 Surface Pressure Analog Model Seven Day Prognosis Based on the 1200Z 12 NOV 1975 Analysis and Verifying at 1200Z 19 NOV 1975. Contour Interval is 3mb.

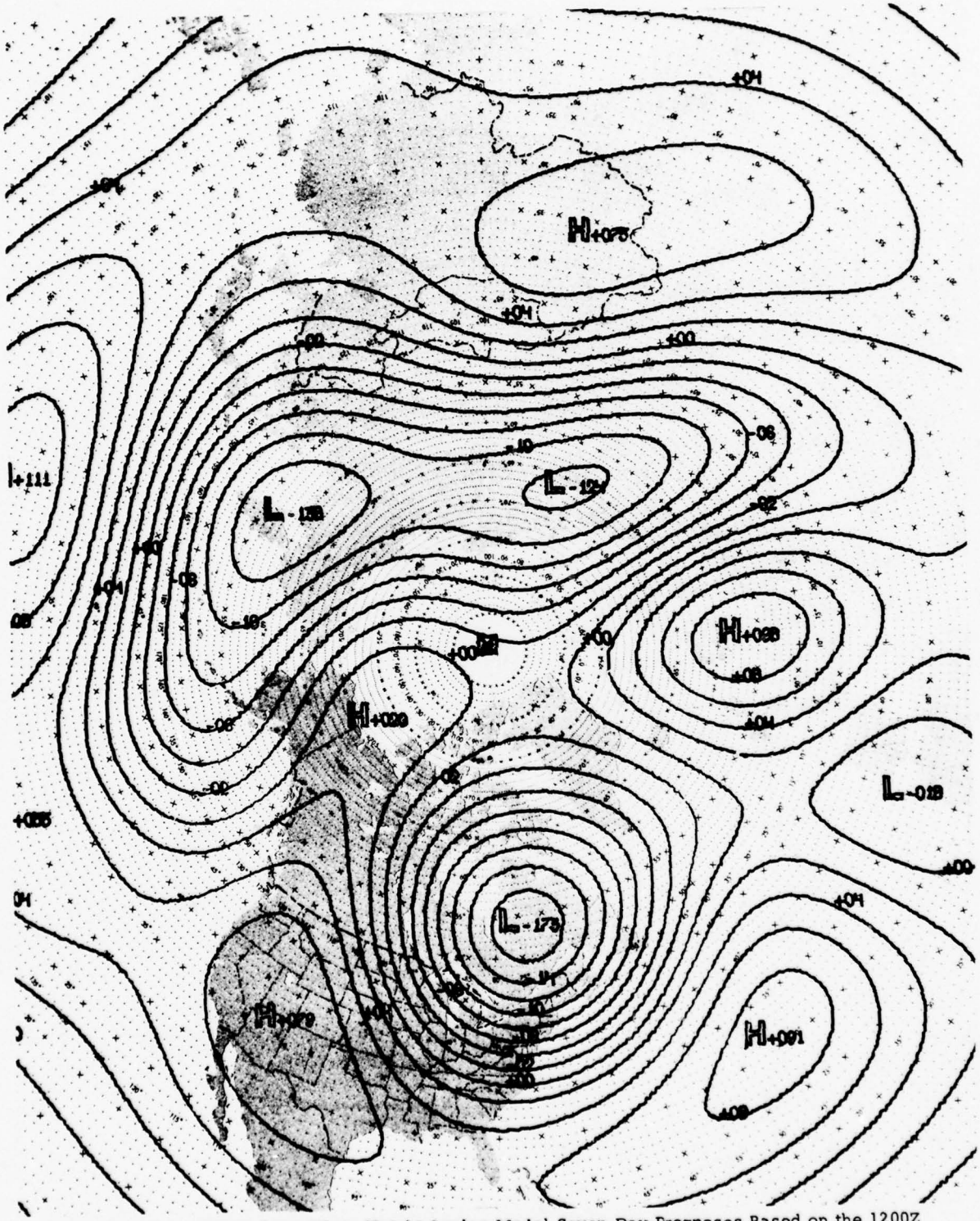


FIGURE 4.10.3 500mb Lone-Wave Height Analog Model Seven Day Prognoses Based on the 1200Z 12 NOV 1975 Analysis and Verifying at 1200Z 19 NOV 1975. Contour Interval is 20 m.

4.12 TROPOPAUSE HEIGHT ANALYSIS AND PROGNOSIS

A. Program Development

The tropopause height chart is useful for determining the level of maximum winds and locating the jet stream. Subjective analysis of tropopause height is a long, tedious operation involving careful examination of lapse rates in high-level layers and application of various ground rules to insure that the final analysis produces a tropopause that meets the WMO tropopause definition. The FNWC tropopause program developers sought a simple, objective technique that would give results comparable in accuracy to good hand analysis.

Since the tropopause is defined by characteristic changes in lapse rate, development of some scheme for combining lapse rates in layers above and below the tropopause seemed a logical approach to the problem (Ref. 1). Various combinations were tested, using a large data sample of objectively analyzed upper-air charts. The best tropopause definition was at the point of intersection between the 500- to 400-mb temperature lapse rate extrapolated upward and the 150- to 100-mb lapse rate extrapolated downward. The level of intersection averaged 700 feet below the observed tropopause.

The assumption that the tropopause height map is a good approximation of the level of maximum winds was tested with data from a 5-year period. Results showed that, on the average, the level of maximum winds (in the jet core) is found at 2300 feet below the derived tropopause heights. These test results were verified by two independent studies.

The formula for computing the tropopause height incorporates a 3000-foot constant to account for the 700 and 2300 foot deviations discussed above. This means that the Tropopause Height charts truly represent the Level of Maximum Winds, but the true tropopause height is 3000 feet higher.

B. Program Input

1. Height and temperature analysis and 0-48 hr prognoses for the 500-, 400-, 150-, and 100-mb levels.

C. Program Computations

1. The 500- to 400-mb temperature lapse rate is extrapolated upward to its intersection with the 150- to 100-mb lapse rate extrapolated downward. Height at the intersection is taken as the tropopause height.

D. Program Limitations

The tropopause height program uses upper-air parameters that are continuous in the horizontal, so the derived chart pictures the tropopause as a continuous surface. Actually, the tropopause has a leaf structure, with one or more breaks between Equator and the Poles. The jet stream core is found at these breaks. Since the jet core location can be determined from other parameters, such as a 500-mb isotherm concentration, the continuous surface presentation of the tropopause by the model is not a serious limitation.

E. Uses of the Product

The level of maximum wind is outlined by the tropopause height contours. Wind direction is normal to the tropopause height gradient. Speed can be estimated from the gradient, and confirmed by comparison with winds taken from the constant pressure chart nearest to the tropopause height.

For forecasting, the tropopause height charts can be used for:

1. Flight wind forecasting at or near the LMW level. Using jet stream winds to best advantage is important to modern high-performance aircraft.

2. Obtaining jet stream definition which, in turn, can be applied to forecasting clear air turbulence and in application of forecasting rules relating to trough and cyclone intensification. Jet stream turbulence most often occurs just below and to the left of the jet stream core (22,000-28,000 feet) and directly above and to the right of the core near the tropopause (35,000 to 50,000 feet). On intensification, a perturbation on a trough or any weak but already developed low will deepen in association with a well-defined jet stream. The low should be located to the left and forward of the jet maximum. The most rapid deepening will occur when the low reaches a position east of the long-wave trough (shown by the trough in the jet axis).

3. Aircraft can be sent to flight levels above the tropopause if conditions of smooth air, few clouds, and low incidence of contrails are desired. Keep in mind here that the tropopause height shown on the chart is actually 3000 feet below the true tropopause.

F. Relationship to Other Products

The tropopause program is used in the P.E. model.

G. Program Output

1. Tropopause Height (meters) analysis and prognoses for 0, 6, 12, 18, 24, 36, and 48 hrs. (Catalog No. Z01, Figure 4.12.1)

H. References or Suggested Reading

[1] Eddy, A., 1963; "A Statistical Model for Mid-Latitude Tropopause and Jet-Stream Layer, J. Meteor., 2, 219-225.

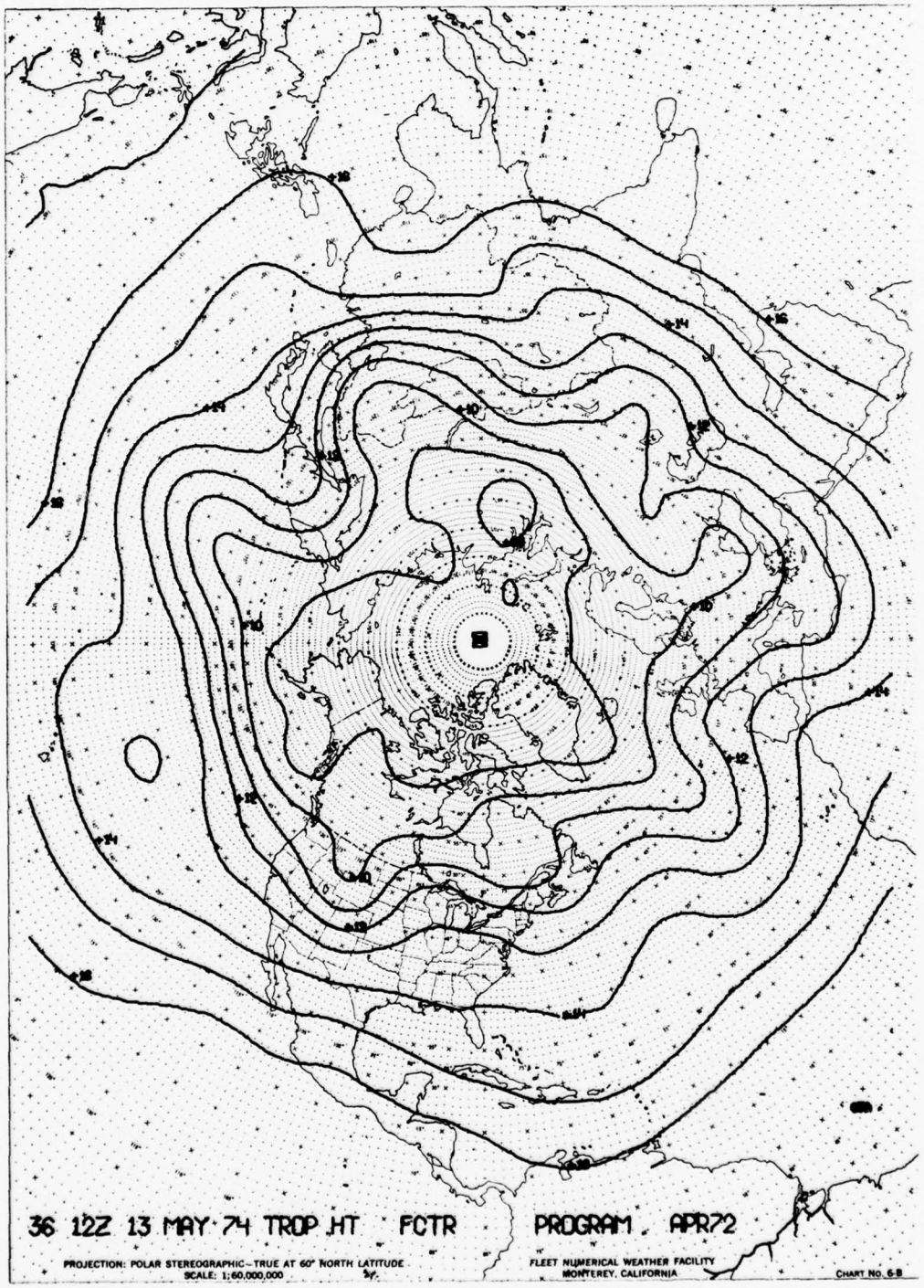


FIGURE 4.12.1 Tropopause Height 36-hr Prognosis (Z01)

4.13 FREEZING LEVEL ANALYSIS AND PROGNOSIS

A. Program Development

The program used to produce freezing level charts is quite simple. Calculations are made by the computer just as they would be done by hand. The height of the lowest freezing level above sea level is obtained by vertical interpolation of temperature between constant pressure levels.

B. Program Input

Height and temperature analyses and prognoses for 1000-, 850-, 700-, 500-, and 400-mb surfaces for 0, 6, 12, 18, 24, 36, and 48-hour periods.

C. Program Computation

1. The computer checks each mandatory upper level in succession, starting at 1000 mb. When the first reading below 0°C is encountered, interpolation to 0°C is performed between this level and the level below.

D. Program Limitations

The linear interpolation used between levels may introduce an error, since the process would not account for inversions that might be present. A further error might arise because of poor analysis or prognosis of one or more of the constant pressure surfaces used as input. However, except in unusual cases, the height error on the freezing level should be within 100 feet.

Only the lowest freezing level is selected in cases where two or more freezing levels may exist.

The interpolation extends only to terrain level. Thus, in regions where atmospheric temperatures are below freezing, isolines of freezing level will correspond to smoothed terrain heights.

In regions of strong freezing level gradients, such as in fronts, the freezing level prognosis will tend to be inaccurate because of the smoothing processes involved in deriving the prognostic charts.

E. Uses of the Product

Freezing level charts can be used in conjunction with other upper-air analyses for outlining layers of potential aircraft icing. The most severe icing occurs in the 0°C to -10°C layer, but it can occur at temperatures of -10°C to -25°C if the right moisture situation exists. Clouds of the cumuliform type are more apt to produce serious ice formation than others. Icing in clear air can occur above the freezing level if the temperature-dew point spread is less than 3°C; the aircraft motion triggers the sublimation process. Aircraft flying at 400 knots or more are not likely to have ice formation because of the heat produced by skin friction. This heating can amount to 20°C to 40°C, depending upon altitude.

The freezing level charts can be used, in a precipitation situation, to forecast a change from rain to snow. When the freezing level is forecast to drop to 5000 ft, forecast a change from rain to snow at that time.

Lightning strikes on aircraft are most likely to occur at the 0°C level. 0°C also happens to be the temperature at which the most dangerous (too rich) mixtures of aviation gas occur. If aircraft are being cleared through areas where lightning is probable, the 0°C level should be avoided.

F. Relationship to Other Products

The freezing level charts are not used as input to any other FNWC products.

G. Program Output

Freezing level analysis and prognoses (meters) for 0, 6, 12, 18, 24, 36, and 48 hours. (Catalog No. Z02, Figure 4.13.1)

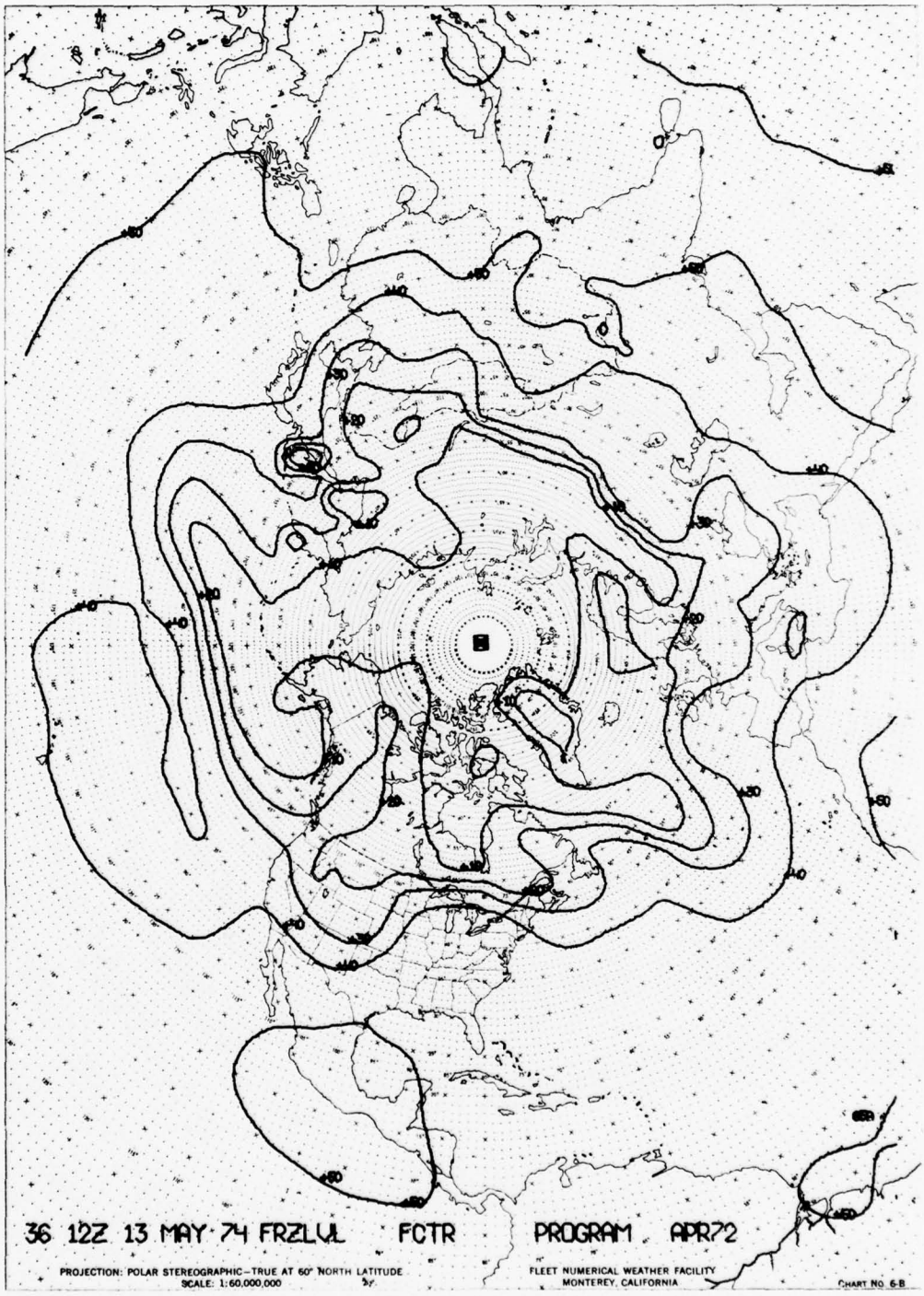


FIGURE 4.13.1 Freezing Level 36-hr Prognosis (Z02)

4.14 TURBULENCE FORECASTS

A. Model Development

Clear Air Turbulence (CAT) is a familiar phenomenon to all air travelers. As a flight hazard, CAT has grown in importance as faster and larger aircraft operate in the 30,000 to 45,000 foot layer, where CAT occurs with the greatest frequency. Structural damage is the main concern in military flight operations. Commercial airlines fear this, too, and they have the added consideration of passenger comfort. Customers have an understandable lack of enthusiasm for being bounced off the overhead by unexpected severe turbulence.

CAT has been studied intensely in the past decade, but the experts in the field readily admit that our understanding of CAT is far from complete. Wind shear and vertical stability seem to be the two most important causative factors, but the relative degree of influence and working relationship of these two is not well understood. There are other factors involved, too, such as the breaking of gravity waves in the free atmosphere.

Forecasts of a poorly understood phenomenon of small scale and transitory nature are bound to be of poor quality. But, since there is an operational requirement for turbulence forecasts, an attempt must be made to provide them.

Forecasts of CAT at FNWC are in two categories: high level (400-100mb) and low level (1000-850 mb). The forecasting methods differ, and the two levels will be discussed separately.

High Level

Because of the limited knowledge about causes and structure of CAT, no forecasting system based on a dynamic model was possible. The approach had to be empirical. The many observations on CAT showed that the highest consistent correlation with CAT occurrence was with strong vertical wind shear and with vertical instability. Stability values and the horizontal advection can be readily calculated from upper-air analyses and prognoses, while predicting the movement of wind shear patterns is a more difficult problem. The FNWC modellers chose stability as the forecast parameter.

The parameter, CCAT, is computed as a function of the horizontal advection of vertical stability. The CCAT equation shows how the parameters fit together:

$$CCAT = \frac{\eta g}{fT}\left[V \cdot \nabla \frac{\partial T}{\partial Z}\right] .$$

$V \cdot \nabla$ = horizontal advection (V is the mean geostrophic wind).

$\frac{\partial T}{\partial Z}$ = the lapse rate.

$\frac{\eta g}{fT}$ = includes the absolute (η) and earth's (f) vorticity, and acceleration of gravity (g).

The values for CCAT range from 0 to 200, and are divided into turbulence categories of Light (0-50), Moderate (50-100), Severe (100 or more). These categories were determined from the turbulence cases that were used in development of the formula. The formula itself is adapted from a theoretical study on the structure of turbulence (Ref. 1).

Low-Level Turbulence

Low-level turbulence, as defined for the FNWC model, is that which occurs in the 1000-mb to 850-mb layer. These levels were chosen because of available FNWC analyses and prognoses. The low-level turbulence forecasts are useful for low-level aircraft penetrations and occasionally for refueling operations.

Low-level turbulence is caused by friction and thermals. Friction can be that from the wind blowing over rough surfaces, or that within the body of air itself when a faster layer blows over a slower layer; this is mechanical turbulence. Thermals arise from instability caused by heating in the lower layers.

The factors to be considered, then, in developing a forecasting formula are: wind speed (there is little turbulence in a 5-knot wind), vertical stability, and vertical shear of the wind.

The mean wind velocity is easily derived from the constant pressure analyses. The other factors are included in a Richardson number. This is a number that has been used for years in the study of shearing flows of a stratified fluid, particularly air and water. The number, which has been verified in countless experiments, gives the ratio of work done against gravitational stability to energy transferred from mean to turbulent motion. When the Richardson number is below a certain critical value, instability is present, and the smooth flow will break up into eddies--the cause of turbulence.

The Richardson number is not complicated:

$$Ri = g\beta / (\partial v/\partial z)^2$$

- g: acceleration of gravity
- β: a representative vertical *stability, usually the* change of potential *temperature with height*
- $\partial v/\partial z$: a characteristic vertical shear of the wind

The interplay of parameters in the Richardson number is shown on a clear, cold winter night. As the layer of air near the ground cools, stability increases and the numerator of Ri grows larger and larger. The wind, meanwhile, decreases to near zero at the surface, while remaining strong aloft. The wind shear term in the denominator increases. But, turbulence does not develop in the normal case because the great thermal stability keeps Ri from ever going below the critical Richardson number. The formula for the FNWC model is:

$$PI = \text{Velocity}^2 \times \left[1 - \frac{\text{Richardson number}}{\text{critical Richardson number}}\right] .$$

After testing, the critical Richardson number was set at 10. The PI stands for Panofsky Index, since the FNWC formula was an adaptation from one of Panofsky's.

The answers for PI come in numbers like 30×10^5; the large numbers arise because computations are done in centimeters per second. For output the 10^5 is dropped, and the numbers of 30 or 40 or 50 are sent to the users. The higher the number, the greater the turbulence.

B. Program Input

1. Height and temperature analyses and prognoses for 400-, 300-, 200-, and 100-mb surfaces (For CAT).
2. Height and temperature analyses for 1000 mb and 850 mb (For low-level turbulence).

C. Program Computation

High Level

1. Compute vertical stability at grid points.
2. Compute geostrophic wind at grid points.
3. Compute CCAT parameter.
4. Output relative values of CCAT values in isoline form.

Low Level

1. Compute geostrophic wind at grid points.
2. Compute vertical stability between 1000 mb and 850 mb.
3. Compute Richardson numbers.
4. Compute low-level turbulence.

D. Program Limitations and Vertification

High-Level Turbulence

The various CAT forecasting methods all produce rather disappointing results. Skill scores run about 15-20% on all methods. The CAT program is limited in efficiency and held back from any dramatic improvements for these reasons:

1. Meteorological data available for operational forecasting do not provide sufficient vertical, horizontal, or temporal resolution to compute desired parameters in the mesoscale structure where turbulence occurs. The spacing of the upper-air network is a case in point.
2. The meteorological parameters used to forecast CAT--parameters that correlate highly with CAT occurrence--are difficult to forecast with high accuracy.
3. Most reports of CAT are subjective and only positive encounters are reported. Reports vary with different pilots, with type of aircraft and aircraft speed.
4. Knowledge of the causes and nature of turbulence is still incomplete.
5. Because large-scale parameters must be used to forecast a small-scale phenomenom, any CAT model will tend to overforecast area-wise. Forecast CAT areas will tend to be larger than the actual areas.

Low-Level Turbulence

The PI Index should verify quite well, as it is based upon sound theoretical formulas and the data used in the forecast are drawn from low-level analyses where data are plentiful. No verification of this model has been attempted.

E. Uses of the Products

High-level turbulence forecasts can be provided as part of the regular flight clearance routine. The forecasts should be provided for any air refueling operations planned for these relatively high altitudes. The forecasters present the information on the basis of the turbulence categories--0-50 light, 50-100 moderate, and 100 or greater as high.

Low-level forecasts can be used for low-level penetrations, either actual or exercise. In rare cases, air refueling operations can use these forecasts.

It should be kept in mind in presenting turbulence forecasts that the turbulence effects increase by the square as the aircraft speed increases.

F. Relationship to Other Products

The turbulence forecasts are purely for operational use, and they are not used in the production of any other FNWC products.

G. Program Output

1. Clear Air Turbulence analysis and prognoses for 0, 6, 12, 18, 24, 36, and 48 hours for the 400-mb to 300-mb layer (Catalog No. Z03), the 300-mb to 200-mb layer (Catalog No. Z04), and the 200-mb to 100-mb layer (Catalog No. Z06).
2. Low-level turbulence index values (PI) for analysis time (Catalog No. Z08). At present, PI values are provided only for overwater areas.

H. References or Suggested Reading

[1] Theodorsen, T., Structure of Turbulence, Technical Note BN-31, University of Maryland.

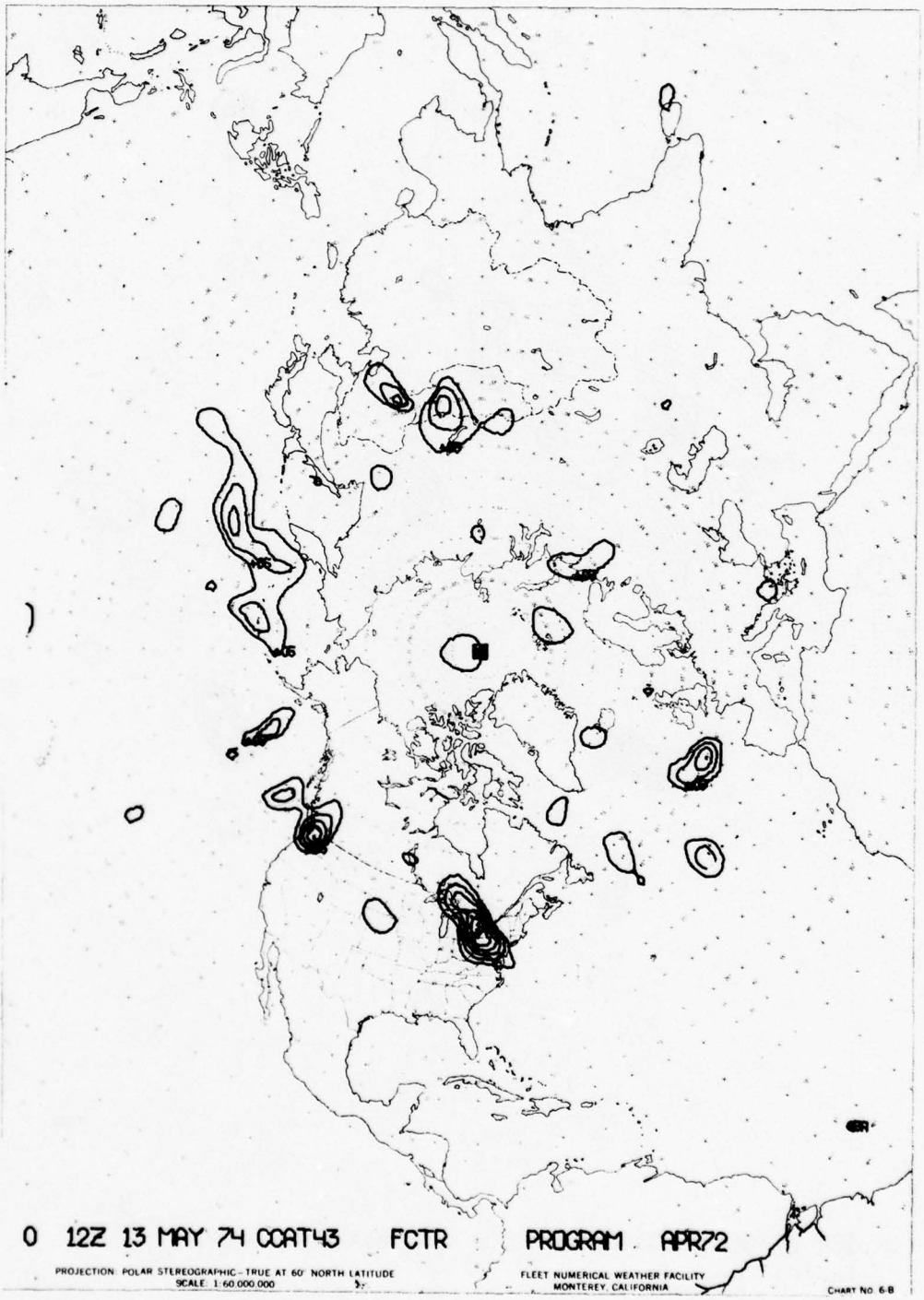


FIGURE 4.14.1 CAT Analysis for 400-300-mb Layer (203)



FIGURE 4.14.2 CAT Analysis for 300-200-mb Layer (Z04)

4.15 ATMOSPHERIC FRONTS

A. Model Development

Frontal analysis has always been a highly subjective process. In any weather office, interpretations of frontal locations and existence vary with each change of the watch. A recent set of comparisons of surface frontal analysis for the same map times, made from output of 16 international and national weather centers, showed wide variations in frontal positions--as much as 300 miles in many cases. Some centers had fronts in places where others had none.

Since fronts are such an important concern in forecasting for military operations, development of an objective numerical frontal analysis scheme at FNWC seemed in order. Advantage could be taken of the many numerically derived data fields available at FNWC that might be useful in frontal analysis. A study was started to (1) determine the best and minimum number of parameters for describing fronts and (2) to develop an objective analysis method for use with the parameter or parameters chosen.

Nearly every possible parameter capable of describing a front was considered and tried in test analyses. To show the thoroughness of the parameter search, the trail-horse candidates are listed: wet bulb potential temperature, equivalent potential temperature, potential temperature, 1000-mb and 850-mb temperatures, temperature at a smoothed terrain level, surface air temperature, temperatures at other than mandatory pressure surfaces, temperatures representative of low tropospheric layers of various depths (1000 mb to 700 mb, for example), and temperature anomalies relative to suitably defined reference atmospheres. Each parameter tested showed good and bad qualities, as a result of such factors as reduction to sea level problems, non-representiveness of surface temperatures, land-sea contrasts, and topography problems. The test results pointed to a solution of using a temperature parameter at a suitable low tropospheric level to minimize terrain effects. Hemispheric moisture patterns are hard to depict accurately, so the equivalent and wet bulb potential temperatures were eliminated on this count. This left potential temperature (θ) standing alone as the chosen parameter. The potential temperature is obtained by calculating the 1000-700-mb thickness from the 1000-mb and 700-mb analyses, and converting the thickness to the mean potential temperature of the layer.

The complete frontal parameter is obtained by application of a mathematical operator (GG) to the potential temperature (θ). GG stands for gradient of a gradient; for the GG θ frontal parameter, it is the directional derivative of the gradient θ along its gradient. The mysteries of the GG operator are explained in Section 3.8. After the operator is applied, the GG θ values at each grid point are analyzed in the horizontal.

Axes of the GG θ patterns accurately depict the warm air boundaries of low-level baroclinic zones of distinct thermal gradient or, more simple, the GG θ fields mark the division between two air masses of different thermal structure. Conventional analysis methods may not account for all such baroclinic zones; the GG θ analysis gives warning of their presence. Further, the GG θ analysis gives an intensity estimate for each frontal zone. This is valuable forecasting and analysis information.

The FNWC GG frontal analyses are not intended to replace the final, hand-touch frontal placement. The large grid size, and possible inaccuracy in upper-air temperature analyses over sparse-data areas, precludes a GG θ accuracy better than $\pm$100 miles. The FNWC frontal analyses are for guidance to the field analyst. They tell him where to look for potential fronts and how strong the fronts might be. In effect, this gives him an educated, scientifically sound, and reliable first guess to start his own analysis.

B. Program Input

1. 1000-mb and 700-mb analyses and prognoses for 0, 12, 24, 36, and 48 hours.

C. Program Computation

1. Compute the 1000-700-mb thickness.
2. Convert the 1000-700-mb thickness to a mean potential temperature field.
3. Apply the GG operator to the potential temperature field.
4. Analyze the GG θ field in the horizontal.

D. Program Limitations and Verification

The GG θ frontal analysis program has a few built-in weaknesses:

1. False indications of a low-level baroclinic zone may appear in mountainous regions because of the inaccuracy involved in reducing surface data to sea level.
2. The GG θ frontal analysis scheme does not work well with occlusions. GG θ is designed to distinguish between air masses with thermal contrast. In many occlusions, isotherms intersect the frontal discontinuity at sharp angles, producing a weak horizontal thermal gradient across the frontal zone. GG θ, thus, finds no front.
3. GG may lag considerably behind a fast-moving thin cold wedge, but usually the major middle and upper clouds will lag with the GG front and the forecaster can adjust accordingly.
4. Regions of fast-forming strong inversion development, with the strong low-level thickness gradients, may produce false frontal indications on the GG θ analysis.

The strong feature of the GG program is that it won't miss a baroclinic zone (even if it does throw in a false one now and then). Subjective analysis can lose fronts with the greatest of ease. Further, GG gives an indication of the strength of the baroclinic zone, so strong and weak fronts can be distinguished, and frontogenesis and frontolysis can be detected well before synoptic data would indicate either condition.

The GG θ approximation to location of fronts is as valid as FNWC's upper-air mass structure model, on which the frontal parameter is based. FNWC's upper-air analysis program is one of its strongest.

E. Uses of the Product

The analyst with his GG θ analysis in hand is like a hunter with a bird dog. He has powerful help in the search problem.

A suggested order of steps in using the GG chart is as follows:

1. Use the GG chart as an underlay to the surface pressure analysis. This will show the analyst approximate locations of fronts and non-frontal troughs, or about where to start looking for them.
2. First analyze the areas of the chart where confidence can be strong. This would be over dense-data areas and in other places where the GG chart shows strong fronts (by the greater number of GG chart isolines around the area). Using GG fronts as a guide, use your own data to pinpoint frontal locations and configurations. If an area is completely devoid of data, use the suggested GG θ frontal position, moving the front somewhat toward the warm air. Keep the frontal-strength indications in mind for later forecasting purposes.
3. Use the frontal strength indicators in connection with past charts to locate areas of frontogenesis and frontolysis. Add or drop fronts as necessary.
4. Over mountainous areas, the GG analysis is suspect. (Mexico and Greenland are examples.) Don't believe GG frontal indications unless you have overwhelming evidence from your own surface reports.
5. Watch for the not-too-frequent cases of a rapidly-moving thin wedge of cold air. GG will lag this, as will the frontal clouds. In this case, rely on your surface reports to locate the cold front.

6. The GG handles occlusions poorly, because the air around the center of circulation tends to be homogeneous, with weak horizontal thermal gradient. GG can't find any baroclinic zone. Your own analysis should be adequate for the occlusion case. They are usually well defined in the isobaric pattern, and have a good history.

The final frontal location analysis derived from following the above procedures should be precise to within a degree, or even half that in dense data areas. Adding the GG intensity indicators to the picture, the forecaster can proceed with confidence.

F. Relationship to Other Products

The GG θ atmospheric frontal analysis is not used in production of any other FNWC products. Its primary use is for guidance to the field analyst in locating fronts on the FNWC surface pressure analysis.

G. Program Output

1. Frontal analysis and prognosis at 0, 12, 24, 36, and 48 hours.

H. References or Suggested Reading

[1] Renard, R. J. and L. C. Clarke, 1965; "Experiments in Numerical Objective Frontal Analysis, Monthly Weather Review, 93, pp. 547-556.

[2] Clarke, Leo C. and Robert J. Renard, 1966; "Objective Frontal Analysis", Technical Note No. 24, Fleet Numerical Weather Facility, Monterey, California, August 1966.



FIGURE 4.15.1 Atmospheric Fronts Analysis (Z10)



FIGURE 4.15.2 Atmospheric Fronts 48-hr Prognosis (Z10)

4.16 TROPICAL CYCLONE STEERING TRAJECTORIES (HATRACK AND MOHATT)

A. Model Development

The strong demand for accurate forecasts of tropical cyclone movement and intensity never ceases. The Navy, with ships at sea and bases at vulnerable locations along shorelines, has been in the forefront in encouraging development of improved forecasting methods. It was only natural, then, that development of some forecasting scheme should be attempted which would take advantage of the numerically-analyzed operational products of FNWC. The numerical-statistical scheme to be described has been under development at FNWC and the Naval Postgraduate School since 1965.

The model developers started work with the knowledge that every conceivable forecast parameter had been used, alone or in combination, in the dozens of tropical cyclone forecasting methods already tried. The problem would not be to discover new parameters, but to pick those with the most promise and develop an improved method for using them. Variations of steering methods had the best track record among the many existing forecast techniques, so development thinking turned in this direction.

The assumptions made in tropical cyclone steering methods are (1) that the tropical cyclone is a perturbation whose movement will be governed by a basic flow generally unaffected by activity within the perturbation, and (2) that movement of the tropical cyclone will be governed by that part of the major flow which affects the storm circulation (this would vary with circulation size in the horizontal and vertical). A choice of just one level for steering involves the assumption that the chosen level is representative of the mean basic flow from surface to the top of the tropical cyclone circulation.

While the basic flow may not be changed by the tropical cyclone, it is masked by the storm circulation. Older steering methods tried to get around this problem by picking steering levels above the storm circulation, or by extrapolating winds from outside the storm's influence. A far better solution to the problem was available at FNWC in the unique Scale and Pattern Separation program. This technique makes it possible to separate small-scale, short-wave disturbances (SD) from the total daily circulation, leaving a residual of the large-scale, long-wave features (SR). Thus, the smaller-scale tropical cyclone circulation can be extracted, leaving the larger-scale steering flow open to view. The first trials on the model for forecasting tropical cyclone movement were started by using FNWC Scale and Pattern Separation products.

The first step in using the SR fields for steering is to compute the geostrophic SR winds; these yield the steering or basic current. The standard finite difference form of the geostrophic wind equation is used to get the winds at grid points. A modification of the sine function in the equation was devised for use south of 30°N. This modification avoids difficulty with the coriolis parameter in these latitudes--a perennial problem in tropical areas whenever the straight geostrophic approximation is used.

The first tests using the SR geostrophic winds for steering involved many different levels--1000 mb, 700 mb, 500 mb, 200 mb--as well as layer combinations of 1000/500 mb, 1000,200 mb, and 500/200 mb. Forecasts made with the SR steering winds (called HATRACK*) were compared with official forecasts in the 1965 season (Ref. 1). The official forecasts were better by about 10 percent than forecasts made from the best-performing numerical steering levels of SR-700 in the Atlantic and SR-500 in the Pacific, indicating that SR steering by itself was not the answer.

In the test above, the forecast and best tracks were similar in shape but the forecast positions lagged their best-track counterparts. This suggested a consistent deficiency in both zonal and meridional components of the numerical steering forecasts and, hence, that the vector error between forecast and best-track positions represents a bias which might be used profitably to modify subsequent numerical-steering forecasts. In effect, the storm behavior tells us there is something a little wrong

*HATRACK = Hurricane and Typhoon Tracking.

with our steering; it might be use of the wrong steering level or layer, the steering-level analysis may be bad, or the steering-level pattern may be undergoing change that is not reflected in the analysis being used for forecasting. Whatever the problem might be, the assumption is that past errors will continue to occur in the same way and a correction can be made to the forecast based on past errors. It is a simple, but unique, application to continuity.

Tests were run on the 1967 North Atlantic data using 6-, 12-, and 24-hr bias corrections on the SR steering forecasts. Only the 500-mb and 700-mb levels were used. The forecasts were improved from 25 to 50 percent, and thus the adjusted HATRACK forecasts were consistently better than the HATRACK and official forecasts (Ref. 2).

A much-improved method of correcting for bias of the HATRACK forecast has recently been devised (Refs. 3,4). MOHATT* (as this scheme is now called) was tested in use against 1967 and 1968 North Atlantic tropical cyclone data. The results showed a still further improvement over the HATRACK method and the original bias adjustment. Again, the forecasts were consistently superior to the official forecasts.

The new bias corrections are largely a function of a linear extrapolation of the 6- and 12-hour HATRACK forecast errors to 84 hours. Figure 4.16.1 shows a sample HATRACK forecast. Figure 4.16.2 illustrates a worksheet example of manually computing the MOHATT forecast from the computer-produced HATRACK information. The MOHATT forecast program is now fully automated.

MOHATT forecasts may be made for the 1000-mb, 850-mb, 700-mb and 500-mb steering levels, using an analysis and its attendant P.E. prognoses. Statistically, the 700-mb level has proven to be the best SR level in the North Atlantic while there is still indecision between 700 mb and 500 mb in the eastern and western Pacific areas. However, all forecast levels are verified regularly in order to search for improvements to the scheme under varying conditions.

B. Program Input

1. Current analyses for 1000 mb, 850 mb, 700 mb, and 500 mb.
2. Prognoses for 1000 mb, 850 mb, 700 mb, and 500 mb for 6, 12, 18, 24, 30, 36, 42, 48, 60, and 72 hours.

C. Program Computation

1. Convert 1000-, 850-, 700-, and 500-mb "D" fields to SR fields.
2. Derive geostrophic wind fields from 1000-, 850-, 700-, and 500-mb SR analyses and prognoses, to 72 hours.
3. Steer the tropical cyclone in 3-hr steps from 3-84 hrs.
4. Calculate bias corrections to the HATRACK forecasts using FNWC program MODHATR (*operational version of MOHATT*).

D. Program Limitations and Verification Limitations

The tropical cyclone steering model has several limitations. The correction for bias compensates for some of them, but obviously not fully or all the developmental test forecasts would have been perfect. The limitations are:

1. Poor basic analyses. The tropical area has been always notorious for data deficiency, particularly in areas not crossed by the usual airline and surface ship routes. The upper-air reports, used to obtain the SR fields, are so widely scattered that both hand and machine analyses will often miss small-scale systems completely. The sudden appearance of small tropical cyclones on the charts is a good example. The bias correction tends to correct for poor analysis, but it will be weak whenever rapid pattern changes are underway.

*MOHATT = Modified Hurricane and Typhoon Tracking.

```
TROPICAL CYCLONE STEERING
PROG MODE
J01 TD05
ANAL TIME     00190871
LEVEL     700 MBS
00190871     137N 0573W  2911
06190871     140N 0587W  2815
12190871     143N 0603W  2815
18190871     146N 0618W  2813
00200871     149N 0634W  2815
06200871     152N 0652W  2817
12200871     155N 0673W  2821
18200871     158N 0694W  2819
00210871     162N 0715W  2819
06210871     165N 0737W  2819
12210871     169N 0758W  2817
18210871     172N 0778W  2817
00220871     176N 0795W  2915
06220871     181N 0812W  2915
12220871     187N 0829W  2915
```

Fig. 4.16.1 Sample HATRACK forecast set for tropical-cyclone CHLOE initiated from 13.7N, 57.3W at 0000 GMT 19 August 1971.

Worksheet for Computing 12, 24, 36, 48, and 72 hour MOHATT Forecasts

Basic Formulae: $E'_t = E_{12} + [(E_{12} - E_6)(t-12)]/6$ $\qquad F'_{t-12} = F_t + E'_t$

F_t = HATRACK forecast position at time t

F'_{t-12} = MOHATT forecast position at time t-12

E_t = Error in F_t, computed as true minus forecast position

E'_t = Estimated error of F_t for forecast interval > 12 hr.

Tropical cyclone 5 (#), CHLOE (name), 700 MB (steering level) HATRACK forecast initiated from 13.7N 57.3W (lat-long) at t_o = 00 Z (time) 19081972 (date)

		Latitude component	Longitude component
at t_o + 6 hr:	a = E_6 =	0.0° lat.* -0.15	+0.8° long.*
at t_o + 12 hr:	b = E_{12} =	-0.3° lat.*	+0.5° long.*
	c = b-a =	-0.15° lat.	-0.3° long.

F'_{12} at t_o + 24 hr = 00 Z 20 (time date):
- Latitude: $F'_{12} = F_{24} + E'_{24}$ (b+2c) = 14.9 + (-0.6) = 14.3° lat.
- Longitude: $F'_{12} = F_{24} + E'_{24}$ (b+2c) = 63.4 + (-0.1) = 63.3° long.

F'_{24} at t_o + 36 hr = 12 Z 20 (time date):
- Latitude: $F'_{24} = F_{36} + E'_{36}$ (b+4c) = 15.5 + (-0.9) = 14.6° lat.
- Longitude: $F'_{24} = F_{36} + E'_{36}$ (b+4c) = 67.3 + (-0.7) = 66.6° long.

F'_{36} at t_o + 48 hr = 00 Z 21 (time date):
- Latitude: $F'_{36} = F_{48} + E'_{48}$ (b+6c) = 16.2 + (-0.9) = 15.3° lat.$
- Longitude: $F'_{36} = F_{48} + E'_{48}$ (b+6c) = 71.5 + (-1.3) = 70.2° long.$

F'_{48} at t_o + 60 hr = 12 Z 21 (time date):
- Latitude: $F'_{48} = F_{60} + E'_{60}$ (b+8c) = 16.9 + (-0.9) = 16.0° lat.$
- Longitude: $F'_{48} = F_{60} + E'_{60}$ (b+8c) = 76.8 + (-1.5) = 75.3° long.$

F'_{72} at t_o + 84 hr = 12 Z 22 (time date):
- Latitude: $F'_{72} = F_{84} + E'_{84}$ (b+12c) = 18.7 + (-0.9) = 17.8° lat.$
- Longitude: $F'_{72} = F_{84} + E'_{84}$ (b+12c) = 82.9 + (-1.5) = 81.4° long.$

SPECIAL RULES:

*(1) For b=0: If $a \geq 0$, set b = +0.1; If $a < 0$, set b = -0.1; and if $|a| > 0.2$, set $|a| = 0.2$

*(2) For a and b with opposite algebraic signs, set a = 0.5b

*(3) For a = 0 and b ≠ 0 or both a and b with same algebraic sign:
If $|a|/|b| > 2.0$, change $|a|$ so that a/b = +2.0
If $|a|/|b| < 0.5$, change $|a|$ so that a/b = +0.5

$(4) For $E'_t/b > +3.0$, change E'_t so that $E'_t/b = +3.0$
For $E'_t/b < -3.0$, change $|E'_t|$ so that $E'_t/b = -3.0$

Fig. 4.16.2 Worksheet for computing 12-, 24-, 36-, 48- and 72-hour MOHATT forecast positions. Example plotted is derived from the HATRACK forecast set in Fig. 4.16.1 and known positions of Chloe at 0600 GMT, Aug. 19, 1971 (14.0°N, 59.5°W) and 1200 GMT, Aug. 19, 1971 (14.0°N, 60.8°W).

2. Operational warning positions frequently have substantial errors. Best-track and operational warning positions, in one study, averaged a difference of nearly 30 miles. This 30 miles would come from a 12-15 mile average error in recon center location, from a poorly defined eye or, more often, from the absence of a recon fix near warning time. If HATRACK starts a forecast from a wrong position, the error will compound with time; the error is unlikely to get smaller than the initial starting error.

3. The bias correction may not work well in cases of sudden acceleration or deceleration of the center occurring near or soon after forecast time.

4. The steering level is supposed to represent the mean flow of the basic circulation. Choice of the proper steering level is difficult. In the Atlantic, the 700-mb level has proven to be best. In the western and eastern North Pacific, there is still an option. The choice must be subjective, at the present state-of-the-art, so despite much soul-searching and quick review of old rules-of-thumb, the choice may wind up at the wrong level. This can only result in forecast error, sometimes severe. There is no way to tell about the steering level choice until the next recon or radar reports arrive. Only then will the forecaster know that he's a bum for having picked 500-mb steering, when he could have been a hero at 700-mb. The bias correction compensates in part for wrong choice of steering level, and will continue to do so through the forecast period until there is marked change in the basic flow pattern.

5. The Scale and Pattern Separation program largely removes the tropical cyclone circulation from the total flow; the cyclone is treated as a small-scale perturbation. Occasionally, a monster tropical cyclone appears on the scene, with a circulation diameter of 800-1200 miles--a little out of the perturbation class. In such cases, the Separation technique is overwhelmed and cannot remove the whole tropical cyclone circulation. This results in the disconcerting development of having the HATRACK program steering the cyclone around its own circulation. With huge cyclones, it may be best to use extrapolation vice an objective forecast scheme like MOHATT. The giant storms usually are not erratic in movement.

6. MOHATT forecasts on those rare storms occurring south of 10°N have not verified well. This is thought to be caused by difficulties in deriving the geostrophic winds--the coriolis parameter problem again. In the south-of-10° cases, little weight should be attached to MOHATT. Move the storms by extrapolation until you're up to 10°N, then fire up the objective scheme.

Verification

Tropical cyclone forecasts receive a more rigorous verification than any other type. The forecasting stakes are high; there are competing forecasting methods; and there are newly developed forecasting methods trying to win a place on the team. The tropical forecasting centers compile elaborate statistics on verification at the end of each season. Each forecasting method is measured against all others, using the simple criterion of where the storms were supposed to go against where they went. The method with the smallest average error is adjudged the best. MOHATT, a function of HATRACK and its statistical modification, has shown skill relative to both objective and subjective forecast methods in the North Atlantic. A comparison of MOHATT to TYRACK and NHC 67 in 1971 is shown in Figure 4.16.3, while the three-year (1971-1973) comparison of official and MOHATT forecasts is shown in Figure 4.16.4. Following Refs. 3 and 4, Figure 4.16.4 shows a stippled area which contains the line of equivalence of the two forecasts. The position of the line is not accurately known; it is dependent on the actual official forecast interval.

E. Uses of the Product

The mechanical application of MOHATT forecasts is uncomplicated. The forecasts assign a position for the tropical cyclone for every six hours out to 72 hours.

F. Relationship to Other Products

The MOHATT tropical cyclone trajectory forecasts play no part in the production of other FNWC products. The program uses upper-air analyses and prognoses at 1000-mb, 850-mb, 700-mb, and 500-mb. These analyses and prognoses are subjected to the Scale and Pattern Separation Program to obtain SR fields at all four levels.

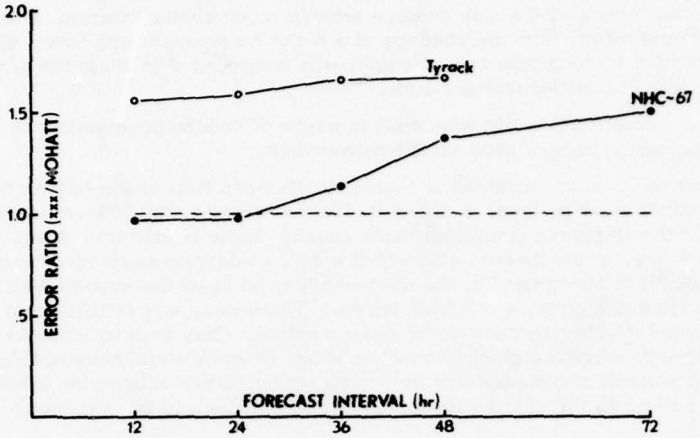
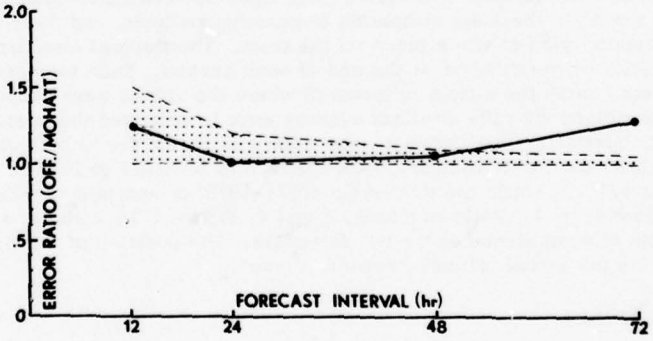


Fig. 4.16.3 Error ratios of NHC-67 and TYRACK to MOHATT (700-mb steering, operational bias) forecasts for 1971 North Atlantic tropical cyclones. Line of equivalent accuracy is 1.0 (dashed). Number of forecasts and MOHATT errors (kt) are also indicated.

MOHATT vs. Official Forecasts

North Atlantic Tropical Cyclones (1971-73)



No. of fcsts:	296	256	186	142
MOHATT Error: (kt)	6.0	6.0	5.5	5.0

Fig. 4.16.4 Comparison of Official and MOHATT forecasts.

G. Program Output

Steering trajectory positions for every six hours out to 84 hours from time = 0 based on analyses and prognostic charts for the four levels of 1000-mb, 850-mb, 700-mb and 500-mb. Modified steering trajectory positions (MOHATT) for every six hours out to 72 hours based on bias corrections to the HATRACK forecast positions.

H. References or Suggested Reading

[1] Renard, R. J., 1968; "Forecasting the motion of tropical cyclones using a numerically derived steering current and its bias", Mon. Wea. Rev., 96, 453-69.

[2] Renard, R. J., and W. H. Levings, III, 1969; "The Navy's numerical hurricane and typhoon forecast scheme: application to 1967 Atlantic storm data", J. Appl. Meteor., 8, 717-25.

[3] Renard, R. J., S. G. Colgan, M. J. Daley, and S. K. Rinard, 1972; "Numerical Statistical Forecasts of Tropical-Cyclone Tracks by the MOHATT Scheme with Application to the North Atlantic Area", Technical Note 72-4 FNWC, Monterey, California, 41 pp.

[4] Renard, R. J., S. G. Colgan, M. J. Daley, and S. K. Rinard, 1973; "Forecasting the Motion of North Atlantic Tropical Cyclones by the Objective MOHATT Scheme", Mon. Wea. Rev., 101, 206-214.

4.18 CONVECTIVE INSTABILITY ANALYSIS AND SEVERE WEATHER THREAT

A. Model Development

Two models are involved here. The first, called CCU for Convective Cumulus, is a model designed to forecast those areas where thunderstorms and heavy convective showers are likely to occur. The second model, called SWEAT for Severe Weather Threat, is designed to forecast areas of probable severe thunderstorm and tornado occurrence. Both models are based on stability indexes, but the differences necessitate separate discussions.

The CCU Model

Many stability indexes have been devised over the years. The familiar Showalter Index is one example. It served a useful purpose in its day, but was somewhat gross in its definition. Forecasters sought refinement.

In the search for a reliable stability index, the FNWC modellers made a careful review of all possible forecast parameters. They finally settled upon basing the index on the simple but fundamental parameter derived from the definition of convective instability--a decrease of equivalent-potential temperature with height (AMS Glossary of Meteorology). Various layers and combinations of layers were tested. The parameter that gave the most consistent results was the difference in equivalent-potential temperature between 850 mb and 500 mb. The calculation is simple, and the forecasts have been quite reliable.

It might be noted here that the CCU analyses in the tropics are characterized by negative values, which just says that mT air is normally convectively unstable. Stable CCU values are the norm for mid and high latitudes. The thunderstorm action starts with intrusions of mT air into higher latitudes.

Severe Weather Threat (SWEAT) Index

The SWEAT index is an Air Weather Service development. The index provides an indication of the potential for tornadoes and severe thunderstorms. FNWC uses the AWS SWEAT formula in unaltered form, with values from FNWC products as input.

The SWEAT index is a good example of an empirically-developed forecasting formula. Over 300 tornado cases from recent years were used by experienced severe-weather forecasters in a study to determine the meteorological conditions sufficient and necessary for the development of tornadoes and severe thunderstorms. The most important parameters involved stability, low-level moisture, and wind shear. After the vital parameters were selected, the study determined weighting factors for each parameter. The final formula was used in all the test cases to establish the SWEAT value at or above which severe weather is almost certain to develop. A very high verification (over 90% for some months) of forecast severe weather areas was achieved in the first six months of operational use of the SWEAT index.

The SWEAT formula is given here to show what parameters and weighting factors are used in the calculations.

$$I = 12D + 20(T-49) + 2f_8 + f_5 + 125(S+0.2)$$

where D = 850-mb dew point,

T = sum of 850-mb temperature and dew point,

f_8 = wind speed at 850 mb,

f_5 = wind speed at 500 mb,

S = sin (500-mb wind direction - 850-mb wind direction).

Note that the SWEAT index forecasts severe thunderstorms, not regular. It has no value as a forecast tool for ordinary thunderstorms. The CCU Index must be used for these.

B. Program Input

CCU Model

1. Height, temperature, and dew-point depression analyses for 850- and 500-mb surfaces.

SWEAT Model

1. Analysis and prognoses at 6-hr intervals from 0-48 hours for 850-mb and 500-mb dew point, temperature, wind speed and direction.

C. Program Computation

CCU Model

1. Compute equivalent-potential temperature at 850 mb and 500 mb.
2. Subtract equivalent-potential temperatures at 850 mb from 500-mb values.

SWEAT Model

1. Extract temperature, dew point, and wind values from 850-mb and 500-mb charts. Apply values in the SWEAT index formula.

D. Program Limitations and Verification

CCU Model

The CCU model is vulnerable to changes in the stability pattern brought about by convective activity itself or by rainfall from a higher cloud layer. Convective activity causes changes in the mid-level moisture, thus the stability; here, it could be said that the changes in equivalent-potential temperature profiles are the result of rather than the cause of increased convective activity. In the rainfall case, a fairly deep layer that is only moderately convectively unstable becomes saturated--not by lifting--but by evaporation of water into it from rain falling from a higher cloud layer. Instability results, with thunderstorms following.

The above two effects, combined with occasional errors in the analysis input, will cause errors in the CCU product. However, in daily use CCU has proved to be highly reliable at showing the areas where thunderstorms will occur, provided the forecaster injects the proper triggering action factor.

The CCU index will not differentiate the severe from normal thunderstorms.

SWEAT Index

The SWEAT index is only to specify and predict areas of potential severe weather activity. Pinpointing the location of small-scale features such as tornadoes is beyond the capability of any existing forecast model.

SWEAT index values give no more than an indication of the potential for severe weather. A high SWEAT index for a given time does not necessarily mean that severe weather is occurring or will occur. There has to be some type of triggering action to realize the potential. The forecaster must inject subjective judgment as to whether some sort of triggering action is likely, and experience counts heavily here. A beginner will get many more busts than the old-hand forecaster.

FNWC has attempted no formal SWEAT verification program. The AWS high verifications are accepted as proof that the model--properly used--is reliable.

E. Uses of the Product

CCU Model

The CCU is of use in area-type forecasts of potential thunderstorm activity. Flight clearances and area rainfall estimates are involved.

CCU fields cannot be used just at face value. Thunderstorms don't necessarily occur in areas where CCU values are negative. If this were so, tropical areas would be covered with thunderstorms nearly every day. The forecaster must evaluate and account for triggering action in the areas of negative CCU values. The triggering action can come from one or more of the following: a front, airflow over high ground, a high-level trough, jet streams, strong low-level heating.

SWEAT Model

The main operational uses of the SWEAT index analyses are for flight forecasting, small boat operations, and air station management. The Air Force uses the Severe Weather Warnings to set alert categories at their airfields. Depending upon the particular type of alert, aircraft are hangared, tied down, or evacuated.

In field use, the forecaster first locates areas in the analysis where SWEAT values are 300 or more. The threshold value for severe thunderstorms is 300; for tornadoes it is 425. Then, over the potential severe weather area, the forecaster superimposes analyses of the most important parameters involved. These would include: low level jets; winds at 850 mb, 700 mb, and 500 mb; confluent and diffluent areas at different levels; moisture patterns; troughs and ridges at 850 mb, 700 mb, and 500 mb. From these patterns, plus the maximum temperature forecasts, the forecaster decides: (1) if the SWEAT index is telling a true story--that the situation is potentially explosive and (2) if there is an appropriate triggering mechanism, such as an approaching trough or the right combination of instability with daylight heating. If everything fits, the forecaster can use his SWEAT values with considerable confidence.

F. Relationship to Other Products

The CCU and SWEAT products are only for use in operational forecasting, and are not used in any other FNWC products.

G. Program Output

1. Convective Instability analysis (Catalog No. Z05).
2. Severe Weather Threat Index analysis and prognoses for 6, 12, 18, 24, 36, and 48 hrs (Catalog No. Z07).

4.19 FLIGHT WINDS FORECAST

A. Program Development

The flight-winds forecast programs are an automation of previous manually prepared flight forecasts. The same data and the same techniques are used, but the computerized forecasts work from a better analysis and wind input basis, and the computer can handle a much larger volume with no degradation of quality.

For several years, FWC Pearl provided computerized flight wind forecasts for the Pacific. The wind forecasts were based upon a tropical wind analysis over the area from 24°S to 37°N and from 90°W to 75°E; from 37°N to 60°N, FNWC wind analyses were used. The Pearl program was excellent, and provided useful clearance information for about 100,000 flights a month during the height of the Viet Nam action.

In 1972, the Global Band model (Section 4.4) was made operational. This model included many more refined analysis techniques than the Pearl model, and the wind-field products were expected to be appreciably better. The two models were compared for accuracy (by FWC Pearl) over a period of many months. The Global Band proved to be as good or better, in addition to providing greater geographical coverage at a finer 2.5° grid mesh. So, in late 1972 the FWC Pearl tropical model was replaced by a combination of Global Band and P.E. models.

In the latter half of 1974 a major reorganization of flight forecast programming responsibility was effected. During this period the Weather Centrals began to assimilate FWC Rota's (Rota, Spain) program FLTPLAN into their operational computer runs. At the same time a flight wind forecasting program similar to the existing Pearl model was implemented at FNWC and flight forecast responsibilities formerly held at FWC Pearl were assumed by FNWC. The remainder of this section is descriptive of only the FNWC flight wind forecast program, since the FWC Rota program is substantially different.

At FNWC, Global Band 24-hr upper-air prognostic u and v wind components and temperatures (T) are obtained by combining the 24-hr P.E. fields with the Global Band analysis fields. North of a seasonally variable blend zone, P.E. grid values are used, below the zone the Global Band analysis values are used, and in the zone a weighted average of the two values.

Flight route forecast parameters are computed using the above derived u, v, T fields. All potential routes are carried on magnetic tape; any route can be called up as needed. The majority of routes are great circle from point to point and for fixed altitudes. No forecasts are included south of 24°S.

The flight wind program interpolates vertically and horizontally as necessary to obtain the desired wind information at flight level along the track. Routes are divided into segments or legs at which flight forecast parameters are computed. The computer output is in the form of a teletype message containing forecast data for each route leg. A sample message shown in Fig. 4.19.1 illustrates format and content of the flight wind forecast output.

Flight wind forecasts are issued routinely every twelve hours, and provided to the Weather Central nearest a clearance facility upon request.

B. Program Input

1. Global Band 24-hr u , v , T prognosis fields for 850-, 700-, 500-, 400-, 300-, 250-, and 200-mb levels.

2. Selected routes from magnetic tape storage.

C. Program Computation

1. Call up desired route from route library tape.

2. Interpolate winds and temperatures horizontally and vertically from grid points to height and location of flight track.

3. Compute effective head/tail winds.

4. Output flight forecast data at each route leg along track.

D. Program Limitations

The principal limitation on the Flight Winds model arises from the necessity of using straight persistence from the Global Band analyses to obtain the 24-hr forecasts for the area between 15° N and 41°S. There are no upper-air prognoses available for this. Persistence works well in the tropics, but in the latitudinal band from about 25° S to 41° S, rapid dynamic changes often take place. Persistence will miss these. To compound the potential error is the fact that the Global Band analysis south of the equator is likely to be weak over those large oceanic areas where observational information is, at best, meager and often nonexistent.

There has never been any formal verification attempted on the Flight Winds model. There is always the day-in-day-out verification provided by incoming flight crews. If the flights arrive within five to ten minutes of schedule, no particular notice is taken of this good forecast. If arrival time is missed by 15-30 minutes, word filters back immediately to the issuing forecast center, and steps are taken to modify future forecasts. In general, the flight wind forecasts have a very good reputation among aviation personnel. A high grade from this critical customer group would indicate that the product is of high quality.

E. Uses of the Product

The flight wind forecasts are used directly on flight cross sections. The clearance officer must compute a mean wind vector for climb-out and let-down; this part of the route is not included in the Fleet Numerical Weather Central forecast.

F. Relationship to Other Products

The flight wind model products are not used as input to any other products.

G. Program Output

1. Flight wind forecasts for selected routes.

```
FKPN 89 KNWC          210000Z  Z16LCZ24
RUSM-PGUM GC RT
00Z 21 APR 76---VALID 00Z 22 APR 76


ZN      9000 FT      11000 FT      13000 FT      15000 FT      17000 FT
     DDFFFTTTWWWW  DDFFFTTTWWWW  DDFFFTTTWWWW  DDFFFTTTWWWW  DDFFFTTTWWWW
60   31016 -2  11  30021 -5  13  30026 -9  14  30031-12  15  30036-16  17
61   30011  1   6  29016 -2   7  29020 -6   7  29025 -9   8  28029-13   9
62   28022  6   3  28025  3   3  28029 -1   4  28033 -4   5  28037 -7   5
63   29014  8   6  29017  5   7  29020  2   8  29023 -1   8  29026 -4   9
64   03007 10   5  02007  7   6  01007  4   6  35007  0   7  34007 -3   7
65   08023 11   0  08023  8   1  07022  4   2  07020  1   4  07019 -2   5
66   08018 10   1  08019  7   2  07021  4   4  07022  1   5  06024 -2   7
12Z     5/   3       6/   4       7/   5       8/   6       8/   7
 TWF       4            5            6            7            8

ZN      19000 FT      21000 FT      23000 FT      25000 FT      27000 FT
     DDFFFTTTWWWW  DDFFFTTTWWWW  DDFFFTTTWWWW  DDFFFTTTWWWW  DDFFFTTTWWWW
60   29041-20  18  29045-24  19  29050-29  20  29055-34  21  29060-39  21
61   28034-16  10  28040-21  10  28045-25  11  28052-30  11  28060-35  11
62   28042-11   6  28047-15   6  28052-20   7  28059-24   7  28065-29   8
63   29029 -7   9  28032-12  10  28036-16  10  28038-21  10  28041-25  10
64   33008 -7   8  33009-11   8  33009-16   8  32009-21   8  32010-26   8
65   06018 -6   7  05017-11   8  05017-15  10  05015-20   9  05013-25   7
66   06025 -6   9  06027-10  11  06029-15  13  06027-19  11  06024-24   8
12Z     9/   8      10/   9      10/  10      10/   9      11/   8
 TWF       8            9           10           10            9

ZN      29000 FT      33000 FT      37000 FT      41000 FT
     DDFFFTTTWWWW  DDFFFTTTWWWW  DDFFFTTTWWWW  DDFFFTTTWWWW
60   29065-44  22  29074-51  23  28081-57  21  28087-62  18
61   28068-40  12  28085-48  13  28101-56  12  28118-64  10
62   28072-33   8  28086-42   9  28097-52  10  28108-61  10
63   28044-30  10  28047-40  10  28048-51  11  28049-61  12
64   31010-30   7  30010-40   7  30013-50   7  29016-60   8
65   05011-30   6  06007-40   2  04004-49   3  33005-59   5
66   07022-29   4  09019-39  -3  12017-49  -9  14018-59 -15
12Z     11/   7      12/   5      12/   4      11/   5
 TWF       9            8            8            8
```

FIGURE 4.19.1 Flight Wind Message

4.20 CONTRAIL PROBABILITY FORECAST

A. Model Development

Forecasting of contrails is only a military problem. Commercial aircraft would just as soon have contrails, as a collision prevention measure. Military aircraft benefit from being hidden as much as possible. Further, contrails are a minor unfavorable weather factor in refueling operations by reducing visibility in the rendezvous area--again of military concern only.

Exhaust contrails arise from the addition of moisture to the atmosphere from aircraft exhaust gases. Aerodynamic contrails are caused by the pressure reduction that accompanies airflow around wing tips, propeller tips, and other aircraft surfaces. The air is cooled enough to bring it to saturation. The aerodynamic contrails are usually less dense and persistent than exhaust trails.

Since formation of either type of contrail is basically a function of only temperature and relative humidity, the probability forecast for contrails is a relatively easy computation. The amount of moisture and heat added by a typical aircraft jet engine can be determined from engineering design and related to free air temperature. Aerodynamic contrail formation is a function almost entirely of the temperature and relative humidity of the air mass in which the aircraft is flying.

Theoretical and empirical knowledge of the variables involved has been combined into tables for various altitudes that give values for temperature (Tr100) where 100% relative humidity is required for contrail formation and temperature (Tr0) where 0% relative humidity is required for contrail formation. These two temperatures are used with the free air temperature in a formula that gives probability of contrail formation. The formula is:

$$\text{Probability} = \frac{Tr100 - T}{Tr100 - Tr0}$$

The formula is very reliable provided the free air temperature input is accurate.

B. Program Input

1. 0-, 6-, 12-, 18-, 24-, 36- and 48-hour temperature prognoses for the 400-, 300-, 200-, and 100-mb levels.

C. Program Computation

1. Compute probability of contrail formation at grid points for the input pressure levels.

D. Program Limitations

The only limitations to accuracy are (1) reliability of the input temperatures, and (2) any new aircraft peculiarities not accounted for in the original engineering calculations.

Forecasts have been verified in many hundreds of cases. Results have been consistently good.

E. Uses of the Products

The products are used operationally in flight planning. Only two situations are of concern: remaining hidden from the enemy and not remaining hidden during a refueling operation. The flight planner adjusts his flight level according to the probability forecast.

F. Relationship to Other Products

Program GEMMSG extracts data from the contrail fields at specific locations and taus. GEMMSG outputs a contrail probability message in a format similar to Figure 4.20.1.

G. Program Output

1. 0-, 6-, 12-, 18-, 24-, 36-, and 48-hour contrail probability forecasts for 400 mb (Catalog No. G40), 300 mb (Catalog No. H40), 200 mb (Catalog No. I40), 100 mb (Catalog No. K40).

H. References

[1] Forecasting of Condensation Trails, Air Weather Service Manual 105-100.

Z08A 36
CONTRAIL 36-HR PROG FROM 12Z 13 AUG 73 PROBABILITY

N	000	40E	80E	120E	160E	160W	120W	80W	40W
85	C9799	C9999	C9999	C9599	C7999	C4099	C4099	C5099	C8199
80	C9997	C9994	C9997	C9999	C5099	C0099	C2099	C6099	C9799
75	C9994	C9991	C9997	C9999	C3099	C0099	C2199	C7499	C9998

FORMAT: $CP_{L4}P_{L3}P_{L2}P_{L1}$

Level 4 (L4) = 400 MBS
Level 3 (L3) = 300 MBS
Level 2 (L2) = 200 MBS
Level 1 (L1) = 100 MBS

Probability of occurrence of contrails (P):

9	90 to 100%
8	80 to 89%
7	70 to 79%
6	60 to 69%
5	50 to 59%
4	40 to 49%
3	30 to 39%
2	20 to 29%
1	10 to 19%
0	0 to 9%

EXAMPLE: 75N 120W C2199

Level 1 - 20 to 29%
Level 2 - 10 to 19%
Level 3 - 90 to 100%
Level 4 - 90 to 100%

FIGURE 4.20.1 Contrail Probability 36-Hour Prognosis Message for Area A

4.21 RADIOLOGICAL FALLOUT

A. Program Development

The method of computation and instructions for use of Radiological Fallout (RADFO) Winds are described in the NAVWEASERVCOMINST 3441.1; and ATP-25 (NAVY) (AIR), Nuclear Fall-Out Forecasting and Warning Organization.

The FNWC program is not original; it represents only a programming job built to the prescribed specifications, using FNWC wind analyses.

B. Program Input

Forecast wind direction and speed for the 1000-, 850-, 700-, 500-, 400-, 300-, 200-, 100-, and 50-mb levels.

C. Program Computation

1. Compute mean vector winds in the 1000- to 200-mb and 1000- to 50-mb layers for the low-yield and high-yield effective fallout winds, respectively. Weight the winds by the thickness of layers between each standard level.

2. Compute low- and high-yield fallout template number from wind shear.

3. Based on effective fallout wind and weapon yield, determine distance along the fallout axis to the 200r contour, where the 200r contour encompasses the area receiving a minimum dosage of 200 roentgens in 48 hours.

D. Program Limitations and Verification

The RADFO program is highly dependent on the quality of the FNWC upper-air wind prognoses. The latter charts have been verified repeatedly in aircraft flight operations, and the winds have proven to be accurate within 10° in direction and 20 kts in speed. Since these generally accurate winds are averaged over deep layers and are intended for use with weapons whose yields can only be coarsely estimated, the RADFO forecasts can be considered satisfactory and the program, thus, has no limitations.

The program products have never been verified. Dropping an atomic bomb would be necessary.

E. Uses of the Product

Use of the RADFO products is detailed in the NAVWEASERVCOMINST 3441.1; and ATP-25 (NAVY) (AIR), Nuclear Fall-Out Forecasting and Warning Organization. The rules therein should be strictly followed.

F. Relationship to Other Products

RADFO forecasts are derived from FNWC forecast winds at all levels up to 50 mb, but are for a specific purpose and therefore have no connection with other FNWC products.

G. Program Output

1. RADFO Pre-Burst Prediction containing forecast low- and high-yield effective fallout wind speed and direction, fallout template number, and distance to the 200r contour. (Catalog Nos. Z09, Z15, Z16, Z17, Z18, Z19, Z20). Messages are sent on the first Sunday of each month, or upon request. A sample message is shown in Fig. 4.21.1.

2. RADFO Warning containing above parameters for an actual nuclear detonation. Message available upon request. Required inputs are time, location, and approximate yield of the detonation. Sample output is given in Fig. 4.21.2.

```
PRE-BURST PREDICTION , 24HR FCST FROM 00Z 11 AUG 73
FORMAT QLLLL TDDSS DDDDD TDSS DDDDD
02075 21420 00013 21523 00171      02080 51112 00010 41112 00124
02085 11107 00008 11106 00086      12090 10904 00006 10804 00068
12095 11206 00008 10906 00086      12000 11207 00008 11007 00094
02575 41111 00010 21112 00124      02580 51411 00010 21312 00124
02585 11707 00008 11607 00094      12590 11602 00004 10703 00058
12595 12603 00005 13004 00068      12500 11705 00007 11703 00058
03075 11306 00008 11106 00086      03080 21912 00010 21814 00134
03085 22213 00011 22214 00134      13090 22518 00012 22520 00161
13095 22719 00013 62821 00164      13000 22714 00011 62717 00148
```

FIGURE 4.21.1 RADFO Pre-Burst Prediction for Selected Points.

```
FALLOUT WARNING
12595 1103/ 05000 13004 00068
```

FIGURE 4.21.2 RADFO Warning for 25N 95W.

4.22 DITCH HEADINGS

A. Program Development

The safest ditch heading is that which will align the aircraft parallel to the dominant swells or waves to reduce impact against sloped water. To reduce ditching speed with maximum lift, the aircraft should be heading into the wind as much as possible. Ditch headings are included in flight folders for all over-water flights, providing pilots with information on the best heading at any point along the route for making a crash landing. In an emergency, there may not be time to determine local sea state and wind direction.

Grid-point values for wave direction are read off the Primary Wave Train Direction field, to give two possible headings. These headings are then matched with wind directions at corresponding grid points in such a way as to have the wind blowing toward the forward part of the plane, on the chosen heading.

B. Program Input

1. Primary Wave Train Direction prognosis for 24 hrs.

2. Marine Wind Direction prognosis for 24 hrs.

C. Program Computation

1. Read off direction of waves at grid points from Combined Wave analysis to determine two possible ditch headings parallel to the waves.

2. Read off wind directions at grid points. From the two possible headings, select the one where the wind is blowing toward the heading.

D. Program Limitations

The accuracy required for this product is not great, as the pilot making a ditch landing can correct for minor errors in the forecast. The accuracy of wave and wind directions will probably never be so poor as to produce a ditch heading 180° out.

E. Uses of the Product

Ditch headings are used at aviation clearance desks. Headings are entered at appropriate intervals on the clearance cross section. The FNWC output is used by civilian and Air Force activities, in addition to the Navy.

F. Relationship with Other Products

The Ditch Heading program output is not used in any other FNWC product.

G. Program Output

1. Hemispheric Ditch Heading prognosis for 24 hrs. (Catalog No. B99)

FXPA 03 KNWC NR04 281200Z B99H 24
DITCHHGD 24 HR PROG FROM 12Z 28 JAN 73 DIR/10 TRUE

N	180	175W	170W	165W	160W	155W	150W	145W	140W
70	29	31	26	31					
65	34	34	29						
60	33	33	27	27				11	
55	19	20	18	00	35	16	16	33	02
50	20	20	18	00	35	17	17	06	07
45	06	19	20	34	35	17	00	36	18
40	26	17	16	34	35	35	36	18	19
35	13	22	16	34	23	34	21	19	19
30	24	22	04	27	25	23	20	19	22
25	06	05	12	28	29	05	06	04	04
20	13	13	13	33	06	08	06	06	24
15	33	31	10	35	06	06	24	24	23

FIGURE 4.22.1 DITCH HEADING MESSAGE

4.23 MARINE LAYER WIND PROGNOSIS

A. Development of the Model

The Marine Layer Wind products come from the Spherical Marine Wind Prognosis Programs; equations used are included in Appendix P. To summarize, the Marine Layer Wind Prognoses are derived from the Northern Hemisphere Primitive Equation surface pressure prognosis. The steps involved are:

1. Calculate surface geostrophic winds, which serve as a first approximation of the wind near the ocean surface. The standard geostrophic wind equation is used to compute u and v components at each grid point. The pressure gradients are computed from the grid-point data by a fourth-order differencing equation.

2. A curvature correction is applied to the geostrophic winds to approximate the gradient wind speed.

3. Correction to the gradient wind is applied to account for stability conditions in the friction layer and the variation of Coriolis force with latitude. A correlation exists between deflection angle and lapse rate in the friction layer and between lapse rate and horizontal sea-surface temperature advection. The model, then, derives the stability and Coriolis force corrections using the advection of sea-surface temperature.

The several corrections discussed above are combined in empirically-developed equations to obtain surface wind speed and direction, and u and v velocity components--the Marine Layer Wind prognoses.

B. Program Input

1. Surface temperature climatology.

2. Surface pressure prognoses, at six hourly intervals to tau 72.

3. Sea-surface temperature analysis; 0 hrs.

C. Program Computation

1. Compute first guess of the wind field from the surface pressure analysis.

2. Apply curvature correction to first-guess wind field.

3. Compute advection correction to vary inflow angle from zero to a maximum of 35°. Speed is also affected by this correction.

4. Compute temperature correction, which automatically provides for a latitude correction.

5. Compute u,v components from the completed Marine Wind direction and speed.

6. Model forecast tropical storm circulations into the wind prognoses as warnings are available, using an empirical wind speed distribution.

D. Program Limitations, Reliability and Verification

The key assumptions made in the Marine Layer Wind model are (1) that the surface pressure analysis is nearly perfect, and (2) that this pressure analysis can be converted to a wind analysis that truly represents the wind existing at any selected point. The pressure-to-wind conversion is based on standard theoretical and established empirical equations that were selected to closely approximate actual conditions; the only doubt is that all possible corrections are included. The wind model, then, is limited by the P.E. SLP prognosis accuracy.

The Marine Layer Winds are verified periodically. The verification compares ship wind reports with similar values interpolated from the wind analyses.

Sample 12-hourly verification summary

Verification Summary
784 Reports

Area RMS	DD error	=	55 deg
Area Average	DD error	=	±3.0 deg*
Area RMS	FF error	=	7.5 kts
Area Average	FF error	=	±1.0 kts

Negative error indicates analyzed < reported

Area average DD and FF error can be interpreted as a bias in direction and speed for any particular field.

E. Uses of the Product

The primary use of Marine Layer Winds in the field is for area forecasts and for the individual ship, WEAX-type forecast. Use of the wind charts is uncomplicated, involving only conversion of chart values to description for the forecast period involved. For a 36-hour area forecast, the 0-, 12-, 24-, and 36-hr wind charts would be examined and interpreted to incorporate indicated changes. For a certain area, it might turn out that for 12 hours the winds would be easterly, 15 knots. The 24-hour chart might show a backing and an increase; the forecast would read accordingly.

For the single ship forecast, the above interpretative process would be followed, but the forecaster would have to account for the added complication of ship movement.

If the field forecaster does not have available the pertinent FNWC products, he would have to use the Marine Winds directly in all forecasts involving drift--oil spills, ice, floating objects--and in state of the sea forecasts. The way to use the winds in these cases is described in several forecasting manuals. It is usually a matter of entering nomograms with the wind values to come up with a "wind effect" answer for use in the equations being used for the particular problem.

F. Relationship to Other Products

The Marine Layer Winds are used in several FNWC programs.

1. Search and Rescue--the winds are the most important component of the SAR calculations.
2. Ocean Surface Currents--the winds are over one half of the effect.
3. Spectral Wave--winds are the total generating force involved.
4. Hydrodynamical Numerical Model.

*NOTE: Average DD error < 0 implies error in a backing direction.

5. Ditch Headings--wind direction is matched with wave direction to make the final choice of ditch heading.

6. Ice Forecasting--winds and currents determine ice movement.

7. Oil Spills.

8. Sea/Swell in semiclosed seas and coasts--Marine Winds are hand modified in this model.

G. Program Output

1. Wind Field Generated FNWC Marine Wind Speed and Direction prognoses for 6 to 72 hours in 6-hr increments. (Catalog No. A27, Fig. 4.23.1; A28, Fig. 4.23.2)

2. Wind Field Generated FNWC Marine Wind U and V component prognoses for 6 to 72 hours in 6-hr increments. (Catalog No. A28, A29 and A30)

3. Surface Marine Layer Wind, GEM message. (Catalog No. A24, Fig. 4.23.3)

H. References

[1] Hubert, W. E. and B. R. Mendenhall, 1970; "The FNWC Singular Sea/Swell Model", Technical Note 59, Fleet Numerical Weather Central, Monterey, California, 29 pp.

[2] Lazanoff, S. M., N. M. Stevenson and V. J. Cardone, 1973; "A Mediterranean Sea Wave Spectral Model", Technical Note 73-1, Fleet Numerical Weather Central, Monterey, California, 83 pp.

NOTE: Since the empirical algorithm is applied on the spherical 2 1/2 degree latitude/longitude grid, other projections (i.e., northern and southern hemispheric polar stereographic and global band mercator) are interpolated from the spherical grid. This ensures consistency of the products.

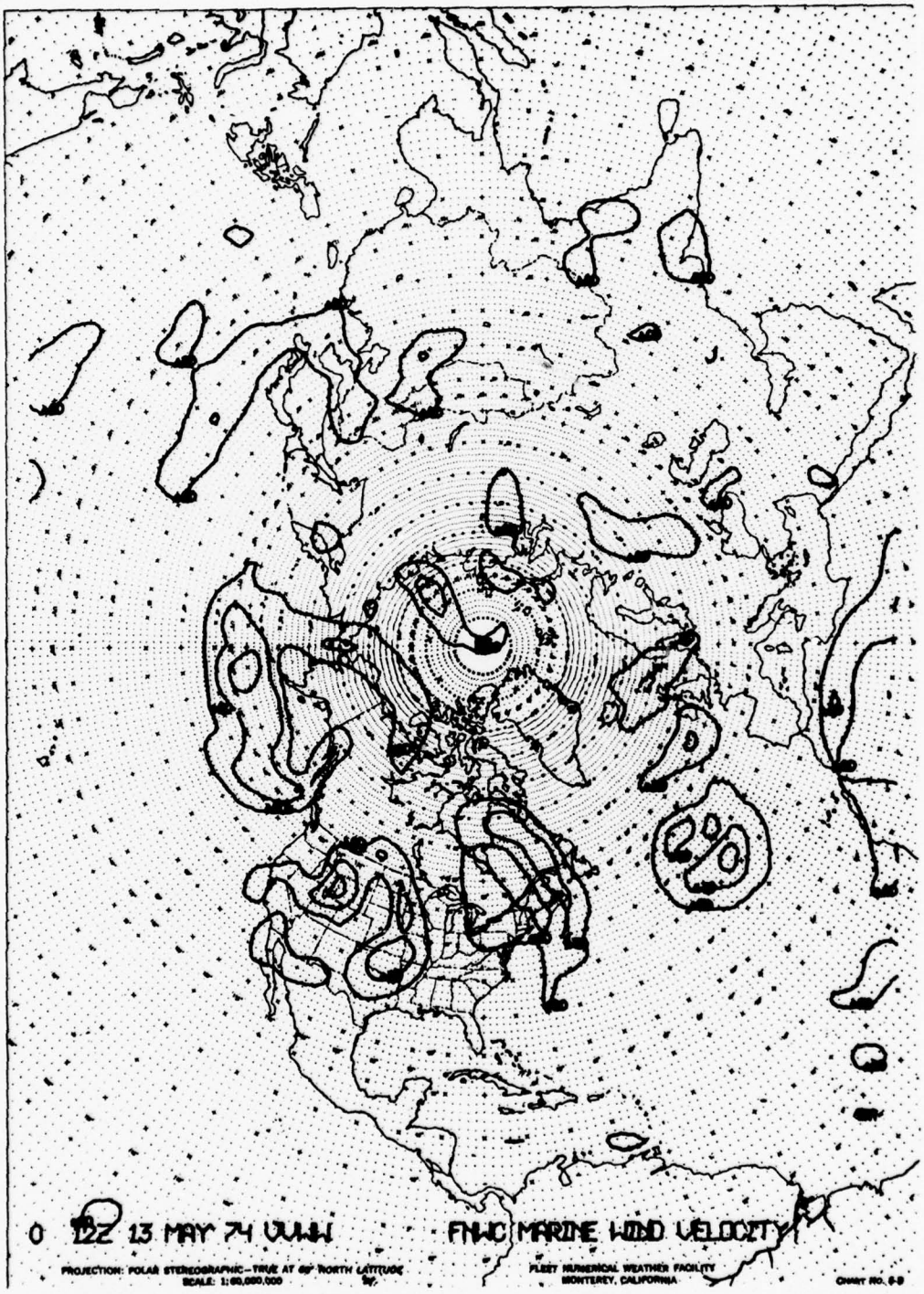


FIGURE 4.23.1 Wind Speed Analysis (A27)

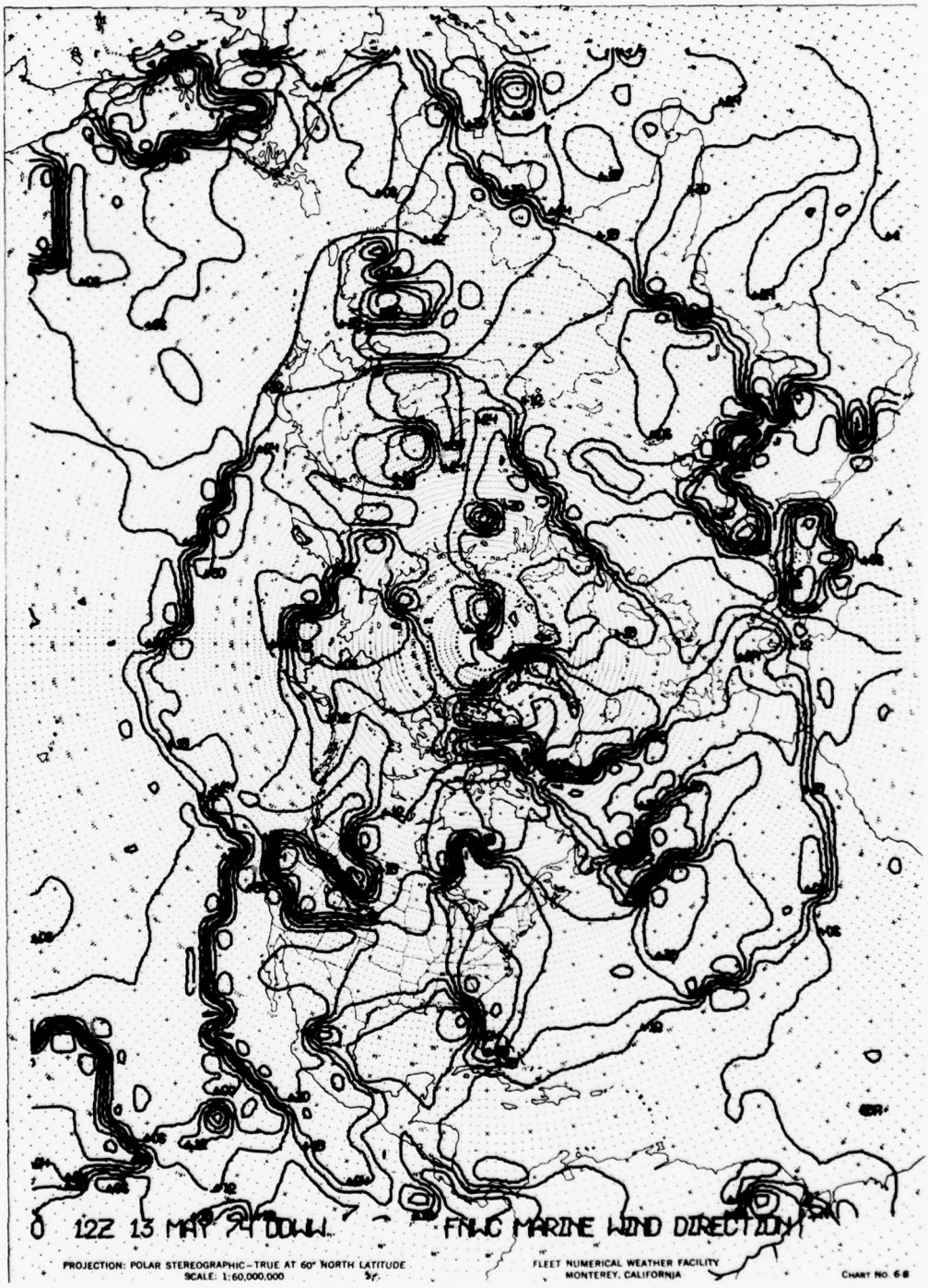


FIGURE 4.23.2 Wind Direction Analysis (A28)

FXPA 02 KNWC NR02 281200Z A24G 36
SFC WIND 36 HR PROG FROM 12Z 28 JAN 73 DIR/SPEED

N	140E	145E	150E	155E	160E	165E	170E	175E	180E
70	27016	29015	31012	34009	36007	01006	02010	01018	01023
65	04009	03015	01013	34008	30007	31009	34013	36015	36012
60	04015	06015	09012	13014	11011	05011	36009	30012	26017
55	32014	29014	30009	03016	05033	07040G	10044G	12039G	14023
50	28009	26018	30030	33040G	33040G	33019	11011	11044G	13052S
45	11006	16009	33012	31028	31047G	30055S	29046G	26022	17029
40	15006	17012	24011	27019	29030	29048S	30060S	28025	23024
35	20015	19020	22007	31006	33009	33016	33043G	29014	21027
30	13015	13016	07011	05012	04015	03020	36022	22013	20016
25	13012	09019	07020	05018	04017	02014	21004	20014	21008
20	08007	05013	09013	05015	06011	05007	14014	13009	07007
15	06023	08013	09016	05013	06015	07013	10019	08022	06021

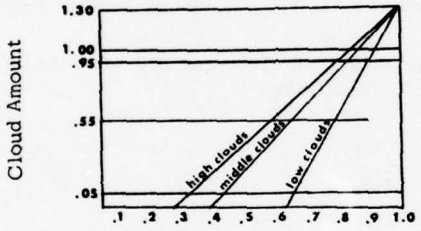
STORM WARNING AREA G G-GALE FORCE WINDS/S-STORM FORCE WINDS

FIGURE 4.23.3 Surface Marine Layer Wind GEM (A24)

4.24 CLOUD COVER

A. Program Development

Cloud cover forecasts are based on empirically determined relationships between relative humidity and cloud amount. Cloudiness occurs at space-averaged relative humidities much less than 100%. Humidity averages represent the mean of a frequency distribution of small-scale humidity variations, so some condensation may be occurring due to saturation at the high end of the distribution. From this situation, the amount or density of condensation (cloudiness) could be expected to increase with increasing mean humidity. This is exactly what has been found, empirically, in studies relating mean relative humidity to clouds reported in thousands of observations. From these studies, graphs of the type shown below were developed.



(After Smagorinsky)

The cloud cover program uses empirical equations derived from the curves to forecast cloud amounts at different levels in the atmosphere. The basic input is relative humidity values derived from the P.E. Model forecasts of vapor pressure.

The total cloud cover forecast comes from still another empirical equation. This equation was derived from an FNWC study comparing mean relative humidity of the column with satellite nephanalyses covering a long enough period to provide statistical validity. A linear fit for $\overline{RH}$ comes from the equation:

$$N = \frac{A + \overline{RH}}{B} \quad , \quad 0 \leq N \leq 1$$

where $A = -0.350$, and

$B = +0.300$.

B. Program Input

1. Temperature and vapor pressure analysis and prognoses at surface, 1000-, 850-, 700-, 500-, and 300-mb levels at 0, 12, 24, 36 and 48 hours.
2. Sea-surface temperature analysis.

C. Program Limitations

The cloud-cover formulas are designed for layer cloud types, not for the random convective-type cases. The latter would be shown if they were at a grid point, but would probably be hidden if they lay between grid points. With the 63x63 grid, many thunderstorms could easily be "no shows" on the cloud cover charts.

The cloud cover forecasts will tend to be quite accurate in storm areas, where high relative humidities generally exist at upper levels.

D. Uses of the Products

The cloud cover products are used directly in the forecasts, with no cross-product interpretations except in the quality control sense. The most common use is in area forecasts, WEAX, aviation forecasts, and detection of surface units by satellite.

E. Relationship to Other Products

The total cloud cover forecasts are used as input to the Heat Exchange Model--Section 5.10.

F. Program Output

1. Total cloud cover in tenths for 00, 12, 24, 36, and 48 hours. (Catalog No. Z12, See Figure 4.24.1)
2. Tenths of cloud cover at 1000, 850, 700, 500, and 400 mbs, for 00, 12, 24, 36, and 48 hours. (Catalog Nos. C36, D36, E36, F36, G36)

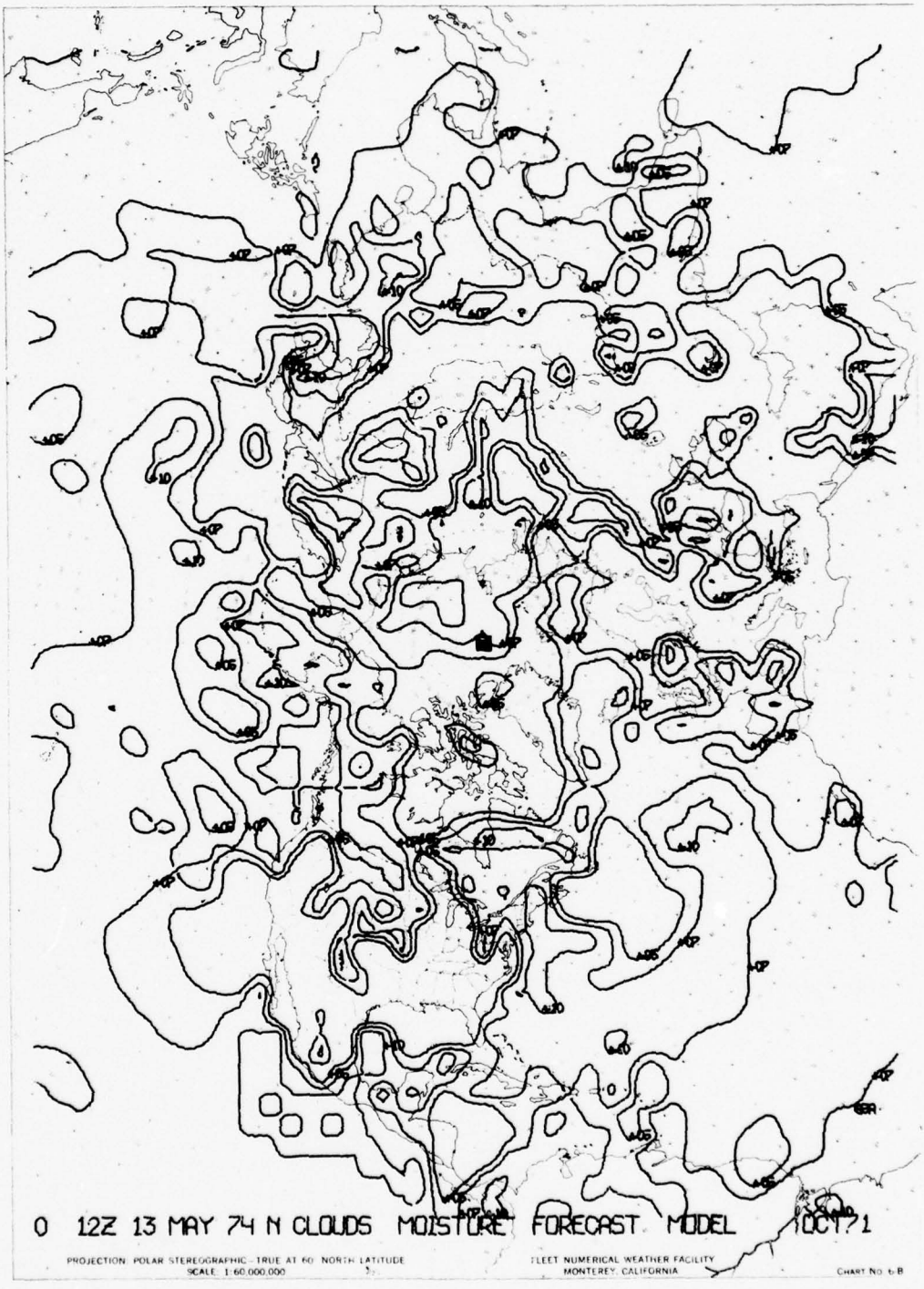


FIGURE 4.24.1 Total Cloud Cover Chart (Z12)

4.25 HORIZONTAL WEATHER DEPICTION (HWD)

Horizontal Weather Depiction (HWD) is an automated display program designed to improve the method of presentation of FNWC products to the operational users. The program extracts information from pertinent FNWC environmental fields, then combines and arranges the required information into a format that best fits the specialized needs of the users. The HWD program plays no part in producing the fields from which the information is drawn.

The HWD program is in the developmental stage. Because some parameters are difficult to treat automatically, it will probably be a few years before full automation is attained for the full range of HWD composites.

The HWD program development was motivated primarily by a desire to provide a better, more usable product to the user; the present system provides too much extraneous information. A surface operation, for example, might receive a variety of constant pressure analyses, clouds and temperatures for all levels, and other nonapplicable output. What the surface operator wants is one or two HWD charts showing surface pressure, winds, visibility, low-level clouds, currents, etc. The HWD program will provide this more personalized service, tailored to the particular needs of the customer. A secondary goal of the HWD program was the saving of manpower by centralizing basic chart preparation at FNWC, rather than having the same charts prepared independently and nonuniformly at the many Naval Weather Service detachments at sea and ashore.

The HWD effort will result in a major change in customer service. The direction of effort is toward automatic HWD chart preparation in the form of composite graphics, where the graphics will display all the necessary environmental parameters of one environmental envelope and the environmental envelope will include the operating area of some type of naval operation. Preliminary planning has led to the breakdown of classes of naval operations and the basic HWD or Ocean State Depiction (OSD) charts to support them, as shown below. Analysis and prognostic charts are required for all cases.

1. HWD--General Marine (two HWD charts)
   a. Combined-wave heights
   b. Ocean currents
   c. Marine wind barbs
   d. Visibility restrictions (fog, rain, snow)
   e. Air temperature
   f. Sea-surface temperature
   g. Ice conditions
2. OSD--Pro/Antisubmarine Warfare (two OSD charts)
   a. Sound propagation loss profiles as function of range
   b. Subsurface thermal structure at selected levels
   c. Potential mixed layer depth
   d. Ambient noise
3. OSD--Logistic Operations
   a. Surface isobars
   b. Marine wind barbs
   c. Combined-wave heights
   d. Surface fronts

4. HWD--Low Level (Close Air Support)
   a. 850-mb wind barbs
   b. Low-level cloud cover
   c. Slant-range visibility
   d. Weather (probability of icing and turbulence)
5. HWD--Mid Level (Turboprop)
   a. 400-mb wind barbs
   b. 500-mb isotherms
   c. 300-mb isotherms
   d. Middle clouds
   e. Weather (icing, turbulence, contrails)
6. HWD--High Level (Jet)
   a. 250-mb wind barbs
   b. 250-mb isotherms
   c. High clouds
   d. Weather (icing, turbulence, contrails)

The above HWD and OSD charts will be transmitted in Broadcast and Addressed modes. The Broadcast Mode will have hemispheric coverage on the 1:60 million scale, and will be sent to all mainline NEDN stations. The Addressed Mode will be for specific areas, or even specific missions, and will be scaled to requirements of the user. The composites will be standardized--only the size of the area and the scale of features will vary between the "broadcast" and "addressed" composites. Chart times will be for 0000Z and 1200Z. Forecast periods will be in 12-hour increments out to 36 hours for charts 1, 2, and 4. Charts 3, 5, and 6 will be in 24-hour increments out to 48 hours.

There are two methods being developed for preparing and transmitting HWD products. The first uses available equipment and communications links to transfer fields in packed raster format. The method is suitable for Varian plots or COMPFAX generation. This system will be used for at least the next few years. The second method, the Naval Environmental Display System (NEDS), is in early development, with testing scheduled for late 1973. The NEDS system involves purchase of relatively expensive equipment. This may delay distribution to Naval Weather Service units, even if field tests show that NEDS is a far superior method.

Both methods will be discussed below--the raster format in more detail since it will be the immediate operational method used.

Raster-Format Method

The raster formatting method can best be described in a step-by-step example using an operationally-used OTSR display (Fig. 4.25.1) of surface pressure, combined-wave heights, and ship positions as input.

1. Data cards are used first to outline the job. These cards tell what fields are needed, where they are stored, what operation is to be performed on the field information, the order of events for the whole job, and whether the final result is to be compacted for transmission.
2. The surface pressure analysis is called up from storage. The HWD program reads the analysis and computes the bit positions for the raster field. The raster field is 14" wide (along the raster) and of whatever length required to produce the chart with 100 rasters per inch. Images and/or contours are created in the raster field by entering a 1-bit wherever a mark is required, continuing until the desired image is created. When all images and/or contours are completely entered into the raster field, it is ready for compacting, transmission, and/or hard copy production as desired.
3. The combined-wave height analysis is called up. The process described above is performed, until all the sea-height isolines are entered (by the 1-bits) on the raster field. The sea height lines are dashed, to differentiate from the isobars. The 12-foot-or-greater sea height contours are made at twice the 1-bit thickness, to act as a flagging device.

4. The ship list is called up. At each ship position, a ship identification number is entered in a box. An arrow showing direction of movement and future positions in 6-hour steps is included. The number of 6-hour positions plotted is optional with the customer. The HWD chart has a Ship Directory Box stuck off in an out-of-the-way corner. Ships are listed by name, call sign, and identification number.

5. The field is generally compacted before transmission. Compaction for the raster fields amounts mostly to taking out the zero bits that, in the fields like the one described above, would amount to over 90%. With 1,960,000 bit positions involved, it would be a waste of time to transmit, say, 1,750,000 zeros. The compaction method is to give a count of zero bytes (6 bits), then the actual bytes containing one or more bits, continuing until a number of zero bytes are encountered, etc. This procedure permits the length of the message to be decreased up to 80%, depending upon the number of bits in the primary field. At the terminal station, the computer uses these compaction numbers to reconstruct the full field.

After step 5, the HWD chart is ready for transmission. After receipt at a terminal, the raster field is reconstructed. Then, a program is run to superimpose the geographical background. This is done at the terminals so that the background will not have to be transmitted with each HWD chart.

Naval Environmental Display System (NEDS)

The NEDS is under development, and is expected to go through testing in the last half of 1973. The time frame for full deployment to Naval Weather Service activities cannot be stated at this time.

Transmission of information in the NEDS can be over any type of communications link. The prototype equipment will use a 100-wpm teletype line, compatible with AUTODIN, fleet RATT broadcast, and the automated weather network teletype system (NETS, Sect. 3.1).

Fields are sent in variable compacted vector (VCV) format. This format is translatable to pen commands (as used in the CALCOMP system), or to the raster format described in the preceding system. The VCV format is so efficient that, in transmission time, it is nearly as efficient as the standard NEDN band-index field format.

The NEDS fields are sent over a continuously-running teletype line. At the terminal, the fields go directly to disc storage. From here, just by punching a button, the fields can be put on display on a 21" TV-type tube. The forecaster works directly from this picture. If he wants comparisons, he can call up any other fields in rapid succession and in any order. The system has a zoom capability. The forecaster can pick out any small area of interest and enlarge it up to six times.

A Varian plotter is included in the NEDS terminal equipment. Again, the punch of a button produces a hard copy of the field or fields being displayed on the TV screen.

4.26 ADVECTION FOG

A. Program Development

The forecast for Advection Fog probability is based on a system of multi-parameter tests, where each parameter is weighted on the basis of test results. The weights of all parameters are summed, divided by 5, and normalized to give a value range of zero to one, representing probability. 0.1 would be 10% probability; 0.9 would be 90%.

Advection Fog has five tests:

1. When surface air temperatures are near 0°C, there is a high probability of fog. (Based on S. Petterssen) Weights favoring fog are assigned in the ±5°C range from 0°C.
2. When condensation is taking place, there is usually an effective fog condition. This test is done by using evaporation calculations from moisture parameters. If evaporation is negative or zero, a certain weight is assigned to allow for the condensation factor.
3. If the near surface relative humidity exceeds a certain critical value (> 95%), a high weight is assigned on fog probability.
4. An air mass discriminant is applied. If the surface geostrophic wind is being advected toward warmer (or colder) surface conditions, the air mass would be classified accordingly--as in the old k and w air-mass system. A warm air mass would call for a high weight. The weight assigned is based upon calculations of the air mass wind component normal to the isotherms.
5. A weight is derived from application of a Fog Criterion. The criterion is based upon the change in dew point that occurs during the mixing of two air masses of dissimilar character. The resulting dew point depression in the mixed air is related to fog probability, which establishes a certain criterion value. If calculations on the current case yield a value less than the criterion value, a strong probability weight is assigned.

User activities receive the fog probability forecasts in the form of a field, where each grid point has a fog probability value.

B. Program Input

1. Sea-surface temperature analysis.
2. Surface air temperature analysis.
3. Surface vapor pressure analysis.
4. Sea-level pressure 6-hourly analysis.
5. P.E. prognoses of the above parameters from 0-48 hours.

C. Program Computation

1. The various tests are calculated as described above for parameters at Tau's equal to 0, 6, 12 to 72 hours. The fog probability FTER is calculated for all land and sea points.

D. Program Limitations

The five-parameter test method is admittedly somewhat gross in character, but has enough built-in controls to insure a correct answer--given correct humidity values. The program gives excellent results in cases of broad-scale fog. The weakness of the program stems almost entirely from use of the large 63x63 grid. Local effects just cannot be accounted for, and fog is particularly susceptible to

small-scale effects such as cold air drainage, small bodies of water, and man-made air pollution. Forecasters, in using the Advection Fog products, should always make allowance for known local effects.

E. Uses of the Product

Fog forecasts have many applications in the Navy for aviation and ship operations. Fog probably causes more cancellations, postponements, and incompletions than any other weather element. It would be very comforting to have a sure-fire fog forecasting method for all situations. The products of the Advection Fog model are not in this category.

Forecasting fog is one of meteorology's hardest problems. This is because there are so many factors involved--moisture, temperature, wind, geography, stability, cloud cover, and several more. Over land areas, the problem is strictly local in nature.

The fog probability forecasts should be used as an alerting device. They tell the forecaster that he will have air with temperature-moisture relationships suitable, borderline suitable, or not suitable for fog formation. From this base, the forecaster must then inject local considerations such as topography, nearby bodies of water, concentration of locally-produced condensation nuclei, fronts, etc. For forecasts over the ocean, the fog probability forecasts can be used almost as is, except that moving fronts must be accounted for in the timing of fog formation or dissipation.

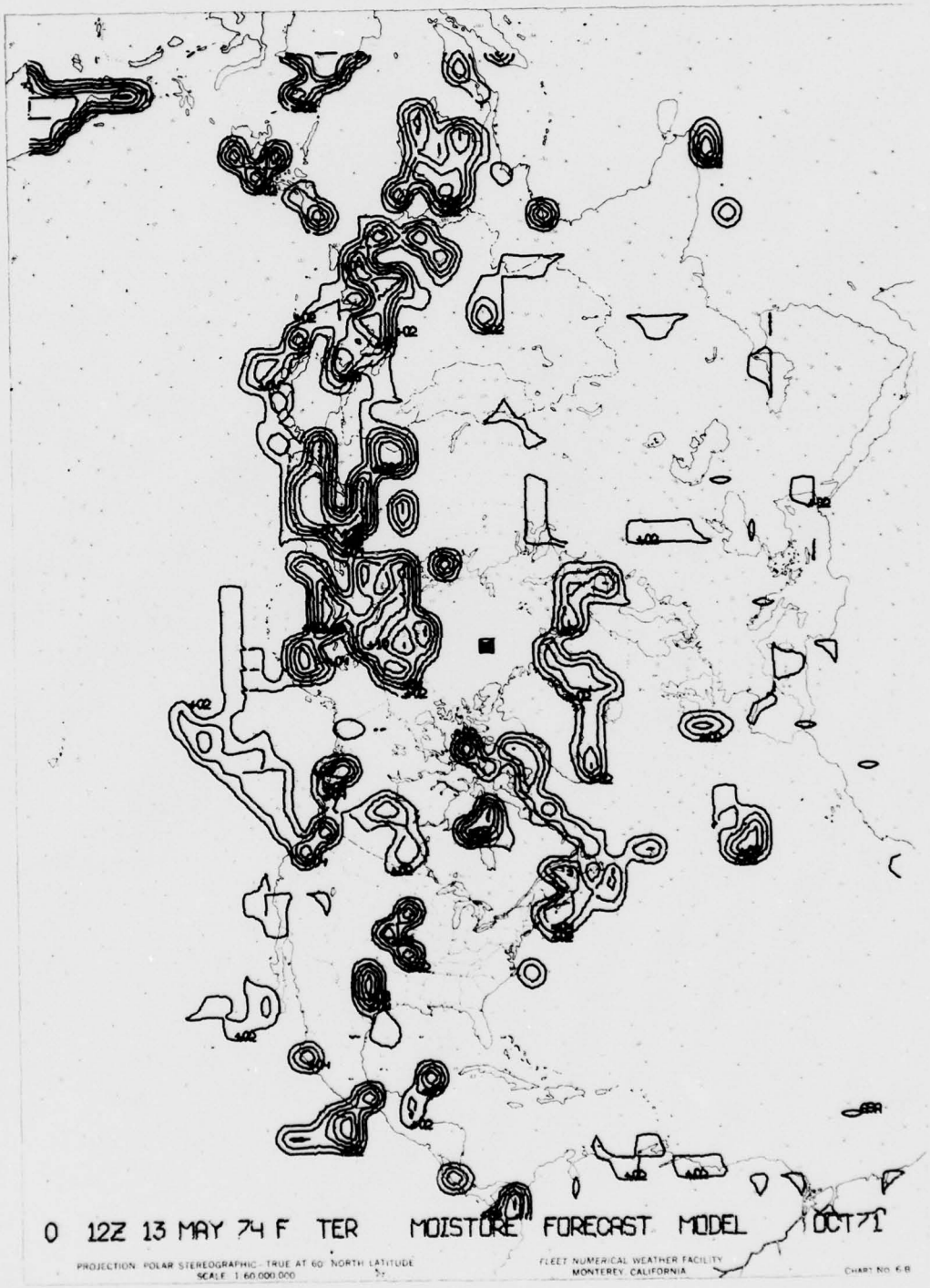


FIGURE 4.26.1 Advection Fog (Z13)

4.27 WIND EXTRACTION

A. Program Development

The wind extraction program is designed to apply the geostrophic wind equation to upper-air constant pressure surface analyses to produce u and v components, direction, and speed of the wind. The 63x63 FNWC grid is the coordinate system for the u,v components rather than the compass directions.

B. Program Input

1. All constant pressure analyses and prognoses from 1000 mb to 10 mb.

C. Program Computation

1. Compute u,v components of the geostrophic wind for each upper-air analysis level.

2. Convert u,v components to wind direction and speed at each grid point.

D. Program Limitations

Derived winds will faithfully reflect errors in the upper-air analyses and prognoses.

Wind speeds computed according to the geostrophic wind equation will be greater than actual speeds in regions of cyclonic trajectory curvature and less than actual speeds in regions of anti-cyclonic curvature. In both cases, the magnitude of the error increases with curvature and wind speed and decreases with latitude.

Errors due to computation on a finite mesh length grid will also be involved. These will serve to reduce computed wind speeds over the whole grid and will be a maximum in regions of strongest curvature, regardless of sign.

It follows that in regions of cyclonic curvature the two errors will tend to cancel one another resulting in fairly close agreement between computed and actual winds. In regions of strong anticyclonic curvature, however, the errors are additive and will result in computed speeds much slower than actual.

The geostrophic approximation does not hold well in the tropics, so winds below about 17°N will tend to be inaccurate.

E. Uses of the Product

The primary uses of the geostrophic wind fields are for preparing forecasts of flight winds, radiological fallout winds, and ballistic winds. For the flight winds (see also Section 4.19) forecast, geostrophic winds are obtained from the input field along approximate great-circle flight routes (i.e., straight lines on a polar stereographic projection). The points are determined by the intersection of five-degree latitude and longitude lines with the flight track. The forecaster must keep in mind that: (1) the winds are point winds, and (2) there are problems inherent in the computation of geostrophic winds on a finite mesh length grid (See D, above).

Ballistic winds and radiological fallout winds are computed by standardized methods outlined in several U. S. Navy manuals. The computations lead, in a general sense, to a stratification of the upper air into layers, where for each layer one representative wind is determined that combines the effect of all the winds within the layer that would affect a bomb, projectile, or radiological fallout debris.

An inspection of the wind fields can be of help to the forecaster in organizing his thinking. From the fields, he can see the location and strength of the jet stream; there are many forecasting rules of pertinence for this case. He can move surface or upper air systems in accordance with the established rules for applying percentages of the geostrophic wind speed (plus direction). Patterns favorable for intensification of lows and highs can be seen in the wind field patterns (the constant pressure charts are normally used for this). Potential areas of CAT can be located by collocation with areas of strong wind shear.

F. Relationship to Other Products

The wind field products are direct input into the RADFO, ballistic wind, flight wind, and P.E. programs. The accuracy of the first three is dependent upon the wind fields, which, in turn, are dependent on the accuracy of the upper-air prognoses.

G. Program Output

1. Geostrophic u,v components; wind speed and direction; at 00, 12, 24, 36, 48, and 72 hrs for 1000 mb (Catalog Nos. C20-23), 850 mb (Catalog Nos. D20-23), 700 mb (Catalog Nos. E20-23), 500 mb (Catalog Nos. F20-23), 400 mb (Catalog Nos. G20-23), 300 mb (Catalog Nos. H20-23), 200 mb (Catalog Nos. I20-23), 250 mb (Catalog Nos. T20-23), 150 mb (Catalog Nos. J20-23), 100 mb (Catalog Nos. K20-23), 50 mb (Catalog Nos. L20-23), 30 mb (Catalog Nos. M20-23), 10 mb (Catalog Nos. N20-23). 925 mb u,v components only (Catalog Nos. R20-21).

Note: Surface wind fields are available from the Global Band model (Section 4.4) and the Marine Layer Wind model (Section 4.23). Global Band u,v, isogon, and isotach fields for analysis time are available at standard levels from 850 mb to 200 mb.

Catalog No. X24 is the GEM MSG catalog number (where X designates a letter indicating the level computed). Wind direction and speed are derived from "D" fields. The output is a five-digit number (DDFFF), where DD is the wind direction to the nearest 10 degrees and FFF is the wind speed to the nearest knot. Example: if DDFFF = 28042, the wind is from 280° true at 42 knots.

5. OCEANOGRAPHIC PROGRAM DESCRIPTIONS

5.1 SEA-SURFACE TEMPERATURE ANALYSIS (SSTFIB)

A. Model Development

Synoptic analysis of Sea-Surface Temperature (SST) presents a difficult problem because of marginal or poor data distribution and variable data quality. There are 1200 to 1400 SST reports available each 12-hour period; however, these are spread very non-uniformly, tending to be concentrated along the shipping lanes, leaving large areas devoid of data. Most of the reports have an uncertainty of at least 1°C in measurement, and there is a further uncertainty in the ship positions which is sometimes considerable. This positional uncertainty can become especially troublesome in areas of strong surface temperature gradient.

Hand analysis of SST normally followed the pattern of starting the analysis in areas of dense coverage, with a constant evaluation of reports as the work proceeded. Evaluation was made by comparing neighboring reports, checking how reports fit with the previous analysis and, finally, comparing with climatology. In areas with no reports (and none in past analyses), the previous analyses and climatology would be weighted appropriately.

The whole analysis process was so tedious and unproductive that synoptic SST analysis was not routinely performed until FNWC undertook development of a computerized model. Synoptic SST analyses are an important input to many of FNWC's meteorological and oceanographic products.

The first FNWC SST analysis model performed well and was used operationally for several years. A new and more powerful analysis technique--Fields by Information Blending (FIB)--has been under development over the past few years in various types of analyses. The FIB method can analyze any single-valued parameter, using spot values or observations as well as one or more independent fields for input. The analysis of SST, with the peculiar data problems involved, appeared to be an area where FIB could be applied to great advantage. The FIB method was therefore adapted to SST analysis. The model was tested for a period of time under operational conditions and was placed into operation in mid-1971.

The FIB numerical analysis technique faces the same problems as those of the hand analyst, and FIB solves the problems in the same general way. The FIB solution has the added advantage of the computer's power and ability to produce consistent, accurate, and timely results.

The SST analysis model will be explained by following the sequence of operations step-by-step. By this, the similarity to the hand-analysis pattern can be seen, along with the assumptions and analysis refinements implicit in the FIB technique. Many formulas are involved, as usual, but these will be included in Appendix O for those who require the technical detail.

A formal definition of FIB is: Numerical analysis of fields by the assimilation and blending of information in observations and in field estimates of the object parameter, its linear-differential properties, and its characteristics; combining information from three sources in time--current, near past, and well past. This breaks down into the component operations of: initialization, data preparation, information assembly, blending, reevaluation, and recycling of the analysis.

Initialization

The analysis scheme requires a first-guess field (one or more) and first-guess gradients, with associated reliabilities. The initialization phase develops these fields.

Reliability, as used in FIB applications, has an exact meaning involving the standard deviation of the errors associated with measurement of an unknown quantity. Reliability defines the worth of a measurement; a report with high reliability signifies that it is more likely to be nearer the true value than a report with low reliability. Thus, if several observations influence a grid-point value, the best combined estimate at that grid point weights the individual estimates by their respective reliabilities, and the total reliability of this best estimate is the sum of the contributing individual reliabilities.

The analysis starts with the 12-hour-old temperature field. To control this field in areas that are data sparse over long periods of time, it is moved a small amount (maximum of 3%) toward climatology before considering any new reports. In some applications, climatology has been given equal weight to each unit of the period to be averaged; viz., if you were working in August and were using a three-month-average period, then July, August, and September would be counted equally. This would result in a jump at the beginning of September when July dropped out and October came in. The FIB method uses a weighting system which changes with each 12-hour analysis. The current month gets a 0.5 weight (50%). If the analysis time happens to be 0000Z on the 20th day of a 30-day month, the preceding month would get an (11/30)·0.5 weight (18%), and the following month would be weighted at (19/30)·0.5 (32%), of that month's climatological value. This method provides a smooth, slowly-changing climatological value.

The 12-hour-old analysis and the weighted climatology are combined to give the first-guess temperature field. This first-guess field is a best estimate of current conditions, without considering any new data or any type of dynamic forecasting. It is the starting point of the analysis; modification to this will be made as dictated by current observations.

The second step in initialization is to compute the first-guess temperature-gradient fields. These are needed later in defining the spreading of information between grid points in the final analysis. The gradient fields could be obtained directly from the first guess, but experience with this method showed that sporadic reports from data-sparse areas had more influence than they should. A more conservative and reliable method is to compute the anomaly of the first-guess field, using the climatology field as a base. This anomaly field (first guess minus climatology) is smoothed very lightly, and then added to the climatology field to create a new base field. The first-guess temperature gradients are then determined from this new base field by taking differences along the two grid coordinate directions. The anomaly smoothing suppresses very small-scale (single grid point) anomalies by tending the first-guess gradients toward climatological gradients at the anomalous points. The larger-scale anomalies which are more continuous in time are retained.

With first-guess field gradients in hand, the next step is to compute the reliability of this gradient information. This will tell us how far information is to be spread between grid points and how much one grid point should influence another. Both local and advective components must be considered in determining gradient reliability. Local effects include all types of small-scale effects, such as water depth differences, different mixing rates, proximity of land, river run-off, cloudiness, etc. The advective effects include movement of warmer or colder water through a grid point, and also account for the uncertainty in a tight gradient where a small change in location may make a big difference in the water temperature. A lower reliability would be assigned in the latter situation. The local and advective influences are combined to give gradient reliabilities at each point in both grid coordinate directions.

Data Preparation

The SST observations, taken from all available sources, are subjected to several checks and processes which:

(a) Eliminate reports not containing SST observations.

(b) Eliminate reports outside the grid.

(c) Eliminate exact duplicates--same station, time, and reported value.

(d) Reject reports colder than -2.1°C or warmer than 34°C, and those which exceed a calculated difference from the first-guess field. This allowable difference ranges from 5°C in zero-gradient areas to 10°C and higher where gradients are strong.

Each report which passes the above tests is assigned a reliability. This value is based on class of report (a bathythermograph report would have higher reliability than an injection-temperature report), age of the report, station location accuracy (in steep gradients, a 20-mile navigation error makes the report less reliable), and extrapolation distance to grid point (extrapolation is always an approximation, and error may be introduced).

Assembly

Each report which has passed the initial error tests is extrapolated with its assigned reliability value, along the first-guess gradient to the nearest grid point. Its temperature and reliability values are combined with the temperature and reliability information already accrued at that point. (The starting

point to the assembly is the base field discussed in the Initialization section.) When all reports are combined, we have a best estimate of the temperature at the grid point without considering surrounding grid-point information. The combined reliabilities indicate the quality of grid-point information, again without considering surrounding information.

Blending

After all information is assembled at grid points, a blending technique is applied to produce a temperature analysis. Blending by the computer at this stage corresponds to the hand analyst drawing the isotherms. The analyst draws with confidence when he has lots of data; the computer does the same at grid points where the information reliability is high. The analyst extends the influence of observations into data-void areas; the computer does, too, but more skillfully, using gradient and temperature reliabilities. The analyst injects climatology into the analysis in areas lacking in data for some time. The computer has already done this during first-guess construction.

Reliability of Analyzed Temperature Field

In the process of blending, grid-point information is spread to surrounding grid points through gradient knowledge. The degree of spreading is related to the reliability at a grid point and reliability of the surrounding gradients. After blending, each grid point will have a new temperature value, reflecting surrounding information as well as information at the grid point itself. There should, therefore, be a new higher weight associated with this new value. An extreme case might be that of one grid point with no information except first guess, surrounded by four grid points with copious report information. Before blending, the lonely grid point would have near zero reliability; after blending, information from his well-endowed neighbors would have been spread toward him and he would have acquired greater respectability (reliability).

The reliability of the blended or analyzed temperature field is calculated at this point for use in a reevaluation, a second gross error check and a first guess reevaluation.

Second Gross Error Check

After the first analysis is completed and its reliability determined, a second gross error check is made on each observation and, for each accepted report, a new reliability is determined. The error check is made by removing the influence of

the observation from the analysis, and then comparing its value with that inferred by all the remaining information. If agreement is good, the reliability of the observation being checked is not reduced for use in the next analysis cycle. Poor agreement causes a lowering of the reliability. When the observation differs by more than an assigned error limit, is is flagged and will not enter the subsequent analysis.

As an example of how the above procedure works, consider three SST reports surrounding a grid point. Assume two are reporting similar temperatures and the third reports a value several degrees different. The first analysis includes the influence of all three reports, perhaps equally weighted, along with the first guess field information. When the third ship report is removed from the field to be checked by comparison with all remaining information, it would be apparent that ship #3 matched poorly. The observation would either be rejected or be assigned a lower reliability and thus have little effect in the subsequent analysis.

Final Analysis

Upon completion of the second gross error check, the full analysis cycle is repeated, combining the observations and their new reliability values with the first-guess field which has also been reevaluated in a manner similar to the report reevaluation. In most of the SST analysis applications, the reevaluation is done twice for a total of three analysis cycles.

Decay of Final Temperature Field Reliability

The reliability of the final analysis field is decayed for the uncertainty that will develop in the intervening 12-hour period before the next analysis. This field is then stored for use as the first-guess field reliability in the next analyses.

B. Program Input

1. SST analysis and reliability fields, 12-hours-old.
2. Climatological SST fields for current, preceding and following months.
3. Sea-surface temperature observations of all types which have been received since the last analysis. (Older bathythermograph reports, if received late, are allowed to enter with reduced weight.)
4. Bogus entries created by the watch team to force the analysis to reject a specified observation, to accept a specified observation, or to take on a given value at a given location.

C. Program Computation

1. Compute current climatology.
2. Compute mean climatology gradient.
3. Compute climatological weight field.
4. Tend previous SST analysis toward climatology.
5. Smooth climatic anomaly field.
6. Compute first-guess gradients.
7. Compute reliabilities of gradients.
8. Prepare data.
9. Assemble data at grid points.
10. Blend assembled data to obtain temperature.
11. Compute reliability of temperature field. (Go to 14 if this is the final pass.)
12. Error check and reevaluate reports.
13. Reevaluate first guess. (Go back to 9 if not final pass.)
14. Decay temperature reliability and save for next analysis.

D. Program Limitations and Verification

The assumptions concerning computation and use of reliability and climatology in FIB/SST are quite conservative, and work toward keeping the analysis smoothly continuous in time. The only real limitations on the program are data distribution and quality. In the large no-data areas which occur at every analysis time, the analysis must necessarily be considered less reliable. Here, other than spreading from data areas, history and climatology are the main inputs to the analysis. Even in areas where data are plentiful, there is still an uncertainty of at least 1°C in the analysis due to inaccuracies in the reports and small-scale or temporary features. This is demonstrated in nearly every analysis when ships at or near the same location consistently report different temperature values over a range of 2° to 3°C.

In the FIB/SST program, the analysis is compared to all available reports at the end of each run. On the average, 50% of the reports are with 0.5°C of the analysis values and 75% are within 1°C. This is accomplished with a relatively smooth analysis product.

E. Uses of the Product

The SST analysis is used primarily as input to other FNWC products (see Part F), but it has some uses in the field. There is no technical difficulty in using SST charts; the temperatures at points of interest are simply read off the chart.

SST charts are useful in forecasting advection-type fogs. These fogs generally occur when sea air is cooled to dew point temperature by passage over colder water; the rarer steam fogs occur when cold air with a low vapor pressure passes over warm sea water. The forecast parameters include air/sea temperature difference, humidity of the air, air trajectory, and pressure gradient.

SST analyses can be used to outline areas where super-gradient surface winds may be expected. This situation arises when cold winds blow over warmer water; northerly wind off the continental U. S. blowing over the Gulf Stream is a common case. The warm water heats the air, causing instability and low-level turbulence. The turbulence has the effect of transferring the energy from the stronger upper winds down to the surface, thus giving higher (up to double) average wind speeds and gusts than would be expected from surface gradients.

Sea-surface temperature information is provided during briefings for all over-water flight operations.

Fishing operations are conducted to a large extent on the basis of sea-surface temperature distribution.

SST charts are useful in a general way in tropical cyclone forecasting. When sea-surface temperatures in a tropical area are below 27°C, tropical disturbances rarely develop. At temperatures of 27°C to 29°C, tropical cyclones generally remain in the 75-100 knot category. At 30°C, and above, the super-storms are able to develop. In general, the chances of tropical disturbance formation increase with higher sea-surface temperatures. Tropical cyclones of all intensities tend to follow paths over areas of warmer water.

Topical cloud systems moving into areas of warmer sea-surface temperatures will tend to increase in intensity. Cooler sea temperatures will tend to decrease intensity.

In an emergency, the SST charts can be used to build a subsurface thermal structure profile. If you were forecasting for an ASW exercise and for some reason no acoustic products were available, the SST chart could be used as a starting point for building subsurface temperature profiles. By adding knowledge of the MLD and the thermocline, sonic ranges could be computed in a rough manner.

F. Relationship to Other Products

The SST analysis is used as input in at least 12 other FNWC products. The role played by the SST analysis is described in more detail than shown below in the separate product descriptions.

1. P.E. Model - to compute sensible heat flux over water.

2. SST anomalies - the SST analysis and SST climatology are used for this product.

3. Oceanic Fronts - fronts are determined by application of the "GG" operator (second derivative) to the SST analysis. [4]

4. Marine Layer Winds - these are surface geostrophic winds used in the Sea/Swell program. Corrections to the computed surface winds for stability and latitude are mostly derived from the SST analysis.

5. Ocean Currents - the SST analysis provides temperature data for the thermal components of the Ocean Current model.

6. Surface Temperature and Vapor Pressure - the SST analysis is used as a base for checking reported surface

air temperatures and computed surface dewpoint depression temperatures.

7. Global Band Surface Pressure and Wind Analyses - the SST analysis is used to correct surface geostrophic winds as in F4 above.

8. Ocean-Atmosphere Heat Exchange Analysis - the SST analysis is one component of computations for back radiation, sensible heat exchange, and latent heat exchange.

9. Acoustic Products - the SST analysis is the temperature anchor-point for computation of these products related to underwater sound analysis.

G. Program Output

Analyses of sea surface temperatures, and SST anomalies relative to climatology, are performed twice daily for the following areas. Units are °C.

Catalog No.	Product	Mesh Size*
B10	Northern Hemisphere SST	1
P11	Northern Hemisphere SST Anomaly	1
B10	Southern Hemisphere SST	1
P11	Southern Hemisphere SST Anomaly	1
P66	Gulf Stream SST	1/8
P68	Gulf Stream SST Anomaly	1/8
P56	Newfoundland Basin SST	1/8
P58	Newfoundland Basin SST Anomaly	1/8
P51	Kuroshio SST	1/4
P52	Kuroshio SST Anomaly	1/4
P59	Mediterranean SST	1/4
P60	Mediterranean SST Anomaly	1/4
B11	Southern California SST	1/8
B12	Southern California SST Anomaly	1/8
P62	Norwegian Sea SST	1/8
P63	Norwegian Sea SST Anomaly	1/8
P90	Iberian Basin SST	1/8
P91	Iberian Basin SST Anomaly	1/8

*Mesh size is relative to the standard FNWC 63x63 hemispheric grid.

H. References or Suggested Reading

[1] Holl, Manfred M., Bruce R. Mendenhall and Charles E. Tilden, 1971; "Technical Developments for Operational Sea Surface Temperature Analysis with Capability for Satellite Data Input", Final Report, Contract No. N62306-70-C-334, Meteorology International Incorporated, Monterey, California, September 1971.

[2] Tilden, C. E., J. R. Clark and M. M. Holl, 1969; "Techniques for the Utilization of Satellite Observations in Operational Mapping of Sea Surface Temperature", Final Report, Contract No. N62306-C-0288, Meteorology International Incorporated, Monterey, Calfornia.

[3] Danard, M. B., M. M. Holl, and J. R. Clark, 1968; "Fields by Correlation Assembly - A Numerical Analysis Technique", Monthly Weather Review, Vol. 96, No. 3.

[4] Clarke, L. C. and T. Laevastu, 1966; "Numerical methods for synoptic computation of oceanic fronts and water type boundaries and their significance in applied oceanography", Technical Note No. 20, U. S. Navy, Fleet Numerical Weather Central, Monterey, California, 38 pp.

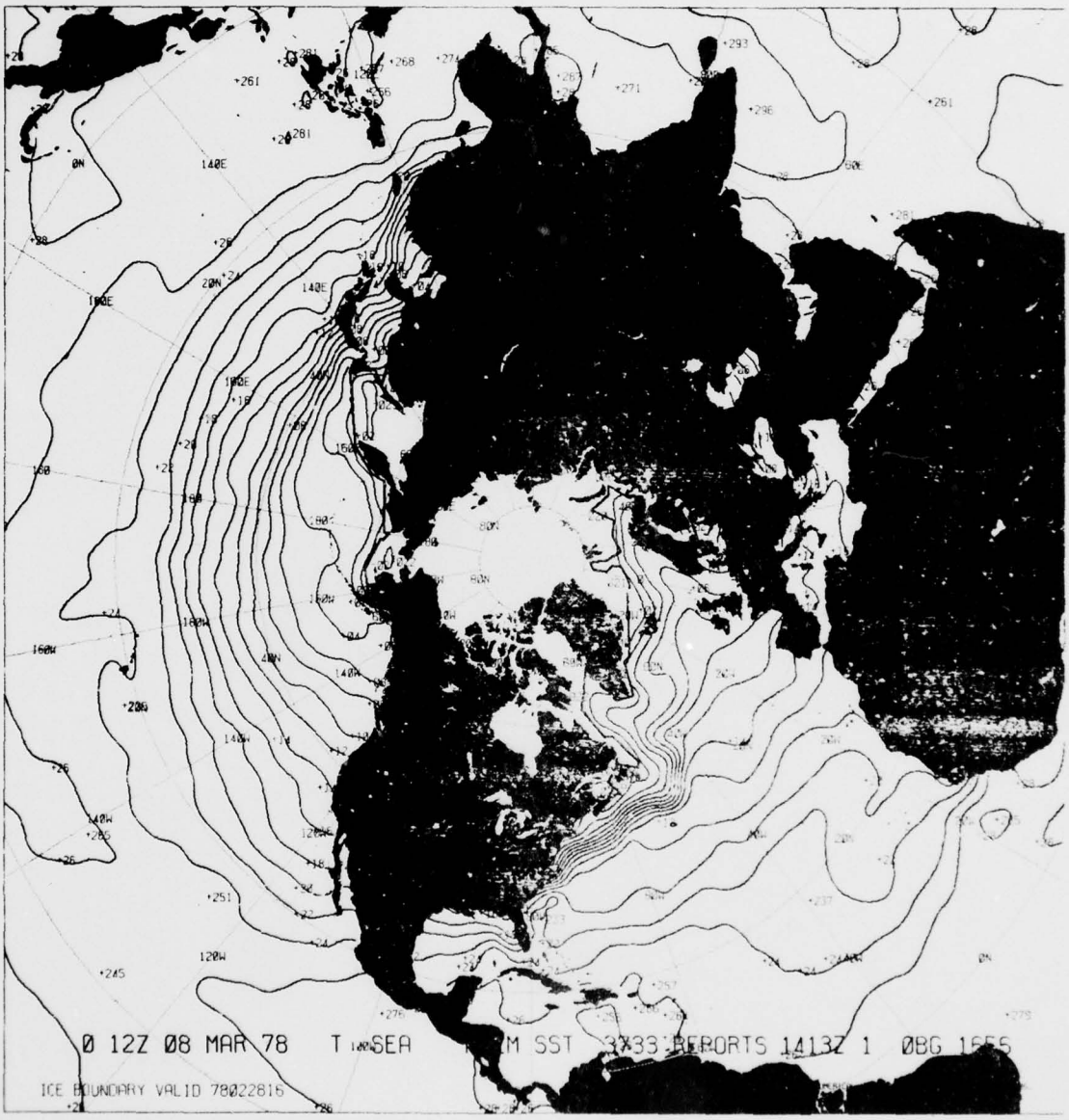


FIGURE 5.1.1 Northern Hemisphere SST Analysis (B10)

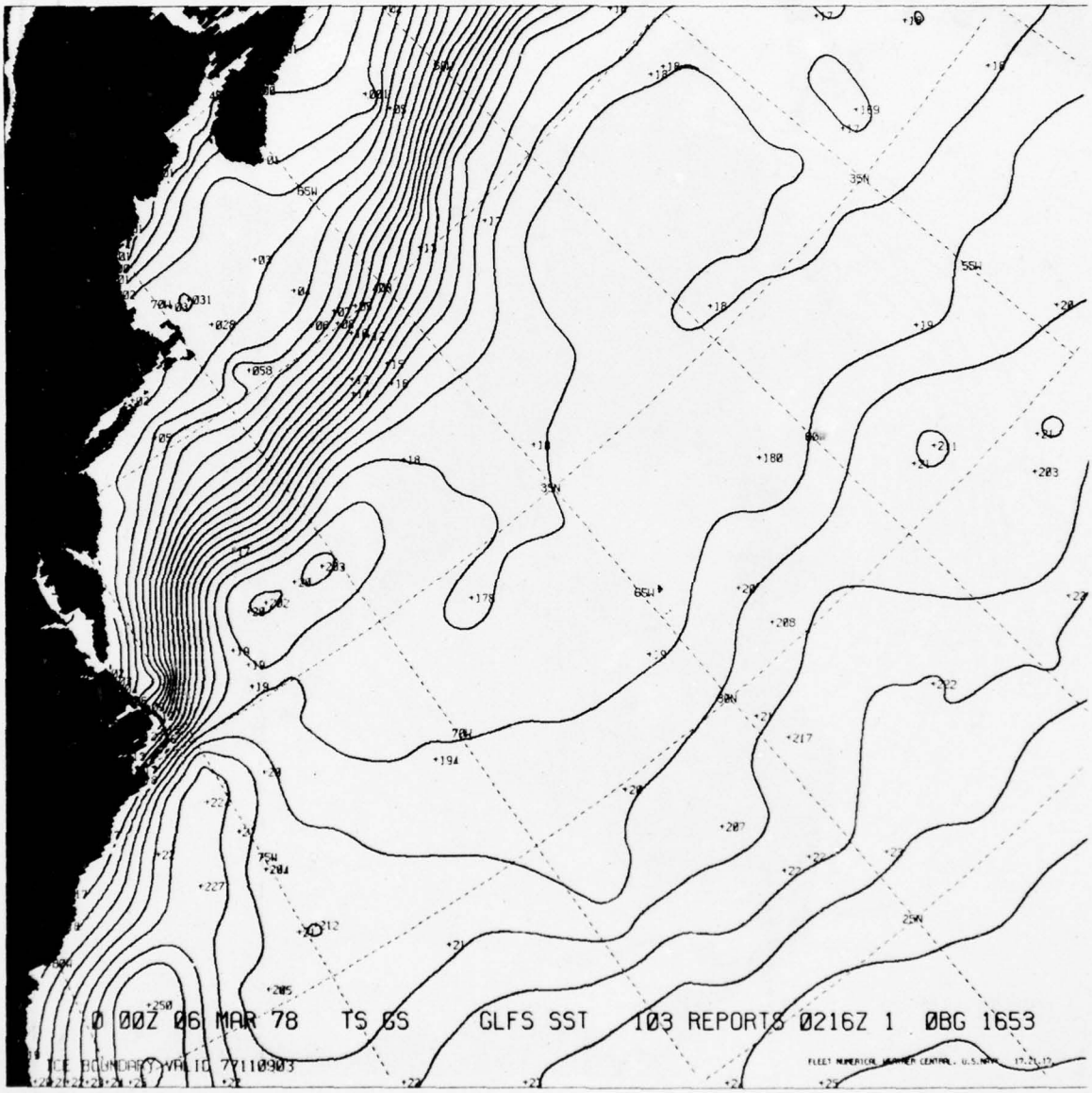


FIGURE 5.1.2 Gulf Stream SST Analysis (P66)

5.2 SEA-SURFACE TEMPERATURE ANOMALIES

A. Model Development

An anomaly is the deviation in a given region or location over a specified time (day, week, month, season) from the normal (long-period average) value for the same region or location and time. Thus, SST anomalies can be computed as the difference between the daily SST analysis and some long-period average. SST anomalies have several causes--advection of colder or warmer water, upwelling, excessive local heating, current convergence, excessive cloudiness, and winds (advection and mixing).

SST anomalies have been studied extensively in an effort to determine their relationship to the atmospheric circulation. Large-scale and persistent SST anomalies have been linked to changes in climate, changed areas of good fishing, and seasonal hurricane frequency. Small-scale, short-term SST anomalies can be related to short periods of a certain type of weather, as can be seen along the California Coast with a strong negative anomaly offshore.

SST anomaly charts have been produced at FNWC for several years, using various techniques, and used extensively in studies of air/sea interaction. While the old anomaly charts were satisfactory, the possibility of producing much improved ones seemed likely when two new tools appeared--the SSTFIB analysis program and the development of a stored, up-to-date SST climatological bank. Program development was started in mid-1971.

The SSTFIB analysis technique is fully described in Section 5.1. It represents the latest and most accurate method of analyzing SST by computer. The reliability of the analysis in areas of even a limited number of reports will be within one degree, and within reporting accuracy where there are more reports. In areas where there are no reports, the weight of climatology in the SSTFIB analysis program will predominate, so that anomalies may not show--as might be expected when it's only matching climatology against climatology. The comforting thing in these no-data areas is that you won't be told there's a big anomaly there when there isn't. Better to be told nothing than a lie. In general, the SSTFIB analysis is a very firm foundation from which to start the anomaly calculations.

Climatology of the oceans has had a very checkered career, and it has only been in the past few years that historical information from all seafaring nations has been gathered together for statistical and analytical treatment. Before this, research studies were based on such samples as 10 years over some small area, added to 15 years from an adjoining area, etc. For the new anomaly model, world-wide coverage of SST reports based on over 100 years of data was available from various recent Hydrographic Office publications. Using these, a data bank of monthly mean SST values was created and stored for each point of the 125x125 grid. Application of the climatological values in the anomaly program is unique. The usual practice has been to give equal weight to each unit of the period to be averaged; viz., if you were working in August and using a three-month average period, July, August, and September would be counted equally. This would result in a big jump when the working month shifted to September, July dropped out, and October came in. The new method uses a weighting system which changes with each 12-hour analysis. The working month gets a 0.5 weight. If it happens to be the 20th day of a 30-day month, the preceding month would get a $11/30 \cdot 0.5$ weight, and the following month would be weighted at $19/30 \cdot 0.5$ of that month's climatological value. The method provides a smooth, slowly-changing SST climatological value for comparison against the analysis value.

B. Program Input

1. Sea-surface temperature analyses for the current 12-hr period.
2. Monthly mean sea-surface temperature climatology.

C. Program Computation

1. Compute weighted mean SST climatological value at each grid point.
2. Subtract climatological value from analyzed value at each grid point.

D. Limitations

The tropical regions south of 20°N are notorious for lack of data, both synoptic and climatological. In the North Pacific, for example, at least 75 percent of the tropical-area climatology is based on fewer than ten reports per 1° block. This makes the climatology suspect. And in this area with very few synoptic SST reports, the SST analysis will be weak.

In all parts of the ocean, there are comparatively large areas where days, even weeks, may pass without a single SST observation. In these areas, the SST analysis will gradually creep toward climatological values. Ship coverage charts can be used to alert forecasters to these places where the SST analysis may be poor.

The Indian Ocean has less historical data than any of the oceans, particularly away from coastal areas. SST anomaly charts in the Indian Ocean should be used with caution.

E. Uses of the Product

SST anomalies of the large-scale, persistent type can be used to better advantage in long-range than in day-to-day forecasting. There are, though, some uses in the latter category. Examples of possible SST anomaly chart use follow:

1. SST anomalies in areas of upwelling show the intensity involved. Upwelling off the San Francisco area is one good case. A 2 to 3 degree negative anomaly alerts a forecaster to the probability of increased fog and low stratus moving inland with any onshore wind. A persistent strong positive anomaly off the Peruvian coast could warn of the dreaded El Niño, when fish and birds die by the millions and there is a terrible stench for hundreds of miles in all directions.
2. SST anomaly charts are of great value to the fishing industry, particularly in tuna fishing. Albacore fishing is best between 17° and 19°C. Anomalously warm SST temperatures off California and Oregon warn that the best fishing areas will shift farther north.
3. Middle latitude areas of persistent warm anomalies are action centers for the initiation of cyclogenesis and strong intensification of cyclonic activity. The cause is increased flow of heat and moisture.
4. A strong cold SST anomaly in the area of the semi-permanent high cells will cause the highs to build strongly.
5. Warm anomalies at high latitudes cause the building and maintenance of blocks during the cold seasons.
6. Unusually inactive hurricane seasons have been linked to persistent cold SST anomalies over the western Atlantic. These were anomalies that averaged 5°C below normal in the center of the cold pool, and persisted throughout the hurricane season.
7. Subsurface thermal structure can be estimated using SST anomaly charts. Surface temperatures generally extend to the bottom of the Mixed Layer Depth.
8. There is correlation between 700-mb height and SST anomalies. Positive 700-mb height anomalies are found over positive SST anomalies, and negative over negative.
9. Strong positive anomalies in equatorial waters, strong enough so that the sea water temperature is greater than air temperature, are a sign that big monthly totals of rainfall may be expected in the area of the anomaly. The excessive rainfall occurs because of the strong upward transfer of moisture and intense convection.
10. Strong positive anomalies in tropical waters are favored areas for the formation of tropical cyclones. Once formed, tropical cyclones have a remarkably persistent tendency to move into or along the areas of greatest positive SST anomaly.
11. West Coast anomalies can be used for temperature forecasting. Strong cold anomalies mean low temperatures inland.

F. Relationship to Other Products

The SST anomaly charts are not used as input for generation of any other FNWC products.

G. Program Output

1. SST anomaly charts for 00Z and 12Z (as described in paragraph G, section 5.1).

2. SST 5-day mean anomaly (Catalog No. P12).

3. SST 5-day mean (Catalog No. P13).

H. References or Suggested Reading

[1] Laevastu, T. and W. E. Hubert, 1970; "The Nature of Sea Surface Temperature Anomalies and Their Possible Effects on Weather", FNWC Tech. Note No. 55.

[2] Hubert, W. E. and T. Laevastu, 1966; "Sea Surface Temperature Anomalies for the Northern Hemisphere during the First Half of 1966", FNWC Tech. Note No. 23.

[3] Hubert, W.E. and T. Laevastu, 1966; "Short-Period Changes and Anomalies of Temperature in the Oceans and Their Effects on Sound Propagation", FNWC Tech. Note No. 18.

Climatology Sources

Pacific: Monthly Charts of Mean, Minimum, and Maximum Sea Surface Temperature of the North Pacific Ocean. SP-123, U. S. Naval Oceanographic Office, 1969.

Atlantic: Oceanographic Atlas of the North Atlantic Ocean, Sec. II. Physical Properties. Pub. No. 700, U. S. Navy Oceanographic Office, 1967.

Arctic: Oceanographic Atlas of the Polar Seas, Part II Arctic. H. O. 705, U. S. Navy Hydrographic Office, 1944.

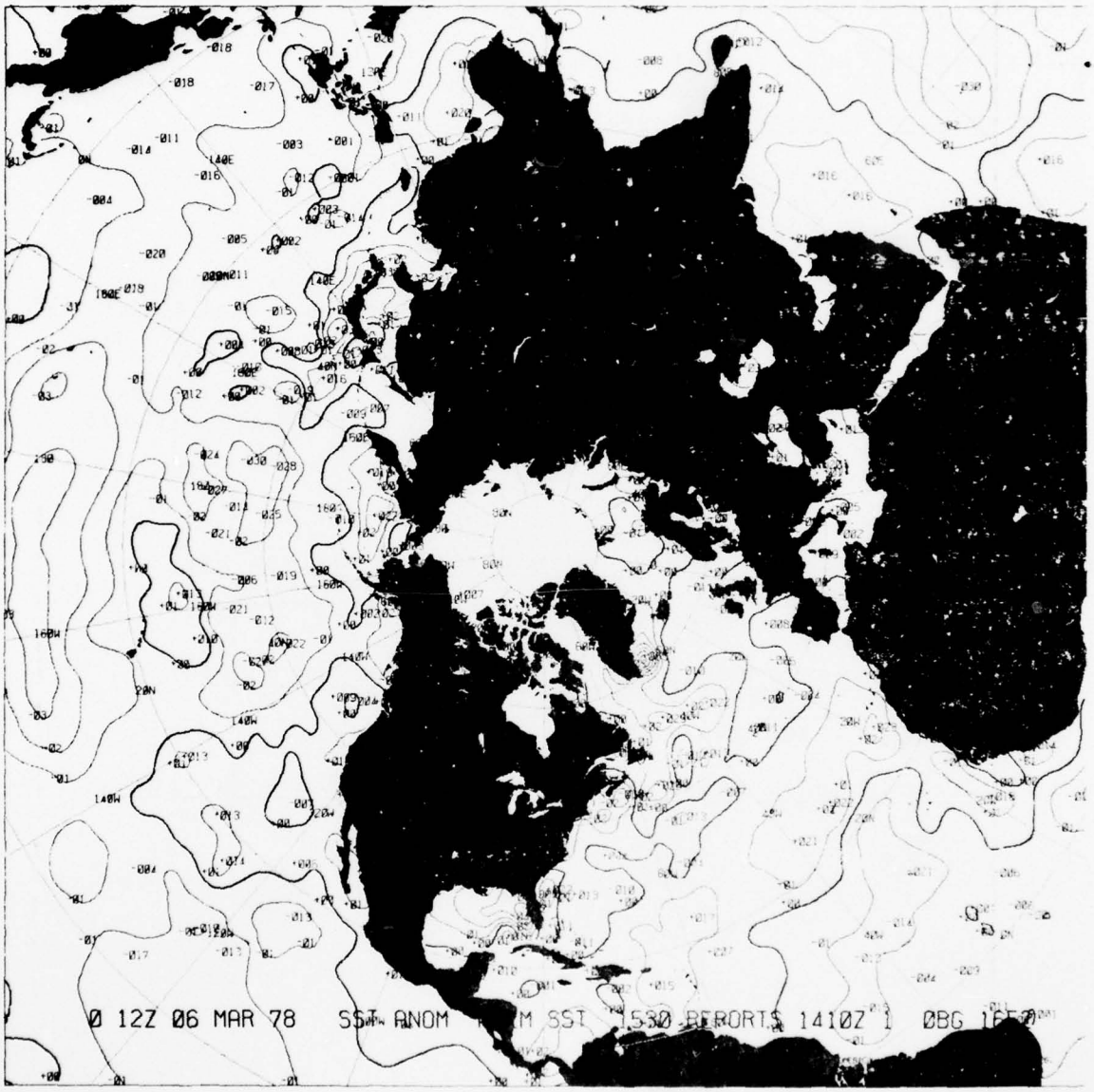


FIGURE 5.2.1 SST ANOMALY (F11)

5.3 BATHYTHERMOGRAPH ERROR SUMMARY

A. Project Development

The Bathy Error Summary (BES) project has been developed to monitor BT reports from ships and air squadrons. These reports are vital as a basis for ocean acoustic predictions for ASW applications. The sparse coverage and non-uniform distribution of the approximately 250 reports received daily at FNWC necessitates that error identification and correction be given constant attention.

B. Program Input

1. Bathythermograph reports with incoming reports error status.

C. Processing

Bathythermograph reports received at FNWC are first processed by an error checking program which sets error bits in a data list recording the report's error status. The BES program processes this data and generates plain language messages and printed summaries of reports for specified time periods.

D. Program Limitations

The BES system logic is able to recognize certain types of coding errors and correct some of them. For example, date-time-group year and month coding errors can be corrected under the assumption that the reports are recent. In other instances, format may be incorrect or numbers may be out of range, or improperly related to each other. In such cases, an error can be restricted to a certain part of the BT report, but not necessarily corrected by machine. Some of these reports can be manually corrected; others must be considered unusable.

E. Uses of the Products

1. Monthly BES Report--Summaries are prepared, monthly, for each U. S. ship and squadron (Fig. 5.3.1), including listings of format errors detected and how many times; the number of reports received, how many were correct, how many were in error but computer correctable, and how many were uncorrectable; and the corresponding percentages of correct, correctable, and uncorrectable reports.

2. Special BES Report--Special summaries are produced, on request, for ships or squadrons reporting BT's; any time period may be specified. The format is the same as that of the monthly reports, except that the previous month's percentages are omitted.

3. Bathy Error Message--When an error is noted several times for a particular reporting activity during the course of daily quality control of incoming BT's, a message is sent to that activity pointing out the error and requesting that future reports not repeat the same error.

Monthly fleet summaries are available for the Atlantic and Pacific fleets for both AXBT reports and SXBT reports.

F. Relationship to Other Products

No other FNWC products require the BES program products as input.

G. Program Output

1. Monthly BES Report.

2. Atlantic Fleet Monthly Summary.

3. Pacific Fleet Monthly Summary.

These three products are sent by U. S. mail to the Navy and Coast Guard units and staffs requesting them.

4. Special BES Report.

5. Bathy Error Message.

These two products are sent via AUTODIN just after the requested monitor periods.

H. References

[1] OCEANAVINST 3160.9B, "Collection and Reporting of Bathythermograph Reports".

PERIOD 01 JULY 76 TO 31 JULY 76

1. ALL BATHYS RECEIVED

TYPE ERROR	MACHINE CORRECTABLE	NON CORRECTABLE	TOTAL
REPORT DOES NOT CONSIST OF 5 CHARACTER GROUPS SEPARATED BY SPACE	0	1	1
NON-NUMERIC CHARACTER IN NUMERIC GROUP	0	1	1
DEPTH IN DEPTH/TEMPERATURE GROUP INDICATES DEPTH NOT INCREASING	0	1	1
TOTALS	0	3	3

TOTAL REPORTS RECEIVED (T)			11
NUMBER OF CORRECT REPORTS		(P)	10
NUMBER OF MACHINE CORRECTED REPORTS USED AT LEAST TO FIRST LEVEL BELOW SURFACE		(C)	0
NUMBER OF REPORTS NOT MACHINE CORRECTABLE REQUIRED MANUAL CORRECTION WHERE POSSIBLE		(J)	1
PERCENT CORRECT	P/T		90.9
PERCENT UNUSABLE	J/T		9.1
PERCENT PARTIALLY USABLE	C/T		0.0

2. FOR COMPARISON, STATISTICS FOR PERIOD 01 JUN 75 30 JUN 75 FOLLOW

TOTAL REPORTS RECEIVED (T)		1
PERCENT CORRECT	P/T	100.0
PERCENT UNUSABLE	J/T	0.0
PERCENT PARTIALLY USUABLE	C/T	0.0

FIGURE 5.3.1 The Monthly Bathythermograph Error Summary Report

5.4. OCEAN THERMAL STRUCTURE MODEL

A. Development of the Model

The Ocean Thermal Structure (OTS) model is based on a parameterization of the vertical temperature profile, for which studies commenced in 1969. The problem in modeling OTS was to develop a set of parameters which captures the significant variability of the vertical structure while having sufficient horizontal continuity to be subjectable to horizontal analysis. The technique used for the analyses is the FIB methodology (see Section 3.10) developed by Meteorology International Incorporated.

The OTS model, installed operationally at FNWC in 1976, consists of several programs. Each program serves a specific function in developing the requisite parameterization.

B. Program Input

1. Climatology for the OTS parameters was constructed from bathythermograph data supplied by FNWC.

2. BT data up to 72 hours old, received since the last analysis, are used for each current run.

3. Field parameters from the last (24-hours-old) OTS model run are used for initialization.

4. SST, wave and wind fields from other FNWC analyses are used in the computations.

5. Bogus entries, created by the watch team, are used to force the analysis to accept or reject a specified report or to take on a given value at a given location.

C. Program Computation

1. Diagnose the parameter information in the BT reports. (Program DGTSTR)

2. Perform horizontal analysis of parameter fields using the parameter information from the BT data. (Program FIBOTS)

3. Produce vertically blended temperature profiles from shallow parameter fields, and deep climatology temperature fields. (Program RCNTF)

The primary layer depth (PLD) is the key parameter diagnosed by program DGTSTR. The PLD is the level of greatest negative curvature* in the BT profile. Other layer depths for which the negative temperature curvature is greater than some

threshold** value are called secondary layer depths; up to eight secondary layer depths are retained. Parameter values are determined at fixed levels (200 feet to 1200 feet at 200-foot intervals) and at variable levels. The variable levels are associated with the layer depth values and move up or down together with the layer depth.

The horizontal analyses are made by program FIBOTS. The PLD and secondary layer depths from each parameterized BT report are considered as potential layer depths for the final horizontally analyzed PLD.

Vertically blended profiles from the horizontally analyzed fields and deep temperature climatology are constructed by program RCNTF. The grid-point profiles are reconstructed and blended, then the horizontal fields are reassembled. This constitutes the final step in a three-dimensional blending.

*NOTE: A level exhibits negative temperature curvature if the rate-of-temperature-decrease-with-depth below the level is greater than the rate-of-temperature-decrease-with-depth above the level.

**NOTE: The threshold value for curvature for secondary layer depth is presently set at $-.5°C/50\ ft^2$.

D. Program Limitations and Verification

The OTS model produces a 3-dimensional structure parameterization of the temperature variations in the ocean. This parameterization is constructed by performing a vertical blending of horizontally analyzed fields. Data limitations include BT report errors, short BT's, and a number of reports. Errors are well screened by the FNWC ADP programs, and machine or manually corrected where possible. BT reports which do not extend past the depth of the first-guess PLD depth by at least 50 feet are discarded to insure that shallow secondary layer depths do not override a strong layer depth which may exist below. In this manner, shallow bias in the PLD analysis is eliminated. The major limitation to the analysis at present is that only some 200 reports are received daily over the Northern Hemisphere and they are not evenly distributed in space.

E. Uses of the Product

Primary uses of the OTS products are for input to other FNWC programs.

F. Relationship to Other Products

The ocean thermocline structure is a determining factor in the ocean-acoustic environment. OTS model output is used as input to the FNWC acoustic models.

G. Program Output

	Field	Catalog Number
1.	Primary Layer Depth	B38
2.	Temperature at 200 feet	P25
3.	Temperature at 400 feet	P26
4.	Temperature at 600 feet	P27
5.	Temperature at 800 feet	P28
6.	Temperature at 1000 feet	P29
7.	Temperature at 1200 feet	P30
8.	First Temperature Difference (200ft-Surface))	P14
9.	First Temperature Difference (400-200)	P15
10.	First Temperature Difference (600-400)	P16
11.	First Temperature Difference (800-600)	P17
12.	First Temperature Difference (1000-800)	P18
13.	First Temperature Difference (1200-1000)	P19
14.	Temperature at PLD	P32
15.	Temperature at PLD+100 ft	P37
16.	Temperature at PLD+200 ft	P38
17.	First Temperature Difference [(PLD) - (PLD-100 ft)]	P39
18.	First Temperature Difference [(PLD+100 ft) - (PLD)]	P31
19.	First Temperature Difference [(PLD+200ft) - (PLD+100ft)]	P40
20.	First Temperature Difference [(PLD+300ft) - (PLD+200ft)]	P07
21.	Second Temperature Difference [centered at (PLD+100ft)]	P08

H. References

[1] Mendenhall, Bruce R., 1975; "Implementation of the Daily Ocean Thermal-Structure Parameter Analysis Capability (FIB/OTS)", Performance Report of Task Three (and Final Report), MII Project No. M-214 (Contract No. N00228-75-C-2364, Fleet Numerical Weather Central), Meteorology International Incorporated, Monterey California, 9 pp.

[2] Weigle, William F., 1973; "The Development of a New System for the Analysis of Ocean Thermal-Structure Distribution", Final Report, MII Project No. M-177 (Contract No. N66314-72-C-1370, Fleet Numerical Weather Central), Meteorology Internaltional Incorporated, Monterey, CA, 38 pp.

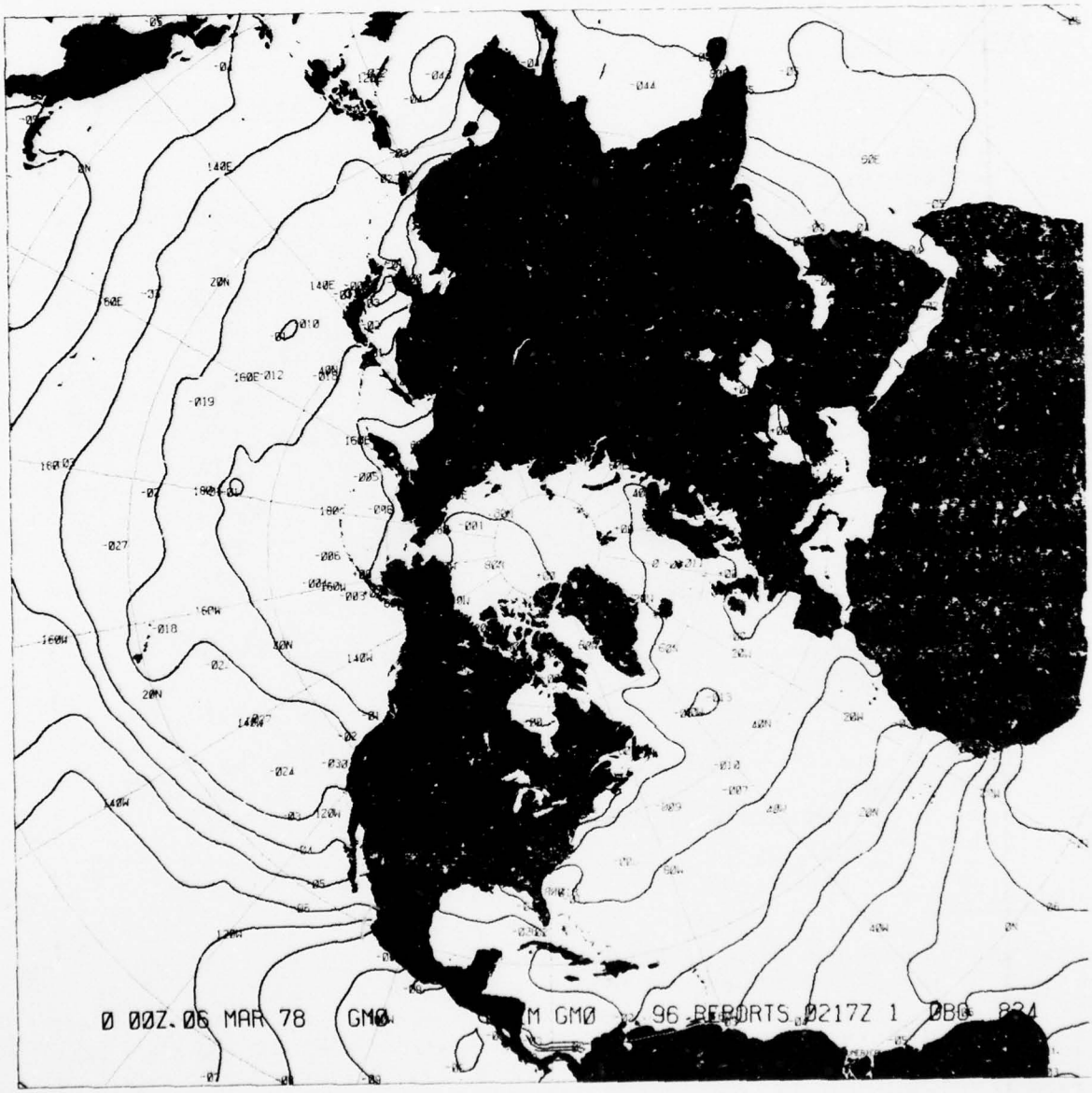


FIGURE 5.4.1 Temperature Gradient at the Primary Layer (F31)

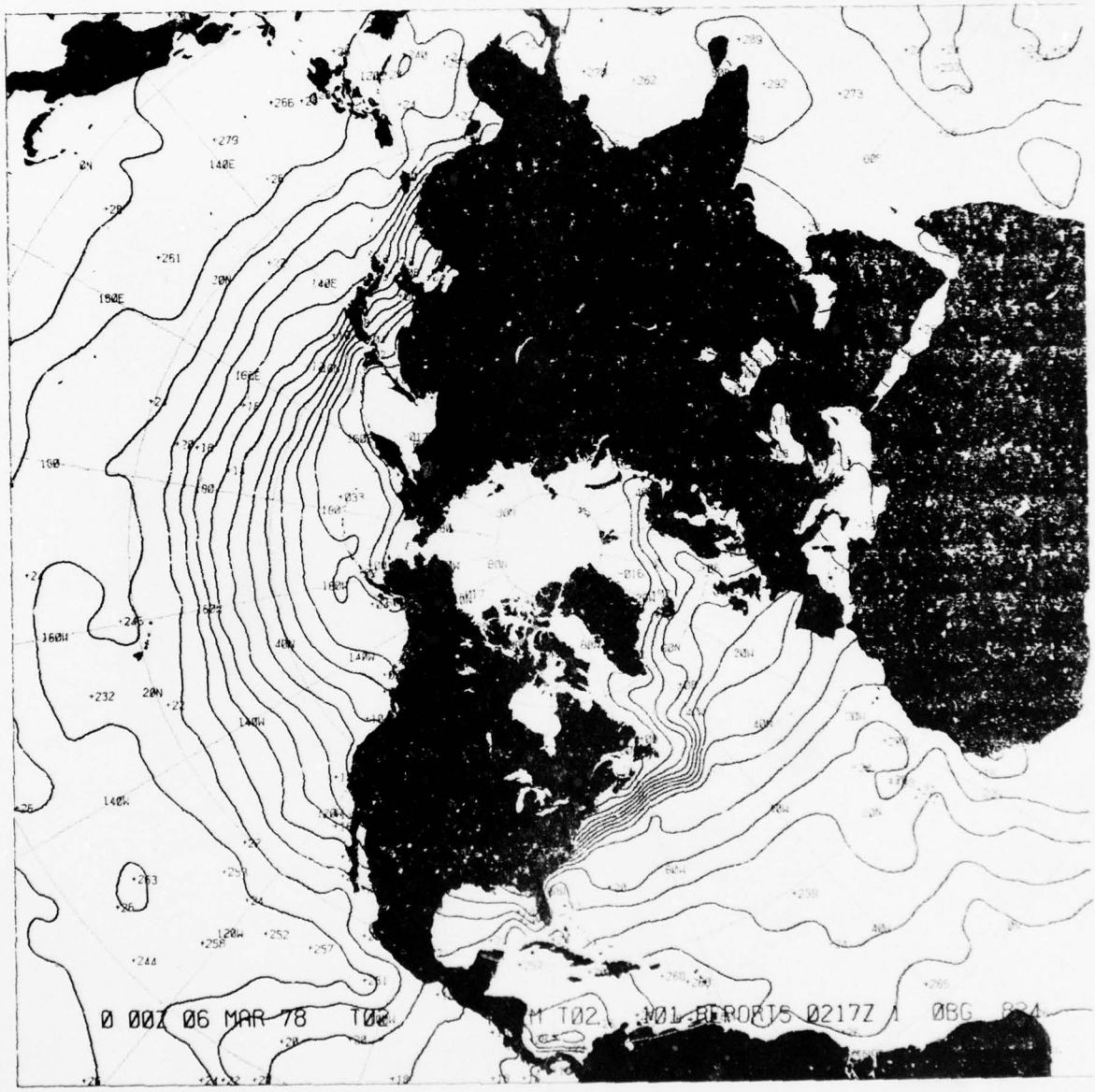


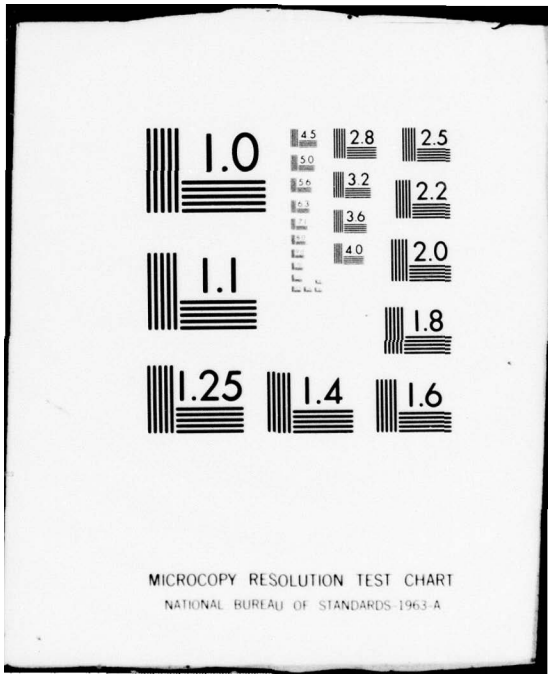
FIGURE 5.4.2 Temperature at 200 ft (P2F)

AD-A065 511 NAVAL WEATHER SERVICE COMMAND WASHINGTON D C F/G 4/2
U.S. NAVAL WEATHER SERVICE NUMERICAL ENVIRONMENTAL PRODUCTS MAN--ETC(U)
FEB 79 E T HARDING

UNCLASSIFIED NAVAIR-50-16-522-REV NL

3 OF 4
AD
A065511




1.0
1.1
1.25
1.4
1.6
1.8
2.0
2.2
2.5
2.8
3.2
3.6
4.0
4.5
5.0
5.6
MICROCOPY RESOLUTION TEST CHART
NATIONAL BUREAU OF STANDARDS-1963-A

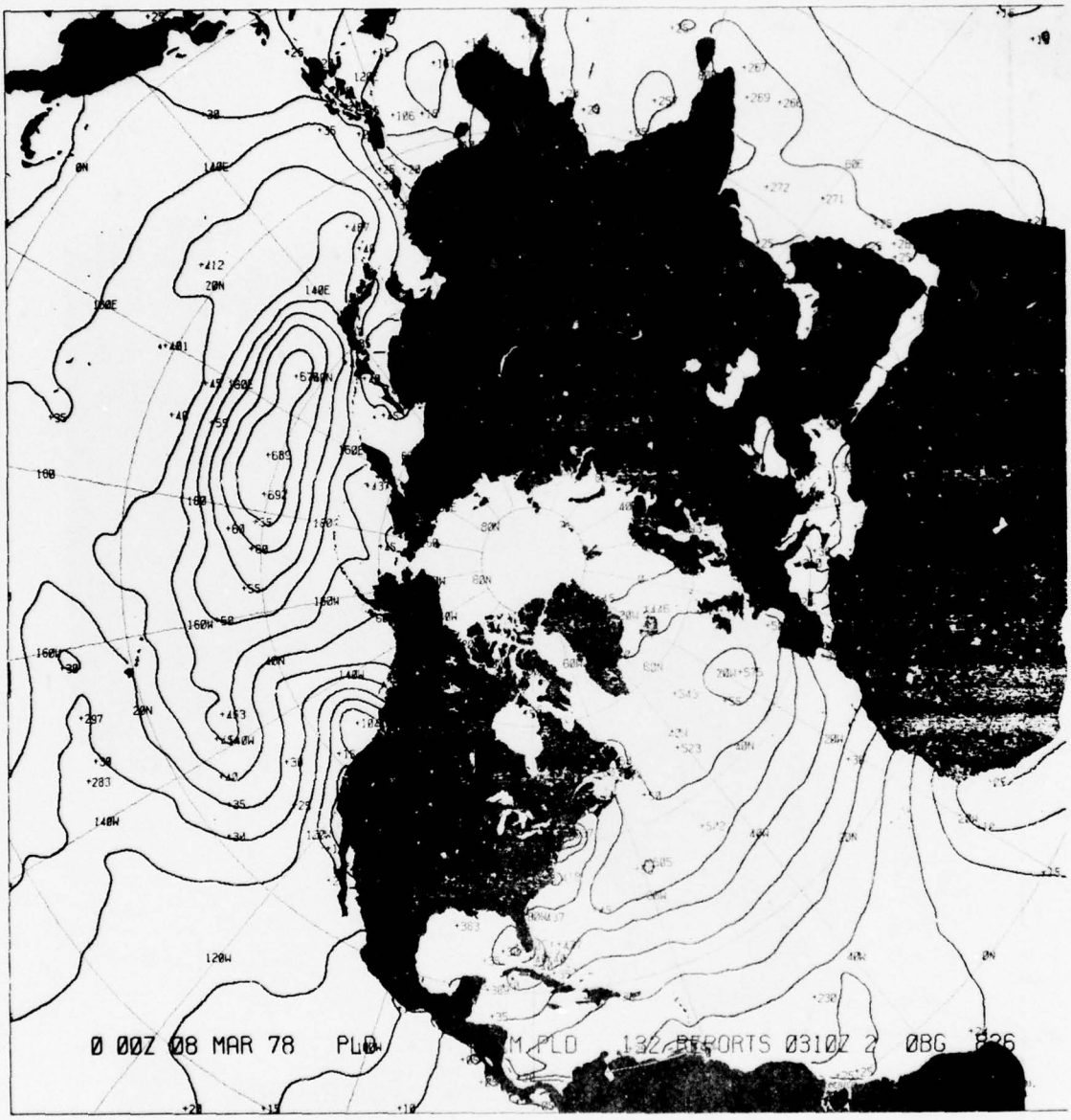


FIGURE 5.4.3 Primary Layer Depth (B38)

5.9 OCEAN SURFACE CURRENT ANALYSES AND PROGNOSES

A. Development of the Model

Ocean currents are caused by force imbalances derived from temperature and salinity variations, wind stress, water waves, tidal motions, and other less important environmental features. Prior to development of the surface current models, all ocean current information came from oceanographic atlases.

For the hemispheric current model, the surface current structure problem has been reduced to a dependence on local wind driven flow (including mass transport by waves) and on permanent thermal flow. In the Grand Banks area of the North Atlantic, the Labrador Current driving forces depend, more than the general ocean current, on salinity variations which contribute to the thermohaline flow.

The Grand Banks surface current program was developed in response to a U. S. Coast Guard request in December of 1973. It is directed toward assisting the Coast Guard in monitoring the position of drifting ice to fulfill the responsibilities of the United States involvement in the International Ice Patrol. The Grand Banks Surface Current Analysis provides a fine mesh analysis in an area where salinity variations have a non-negligible contribution to thermohaline flow.

B. Model Input

1. Ocean Surface Current
   a. Sea-Surface Temperature analysis.
   b. 600-foot level sea temperature analysis.
   c. Surface pressure analysis.
   d. Surface pressure prognosis, 24 hours.
2. Grand Banks Surface Current
   a. Ocean Surface Current analysis.
   b. Sea-Surface Temperature analysis.
   c. Temperature climatology.
   d. Dynamic topography (includes salinity input)
   e. Marine Wind Fields.

C. Program Computation

1. Ocean Surface Current
   a. Calculate the mean temperature field for the layer from the surface to the 600-foot level.
   b. Determine the horizontal temperature gradient.
   c. Apply thermal current equations to the gradient field to compute u and v components of the surface current due to temperature variations.
   d. Compute geostrophic wind from the SLP analysis and the 24-hour prognosis.
   e. Compute a marine (surface) wind from the geostrophic wind.
   f. Compute u and v components of the surface current due to surface wind.

g. Generate the surface current by combining the wind and thermal components.

h. Generate non-divergent stream function analysis in order to display current speed and direction in one continuous field.

2. Grand Banks Surface Current

a. Produce fine grid wind analysis from marine wind analysis from marine wind fields and marine wind data.

b. Produce surface current approximations from dynamic topography.

c. Produce thermal current component from temperature climatology and sea-surface temperature analysis.

d. Produce Ekman* component of surface current from wind fields.

e. Interpolate summed values of thermal and wind components of the surface current to a 20-minute (39x45) grid mesh over the area 40° through 50°N latitude, 43° through 57°W longitude.

D. Program Limitations and Verification

The FNWC total ocean surface current is the vector sum of the thermal and wind driven components. It is adequate for hemispheric-scale analysis, but it cannot show small features of considerable interest; it is designed to picture current patterns over deep water.

Small scale currents such as the Florida Current and the Alaskan Stream are of sub-grid scale. Salinity dominated currents such as the Greenland Current System and the Labrador Current are not well described without consideration of salinity distribution. Coastal areas or areas near island chains are affected by coastal contours, tidal currents, shallow water, and other boundary effects not accounted for by the model.

Macroscale features such as the anti-cyclonic circulation associated with the subtropical semi-permanent, high pressure wind circulations are well depicted. In the northwestern portions of these regions where the surface layer thermal gradients are strong, producing thermal current components in the same direction as the prevailing wind effect current, the two components are additive. The Gulf Stream and the Kuroshio Current are examples of these additive effects.

Verification of surface current products is seldom feasible in the field; observations would be available only in rare situations. Field units must rely on the FNWC verification program.

Verification at FNWC is not the direct type since observations of surface currents are so rare. Current observations are normally recorded by oceanographic research-type vessels. Such data seldom have real-time synoptic utility that could serve as direct verification of the analysis. Current measurements typically find their way into atlas summaries and oceanographic reports, and are usually not available to the oceanographic community for weeks or months after observations are made. Ship navigation drift data, which serves as the preponderance of data for the compilation of surface current atlases, generally give speed values significantly lower than real currents. The FNWC current model agrees well with atlases in direction but is somewhat higher in speed. FNWC monthly mean currents, however, are almost identical with monthly mean currents in available atlases. The maximum major current velocities, such as the Gulf Stream and Kuroshio, are well within accepted ranges.

Other indirect means are used to verify the FNWC surface current product. Sea-surface temperature (SST) is the only oceanographic parameter which allows for a reasonably complete synoptic analysis on the hemisphere scale. SST resolution is such that SST changes can be determined for periods of 24, 48 hours, etc. From these changes, the local changes computed from air/sea heat exchange equations are subtracted. If the remainder correlates well with the advection of SST resulting

*NOTE: Ekman theory states that wind imparts momentum to the sea through a stress directed 45° to the right of the wind direction; and that the resulting mass transport is directed 90° to the right of the wind direction, for the northern hemisphere.

from current transport, the computed currents can be assumed to be reasonably correct. Such experimental verification has determined that the surface current analysis performs well.

Verification of the Ocean Surface Current products will occasionally result from correlation of drift estimates with actual drift observations from a Search and Rescue incident.

U. S. Coast Guard reports on the usefulness of this product are expected to be received during the breaking ice season of 1976. These reports will constitute the only information, at this time, on the reliability of this product. The first Coast Guard reports have been favorable.

E. Uses of the Product

Dealing with sub-grid-scale features or salinity dominated features requires reversion to climatology or use of a small scale analysis which considers dynamic topography (salinity). The Grand Banks Surface Current analysis, used for iceberg drift monitoring, is an example of small-scale salinity dominated problem.

The primary use of ocean surface products in the field is for drift calculations. The surface current products give current vectors by inspection, and these can be added to any other vectors (usually wind) involved in the drift calculation. The Grand Banks surface current field is sent over the NEDN in message format to FWC Norfolk and then relayed, via teletype, to Governers Island, New York.

The common drift problems include:

1. Search and Rescue, where one hundred percent of the current component is added to the wind drift effect.

2. Marine Navigation, where the current component is included in the dead reckoning navigation computation. The current effect is appreciable when strong currents like the Gulf Stream are involved.

3. Ice and iceberg drift, where the full current component is used.

4. Pollution drift, such as in oil spills or dispersion of other pollutants. Full Current component is added to wind and diffusion terms.

5. Optimum Track Ship Routing, where surface currents can be used to save transit time.

In almost all types of fisheries work there is a need to know the actual currents and to adjust fishing operations accordingly. In areas of surface divergence, the deeper, nutrient-rich waters are brought into the upper layers where a higher production of organic matter ensues and the number of fish increases. Convergent areas cause (dynamically) a concentration of zooplankton and again there is a concentration of fish.

F. Relationship to Other Products

The surface current analysis and prognosis is an important input to the FNWC Search and Rescue Program, and to the Grand Banks surface current analysis. The latter is not used as input to other FNWC programs.

G. Program Output

1. Surface Current analysis and prognosis, 0 and 24 hr.
   (a) Current Stream Function. (Catalog No. B30) Figure 5.9.2
   (b) Current Transport. (Catalog No. B31) Figure 5.9.1
   (c) U Component of Current Speed. (Catalog No. B32)
   (d) V Component of Current Speed. (Catalog No. B33)
   (e) Current Direction. (Catalog No. B36) Figure 5.9.3

2. Grand Banks Surface Current Analysis

(a) A message (Catalog No. B37) containing 5-digit groups.

Each group is identified by latitude and longitude, and has the form ddsss where dd is a two-digit direction in tens of degrees, and, sss is a three-digit speed in tenths of a nautical mile per 12 hours.

H. References and Suggested Reading

[1] Hubert, W. E. and T. Laevastu, 1965; "Synoptic Analysis and Forecasting of Ocean Currents", FNWC Technical Note No. 9, June 1965.

[2] Hubert, W. E., 1965; "Computer Produced Synoptic Analyses of Surface Currents and Their Application for Navigation", Navigation, Vol. 12, No. 2, 101-107.

[3] Soule, F. M.; "The Normal Dynamic Topography of the Labrador Current and its Environs in the Vicinity of the Grand Banks of Newfoundland during the Iceberg Season", Woods Hole Oceanographic Institution, Reference No. 64-36.

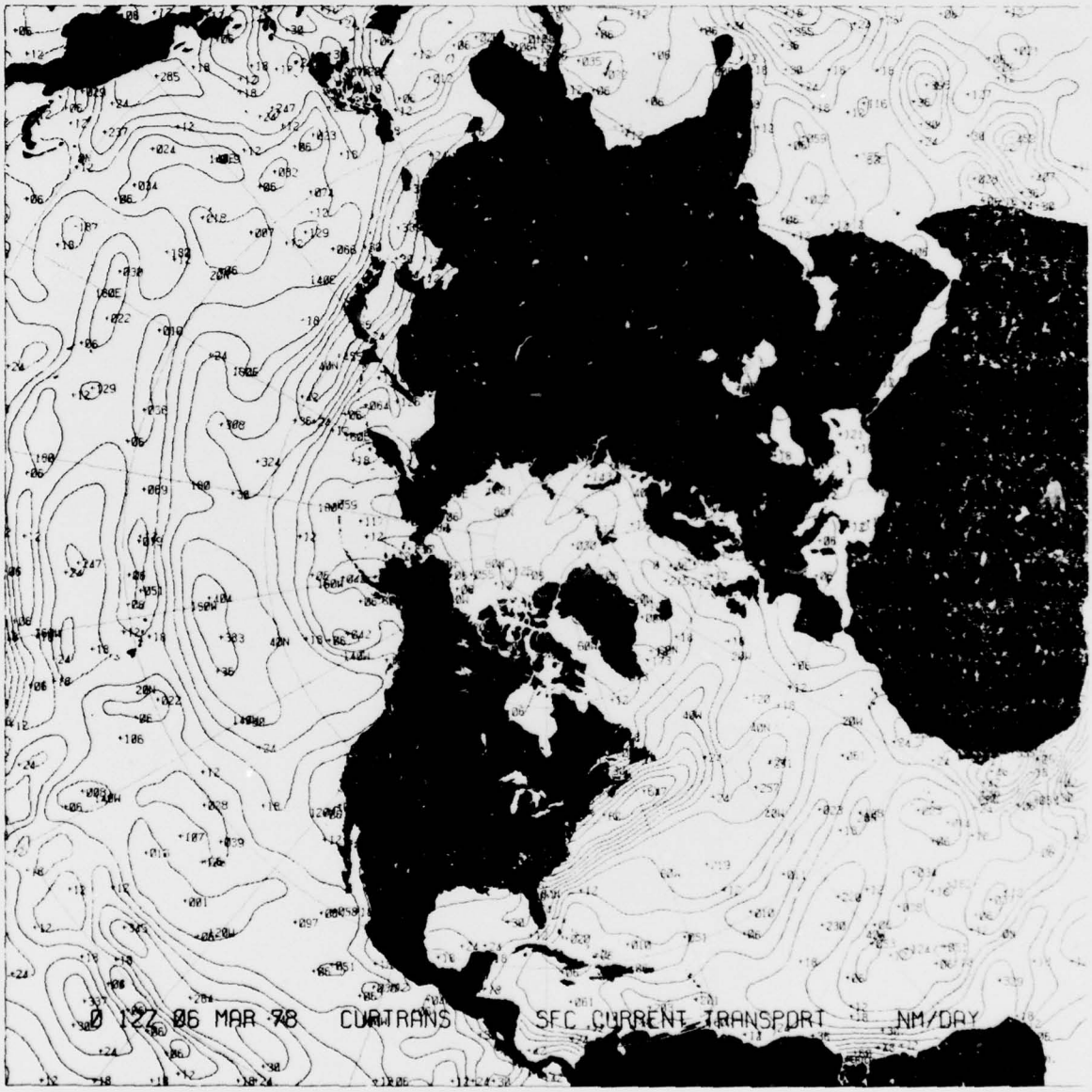


FIGURE 5.8.1 Surface Current Transport (B31)

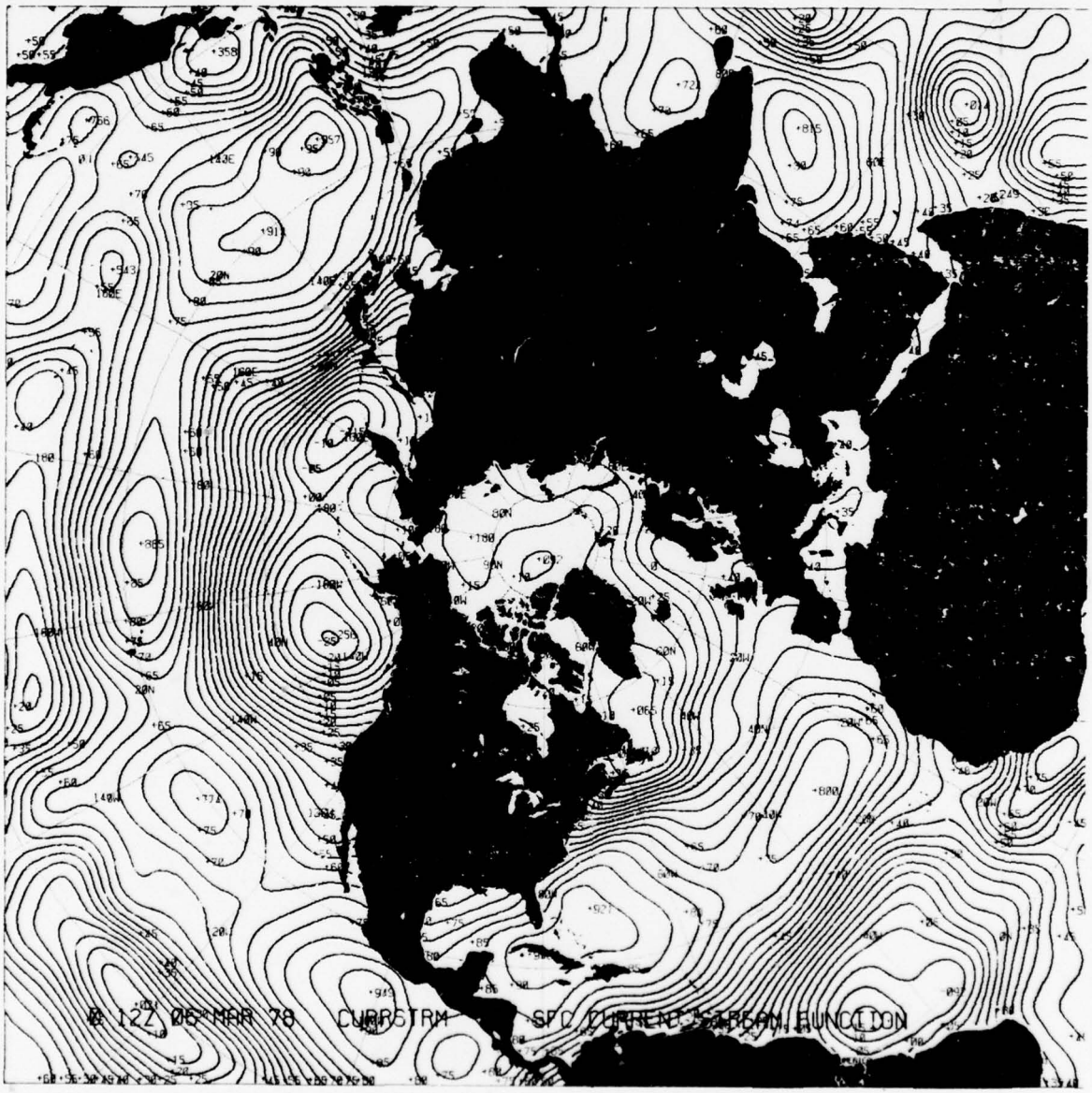


FIGURE 5.9.2 Surface Current Stream Function (B30)

5.13 OCEAN FRONT ANALYSIS

A. Model Development

Ocean fronts are a familiar phenomenon to those who sail the seas. These sailors have seen the usual frontal signs many times--water color changes, rapid sea-surface temperature change, variable character of surface waves, and accumulation of debris and sea smoke.

Ocean fronts, in the general sense, are just like atmospheric fronts. Both separate masses of different physical and chemical properties (also biological in the oceans). Their behavior is similar in that both move, both range widely in sharpness of definition, both have quasi-stationary segments (more common in ocean fronts), and both change in intensity with time. The principal difference is in the speed with which things happen. A one-day change in atmospheric fronts might equal a week or two of oceanic front action.

The knowledge of positions, nature, intensity and dynamics of ocean fronts has many practical applications. This potential operational value led to the development of the ocean front model at FNWC.

A number of parameters that might be used for describing ocean fronts were considered and tested. Salinity and biological parameters were discarded at once, since synoptic information is not available for either. The choice narrowed to sea-surface temperature and ocean currents, both available at FNWC in daily synoptic analyses.

The ocean current stream function shows speed and direction of ocean currents. Since oceanic fronts are most often boundaries of different current systems, thus different surface water types, use of the stream function looked promising. But, examination of many cases showed that the major boundaries are given in too smoothed a fashion by use of the stream function. Still another attack of calculating gradients of SST and current stream function did nothing to sharpen the frontal delineation.

Use of SST as the sole parameter was the next approach. First, the pattern separation technique (Section 4.9) was applied to the SST analysis to obtain an SST SD pattern (small-scale SST anomalies). The SD patterns defined the ocean fronts very well wherever the SST gradients were strong, but too much detail was lost in areas of weak gradients.

The final parameter candidate was to apply the GG operator (Section 3.8) to the SST analysis. The procedure is the same as that used to obtain atmospheric frontal analyses (Section 4.15), except for the difference in temperature parameters. The general similarity between ocean and atmospheric fronts makes this approach reasonable. Several investigators (Laevastu, Hela, and LaFond) have shown the direct relationship of subsurface thermal structure to fronts at the surface. If the front can be located accurately at the surface, the subsurface front is defined as well.

When the GG operator is used on large-scale SST charts such as the FNWC 63x63 polar stereographic chart, the large mesh size does not allow correct resolution of the SST gradients and the resulting GG pattern is displaced toward warm water. In this case, it has been found that the axis of the GG pattern depicts the core of the warm current. The true current boundary (temperature separation of water masses) is the zero line of the GG pattern on the northern edge. The strength of the temperature gradient is proportional to the number of isolines surrounding the pattern axis.

If the GG operator is used on a SST analysis with a finer mesh size, then the representiveness of the GG pattern becomes more realistic and the axis of the GG pattern shifts toward the true frontal boundary.

B. Program Input

1. Sea-surface temperature analysis.

C. Program Computation

1. Apply the GG operator to the current sea-surface temperature analysis.

D. Program Limitations and Verification

The accuracy of the ocean front program hinges entirely upon the accuracy of the SST analysis. Fortunately, the SST analysis program is one of the stronger ones at FNWC. In shipping lane areas, where reports are numerous, the SST analysis is accurate to within less than 1°C. In sparse data areas, a 2 to 3°C error might be expected to be correct within 50 miles in good data areas, and within 100 miles elsewhere.

The GG ocean front program is completely reliable in detecting frontal zones. It won't miss fronts, nor will it put in spurious fronts.

Direct verification of the program is very difficult because only a few reports a day are received from ships located in or very near the ocean front. A second method, and only a loose one, is to compare the frontal analyses with climatological ocean current positions. About all this shows is that the program is putting in existing fronts in the right geographical area. Inspection of the SST and ocean current analyses will also give this same general information.

The program has been verified in a limited number of cases against aircraft and ship observations taken continuously across ocean fronts. In these cases, the frontal analyses proved to be highly accurate except for small-scale features like eddies along the edge of the Gulf Stream.

E. Uses of the Product and How to Use It in the Field

The ocean front product can be used in several areas--fishing, weather forecasting, navigation, and in several sonar applications.

In weather forecasting, knowledge of ocean front location is useful in locating boundaries of fog and low cloudiness. Over the oceans, most fog is of the advection type. It occurs where cold and warm currents run side by side and the wind flow is from warm to cold water. The notorious Grand Bank fogs exemplify this situation. A forecaster can use the ocean front analysis along with his weather maps to forecast with precision where advection fogs or low stratus will form.

Cyclogenesis occurs most readily along the boundaries between warm and cold water. Forecasters should use ocean fronts as guidelines for locating incipient storms.

Use of ocean front analysis in navigation would be in those cases where ships in transit were using currents as a helping component, or avoiding the current so as not to be slowed. The GG analysis gives the center of the warm current and its boundary, and the ship can navigate accordingly.

The change in thermal characteristics across an ocean front can be appreciable. In 20 miles, SST can change from 0 to 12°C, layer depth from 0 to 200 meters, in-layer gradient from 0 to 10°C. Obviously, changes of this magnitude affect sound velocity profiles and sonar operation. Ocean front effects should be accounted for in all acoustic models and used directly in ASW operations. But, the acoustic models are unable to handle ocean fronts with any precision, primarily because there is rarely any continuous or closely-spaced data across fronts and, even if there were, the analysis grid size is too large to resolve the fine changes involved. A new underwater analysis model is under development that will give the acoustics models a much better delineation of ocean fronts. Until this new model is made operational, ocean fronts must be dealt with by ASW operators in a very gross way. If the operation is in an area where fronts are located, the sonar operators can do one of two things. First, as a front is approached, a series of close-interval underwater soundings can be started and continued through the front. The frontal thermal structure will be defined and the range forecasts can be modified accordingly (Ref. 3 has some applicable rules for hull-mounted sonars and submarine operations.). A second course of action is to assume generalized ocean front thermal structure for, say, three types--weak, medium, and strong fronts. Using this "modelled" front, corrections to the range forecasts can be calculated. Ref. 2 has some examples to assist in the categorization. The ocean front model can help here, too, since the products show both location and relative intensity of the ocean fronts.

F. Relationship to Other Products

The Ocean Front analysis is not used as input to any other FNWC models or programs.

G. Program Output

Objective frontal analyses of SST for the following areas using both gradient (G) and gradient-of-gradient (GG).

Area		Catalog No.
Gulf Stream	G	P94
Gulf Stream	GG	P93
Kuroshio	G	P96
Kuroshio	GG	P95
Iberian Basin	G	Not yet assigned
Iberian Basin	GG	
Newfoundland Basin	G	
Newfoundland Basin	GG	
Mediterranean	G	
Mediterranean	GG	
Norwegian Sea	G	
Norwegian Sea	GG	
Southern California	G	
Southern California	GG	

H. References or Suggested Reading

[1] Clarke, L. C., T. Laevastu, 1966; "Numerical Methods for Synoptic Computation Fronts and Water Type Boundaries and Their Significance in Applied Oceanography". FNWC Technical Note No. 20, June 1966.

[2] Laevastu, T., P. M. Wolff, and E. C. LaFond; "Effects of Oceanic Fronts on Sound Propagation and Possible Implications for ASW Tactics (U)". NUC TP226, Naval Undersea Research and Development Center, March 1971, CONFIDENTIAL.

[3] James, R. W., 1972; "Criticality of Ocean Fronts to ASW Operations". NAVOCEANO Tech. Note 7700-3-72, 1 September 1972.

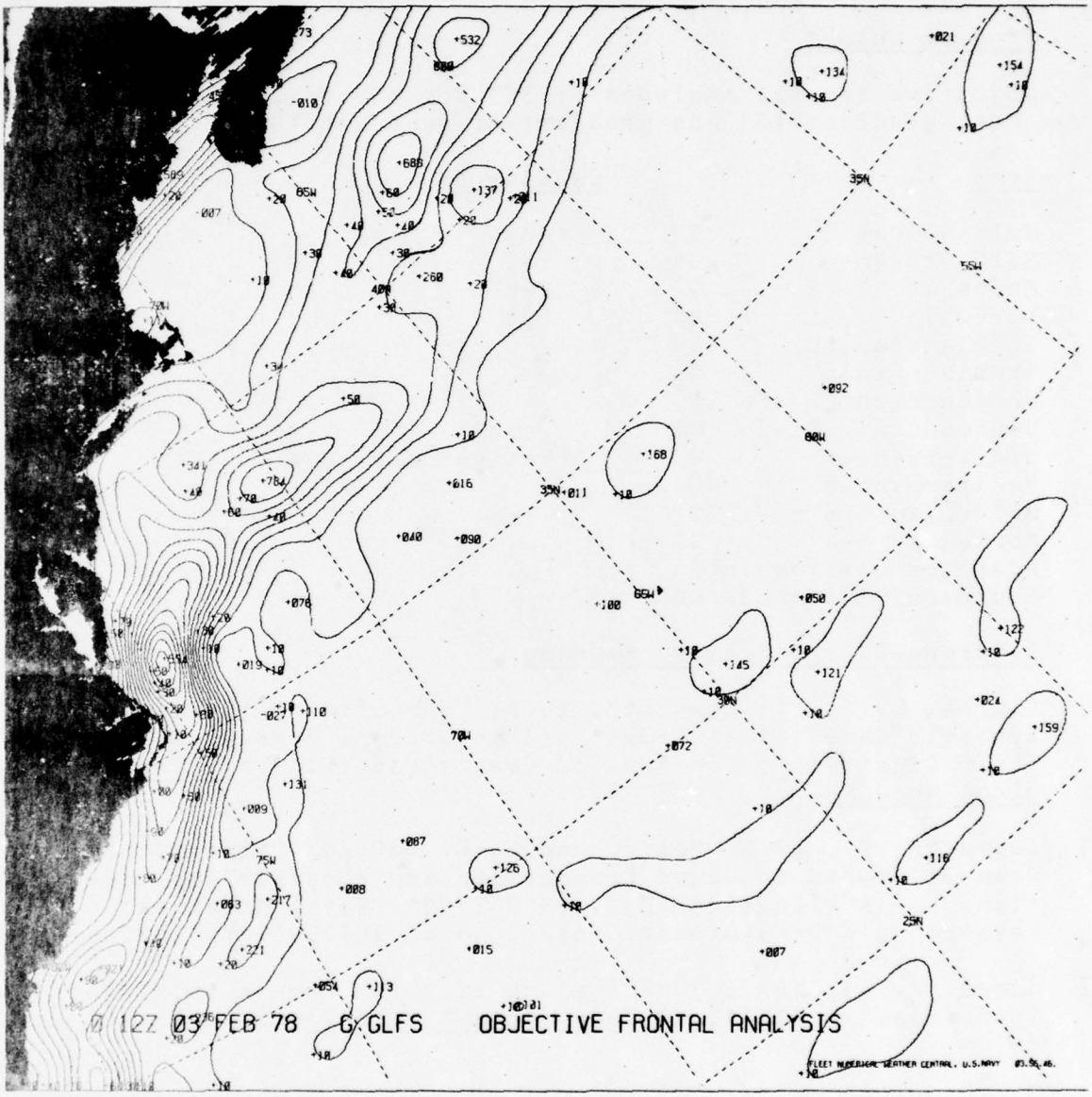


FIGURE 5.13.1 Gradient of SST in the Gulf Stream (F94)

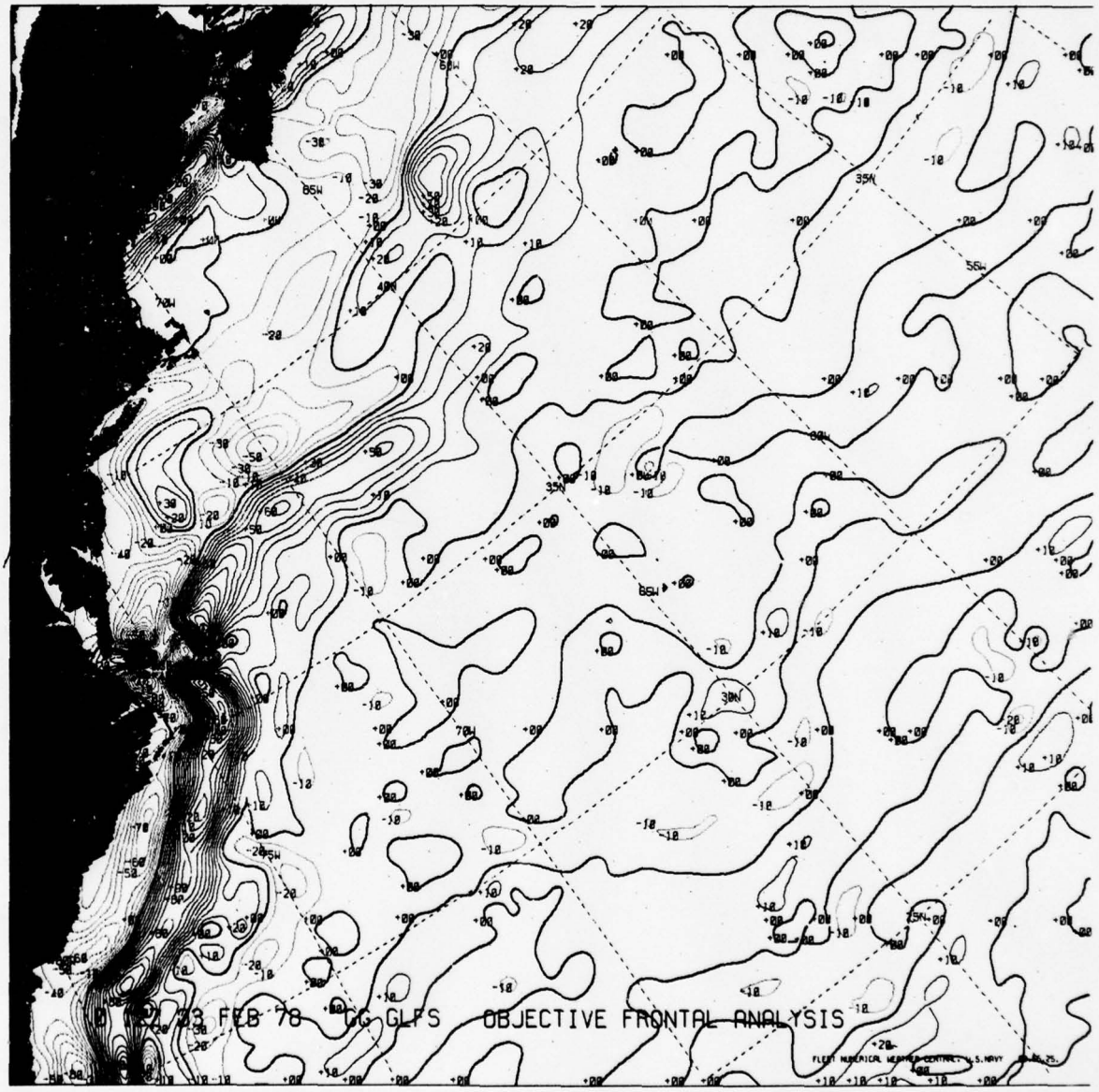


FIGURE 5.13.2 Gradient of SST in the Gulf Stream (P93)

5.14 SEARCH AND RESCUE PLANNING PROGRAM

A. Model Development

An object or person adrift at sea changes position continuously because of current and wind effects, so the Search and Rescue (SAR) plan must include an accurate estimate of the position at which to start the search. The FNWC SAR planning program is designed to provide this estimate rapidly and accurately.

The SAR model is based on the assumption that a drifting object will be affected by only two forces--currents and winds. The surface current component is applied at one hundred percent of the existing current in the search area. The wind effect depends on degree of exposure and shape of the object. Something barely awash will drift at a much different rate from one that has a high freeboard or a large sail area.

Surprisingly little was known until 1970 about how the wind affects drift speeds of objects of varying shapes and exposure. The U. S. Coast Guard, in 1969 and 1970, conducted extensive drift studies on a great variety of objects. Some were tracked for months. Wind effects were isolated from currents, and tables were compiled that show the percentage of total wind to be used for different objects. SAR centers use a series of leeway options, or codes, to specify how wind effects are to be treated in the SAR forecast computation. These options range in complexity from down-wind drift at a percentage of the wind, to non-linear expressions in the case of a life raft with drogue, to cross-wind drift for objects with known sailing characteristics.

B. Program Input

1. Drift characteristics vary with the type of object adrift. Input parameters, determined by the SAR center to describe the characteristics of the object of the search, are as follows:
   a. Leeway code--a function of the surface wind effect on the drifting object.
   b. Starting points--distress positions at the time of drift start.
   c. Datum time--search times for which plot is requested.
   d. (1) Probable navigation error of the search craft.
      (2) Initial probable error in position of the search object.
      (3) Percent of dead reckoning (DR) distance to be applied as DR error.
2. Ocean surface current analysis and prognosis for 0 and 24 hrs.
3. Marine wind speed analysis and prognoses for 0, 12, 24, 36, and 48 hrs.
4. Marine wind direction analysis and prognoses for 0, 12, 24, 36, and 48 hrs.

C. Program Computation

1. Determine surface current vector from surface current analysis.
2. Compute leeway component using Marine Surface Wind analysis and prognoses with assigned leeway code number.
3. Combine current and wind vectors to obtain total drift in 12-hour increments.
4. Calculate search positions for requested search times.

D. Program Limitations and Verification

The FNWC surface current analysis and prognoses are not reliable near coasts or island chains because of tidal and terrain effects. Occasional large errors in the SAR forecasts should be anticipated in these areas.

The SAR program has verified quite well in some actual SAR incidents.

E. Uses of the Product

The SAR forecasts are used almost exclusively in SAR incidents involving searches for people in the water, or in rafts or boats. The forecast positions are used exactly as they come from the computer, but search plans should allow for possible large errors when the search is near coasts or island chains.

The SAR forecasts are useful for tracking sonobuoys, and for locating drifting objects like buoys and floating mines.

F. Relationship to Other Products

SAR forecasts are not used in the production of any other FNWC products.

G. Program Output

Messages that include an estimated position of the search object, position error, and radius of search for each datum time.

H. References or Suggested Reading

[1] Discenza, J. H., 1969; "Computerized Survivor Search Planning", M. S. Thesis, U. S. Naval Postgraduate School, Monterey, California, 117 pp.

[2] Hubert, W. E., 1966; "Computer-Produced Synoptic Analyses of Surface Currents and Their Application for Navigation", Journ. Inst. Navg. 12(2): 202-207.

[3] Hubert, W. E., Lcdr K. G. Hinman, USN, and B. R. Mendenhall, 1970; "The FNWC Monterey Search and Rescue Planning Program (NSAR)", Tech Note 60, Fleet Numerical Weather Central, Monterey, California, 15 pp.

```
CZCGAA304
OTTUZYUW RULGSD G2478 0190100-UUUU--RUWJAGD.
ZNR UUUUU
O 190100Z JAN 72
FM COMCOGARD GANTSEC
TO FLWNUMWEACEN MONTEREY
BT
UNCLAS
ALERT TUG RAMONA ADRIFT
1. REQUEST SAR PLOT
2. DATA:
   A. 301100
   B. 180300Z, JAN, 1602.0N, 06232.0W
   C. 191500Z, JAN
   D. 1602.0N, 06232.0W/10.0/05.0/0.05/2
BT
 2478
```

MESSAGE BREAKDOWN

2A	30 = Leeway code downwind drift at 3% of wind velocity in this case. 1 = Number of starting points. 1 = Number of datum times. 00 = No meaning. Always punched as 00.
2B	Date-time group and position of each starting point.
2C	Date-time groups of datum points. Datum points are the position estimates to be computed for the search times specified.
2D	Last known position. 10.0 = Possible navigation error of search craft. 05.0 = Probable position error of search object. 0.05 = Percent of DR distance to be applied as DR error. 2 = Safety factor multiplier. Search radius to be multiplied by 1.5 in this case.

FIGURE 5.14.1 SAMPLE INCOMING NSAR MESSAGE

O 190200Z JAN 72
FM FLENUMWEACEN MONTEREY
TO COMCOGARD GANTSEC
BT
UNCLAS //N03130//
SAR DATA
A. YOUR 190100Z JAN 72
B. OPNAV INST 3130.5
1. THE FOLLOWING ARE THE DATUM POINTS FOR THE
191500Z JAN SEARCH.
(STARTING TIME/POSIT 180300Z JAN / 16- 2.0N 62-32.0W)
15-59.4N 63- 6.2W POS. ERROR 18.0 RADIUS 28.8 MILES.
2. LEEWAY CODE 30 USED.
BT

RELEASED BY ---Alg--------- TIME 190057Z

FIGURE 5.14.2 SAMPLE OUTGOING NSAR MESSAGE

5.15 HYDRODYNAMICAL NUMERICAL MODEL (HN)

A. Model Development

During the normal course of events, tidal circulation in coastal areas, estuaries and rivers affects a diverse number of parameters including: marine life in the inter-tidal and near shore zones; the flow of man-made sewage and other pollutants dumped into the water; off-shore structures, channel dredging and other engineering projects; and, of course, ship traffic. Furthermore, in areas where intense storms occur, the wind can create storm surges which combined with the tides can kill and injure people and destroy property on the surrounding low lands. Before the advent of high speed digital computers, the prediction of tidal heights and currents was difficult and cumbersome. The tidal circulation in deep water is primarily due to the attraction by the moon and sun; however, the tides in shallow water are also strongly affected by the geography and bathymetry of the area.

In the past tidal constituents derived from measured tide data were used to predict tidal fluctuations for a given location. One serious problem with this technique is that if tide data are required for areas other than the tidal stations, the predictions have to be interpolated between known tidal stations. The interpolated tide values can be inaccurate and more detrimental than useful for real-time operational planning. The U. S. Navy became acutely aware of this problem when using existing tide tables for riverine and coastal operations in the Republic of Vietnam.

Development of the FNWC HN model was inspired to a great degree by U. S. Navy operational requirements in the S. E. Asia area. A knowledge of anticipated current and tidal conditions is particularly important to resupply operations being conducted on open beaches and in estuaries. Amphibious operations are affected by tides and tidal currents, and other operations, such as mining, SAR, and pollutant control can also be affected. So, beyond satisfying the initial S. E. Asia operational requirements, the HN model evolved with great potential for output of products of future value to the U. S. Navy.

The use of a hydrodynamical model for computation of tides and currents was suggested over thirty years ago, and equations were formulated in succeeding years. However, it was not until high-speed computers became available that synoptic use of the HN model became economically feasible and practically possible.

The HN model at FNWC is an adaptation of one developed by Professor Walter Hansen, University of Hamburg. Hansen has used his model for the past twenty years successfully and demonstrated that the basic theory behind the model is correct. Originally, the HN model was designed to be used as a single-layer model; however, FNWC has modified the model so that it can be run in a multi-layer mode.

B. Program Input

Basic inputs to the HN model are the astronomical tidal constituents along the open boundary, surface winds across the grid, bathymetry at the grid points and the Coriolis force. Other inputs which can be used if required are permanent currents, tables for drifting objects, sources and quantity of pollutants and composition of the vertical layers if the model is to be used in the multi-layer mode.

The tidal constituents are derived from measured data. If tide gauges have been maintained in the area of interest for some length of time, it is possible that the tidal constituents for the area can be obtained from the U. S. National Ocean Survey in Washington, D. C. which has access to tidal constituents for all areas throughout the world. If the tidal constituents are not readily available, then the constituents will have to be derived from cotidal and corange charts. If the specified area is small in size, then one set of constituents can be used for the entire length of the open boundary; however, if the area is large, then the constituents should be adjusted along the open boundary.

To increase the accuracy of the model computations, it is essential that the best available bathymetric data be used as input to the model. Since the HN model is not run in a real-time mode, the user of the product has to predetermine the desired wind velocities required for input to the model. This is also true for the permanent current input.

Fields required for input are:

1. Water depths at u and v points over the grid.

2. Sea and land table.

3. Synoptic wind reports over the grid area.

4. Permanent currents in the grid area. Both atlas and FNWC ocean current input is used.

5. Tidal heights using four tidal components.

6. Mixed layer depth, when calculations are performed over deep water.

7. Atmospheric pressure, when calculations are performed over large areas.

Special inputs as desired:

8. Leeway tables for various types of drifting objects.

9. Quantities of pollutants released or initial distribution of temperature, salinity, or any other variable.

C. Program Computation

The changes in water elevation computed at the open boundary are propagated throughout the model model area by the Newtonian equations of motion and the continuity equation. These state that the acceleration in any direction is proportional to the resultant of all forces acting in that direction, and that a change in density at a point requires a mass flux at the point. The basic hydrodynamical equations ((1) through (3), Appendix D), used in the single layer model, are the differential formulations of the equations of motion and the continuity equation. They yield the rate of change of a property, and thus enable a prediction of the amount of change over a given time period. The thickness of the layer is governed by the continuity equation. Vertical motions below the mixed layer are rare because of the stable density stratification.

Major computational steps are organized as follows:

1. Read in:

   a. Water depth at u and v points, and sea-land table at two points
   b. Wind field
   c. Boundary coordinates
   d. Significant tidal constituents at the boundaries
   e. Coriolis parameter
   f. Gravity acceleration
   g. Friction coefficients (bottom and surface)
   h. Air density

2. Print input data for checking.

3. Initialize for all parameters.

4. Compute tides and currents.

5. Compute diffusion and transport of pollutants if required.

6. Compute drift for search and rescue if required.

7. Compute storm surges if required.

8. Output:

   a. Horizontal fields of water level and current speed and direction in one- or two-hour increments.

   b. Water level and current data for selected points as required.

   c. Pollutant diffusion and transport data as required.

   d. SAR data as required.

D. Program Limitations and Verification

The HN model is most accurate in semi-enclosed embayments where the astronomical tides and local winds are the predominant driving forces of the water circulation. In these areas, the accuracy of the model calculations is limited by the accuracy of the tidal constituents at the open boundaries and the state of knowledge of the bathymetry within the area of concern. The model has been successfully applied in areas such as the Gulf of Tonkin, DaNang Bay and Chesapeake Bay.

In areas where the water circulation is influenced more by eddies of oceanic currents such as the Davidson Current and the Gulf Stream than by the tides and winds, the HN model is obviously not as accurate. Monterey Bay, California is an example where this situation occurs. Attempts have been made to simulate the oceanic currents in the computer model and some success has been attained when the magnitude and direction of the oceanic currents can be accurately defined along the open boundary of the computer model and the real oceanic currents do not shift position during the simulation period of the calculations.

The HN model products should be verified for each geographical location by conducting field surveys for the purpose of measuring tides, currents and winds. Often it is impossible, if not impractical, to conduct field surveys for verification. An alternative method of verifying would be to compare the computed results with the climatology data for the area of interest. It is important to remember that because the various combinations of tides, winds, bathymetry and mesh length, among other parameters, can significantly vary from area to area, that some sort of verification should be conducted each time the model is applied to a new area.

E. Uses of the Product

The HN model is best suited for semi-closed bays and estuaries, but has been used for other areas where there has been at least one closed boundary. Since the model is basically a tidal model, the permanent current does not meander once it has reached equilibrium and can only be adjusted by manual input. In order to apply the HN model to a particular area, a rectangular grid must be set up. The grid is used to determine land-sea boundaries and to allow bathymetric input to the model. Two basic criteria are considered when setting up the grid, the operational requirements of the user and the limitations of memory and processing time of the computer to be used to perform the calculations. Both computer space and time requirements increase when the size of the grid is increased; i.e., when the size of the area to be covered by the grid is increased or the mesh length between grid points is decreased. Thus, a balance has to be maintained between operational requirements and the limitations of the computer hardware. It is noted that when the number of layers in the model is increased the number of grid points in the grid is essentially increased by the same factor.

The mesh length and the depth of the area determine the time step of the model (Eq. 15, Appendix D). Note that when the mesh length is decreased or the maximum depth becomes larger, the time step decreases. The processing time of the computer model is partially governed by the size of the time step. A point to be considered when setting up a computer run is that a smaller time step increases the calculation time. The model is already set up to be run for the South China Sea, Gulf of Tonkin, DaNang Bay, Sweeper's Coves, Adak Island, New York Bight area, Monterey Bay, Chesapeake Bay, Straits of Gibralter as well as other areas throughout the world.

HN model products are tailored for direct use in the field. No interpretation is required by the meteorologist/oceanographer. The user has only to read off values from the HN printout or graphical field and adapt them to the problem at hand--navigation, pollutant drift, locating drifting objects, oil spill, etc.

F. Relationship to Other Products

The HN model products are not used in any FNWC models.

G. Program Output

1. Hourly or two-hourly horizontal fields of water level and current speed and direction, either in printout or graphical form. Any desired time interval can be specified. Data for selected points in the field can be provided upon request.

2. Pollution diffusion and dispersal charts showing change of concentration of the pollutant with time. Release of the pollutant may be specified as instantaneous or continuous.

3. Drift computations in coastal water for Search and Rescue operations. Forecast hourly positions of any drifting object are given.

4. Storm surge predictions giving time and height of surge at selected points along a coast.

The products listed above are provided only upon request.

The basic output of the model is water elevation and current speed and direction at every grid point. The computations can be displayed in a printout form as shown in Figures 5.15.1 and 5.15.2 or graphical display as shown in Figures 5.15.3 and 5.15.4. The data could be displayed every time step but for practical considerations dictate that the solutions be output every hour or every two hours depending upon the user's requirements.

H. References

[1] Laevastu, T. and P. Stevens, 1969; "Applications of Numerical-Hydrodynamical Models in Ocean Analysis/Forecasting", Fleet Numerical Weather Central, Monterey, California, Technical Note 51, July 1969.

[2] Laevastu, T. Dr., and K. Rabe, 1972; "A Description of the EPRF Hydrodynamical-Numerical Model", Environmental Prediction Research Facility, Monterey, California, Technical Paper No. 3-72, March 1972.

[3] Lazanoff, S. M., 1971; "An Evaluation of a Numerical Water Elevation and Tidal Current Prediction Model applied to Monterey Bay", U. S. Naval Postgraduate School, Monterey, California, Department of Oceanography Master's Thesis, March 1971.

RESULTANT CURRENT VELOCITY MAGNITUDE(CM/SEC) AND DIRECTION(DEGREES) AFTER T= 50400 SEC

	1	2	3	4	5	6	7	8	9	10	11	12	13	14	15	16	17	18	19	20
1	0, 999	0, 999	0, 999	0, 999	0, 999	0, 999	0, 999	0, 999	0, 999	0, 999	0, 999	0, 999	0, 999	0, 999	0, 999	0, 999	0, 999	0, 999	0, 999	0, 999
2	0, 999	0, 999	0, 999	0, 999	0, 999	0, 999	0, 999	0, 999	0, 999	0, 999	0, 999	0, 999	0, 999	0, 999	0, 999	0, 999	0, 999	0, 999	0, 999	0, 999
3	0, 999	0, 999	0, 999	1, 999	0, 999	0, 999	0, 999	0, 999	0, 999	0, 999	0, 999	0, 999	0, 999	0, 999	1, 251	10, 247	30, 247	39, 223	51, 194	61, 163	75, 213	75, 213
4	0, 999	0, 999	0, 999	1, 999	0, 999	0, 999	0, 999	0, 999	1, 999	0, 999	0, 999	0, 999	0, 999	0, 272	17, 239	21, 226	31, 227	45, 225	64, 232	99, 203	122, 235	123, 235
5	0, 999	0, 999	0, 999	0, 999	0, 999	3, 999	0, 999	0, 999	0, 999	0, 999	0, 999	0, 235	14, 224	20, 219	29, 206	45, 220	64, 216	69, 204	95, 209	96, 220
6	0, 999	0, 999	0, 999	0, 999	0, 999	0, 999	0, 999	0, 999	0, 999	0, 63	2, 109	7, 192	14, 205	25, 192	41, 182	45, 214	49, 180	57, 176	82, 180	92, 180
7	0, 999	0, 999	0, 999	1, 999	0, 999	0, 999	0, 999	0, 999	0, 999	9, 89	5, 79	9, 159	17, 157	29, 161	23, 178	37, 196	54, 177	73, 154	67, 158	67, 151
8	0, 999	0, 999	0, 999	0, 999	0, 999	0, 999	0, 999	0, 999	19, 161	2, 94	0, 59	7, 173	6, 101	19, 108	21, 136	55, 169	58, 173	59, 157	88, 134	93, 134
9	0, 999	0, 999	0, 999	1, 999	0, 999	0, 999	0, 999	0, 999	110, 180	0, 65	0, 65	11, 231	2, 82	5, 88	49, 138	62, 157	38, 176	54, 160	89, 134	99, 134
10	0, 999	0, 999	0, 999	1, 999	0, 999	0, 999	43, 131	98, 155	44, 180	0, 65	0, 65	6, 178	0, 65	0, 65	48, 152	61, 149	61, 150	68, 153	83, 140	83, 140
11	0, 999	0, 999	0, 999	0, 999	0, 999	0, 999	59, 116	63, 172	23, 155	15, 91	4, 135	9, 132	0, 103	6, 99	17, 146	39, 136	36, 132	49, 155	63, 144	63, 144
12	0, 999	0, 999	0, 999	0, 999	0, 999	0, 999	62, 114	34, 165	24, 131	29, 92	15, 101	17, 106	10, 104	7, 113	28, 126	31, 145	92, 149	45, 145	61, 133	61, 133
13	0, 999	0, 999	0, 999	0, 999	0, 999	0, 999	64, 119	28, 157	27, 149	45, 126	24, 97	24, 78	13, 122	15, 174	42, 164	87, 173	51, 166	35, 136	35, 112	35, 112
14	0, 999	0, 999	0, 999	1, 999	0, 999	0, 999	74, 139	29, 124	25, 134	18, 100	18, 64	33, 88	14, 145	49, 170	86, 175	93, 146	21, 164	23, 120	35, 111	35, 111
15	0, 999	0, 999	0, 999	1, 999	0, 999	55, 91	23, 18	37, 90	18, 134	10, 112	0, 89	21, 89	34, 137	74, 143	14, 153	9, 131	24, 134	21, 108	25, 97	25, 95
16	0, 999	0, 999	0, 999	1, 999	27, 91	38, 78	22, 89	35, 98	0, 152	14, 179	0, 65	0, 65	54, 133	16, 132	22, 123	35, 114	22, 102	71, 85	27, 86	23, 86
17	0, 999	0, 999	0, 999	1, 999	25, 50	5, 2	0, 65	5, 87	14, 178	53, 164	79, 125	16, 82	19, 87	25, 89	29, 103	37, 119	26, 92	28, 86	22, 69	22, 69
18	0, 999	0, 999	0, 999	0, 999	32, 80	1, 159	0, 65	3, 96	41, 128	22, 122	28, 92	28, 65	28, 69	35, 87	48, 108	95, 112	71, 85	29, 79	28, 54	25, 54
19	0, 999	0, 999	0, 999	0, 999	34, 99	13, 179	0, 65	2, 83	35, 79	24, 78	38, 72	37, 65	77, 73	95, 99	54, 121	21, 45	36, 78	29, 55	32, 61	32, 61
20	0, 999	0, 999	0, 999	1, 999	37, 130	25, 158	0, 65	1, 82	18, 69	33, 62	48, 69	43, 55	49, 74	78, 75	98, 116	95, 66	74, 65	32, 59	33, 62	33, 62
21	0, 999	0, 999	0, 999	1, 999	74, 174	96, 188	0, 65	2, 84	27, 37	36, 37	36, 34	39, 73	27, 73	85, 93	18, 67	39, 36	35, 60	35, 62	75, 64	35, 64
22	0, 999	0, 999	0, 999	0, 999	135, 165	88, 188	15, 135	20, 54	37, 34	41, 42	35, 63	32, 63	21, 80	79, 102	38, 79	38, 51	38, 57	37, 61	75, 62	35, 65
23	17, 271	67, 212	88, 191	103, 156	46, 185	19, 191	20, 76	24, 42	18, 40	44, 61	38, 44	34, 64	77, 72	49, 89	42, 86	68, 59	38, 59	37, 61	74, 63	34, 67
24	22, 271	44, 219	54, 236	41, 219	24, 198	9, 179	25, 65	27, 91	32, 93	29, 90	38, 62	27, 61	53, 71	31, 64	95, 59	74, 58	32, 56	30, 58	28, 57	28, 57
25	8, 271	16, 271	14, 271	14, 271	7, 272	9, 93	0, 89	11, 99	10, 89	5, 99	7, 88	6, 88	7, 89	1, 89	9, 99	9, 89	9, 89	8, 89	8, 89	8, 89

FIGURE 5.15.1 Example Printout of Current Speed and Direction at a Specified Time

WATER HEIGHT AFTER T= 50400 SEC (CM)

	1	2	3	4	5	6	7	8	9	10	11	12	13	14	15	16	17	18	19	20
1	0	0	0	0	0	0	0	0	0	0	0	0	0	0	0	0	0	0	0	0
2	0	0	0	0	0	0	0	0	0	0	0	0	0	0	0	0	0	0	0	0
3	0	0	0	0	0	0	0	0	0	0	0	0	-68	-70	-73	-75	-77	-79	-91	0
4	0	0	0	0	0	0	0	0	0	0	0	-65	-55	-56	-52	-58	-63	-48	-35	0
5	0	0	0	0	0	0	0	0	0	0	-63	-51	-49	-48	-47	-43	-16	-32	-23	0
6	0	0	0	0	0	0	0	0	0	-59	-58	-46	-43	-42	-17	-76	-22	-23	-11	0
7	0	0	0	0	0	0	0	0	0	-56	-49	-41	-36	-33	-31	-24	-18	-14	-10	0
8	0	0	0	0	0	0	0	0	-55	-57	-58	-39	-38	-27	-24	-15	-16	-13	-1	0
9	0	0	0	0	0	0	0	0	-52	0	0	-32	-27	-24	-14	-16	-15	-7	-2	0
10	0	0	0	0	0	0	-47	-58	-63	0	0	-30	3	0	-14	-9	-8	-6	1	0
11	0	0	0	0	0	0	-44	-58	-46	-42	-33	-28	-22	-17	-15	-9	-8	-5	-1	0
12	0	0	0	0	0	0	-43	-48	-48	-37	-32	-25	-21	-16	-12	-10	7	-6	-3	0
13	0	0	0	0	0	0	-39	-44	-35	-29	-29	-24	-19	-15	-9	3	-15	-2	-1	0
14	0	0	0	0	0	0	-36	-38	-38	-32	-26	-18	-18	-10	-9	0	-13	-3	0	0
15	0	0	0	0	0	-33	-49	-26	-38	-25	-23	-17	-12	-7	-25	-20	-4	-4	-2	0
16	0	0	0	0	-30	-29	-29	-25	-29	-24	0	0	-6	-22	-8	-7	-9	-5	-2	0
17	0	0	0	0	-27	-27	0	-28	-26	-21	-16	-26	-19	-12	-12	-9	-8	-4	-4	0
18	0	0	0	0	-24	-30	0	-18	-17	-25	-23	-17	-14	-10	-8	-14	-7	-6	-4	0
19	0	0	0	0	-22	-28	0	-19	-18	-16	-14	-12	-10	-5	-8	-14	-6	-9	-2	0
20	0	0	0	0	-19	-26	0	-18	-15	-12	-14	-18	-6	-8	-10	-10	-7	-5	-2	0
21	0	0	0	0	-16	-12	0	-20	-14	-13	-7	-3	-5	10	-24	-8	-6	-4	-2	0
22	0	0	0	0	-13	-24	-21	-12	-12	-9	-5	-4	-3	9	-20	-7	-5	-3	-1	0
23	0	-5	-8	-10	-25	-16	-10	-10	-6	-2	-7	-2	-2	-2	-5	-4	-3	-2	-1	0
24	0	6	-6	-8	-8	-4	-4	-8	-1	-3	1	-1	0	-4	-3	-2	-2	-1	-1	0
25	0	0	0	0	0	0	0	0	0	0	0	0	0	0	0	0	0	0	0	0

FIGURE 5.15.2 Example Printout of Water Level (in cm above or below a reference level) at a Specified Time

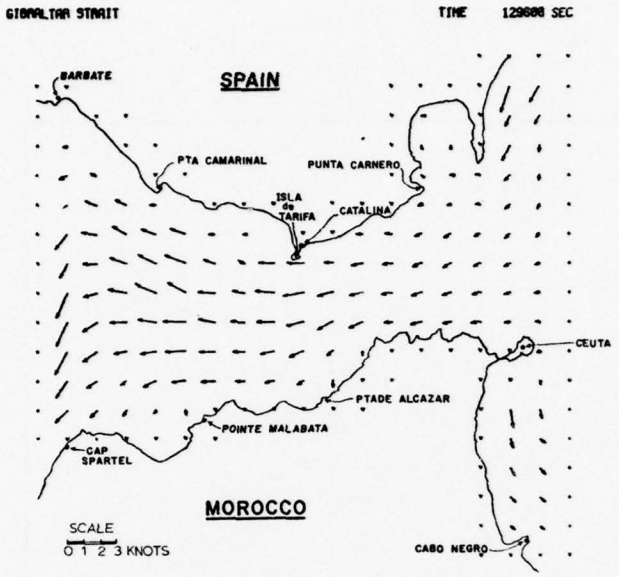


FIGURE 5.15.3 Tidal currents in Strait of Gibraltar three hours after low water at Tarifa. (HN method)

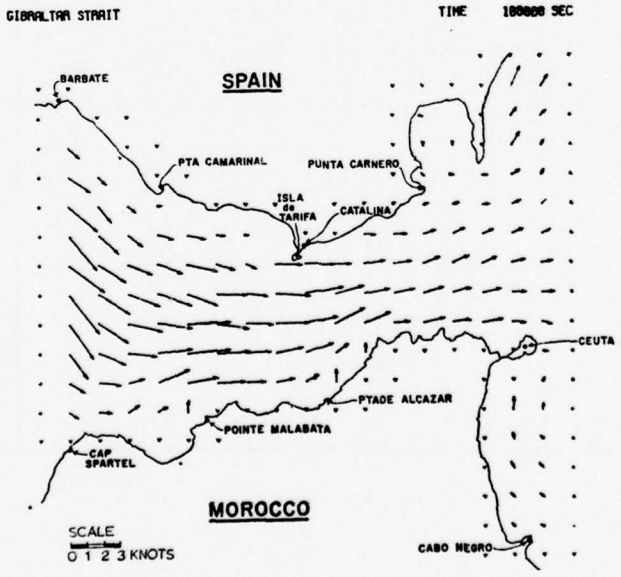


FIGURE 5.15.4 Tidal currents in Strait of Gibraltar three hours after high water at Tarifa. (HN method)

5.16 SPECTRAL WAVE MODELS

A. Model Development

Since the early 1960's FNWC has provided computer-generated ocean surface wave analyses and forecasts for the Navy. Due to limitations in computer capacity and in the accuracy of the wind values used as a wave model input, the operational ocean wave model at FNWC has, until recently, been limited to a "singular advective" model calculation of the principal ocean wave components. Acquisition of larger digital computers and implementation of more accurate atmospheric analysis and forecast models in the late 1960's removed the principal limiting factors to the operation of more detailed and improved ocean wave analysis and forecast models.

The spectral wave model now operating at FNWC derives its name from the fact that it provides a distribution (or spectrum) of energy at specified grid points. This distribution of energy defines the sea surface at each grid point through a two-dimensional (direction/frequency) matrix describing the energy in waves traveling in each of twelve directions and fifteen frequency bands.

Development of wave spectral models commenced with OPNAV tasking of the U. S. Naval Oceanographic Office in 1961 to compile a climatology of spectral wave data from the North Atlantic with an objective to develop a numerical method of providing near real-time wave spectra.

Two wave spectral models, commonly referred to as the Pierson model and the Barnett model, were developed under Naval Oceanographic Office contract and were then converted at FNWC into working computer programs for operational testing. Since the development of the Pierson model more nearly matched the operational characteristics of the FNWC system, this model was adapted for initial operational use as the FNWC spectral model. The first known operational ocean wave spectral model began to be run routinely at FNWC in May 1972 for the Mediterranean Sea (FNWC Tech Note 73-1) and demonstrated the potential improvement to be gained over the singular wave models previously used. In December 1974, the spectral wave model replaced the singular wave model as the operational wave model for the Northern Hemisphere.

B. Basic Theory and Numerical Computation

The current form of the ocean wave spectral model is based on the assumption that, given a continuous specification of the wind over the sea surface, theoretical and empirical methods can be used to compute the resultant energy of the ocean surface. Thus, the energy calculations are directly dependent on other computerized models for analyzing and predicting the wind. At this time, actual wave measurements are not used for direct feedback, but are used in model evaluation and improvement.

The transfer of wind energy to the sea surface has been described as consisting of two main processes: the resonance mechanism, which causes linear growth of the wave energy as a function of time, and the instability mechanism which provides exponential growth. One of the important results of this work is that with initial conditions of a calm sea and a given wind speed, the resonance mechanism is found to predominate. After a certain period of time, the instability mechanism becomes the dominant factor in wave energy growth. Separate winds are required to drive these two processes: A surface level wind (6.1 meters) is used for the resonance (linear) growth and the friction level wind (U_*) is used for exponential growth. The Planetary Boundary Layer Model (PLM) produces these winds and this model takes into account the stability of the boundary layer. For example in an unstable atmosphere, a given wind at the friction level will generate greater energy in the sea than the same wind in a stable atmosphere. Fetch and Duration are an integral part of the growth cycle of spectral models since at each time step the current energy is compared to the fully arisen spectra (Pierson-Moskowitz) to ascertain if energy growth can occur in this particular frequency (i.e., 1/period) band. Energy at each grid point is spread among adjacent directional bands through an equation developed from the Stereo Wave Observation Program (SWOP).

The wave energy in the spectral models is represented by a twelve-direction, fifteen-frequency matrix with each component of the matrix being propagated along its great circle path on the earth's surface at its respective group velocity. The propagation method provides continuity since the propagation sequence will continue until the energy encounters land or is dissipated through wave/wind interaction. A key description of the spectral wave model operation is the history update, the spectral energy values from the previous computer run are updated using newly analyzed wind values so that, at the start of the forecast period, appropriate energy spectra, based upon analyzed wind fields, are available for growth and propagation calculations. That is, the initial conditions are refined at each subsequent run and are not dependent on the atmospheric forecast model. Any loss of the spectral wave history degrades the model performance for a period of time approximating that required for each wave component to traverse the ocean basin or to spread to a negligible level. Two propagation methods are used in the operational spectral models.

(a) Northern Hemisphere Icosahedral-Gnomonic Model

The numerical computation used in this model is the velocity gradient method where the energy field is considered to be continuous. If discontinuities are noted, an additional field is computed to show the relative position of the discontinuous point in relation to its adjacent grid point. In this definition, centers of maxima and minima would be classified as discontinuous.

(b) Mediterranean Model

Since the mesh spacing of this model is only 67 km, the propagation technique used in this model is a much simpler method and is called the "jump technique". This implies that the energy from the directional/frequency matrix is retained at each grid point until sufficient time has elapsed to allow the energy component to reach the corresponding grid point, then the energy is moved as a unit to the next grid point in the propagational sequence.

Since the grids of both models are structured at directional intervals (60° Icosahederal-Gnomic/90° Mediterranean) greater than the 30° directional bands of the directional/frequency energy matrix, propagation of energy at intervals less than the basic grid orientation is accomplished through a "zig-zag" technique where energy is propagated to alternate grid points based upon the model time step. Figure 5.16.1 is a typical propagation sequence.

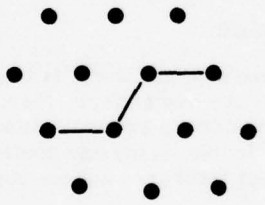


FIGURE 5.16.1 Zig-Zag Propagation Sequence

C. Uses of the Model

Many techniques available to describe the effects of wave motion have been impractical to use operationally because an adequate description of the sea surface has not been available.

1. Ship movements.

Most algorithms for the use of wave information are based on the oversimplifying assumption of the existence of only one, or at most two, predominant sinusoidal wave components, with wave period being a factor of secondary importance. A common example occurs in planning ship movements. Until the present time, wave height and direction were the principal parameters used in routing transiting ships or in planning various Naval exercises and operations. In reality, a ship is more responsive to given wave heights at certain specific frequencies than to greater wave heights at other frequencies.

Efficiency of Optimum Track Ship Routing Services (OTSR) could be increased by generating frequency response curves for all Navy ships and developing computer programs capable of integrating the ship response curve with available spectral wave energy information. In the same way, these data could also be used to plan underway replenishment operations, carrier flight operations, destroyer helicopter operations, towing operations, and other operations where sea state is a critical factor.

2. Inshore and nearshore operations.

Accurate surf and shallow coastal water conditions can be forecast with the wave spectrum information and a detailed coastal bottom topography. This is a potential aid to environmental studies, coastal engineering projects, and coastal operations.

3. ASW applications.

The performance of sonars, in particular, high frequency sonars, and listening devices, is affected by the ambient noise of the ocean. This noise is partially caused by wave action and prior specification of this variable has been by crude estimate. The detailed energy spectra of the spectral wave model can contribute indirectly to the ASW tactical decision-making process through improved SHARPS and ASRAP forecasts. A "whitecap function" currently computed by the wave model and its relationship to ambient noise is currently under study. The use of spectral wave energy information in surface reverberation and scattering calculations appears promising.

4. Additional potential applications of spectral wave information include search and rescue efforts salvage operations, diving and offshore platform operations, unconventional ship design (hydrofoils, surface effect ships) and other motion-or stress-critical situations. For example, surface effect ships, when above the water, are unstable in an environment of certain wave frequencies.

D. Model Output

Fields output by the model are:

	Catalog Number
1. $\overline{H}1/3$, Mediterranean	B50
2. Primary Period, Mediterranean	B51
3. Primary Direction, Mediterranean	B52
4. Significant Wave Height	B53

5.	Primary Period		B54
6.	Primary Direction		B55
7.	Secondary Period		B56
8.	Secondary Direction		B57
9.	White Caps		B58
10.	Secondary Period, Mediterranean		B60
11.	Secondary Direction, Mediterranean	B61	B61
12.	White Caps, Mediterranean		B62

These fields are produced twice daily, tau 0 through tau 72, on the 63x63 Northern Hemisphere grid.

Upon special request from AWN source or FNWC, a page print of wave heights at a point is available in two formats. The period of the waves is displayed vertically, and the direction, horizontally. The significant wave height ($\overline{H}1/3$) is the average of the largest 1/3 of the waves and is used to represent the waves ships will encounter. $\overline{H}1/3$ is the summation, over all bands, of the energy present at a grid point. Average wave height ($\overline{H}$) is the average of all wave heights. The equations for computing $\overline{H}1/3$ and $\overline{H}$ are $4\sqrt{E}$ and $2.83\sqrt{E}$ respectively where E is the sum of the spectral variance (energy). The first format (see Figure 5.16.2) is in units of variance.

78030212 LAT 35.1N LON 59.3W 12Z 2 MAR 78 TAU 24

DIR FROM -LOCAL WIND 298.0DEG 23.4KTS WHITE CAP 1

PERIOD	TOTAL	250	40	10	340	310	280
18.0	4	0	0	2	1	1	0
16.4	60	0	1	16	19	18	5
15.0	168	0	9	58	44	46	10
13.8	219	0	7	69	51	66	23
12.4	606	3	1	109	241	202	45
10.9	470	1	0	105	168	149	45
9.7	321	5	0	74	101	96	42
8.6	295	8	0	71	84	85	46
7.5	159	6	0	34	44	46	27
6.3	146	8	0	30	38	40	28
4.8	75	13	0	7	14	20	19
3.2	23	4	0	2	4	6	5
DIR TOTAL		48	18	577	809	775	295

SIG HT 20.21FT AVG HT 14.29FT THRESHOLD .01

The sum of the period totals of variance (second column on next to bottom line) is the total energy in units of (ft^2x100). In the example, the sum of the energy is 25.56 ft^2, the square root

being 5.055 ft. The resulting $\overline{H}1/3$ = 20.22 ft and $\overline{H}$ = 14.29 ft. The second format (see Figure 5.16.3) is in units of variance density (ft^2/Hz); to convert this to variance it is necessary to multiply by the frequency bandwidth of the respective period domains.

78030212 LAT 35.3N LON 13.5E 12Z 2 MAR 78 TAU 48
DIR FROM -LOCAL WIND 331.6DEG 20.1KTS WHITE CAP 0

PERIOD	TOTAL	0	30	60	270	300	330
12.4	44	0	13	30	0	0	0
10.9	168	5	114	48	0	0	0
9.7	162	59	50	44	6	0	0
8.6	463	93	134	15	17	76	121
7.5	615	181	174	0	0	75	183
6.3	393	116	88	0	19	61	106
4.8	107	30	19	0	8	18	31
3.2	19	4	3	0	2	3	4
DIR TOTAL	488	595	137	52	233	445	

SIG HT 8.49FT THRESHOLD .01

The standard bandwidth is 0.00055 Hz (period = 1800 seconds) but some bandwidths are multiples of this standard bandwidth (see Figure 5.16.4).

Period	25.7	22.5	20.0	18.0	16.4	15.0	13.8	12.4	10.9	9.7	8.6	7.5	6.3	4.8	3.2
Multiple	1	1	1	1	1	1	2	2	2	3	3	3	6	12	24

FIGURE 5.16.4 Variance Density Period Factors

Total variance is derived by multiplying each of the subtotal periodic variances (second column; the directional subtotals can not be used in this case) by the appropriate multiple. In the example shown, multiples of 2, 2, 3, 3, 3, 6, 12 and 24 are used on periodic variance densities in column two. The sum of these components is 8242; dividing by 1800 (multiplying by the standard bandwidth of 0.00055 Hz) gives a variance total of 4.579. Applying the $4\sqrt{\ }$ rule we compute 4x2.14=8.56 ft as the significant wave height. In both examples, especially the variance density format which is currently used only in the Mediterranean, rounding of the data for transmission leads to slightly different results than the computer solution, which is precise.

A useful feature of reading variance format is the direct correlation of component magnitudes to determine dominant period

and direction. In the first example, the primary period is centered around the 10.9 and 12.4 second band while the direction is between 310° and 340°. In the second case, the primary period is between 6.3 and 7.5 seconds and the primary direction is between 000° and 030° (the variances are almost equal).

In both Figures 5.16.2 and 5.16.3, the figures for "Threshold" shows what level of variance was required to be printed as a non-zero value; the initial value is .01; if the bulletin is too long (>68 columns), this level is set to .05 to shorten the bulletin, etc., until the bulletin fits in the TTY format.

E. References

[1] Lazanoff, S. M. and N. M. Stevenson; "An Evaluation of a Hemispheric Operational Wave Spectral Model", FNWC Technical Note 75-3, 1975.

[2] Lazanoff, S. M., N. M. Stevenson and V. J. Cardone; "A Mediterranean Sea Wave Model", FNWC Technical Note 73-1, 1973.

5.17 BATHYTHERMOGRAPH AND SOUND VELOCITY EXTRACTS

A. Program Development

Sound velocity profiles constitute one of the basic inputs to acoustic models. The sound velocity extraction program (EXTRA) acts as an interface, or transformation program among the various data systems (FNWC programs, the data base format, the acoustic model, and standard Navy data formats).

B. Program Input

1. The program uses standard synoptic Ocean Thermal Structure (see Section 5.4) 63x63 fields for the upper levels, and long-term FNWC climatology for the lower levels. Salinity fields are provided by long-term climatology.

2. Inputs from the user can take any of these five forms:*

   (1) ASW prediction area (PTIDENT)

   (2) Latitude and longitude

   (3) Bathythermograph

   (4) Sound velocity profile

   (5) Depth, temperature, salinity profile.

C. Program Computations

1. EXTRA extracts field data for the desired location. The primary layer depth is inserted into the profile using the PLD temperature. The salinity data is interpolated to provide a depth-temperature-salinity array to which Leroy's equation is applied yielding the sound velocity. Sonic layer depth and the deep sound axis are then derived.

2. Where bathythermograph observations are provided, the values are blended and smoothed with field data to provide a complete surface to bottom profile. Bathythermograph profile may also be obtained using program KRILL and program HYDAT (see Sections 5.19 and 5.20).

*NOTE: The specific formats are given in reference [1].

3. Where a sound velocity profile is provided the velocities are converted to equivalent temperatures using Leroy's equation and field salinity data. These data are then blended utilizing the same scheme as for the bathythermograph data.

D. Program Limitations

Program EXTRA is a data base manager - it changes data formats to correspond with the requirements of specific applications. Primarily, EXTRA is used to convert various forms of data into ocean sound velocity profiles formatted for input to the Propagation Loss Model. Limitations of the outputs stem from limitations of the resolution of input and output forms, for example, the standard grids and the standard ocean structure-parameter levels.

E. Uses of the Products

There are several range prediction techniques that convert a single bathythermogram sample or profile to an expected contract range. If propagation loss predictions are not available from the FNWC models, these one-sounding techniques can substitute, with a loss of accuracy. But a fairly good estimate can be provided of the range within which the probability of detection is very high and a range beyond which there is little probability of detection.

F. Relationship to Other Products

Sound speed profiles are used as input to the Operational Propagation Loss Model (Section 5.18).

G. Program Output

Printouts and plots of sound velocity, temperature and salinity as functions of depth are available in various forms. Detailed descriptions of output formats are contained in Section 3.4 of reference [2].

H. Reference

[1] Fleet Numerical Weather Central, 1976; "Oceanographic Services Enviro-Acoustics Products Manual", Vol. II.

[2] DIRNAVOCEANMETINST C3160.4, Vol. 2.

5.18 OPERATIONAL PROPAGATION LOSS MODEL

A. Background

Man's interest in the transmission of sounds underwater actually dates back many years. Leonardo da Vinci described an early "SONAR" system when he spoke of using water-filled tubes to hear underwater sounds. Curiously enough, da Vinci's tube system persisted with only minor modifications until the closing months of World War I, when it was replaced by electronic techniques for converting acoustic energy into another energy form. During World War II and in more recent times, the developments in submarine warfare have forced great strides to be made in the field of underwater acoustics. While potential targets concentrated their efforts to be come less acoustically detectable, their adversaries developed more sensitive and sophisticated detection equipments. A common goal of both is to achieve a thorough understanding of the tactical implications of the way sound is transmitted through the water medium.

Since early in its existence FLENUMWEACEN has been intimately involved in the development of an operational model to predict just how acoustic energy is propagated underwater. FLENUMWEACEN is particularly well-suited for this task, owing to their unique synoptic air/ocean prediction capabilities and the required computer/manpower assets. Of special interest to the operational user is an assessment of how much energy of an acoustic signal is lost on its way from an underwater source to a receiver. The first propagation loss model was in operation by 1965 at FLENUMWEACEN, and subsequent modeling improvements have led to the present Operational Propagation Loss Model activated in 1973.

The primary causative factors behind Propagation Loss are: (1) Spreading Losses and (2) Attenuation Losses. The severity of the Spreading Loss(es) suffered is dependent upon the travel path available to the signal energy, but is basically a function of some discrete amount of sound energy being distributed over an increasingly larger area as it moves outward from the source. Attenuation Losses on the other hand, may be the result of such things as the conversion of some of the sound energy into heat energy (i.e., absorption) and the random scattering of signal energy away from the receiver. All of these causative factors are considered in the current Operational Propagation Loss Model.

The operational user of propagation loss (PL) data requires this information as an input parameter to the SONAR equation; one general form of which is shown below:

$$SE = SL - PL - AN - RD$$

Where,

SE = Signal Excess, in dB
SL = Source Signal in dB, at a 1 yard ref distance
PL = Propagation Loss suffered by the signal, in dB
AN = Ambient Noise present, in dB
RD = Recognition Differential of sensor system

Although particular sensor systems may require the inclusion of additional terms such as Target Strength (TS) or Directivity Index (DI), the SONAR equation provides the tactician with an assessment of his performance against a particular target in a given environmental scenario.

B. Description of the Model

The Fast Asymptotic Coherence Transmission (FACT) model is the Navy Interim Standard Transmission Model for ocean environments which may be treated by means of a single sound velocity profile and a flat bottom. It is a ray-acoustics model designed for the computation of acoustic propagation loss (PL) as a function of range and frequency at given source and receiver depths. Classical ray-trace methods have been augmented with higher order asymptotic corrections in the vicinity of caustics, and phased addition of selected paths to treat the coherence effects so important at lower frequencies. The formulas used come either from well-validated theory, or from empirical data derived from extensive field tests.

Model Assumptions/Limitations

1. When synoptic data are unavailable, the model draws upon climatology for its temperature-salinity input parameters.

2. Input data resolution with respect to bottom contours and/or reflectivity may be a source of error in the PL output.

3. Since no accurate method for computing surface reflection loss has yet been devised, a perfect surface reflection is assumed (no loss). This assumption introduces very little error for signal frequencies below 500 Hz, but at higher frequencies that computed loss will be less than actual.

4. Due to such factors as confused temperature gradients and irregular bottom topography in shallow waters, reliable PL data from the model may be expected only in deep water 100 miles or more away from the coast.

5. Some of the empirical equations used were derived from North Pacific studies, and may not be as effective in other oceans.

C. Model Input Parameters

*1. Vertical Temperature-Salinity Profile Data

**2. Ocean Bottom Depth

***3. Ocean Bottom Reflectivity Characteristics

4. Significant Wave Height Data

5. Acoustic Source Depth(s)

6. Acoustic Receiver Depth(s)

7. Acoustic Signal Frequency(ies)

*Temperature-salinity profile data may be derived from: (1) user-provided BT/TSP data; (2) extracts from FLENUMWEACEN subsurface thermal field data and monthly salinity climatology; or (3) climatological T,S data extracted from purely climatology data.

**Bottom depth input data includes information on depth and slope.

***Bottom reflectivity data refers to the reflectivity characteristics - mud vs granite, for instance.

D. Model Output Usage

Although adaptations of the FACT model have been adapted for use by other FLENUMWEACEN acoustic support products (e.g., ASRAP, PHITAR, etc.), the long-range PL output is only produced upon request. Some of its principal uses include:

1. Tactical and strategic planning.

2. Evaluation of SONAR equipment design.

3. Tactical usage by long-range acoustic sensor systems.

4. Long-Range Acoustic Studies.

The long-range PL output provides signal loss data out to any desired range for specific frequencies, source/receiver depth combinations, bottom topography and reflectivity type(s), and wave height.

E. Uses of the Products

The long-range PL products are not produced on a regular basis - only upon request. The principal uses are for:

1. Tracking by large underwater sound-listening arrays.

2. Placement and arrangement of long-range listening arrays.

3. Sonar equipment design.

4. Tactical and strategic planning.

F. Relationship to Other Products

The long-range PL output is not used in any other FNWC products. Parts of the model have been adapted for use in ASRAP and SUBRAP. This is discussed in Sections 5.21 and 5.23.

G. Program Output

Sound intensity loss data to any desired range and any given source depths, receiver depths, bottom topography, bottom acoustic loss class or classes, wave height, and frequencies.

H. References

[1] Spofford, C. W., 1974; "The FACT Model", Volumes 1 and 2; Acoustic Environmental Support Detachment, Office of Naval Research, Maury Center Report 109 (Vol I) and AESD Technical Note TN-74-04.

5.19 SYNOPTIC BATHYTHERMOGRAPH EXTRACTION (KRILL)

A. Program Development

Program KRILL was developed to extract synoptic bathythermograph data for use in real-time acoustic forecasts.

B. Program Input

1. Synoptic bathythermograph data supplied to FLENUMWEACEN for the previous 72 hours.

2. FLENUMWEACEN synoptic analysis levels from current OP49 fields for extraction position.

C. Program Limitations and Use

The program will produce an OP49 fields profile and extract all data for the previous 72 hours for the requested area. The maximum extraction radius around a point is 500 NM. In areas of high data, a maximum of the ten closest bathythermograph reports are extracted. If no data within 500 NM of the extraction point has been received in the previous 72 hours, only an OP49 profile will be produced.

The user specifies the point of interest, and KRILL returns a graphical plot of the nearest bathy reports along with the vertical profile from the Ocean Thermal Structure Analysis fields. Based upon experience and training, the watch officer selects an appropriate profile, which may then be used as input to the acoustic performance prediction models. KRILL is intended to complement the analysis in those areas of the oceans where the thermal structure is complex and/or rapidly changing. Figure 2.6.3.7 is an example of the KRILL graphical display as it is presented on the terminal for the watch officer.

D. Relationship to Other Products

Bathythermograph data combined with historical salinity data are used to produce sound velocity profile inputs to the Operational Propagation Loss Model (Section 5.18), ASRAP-III (Active and Passive), SHARPS-II and III, PHITAR, TASRAP, SIGRAM, and BASEPS.

E. Program Output

An X-Z plot of temperature profiles for OP49 fields and extracted bathythermographs for any point(s) in the Northern Hemisphere oceans. See Figure 5.19.1.

5.20 HYDROCLIMATOLOGICAL DATA RETRIEVAL PROGRAM (HYDAT)

A. Program Development

To improve FLENUMWEACEN's ability to access and use hydroclimatological data; the Hydroclimatological Data Retrieval Program (HYDAT) was developed for FLENUMWEACEN. The HYDAT program retrieves subsurface soundings from historical and synoptic hydroclimatological data bases.

The extraction process operates on one degree squares. Historical data to 1973 is accessed from monthly storage. HYDAT extracts data, calculates a mean, standard deviation, and selects a typical profile. Data is not directly available for input into acoustic products.

B. Program Input

1. Historical bathythermograph and Nansen cast soundings for the entire month.

2. Synoptic bathythermograph soundings from FNWC S10 file.

3. HYDAT extraction area characteristics (latitude and longitude of center point, square, circle, rectrangle).

C. Program Computations

The program HYDAT performs statistical analysis of extracted hydroclimatological data producing mean, maximum, minimum, and standard deviation temperature values for standard levels to 420 meters. A typical profile is selected based on statistical distribution of sea surface temperature (SST), heat content, and deep temperature. The statistical data, selected "typical" profile, typical profile extrapolated to bottom, and salinity data (if present) are an output to this plotter and/or printer for display. If data indicates this presence of up to three statistically different water masses, HYDAT will output "typical" profiles for each. In addition to the thermal profile, if a salinity profile is present in the data base for the selected "typical" profile, the program will output a salinity plot.

D. Limitations and Verification

HYDAT is limited to extracting data in whole degree blocks. All data found within a one degree block will be processed. The minimum size area for a search is the four one-degree blocks bounding a single latitude-longitude point.

The historical data base for HYDAT is based on Nansen casts

and bathythermographs from 1940 to 1973. HYDAT additionally accesses FNWC synoptic bathythermograph data stored in the S10 file for the previous seven days.

E. Uses of the Product

HYDAT extractions are used in exercise planning and preparation.

F. Program Output

1. An X-Z plot of statistical high, low, mean and standard deviation for area of interest.

2. An X-Z plot of all bathythermographs overplotted. See Figure 5.20.1.

3. An X-Z plot of the "typical" profile both to 410 meters and to the bottom depth of the area. See Figures 5.20.2 and 5.20.3.

4. An X-Z plot of the salinity profile if available for the "typical" profile. See Figure 5.20.4.

6. PRODUCTS FROM OTHER ACTIVITIES

6.1 NAVAL ENVIRONMENTAL WATCH SYSTEM (NEWS)

NEWS is a Naval Weather Service system for providing continuous monitoring and environmental forecasting for surface ships under U. S. Navy control. Ships included are all U. S. Navy, U. S. Coast Guard, Military Sealift Command, and Navy contract ships. Fleet Weather Central Pearl monitors Pacific ships; Fleet Weather Central Norfolk provides service in the Atlantic. NEWS operates only in the Northern Hemisphere at this time, but when a Global P.E. model becomes operational at FNWC, NEWS will cover the world.

The NEWS program (originally written by LCDR R. J. Gray) starts with input from the Operations and Control Center. This input consists of ship location files on magnetic tape. Each ship's current position is given, as are estimated positions for each 12 hours out to 72 hours. Dead reckoning is used to compute future positions, with no accounting made for the influence of environmental factors. The OPCON data base includes indicators which show whether each ship is (1) under Optimum Track Ship Routing (OTSR), (2) has requested Route Weather Forecasts (WEAX), or (3) is under both OTSR and WEAX.

The second input to NEWS consists of grid fields of environmental parameters from FNWC. These fields, covering from 12 to 48 hours in 12-hour increments, include: Degree of cloud cover or precipitation, visibility, surface wind speed and direction. The NEWS program matches the ships' positions with the appropriate FNWC grid field and extracts the required environmental data. Interpolation of parameter values from grid points to ship positions is done by the double-Bessel technique, the same as used in several FNWC programs. (Appendix B illustrates the technique in the FNWC Objective Analysis.)

The output section of the program produces four printouts every 12 hours.

1. Present ship's position and positions every 12 hours for the next 48 hours, with anticipated environmental conditions at each position. This output is stored on magnetic tape.

2. An alert list that includes all ships expected to encounter one or more of the following conditions within the next 48 hours: (a) winds in excess of 25 knots, (b) combined-wave height in excess of 10 feet, (c) visibility less than one mile.

3. Plain-language messages (WEAX) giving the range of environmental conditions expected for the next forty-eight hours for all ships that have requested enroute weather and sea-state forecasts. This printout also gives forecasts for all Ocean Station Vessels and selected islands.

4. Navigational information from synoptic ship reports is extracted and sent to OPCON for use in updating ship lists. The printout includes: call sign, latitude, longitude, course and speed.

An additional output of NEWS is spot forecast information that is overlayed on computer generated fleet facsimile charts.

Quality control on the fully-automated NEWS products is exercised by the FWC Duty Officer. He checks all the WEAX and alert list forecasts against the pertinent operational analyses and prognoses to insure that the NEWS products make meteorological sense. An added quality control measure is to compare the NEWS forecasts with reported weather and seas in the latest ship reports.

An additional output of NEWS is spot forecast information that is overlayed on computer generated fleet facsimile charts.

7. APPENDICES

APPENDIX A

GENERAL ENVIRONMENTAL COMPUTER PRODUCT CATALOG
(issued under separate cover as FNWC Technical Note No. 11)

APPENDIX B

CARSTENSEN OBJECTIVE ANALYSIS OF RANDOMLY DISTRIBUTED SCALAR DATA

Initialization

A. *Form the Laplacian of the initial guess field:*

$$L_{i,j} = \nabla^2 G_{i,j} = G_{i-1,j} + G_{i+1,j} + G_{i,j-1} + G_{i,j+1} - 4\,G_{i,j}$$

B. (Optional) Smooth the Laplacian of the initial guess:

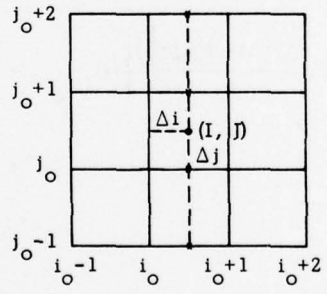
$$\tilde{L}_{i,j} = L_{i,j} + k\nabla^2 L_{i,j} \quad , \quad \text{where} \quad 0 \leq k < \frac{1}{4} \ .$$

Repetitive Section

A. Set up correction fields, to be used for adjusting the guess field to the observations. Repeat the following procedure for each report:

Given a reported value R at $I = i_o + \Delta i$, $J = j_o + \Delta j$, where i_o and j_o are integers and $0 \leq \Delta i < 1$ and $0 \leq \Delta j < 1$.

1. Interpolate in the guess field to obtain a guess value at the point (I,J), using Bessel's central difference formula:



a. Perform four horizontal interpolations:

$$G_{I,j} \equiv G_{i_o+\Delta i,j} = \frac{G_{i_o+1,j} + G_{i_o,j}}{2} + \left(\Delta i - \frac{1}{2}\right)\left(G_{i_o+1,j} - G_{i_o,j}\right)$$

$$+ \frac{\Delta i\,(\Delta i-1)}{4}\left\{\left(G_{i_o+2,j} - G_{i_o+1,j}\right) + \left(G_{i_o-1,j} - G_{i_o,j}\right)\right\}$$

$$+ \frac{\Delta i\left(\Delta i-1\right)\left(\Delta i-\frac{1}{2}\right)}{6}\left\{\left(G_{i_o+2,j} - G_{i_o+1,j}\right) - 2\left(G_{i_o+1,j} - G_{i_o,j}\right)\right.$$

$$\left. + \left(G_{i_o,j} - G_{i_o-1,j}\right)\right\} ,$$

for $j = j_o - 1,\ j_o,\ j_o + 1,\ j_o + 2$.

b. Perform one vertical interpolation:

$$G_{I,J} \equiv G_{i_o+\Delta i,j_o+\Delta j} = \frac{G_{I,j_o+1} + G_{I,j_o}}{2} + \left(\Delta j - \frac{1}{2}\right)\left(G_{I,j_o+1} - G_{I,j_o}\right)$$

$$+ \frac{\Delta j\,(\Delta j-1)}{4}\left\{\left(G_{I,j_o+2} - G_{I,j_o+1}\right) + \left(G_{I,j_o-1} - G_{I,j_o}\right)\right\}$$

$$+ \frac{\Delta j\left(\Delta j-1\right)\left(\Delta j-\frac{1}{2}\right)}{6}\left\{\left(G_{I,j_o+2} - G_{I,j_o+1}\right) - 2\left(G_{I,j_o+1} - G_{I,j_o}\right)\right.$$

$$\left. + \left(G_{I,j_o} - G_{I,j_o-1}\right)\right\} .$$

2. Find the difference between the observed value and the interpolated guess value at the same point:

$$D = R - G_{i,j} .$$

3. Compute weights for the four grid points around the report:

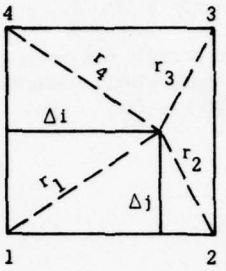
   a. Find the square of the distance in mesh lengths from the report to each of the four surrounding points:

$$r_1^2 = \Delta i^2 + \Delta j^2$$

$$r_2^2 = (1-\Delta i)^2 + \Delta j^2$$

$$r_3^2 = (1-\Delta i)^2 + (1-\Delta j)^2$$

$$r_4^2 = \Delta i^2 + (1-\Delta j)^2$$



   b. Form one minus the square of the distance to each of the four points, setting negative values to zero:

$$S_k = 1 - r_k^2 \quad \text{if} \quad r_k^2 \leq 1$$

$$0 \quad \text{if} \quad r_k^2 > 1 \quad ,$$

   for $k = 1, 2, 3, 4$.

   c. Normalize to find weight factors for each of the four surrounding points:

$$w_k = \frac{S_k}{\sum_{\ell=1}^{4} S_\ell} \qquad \text{for } k = 1, 2, 3, 4.$$

   d. Multiply each weight factor by the reliability coefficient for the report:

$$W_k = (RLB)\, w_k \quad \text{for } k = 1, 2, 3, 4,$$

   where $0 < RLB < 8$.

4. Compute a weighted difference for each of the four points:

$$(WD)_k = W_k \cdot D \,, \quad \text{for } k = 1, 2, 3, 4,$$

where D = (observed value) - (interpolated value).

5. Add W_k to cumulative sums of weight factors, and add $(WD)_k$ to cumulative sums of weighted differences, for each of the four points around the report.

B. Lateral check each report for compatibility with neighboring reports. For each report which fails the lateral check, subtract the weight factors and weighted differences from the sums to eliminate the influence of the report.

C. Adjust each grid point in the guess field by adding the mean of the weighted corrections resulting from each relevant observation. (The value at a grid point is thus changed by observations within one mesh length of the grid point.)

$$A_{i,j} = G_{i,j} + \frac{\sum_{\ell=1}^{P} (WD)_\ell}{\sum_{\ell=1}^{P} W_\ell} \quad ,$$

where P is the number of reports affecting this point. (If $P = 0$, $A_{i,j} = G_{i,j}$.)

D. Modify interior grid points which have no reports within one mesh length, using the over-relaxation technique for solution of the Poisson equation $\nabla^2 A = \tilde{L}$: (Values which have been adjusted to reports are held fixed.)

1. $R_{i,j}^{\nu+1} = \left(\frac{\lambda}{4}\right)\left(\nabla^2 A_{i,j}^{\nu} - \tilde{L}_{i,j}\right)$, where $\frac{1}{4} < \frac{\lambda}{4} < \frac{1}{2}$, and ν denotes scan number.

2. $A_{i,j}^{\nu+1} = A_{i,j}^{\nu} + R_{i,j}^{\nu+1}$.

3. Repeat 1. and 2. until $|R_{MAX}^{\nu+1}| < \epsilon$.

E. (Optional) Smooth the analyzed field with a light smoother designed to eliminate short-wave features without disturbing long-wave patterns.

F. Return to step A. in Repetitive Section for the next cycle. (The guess for the next cycle will be the analysis resulting from this cycle.)

The entire analysis scheme, starting with Initialization, may be repeated one or more times. In each case the "initial" guess will be the analyzed field resulting from the previous scan through the analysis routine.

APPENDIX C

AN APPLICATION OF THE 500-MB SCALE AND PATTERN SEPARATION CHARTS

Relationships between sea-level cyclone development and the movement, intensity and interactions of upper-level disturbances have been treated exhaustively in the literature. Application of these relationships to the synoptic forecast problem, however, has been difficult. This has been due, among other things, to the inability of the forecaster to determine objectively the exact locations, dimensions and intensities of meteorologically significant upper-level disturbances. The Scale and Pattern Separation program (Section 4.9) represents a method for separating two disturbance components from the total circulation at any desired level. The meteorological significance of these components at the 500-mb level and their application to cyclone forecasting will be demonstrated in this appendix.

Long waves (large-scale disturbances) have generally been difficult to separate from the total flow pattern with any degree of precision. The more numerous short waves (small-scale disturbances) normally translate through and distort the large-scale features. In Figure C.1 the 500-mb circulation for 1200Z 1 January 1966 is depicted. The double lines are objectively determined long-wave trough positions. Over one hundred practicing forecasters attending the several FNWC Numerical Environmental Prediction Courses have been asked to locate subjectively the long-wave troughs in this analysis. None have exactly duplicated the positions indicated here. Given the objective long-wave trough locations, the short waves can readily be identified as distortions which serve to mask the larger scale features.

The locations, dimensions and intensities of the small-scale disturbances, manifest as short-wave troughs in the analysis, are depicted in Figure C.2. Effectively, this analysis depicts the relative vorticity integrated over a prescribed scale range with the sign reversed. In the Residual analysis, Figure C.3, the small-scale disturbances have been separated from the complete circulation pattern. Again, objectively determined long-wave trough positions are superimposed. Subjective determination of long-wave trough positions even from this analysis might not result in the exact locations indicated by the double lines. On this particular day, the correspondence is relatively good.

Figure C.4 is the large-scale disturbance analysis. The long-wave trough positions displayed in the previous figures were obtained from this pattern. The double lines were drawn by hand, allowing some slight subjectivity in the process.

One should spend some time noting the relationships between the disturbance components of Figure C.2, C.4 and the total circulation pattern, Figure C.1. Figures C.5 through C.8 provide a comparison with the same charts for a time 48 hours later. The positions of the large-scale disturbance troughs have remained relatively stable over this 48-hour period. Superimposed on the large-scale disturbance analyses are the 24-hour history positions of selected negative SD small-scale disturbances. The center labelled Case A is charted from its position east of the Ural Mountains at 1200Z 28 December 1965 (Figure C.4) to a position over Japan at 1200Z on 4 January 1966 (Figure C.8). The center labelled Case B moves from the New England States to the Adriatic Sea over the same six-day period. In both cases the small-scale disturbance centers were represented by at least one closed contour during the period and are easily identified in Figures C.2 and C.6.

The small-scale disturbance labelled Case C was evident as a sharp trough in the SD pattern for 1200Z on the 28th and 29th of December 1965 (Fig. C.4). On the 30th of December it developed a closed center and broke away from a parent center located in the Gulf of Alaska. Subsequently it moved to a position in the central Atlantic by 1200Z on the 4th of January (Fig. C.8). Case D appeared as a closed center in northern California twelve hours prior to the time of Figure C.8. In three days it moves to the Gulf of St. Lawrence.

The time continuity displayed by all of these small-scale disturbance centers is typical for the winter season. In fact, the center labelled Case A can be traced all the way back to its break-off from a parent center in the eastern Atlantic on 16 December 1965.

The relationship between meteorological events at the surface and the movement of these small-scale disturbances through the large-scale disturbance troughs is displayed in the surface pressure analyses of Figures C.9 through C.13. Small-scale 500-mb disturbance centers are indicated as squares on the surface analyses.

Case A:

As the upper-level disturbance center proceeds across Mongolia (Fig. C.9) and through China (Figs. C.10 and C.11) an associated weak surface low-pressure center moves through the Siberian Anticyclone. This is a manifestation of the upper-level divergence associated with the advection of negative SD (positive vorticity) at 500-mb. Obviously, low-level convergence is sufficient to balance the upper-level divergence. The small-scale disturbance center passes through the large-scale disturbance trough at about 0000Z 4 January 1966 (Figure C.8). Subsequent development at the surface near Japan is quite striking (Figures C.12, C.13 and C.14).

Case B:

The small-scale 500-mb disturbance center is associated with a deep surface cyclone approaching the British Isles on 1 January 1966 (Figure C.9). By 3 January (Fig. C.11), the 500-mb small-scale disturbance center has begun to split. The southernmost center subsequently becomes dominant. By 4 January (Fig. C.12) this center has moved well to the south of the surface cyclone with which it was originally associated and the surface cyclone weakens rapidly. A new surface weakness is becoming organized over Yugoslavia just ahead of the upper-level small-scale disturbance which is at this time moving into the large-scale disturbance trough. Subsequent surface cyclone development is again quite striking (Figs. C.13 and C.14).

Case C:

The 500-mb small-scale disturbance center located over Lake Superior on 1 January (Fig. C.9) is associated with a well-developed surface cyclone. This surface low developed in Wyoming as the SD center moved out of the Pacific and through the large-scale disturbance trough over the west coast of North America on 30 January (Figure C.4).

During the next twenty-four hours the surface cyclone weakens while moving to a position over Newfoundland (Figure C.10). Subsequently the associated small-scale disturbance center moves into and through the large-scale disturbance trough. Surface cyclone deepening is strong (Figures C.10 through C.14).

Case D:

The small-scale disturbance center in California (Figure C.9) is associated with a surface pressure weakness on the Nevada-Utah border. Reference to Figure C.8 shows the SD center position to be under a large-scale disturbance trough at this time. Subsequent rather slow surface cyclone development is seen in Figures C.10 and C.11. By 0000Z 4 January (Fig. C12) the surface cyclone has moved appreciably north of the upper level SD center. Within six hours (Fig. C.13) a surface center jump to a position closer to the upper level disturbance has taken place. The new surface low is located in the Gulf of St. Lawrence while the original surface center has become indistinct over Labrador. Subsequently the SD center moves into the large-scale disturbance trough in the mid-Atlantic. A deep secondary surface low center on the periphery of the primary low southeast of Greenland results.

Conclusions:

1. A 500-mb small-scale disturbance (SD) center, translating in the westerlies, is likely to be accompanied by surface cyclone development as it moves into and through a 500-mb large-scale disturbance trough.
2. A surface cyclone which moves out from under an associated 500-mb small-scale disturbance center is likely to weaken rapidly while another surface center is likely to form closer to the upper-level SD center (under the maximum negative SD advection aloft).

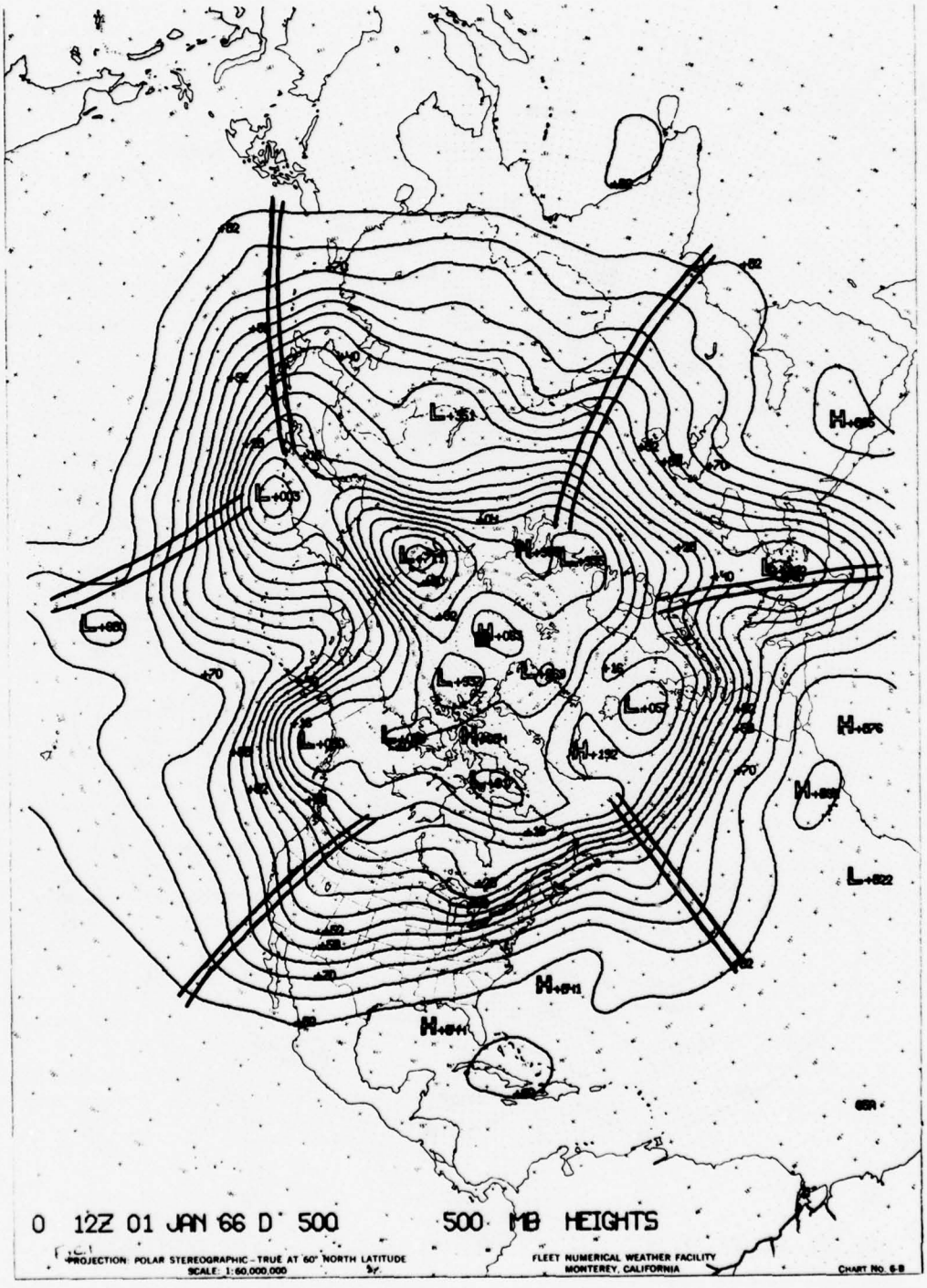


FIGURE C.1 500-MB HEIGHT ANALYSIS FOR 1200Z 1 JANUARY 1966. DOUBLE LINES ARE LONG WAVE TROUGH POSITIONS. SEE FIGURE C.4.

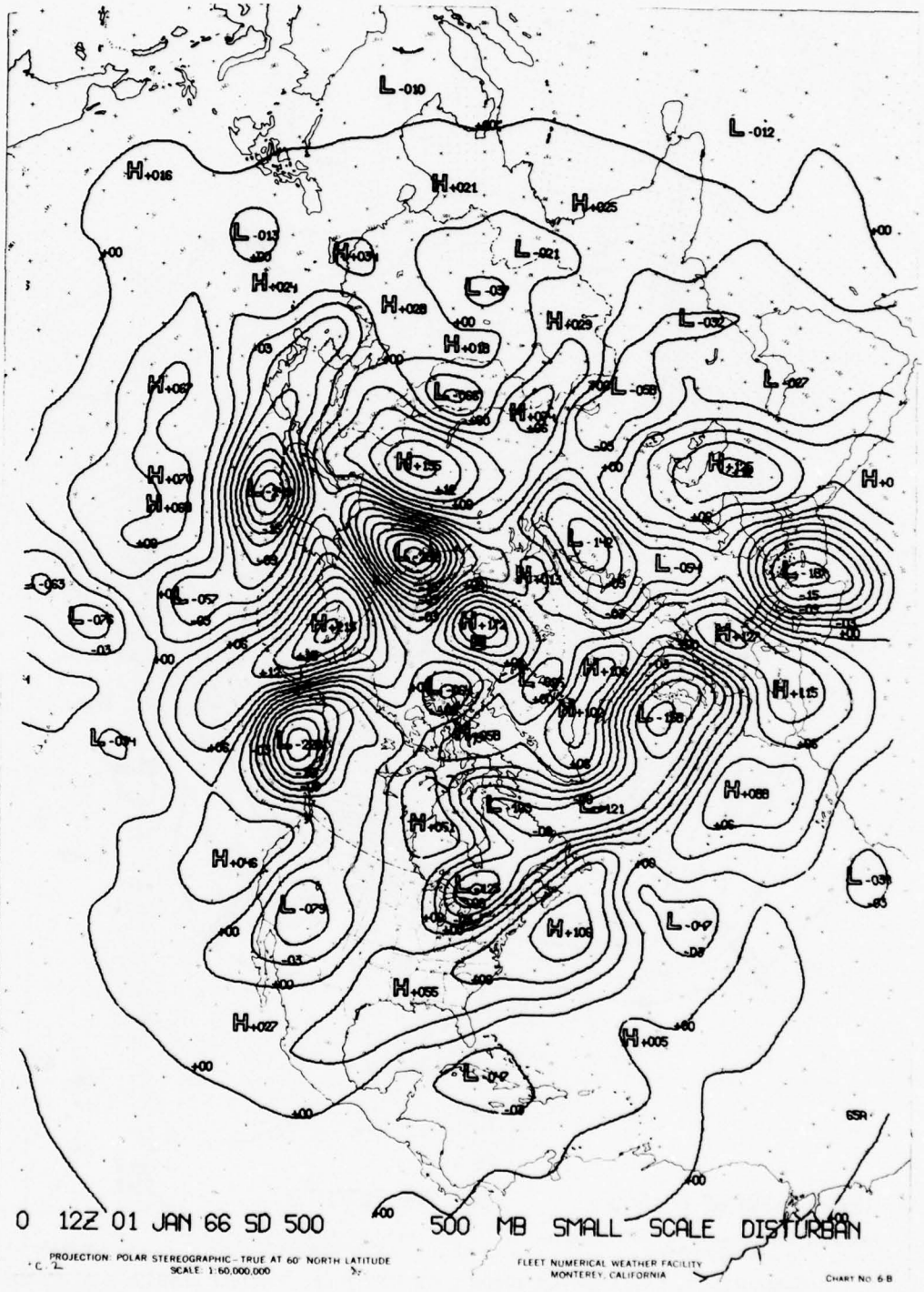


FIGURE C.2 500-MB SMALL SCALE DISTURBANCE ANALYSIS FOR 1200Z 1 JANUARY 1966.

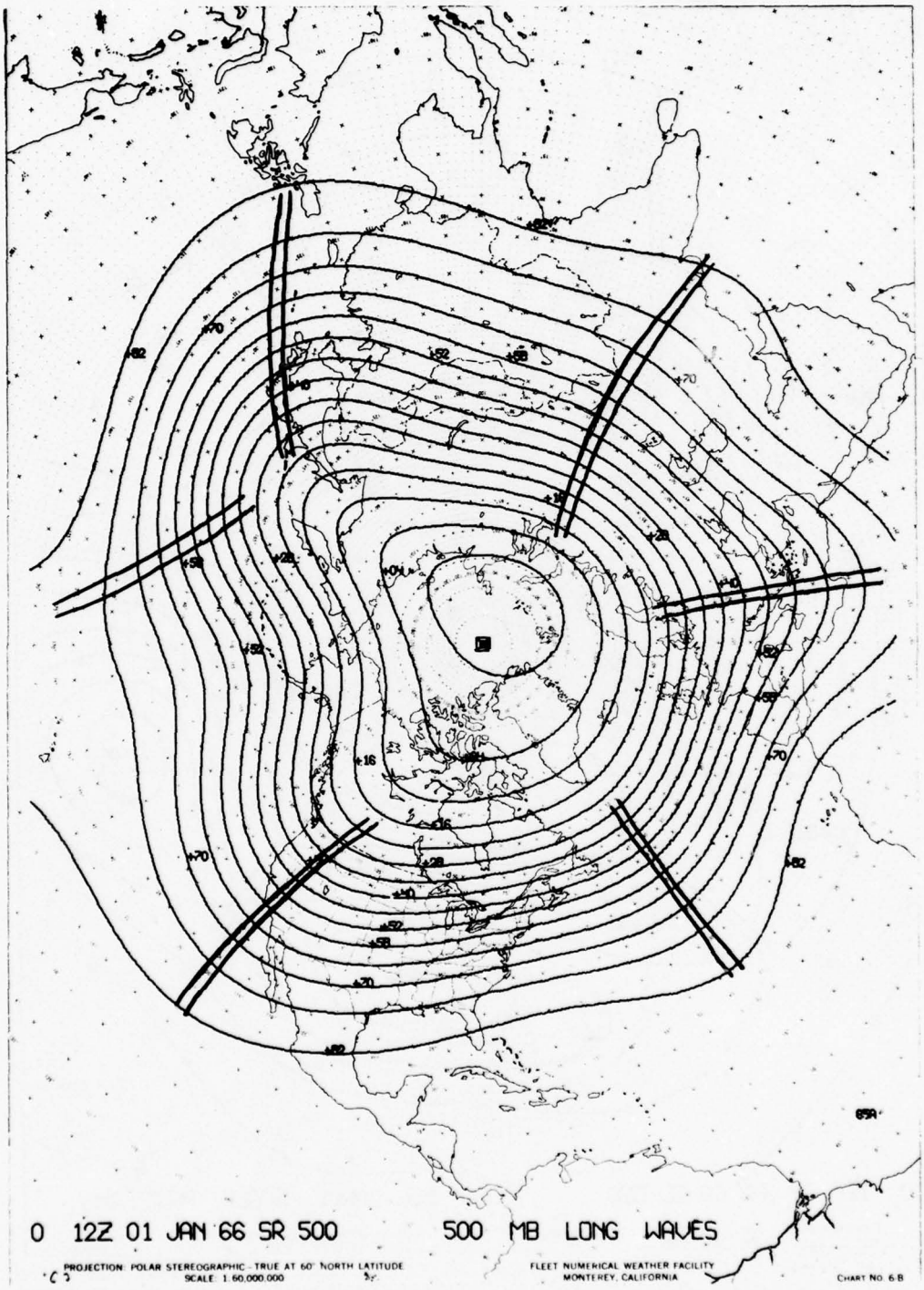


FIGURE C.3 500-MB RESIDUAL ANALYSIS FOR 1200Z 1 JANUARY 1966. DOUBLE LINES ARE LONG WAVE TROUGH POSITIONS.

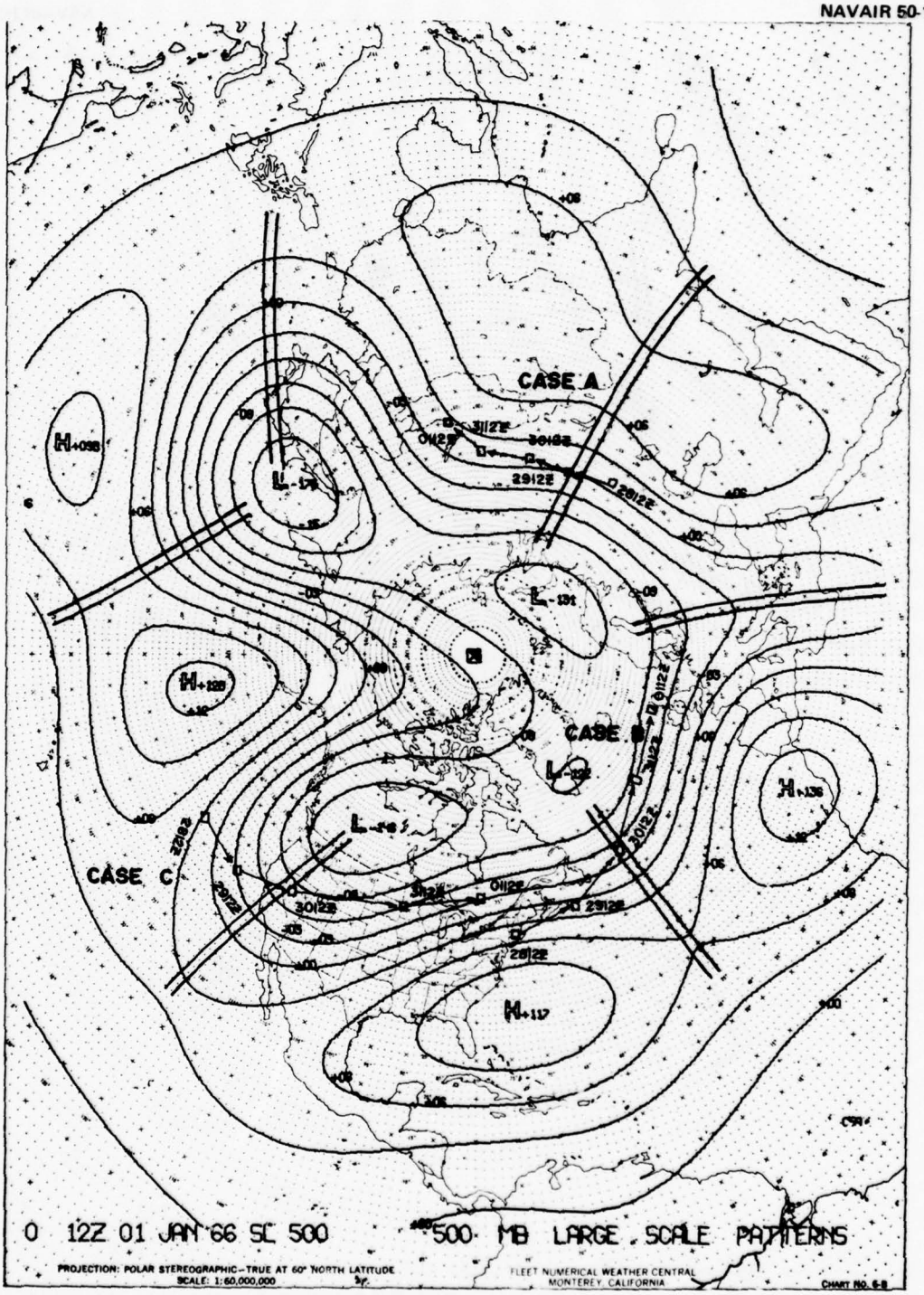


FIGURE C.4 500-MB LARGE SCALE DISTURBANCE ANALYSIS FOR 1200Z 1 JANUARY 1966. OBJECTIVE LOCATION OF LONG WAVE TROUGHS (DOUBLE LINES) IS PROVIDED BY THIS ANALYSIS. SQUARES ARE 24-HOUR POSITIONS OF SELECTED SMALL SCALE DISTURBANCE CENTERS FOR THE PAST 72 HOURS.

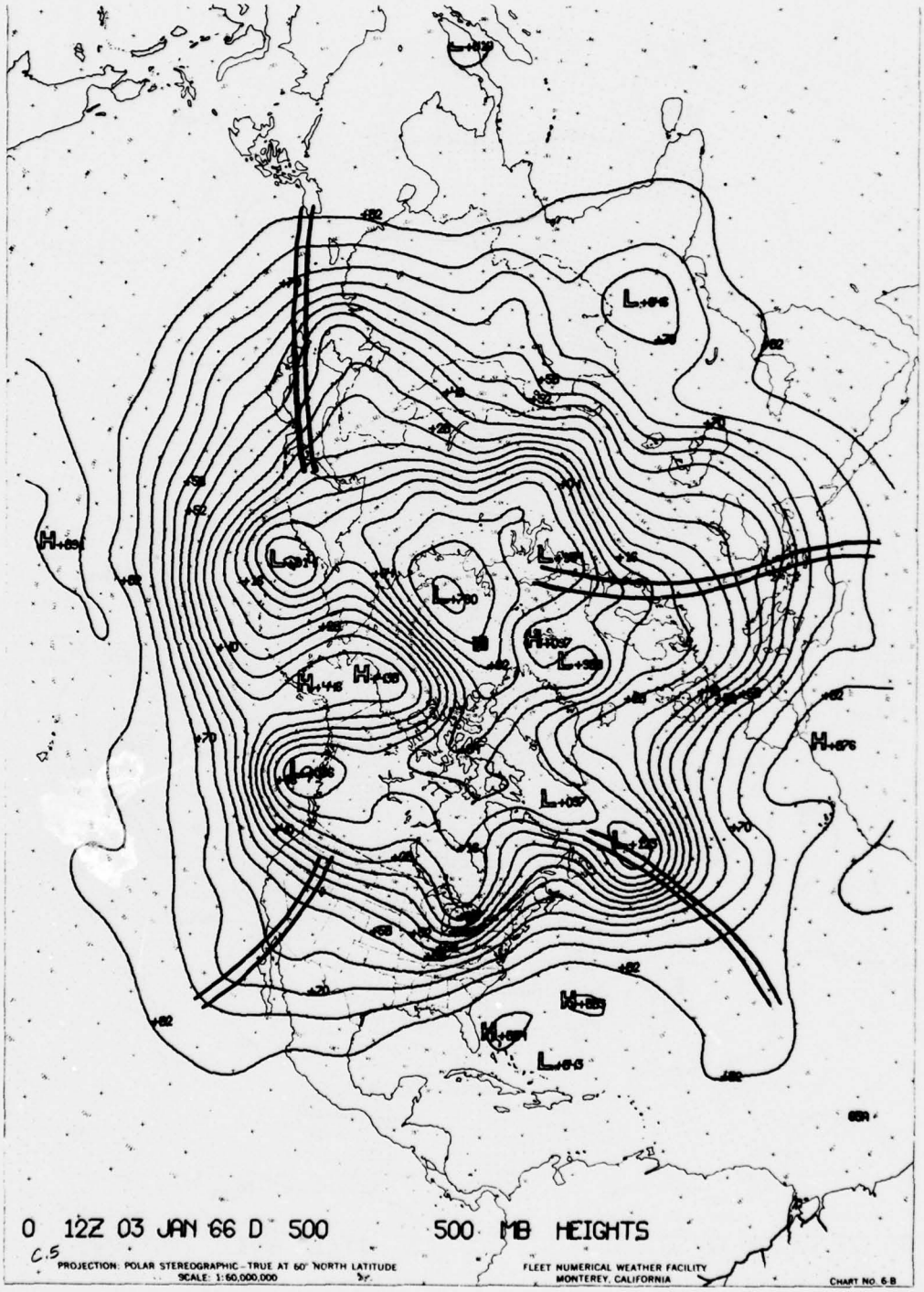


FIGURE C.5 500-MB HEIGHT ANALYSIS FOR 1200Z 3 JANUARY 1966. DOUBLE LINES ARE LONG WAVE TROUGH POSITIONS. SEE FIGURE C.8.

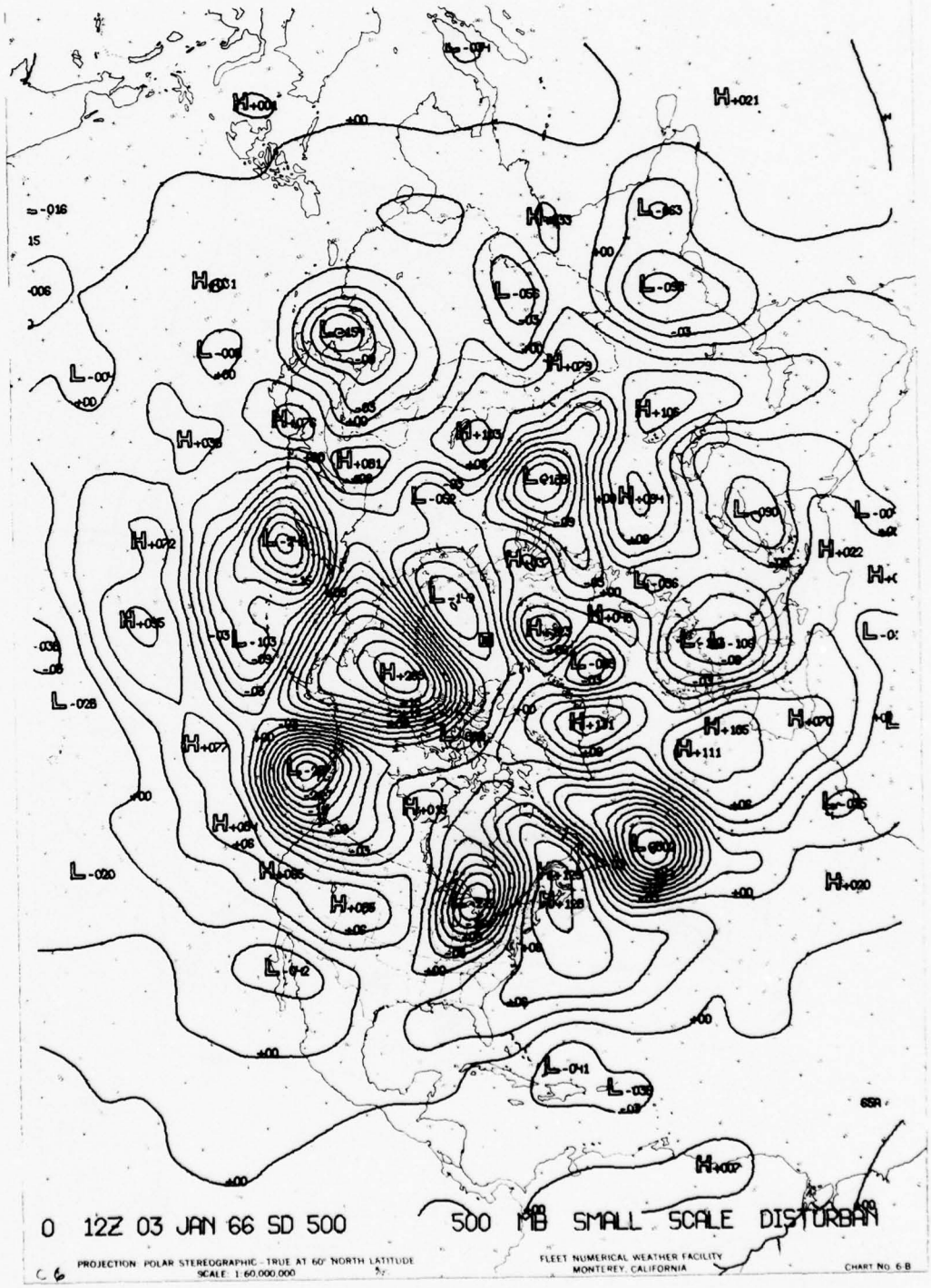


FIGURE C.6 500-MB SMALL SCALE DISTURBANCE ANALYSIS FOR 1200Z 3 JANUARY 1966.

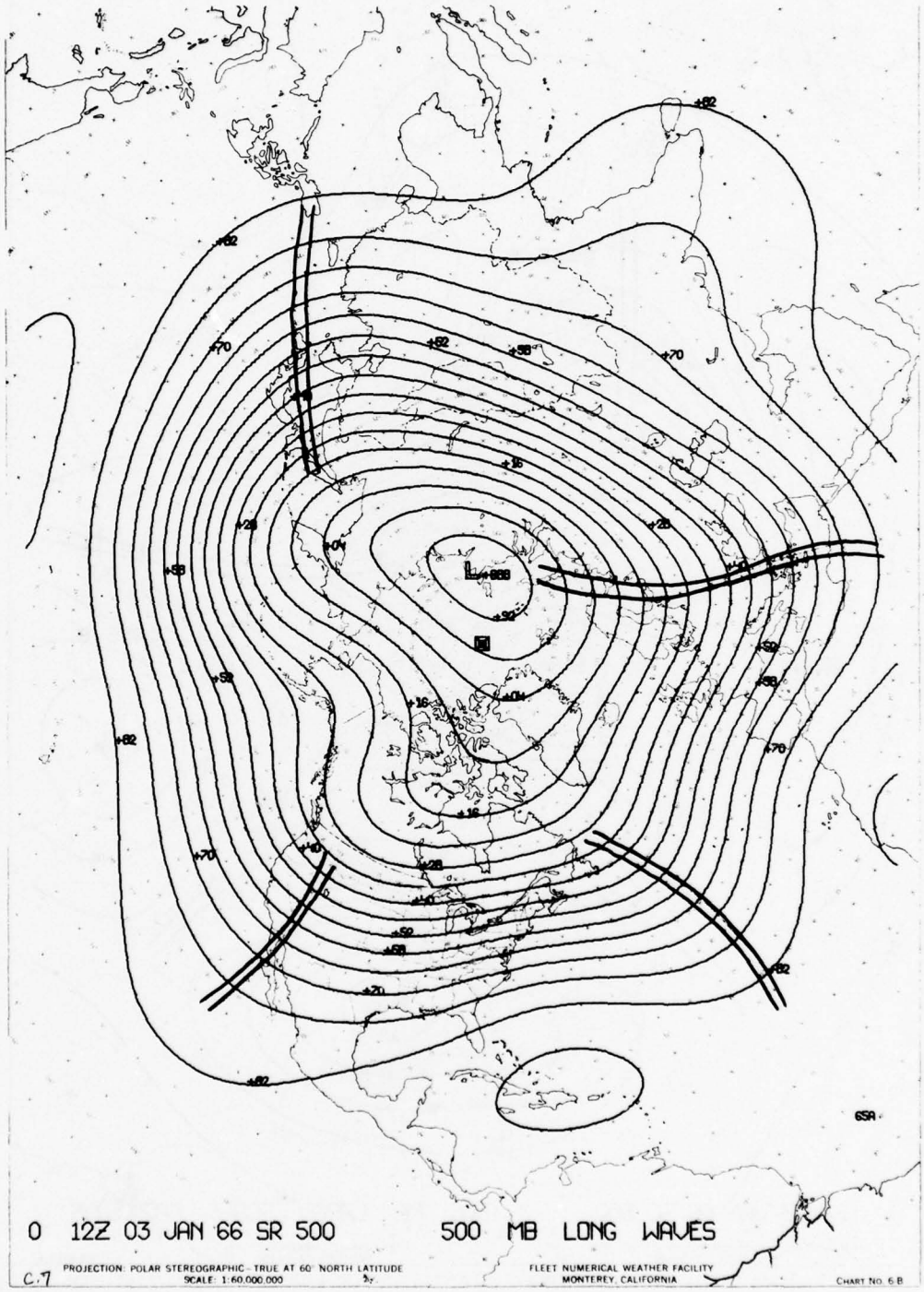


FIGURE C.7 500-MB RESIDUAL ANALYSIS FOR 1200Z 3 JANUARY 1966. DOUBLE LINES ARE LONG WAVE TROUGH POSITIONS.

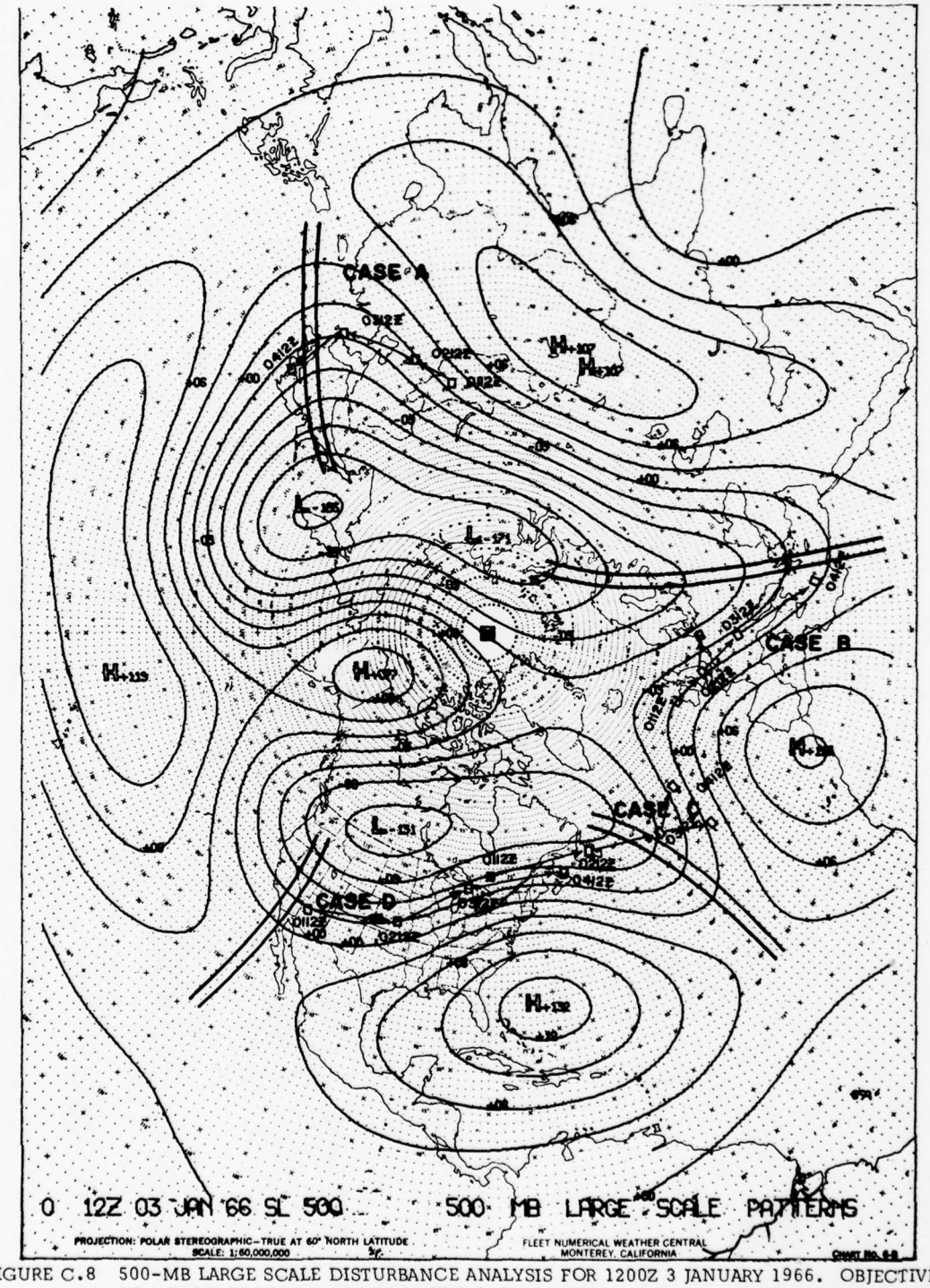


FIGURE C.8 500-MB LARGE SCALE DISTURBANCE ANALYSIS FOR 1200Z 3 JANUARY 1966. OBJECTIVE LOCATION OF LONG WAVE TROUGHS (DOUBLE LINES) IS PROVIDED BY THIS ANALYSIS. SQUARES ARE PAST HISTORIES OF SELECTED SMALL SCALE DISTURBANCE CENTERS.

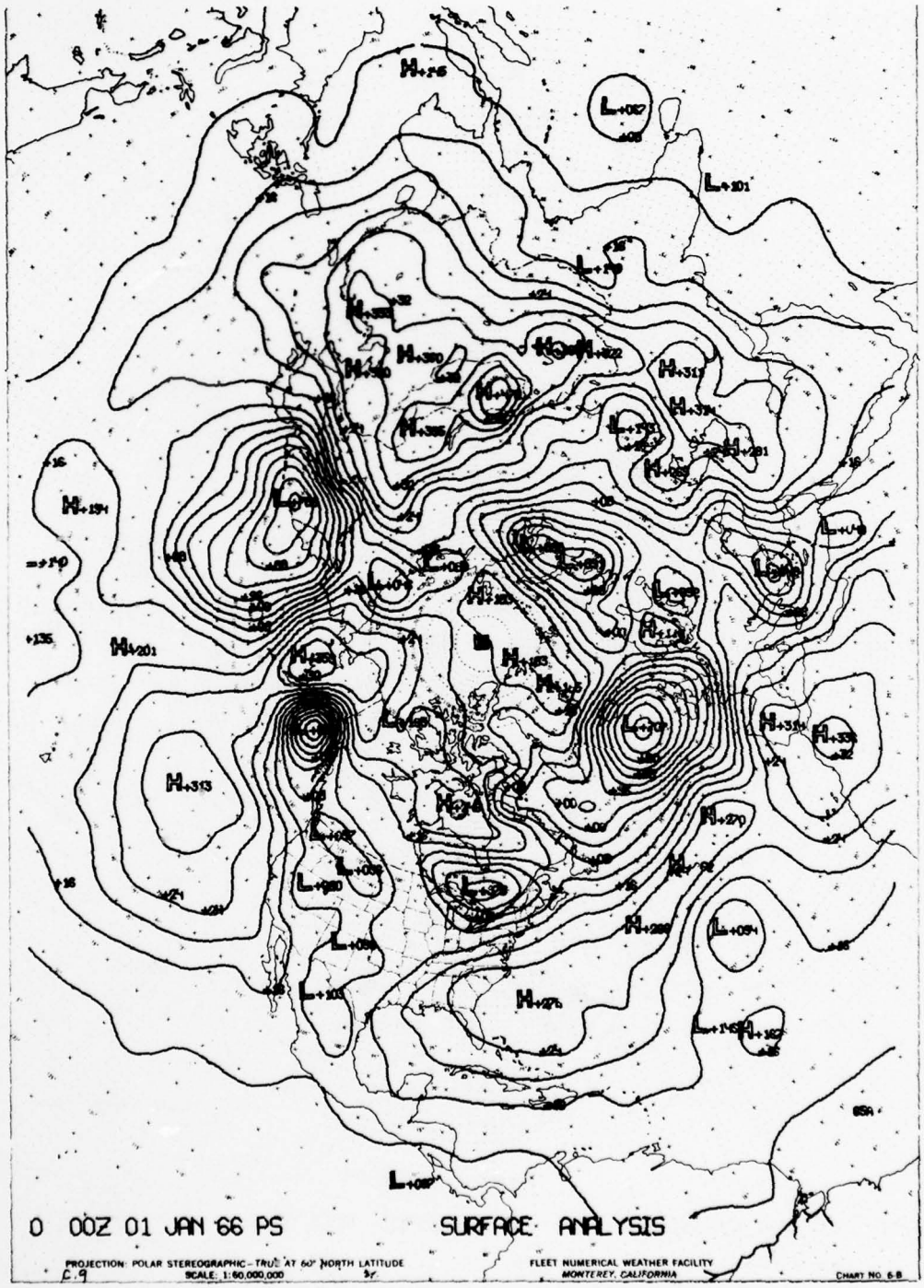


FIGURE C.9 SURFACE PRESSURE ANALYSIS FOR 0000Z 1 JANUARY 1966. 500-MB SMALL SCALE DISTURBANCE CENTER LOCATIONS AT THIS TIME ARE INDICATED BY SQUARES.

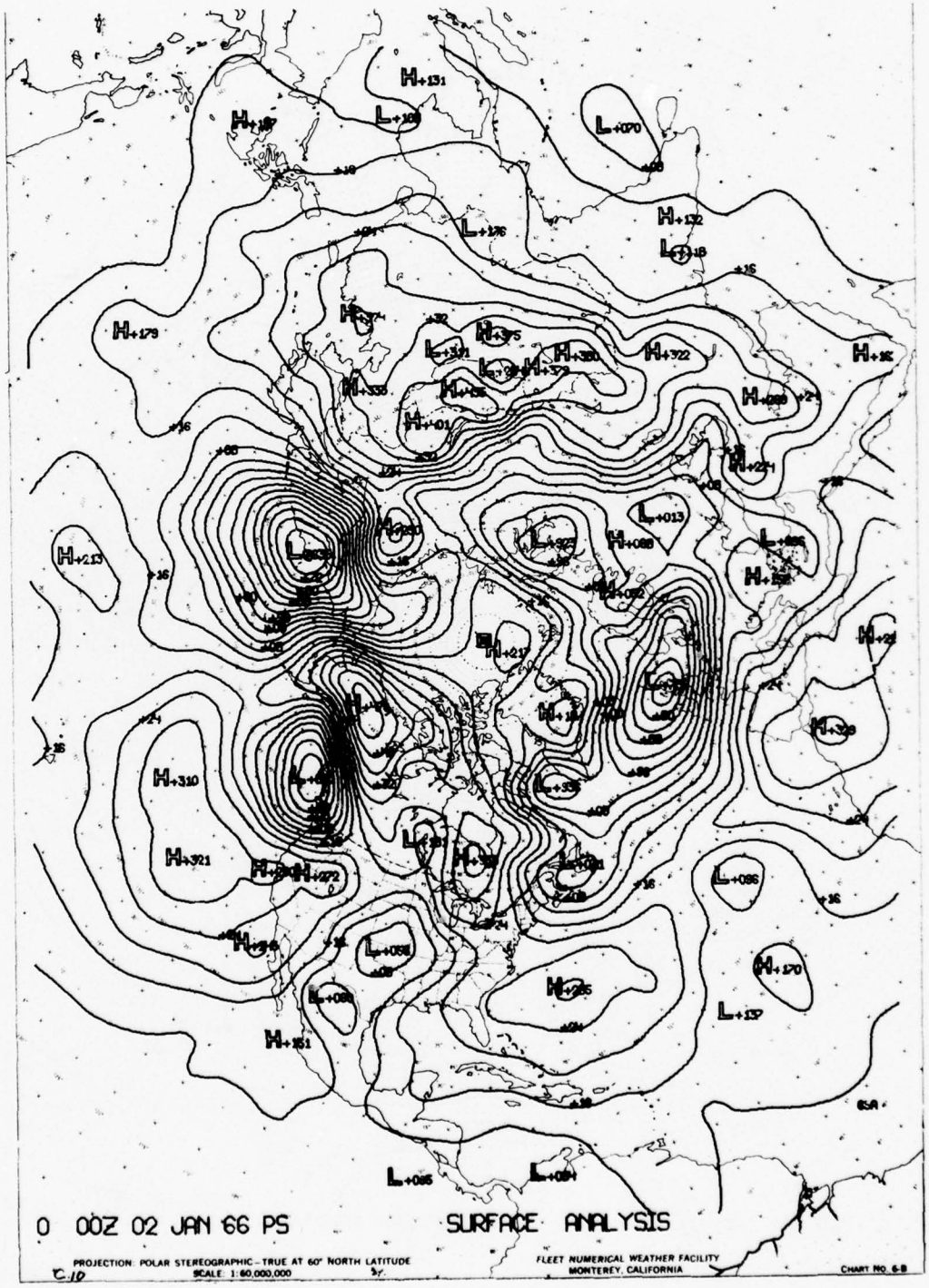


FIGURE C.10 SURFACE PRESSURE ANALYSIS FOR 0000Z 2 JANUARY 1966. 500-MB SMALL SCALE DISTURBANCE CENTER LOCATIONS AT THIS TIME ARE INDICATED BY SQUARES.

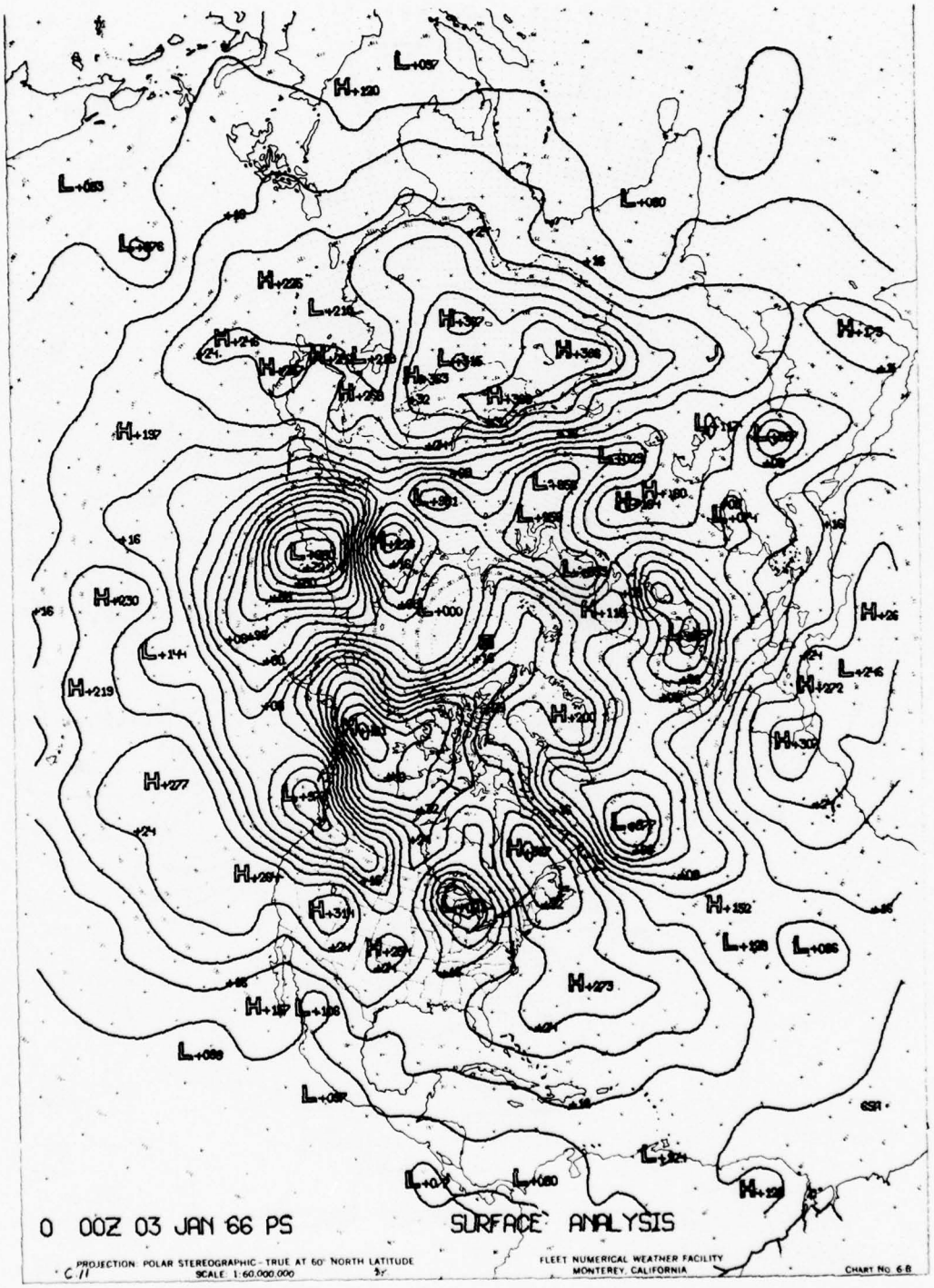


FIGURE C.11 SURFACE PRESSURE ANALYSIS FOR 0000Z 3 JANUARY 1966.

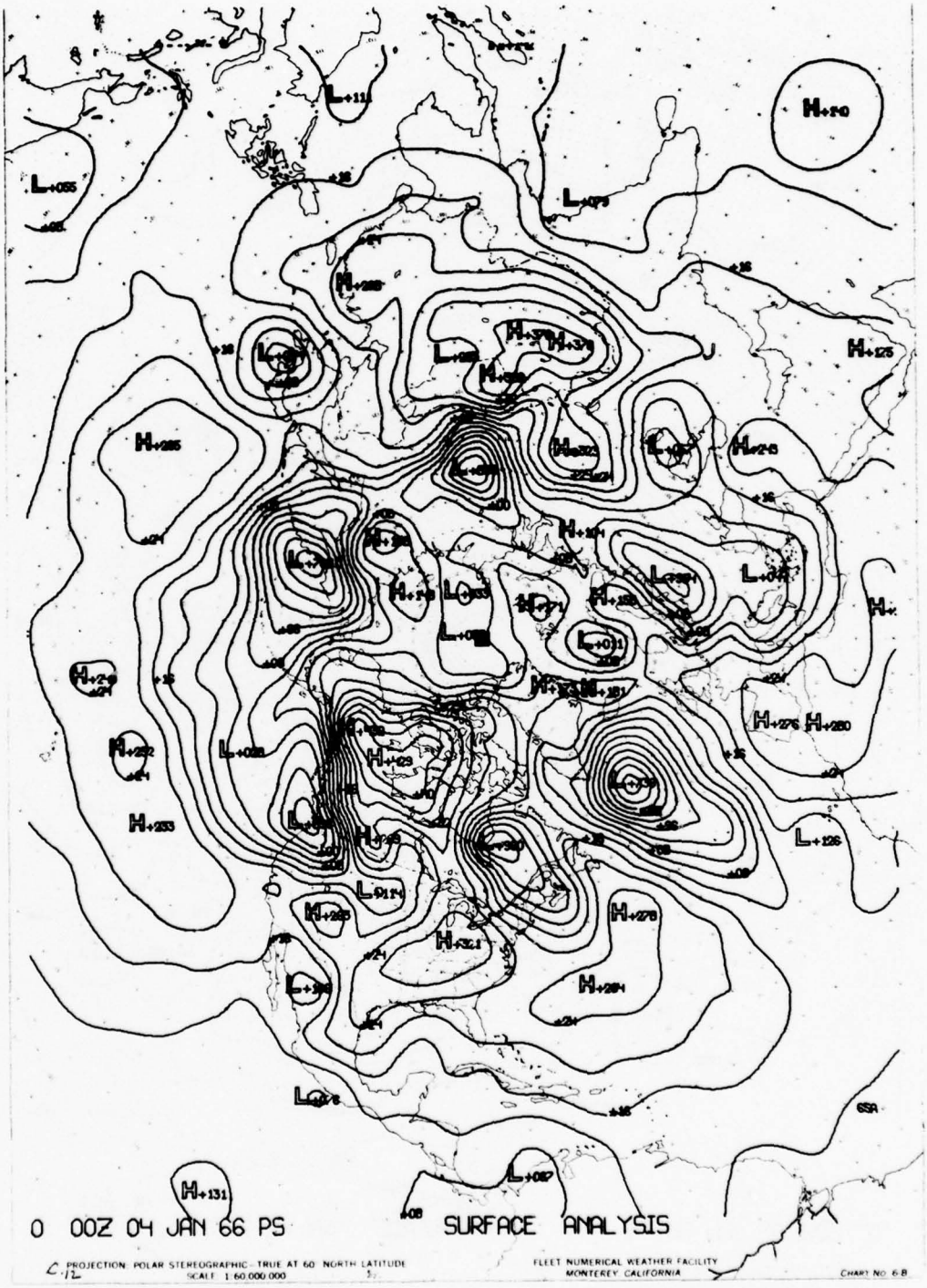


FIGURE C.12 SURFACE PRESSURE ANALYSIS FOR 0000Z 4 JANUARY 1966.

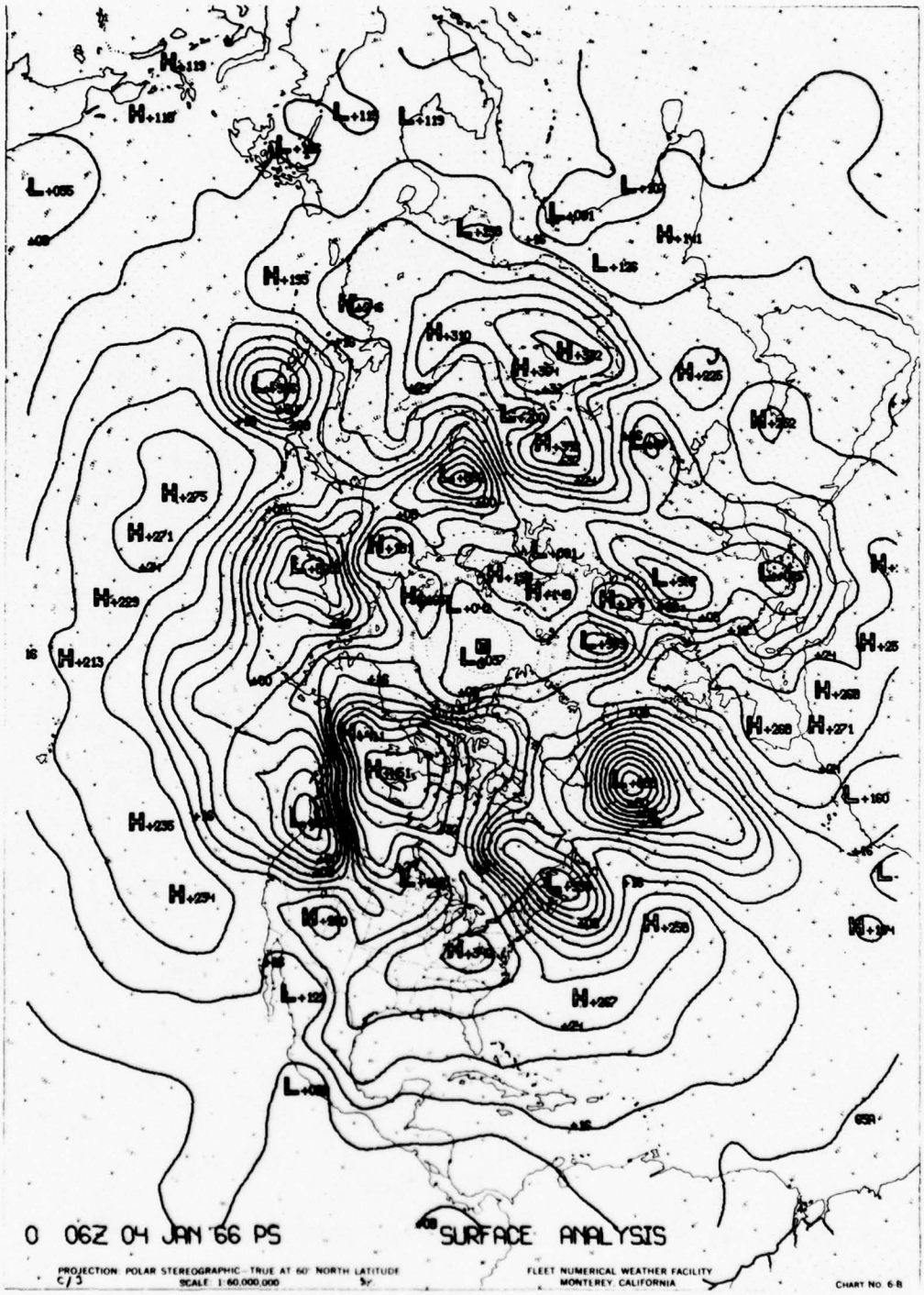


FIGURE C.13 SURFACE PRESSURE ANALYSIS FOR 0600Z 4 JANUARY 1966.

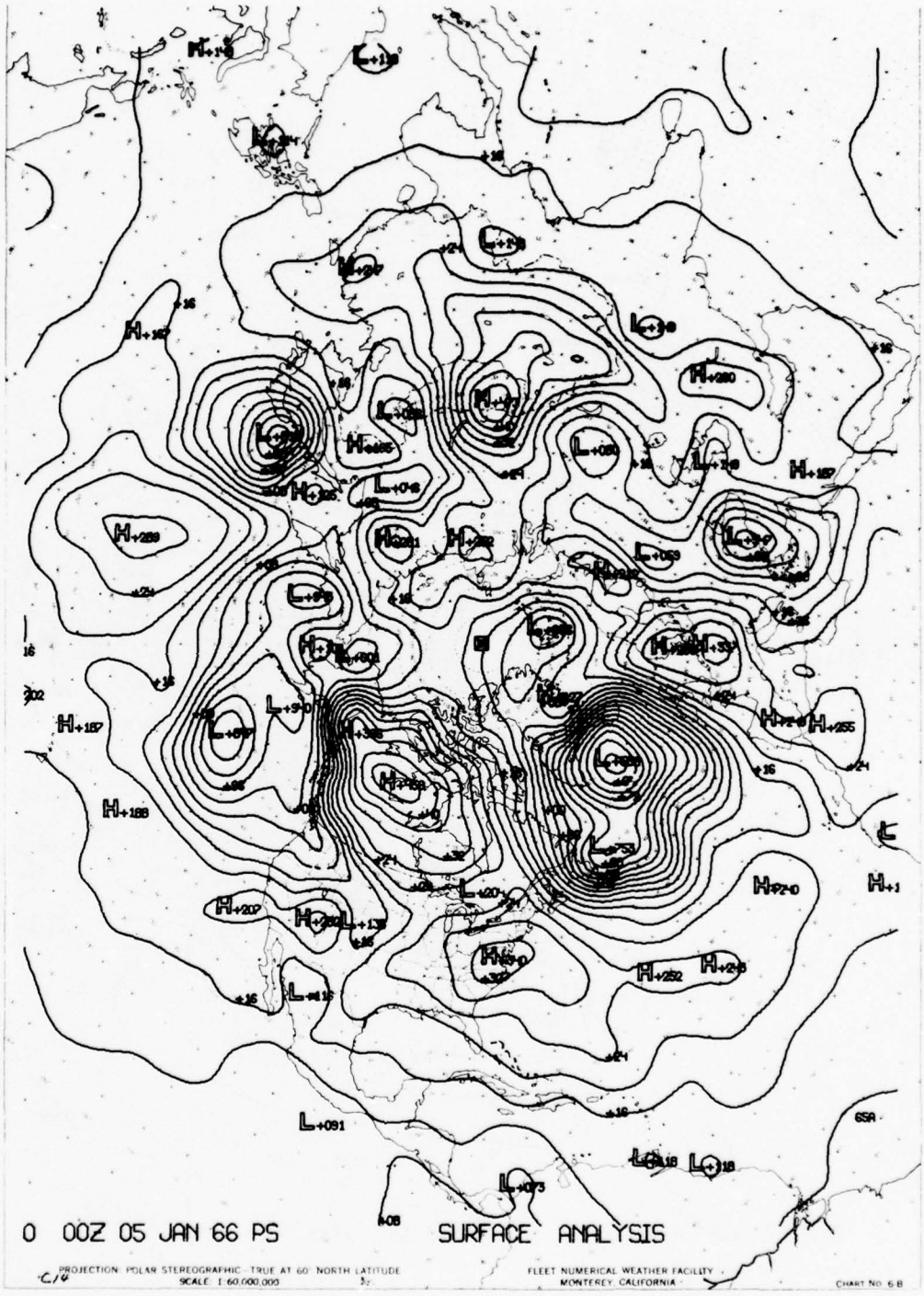


FIGURE C.14 SURFACE PRESSURE ANALYSIS FOR 0000Z 5 JANUARY 1966.

APPENDIX D

BASIC EQUATIONS FOR THE HYDRODYNAMICAL NUMERICAL MODEL

The derivation of vertically integrated hydrodynamical equations and their finite difference forms is described by several authors listed in the References of Section 5.15. Professor Walter Hansen, University of Hamburg, is the principal contributor to the mathematical formulations in the HN model.

The following basic hydrodynamical equations are used in the single layer model:

$$\frac{\partial u}{\partial t} - fv - \nu\nabla^2 u + \frac{r}{H}\, u\sqrt{u^2+v^2} + g\frac{\partial \zeta}{\partial x} = X + \frac{\tau^{(x)}}{\rho H} \tag{1}$$

$$\frac{\partial v}{\partial t} + fu - \nu\nabla^2 v + \frac{r}{H}\, v\sqrt{u^2+v^2} + g\frac{\partial \zeta}{\partial y} = Y + \frac{\tau^{(y)}}{\rho H} \tag{2}$$

$$\frac{\partial \zeta}{\partial t} + \frac{\partial}{\partial x}\left(H_u\right) + \frac{\partial}{\partial y}\left(H_v\right) = 0 \tag{3}$$

Equations (1) and (2) are vertically integrated equations of motion, and Equation (3) is an equation of continuity.

$\tau^{(x)}$ and $\tau^{(y)}$ (wind stress) are usually expressed as:

$$\tau^{(x)} = \lambda\, W_x \sqrt{W_x^2 + W_y^2} \tag{4}$$

$$\tau^{(y)} = \lambda\, W_y \sqrt{W_x^2 + W_y^2} \tag{5}$$

The bottom stress (friction) $\tau^{(b)}$ in formulas (1) and (2) is:

$$\frac{r}{H}\, u\sqrt{u^2+v^2} \quad ; \quad \frac{r}{H}\, v\sqrt{u^2+v^2} \tag{6}$$

Analytical solutions to Eqs. (1) to (3) are of little value, as exact solutions are possible only for basins with regular shape and constant depth and wind distributions. Recourse must be to an explicit method for achieving time-dependent solutions to these formulas using a finite difference approach. The finite difference approximations for Equations (1) to (3) are:

$$\zeta^{t+\tau}(n,m) = \overline{\zeta}^{\,t-\tau}(n,m) - \frac{\tau}{\ell}\Big\{H_u^t(n,m)\,U^t(n,m) - H_u^t(n,m-1)\,U^t(n,m-1) + H_v^t(n-1,m)\,V^t(n-1,m) - H_v^t(n,m)\,V^t(n,m)\Big\} \tag{7}$$

$$U^{t+2\tau}(n,m) = \left\{1 - \left[2\tau r / H_u^{t+2\tau}(n,m)\right] \sqrt{\overline{U}^t(n,m)^2 + V^{*t}(n,m)}\right\} \overline{U}^t(n,m)$$
$$- 2\tau f V^{*t}(n,m) - \frac{\tau g}{\ell}\left\{\zeta^{t+\tau}(n,m+1) - \zeta^{t+\tau}(n,m)\right\} + 2\tau X^{t+2\tau}(n,m) \quad (8)$$

$$V^{t+2\tau}(n,m) = \left\{1 - \left[2\tau r / H_v^{t-2\tau}(n,m)\right] \sqrt{\overline{V}^t(n,m)^2 + U^{*t}(n,m)^2}\right\} \overline{V}^t(n,m)$$
$$+ 2\tau f U^{*t}(n,m) - \frac{\tau g}{\ell}\left\{\zeta^{t+\tau}(n,m) - \zeta^{t+\tau}(n+1,m)\right\} + 2\tau Y^{t+2\tau}(n,m) \quad (9)$$

where

ρ	=	density
x,y	=	space coordinates
t	=	time
u,v	=	components of velocity
h	=	initial depth (when $\zeta = 0$)
ζ	=	surface elevation
H	=	total depth ($H = h + \zeta$)
H_u, H_v	=	depths at u and v points respectively
X,Y	=	components of external forces
$\tau^{(x)}, \tau^{(y)}$	=	components of wind stress
g	=	acceleration of gravity
f	=	Coriolis parameter
r	=	friction coefficient (bottom stress)
ν	=	coefficient of horizontal eddy viscosity
∇^2	=	Laplacian
λ	=	coefficient of friction (drag coefficient)
W_x, W_y	=	wind speeds
$\tau^{(b)}$	=	bottom stress
n,m	=	coordinates of the grid point
τ	=	halftime step
ℓ	=	grid length

in finite difference equations

The averaged velocity and water elevation (sea level) components are:

$$\overline{U}^t(n,m) = \alpha\, U^t(n,m) + \frac{1-\alpha}{4}\left\{U^t(n-1,m) + U^t(n+1,m) + U^t(n,m+1) + U^t(n,m-1)\right\} \quad . \qquad (10)$$

$\overline{V}^t(n,m)$ and $\overline{\zeta}^t(n,m)$ are analogous to $\overline{U}^t(n,m)$ above. (The factor α can be interpreted as a "horizontal viscosity parameter". Its normal value is 0.99.

$$U^{*t}(n,m) = \frac{1}{4}\left\{U^t(n,m-1) + U^t(n+1,m-1) + U^t(n,m) + U^t(n+1,m)\right\} \quad . \qquad (11)$$

$V^{*t}(n,m)$ is analogous to the $U^{*t}(n,m)$ above. The time step is 2^τ. The total depth (H_u, H_v) is computed as:

$$H_u^{t+2\tau}(n,m) = h_u(n,m) + \frac{1}{2}\,\zeta^{t+\tau}(n,m) + \zeta^{t+\tau}(n,m+1) \quad . \qquad (12)$$

The effects of wind (external force) are computed with the following formula:

$$X^t = \frac{\lambda\, W_x^t \sqrt{\left(W_x^t\right)^2 + \left(W_y^t\right)^2}}{H} - \frac{1}{\rho r}\,\frac{\partial P_o}{\partial x} \qquad (13)$$

$$Y^t = \frac{\lambda\, W_y^t \sqrt{\left(W_x^t\right)^2 + \left(W_y^t\right)^2}}{H} - \frac{1}{\rho r}\,\frac{\partial P_o}{\partial y} \quad . \qquad (14)$$

In small-area computations the pressure gradient term is usually neglected.

The maximum length of the time step is determined by the grid length and maximum depth found in the area according to the Courant-Friedrichs-Lewy criterion:

$$0.5\Delta t \leq \frac{0.5\,\ell}{\sqrt{2gH_{max}}} \qquad (15)$$

where Δt is time step (sec); ℓ is grid length (cm); g is acceleration of gravity; and H_{max} is the maximum depth in the area of computation (cm). Any attempt to increase the time step above the criterion has resulted in the "blow up" of computations (computational instability).

If the computational area contains only a relatively small section of greater depths, a "false bottom" can be assumed in these areas (e.g., areas > 500m can be assumed to be 500m deep). This will often result in a considerable increase in the time step, or a decrease of the grid length if total computation time is a critical factor. Experiments have shown that the error introduced with the above procedure is, in most cases, acceptable for practical applications of the model.

The principal forcing function for the HN model is the tides at the open boundary points. Predicted tides are generated along the open boundary for each time step using the following equation:

$$R = A_o + \sum_{n=1}^{N} f_n A_n \cos\left[a_n t + \left(V_o + U_n\right) - K_n\right] \qquad (16)$$

where, R = height of the tide at any time,

A_o = mean height of water level above datum line,

A_n = amplitude of the nth amplitude,

f_n = factor for reducing amplitude A_n to year of predictions,

a_n = speed of the nth constituent,

t = time calculated from initial epoch such as beginning of predictions,

$\left(V_o + U_n\right)$ = value of equilibrium of the nth constituent when $t = 0$,

K_n = epoch of the nth constituent.

The terms f_n and $\left(V_o + U_n\right)$ are only used when the user is interested in applying the HN model to a specific time period and can be found in U. S. Coast and Geodetic Survey (now known as National Ocean Survey) Special Publication 98. The values of A_n are also found in this publication.

Normally, the calculations are begun when t equals zero; however, the calculations can be begun at any time.

In practice only the principal tidal constituents, M_2, S_2, O_1 and K_1 are used in the computations since the amplitudes of the other constituents are usually quite small in magnitude and will not significantly alter the calculations.

APPENDIX F

OCEAN SURFACE CURRENTS

(a) Wind Effect Component C_W

The wind effect component for the ocean surface current Tau = 0, $C_{W(0)}$, is computed using the surface wind derived from the FNWC sea-level pressure analysis. The wind effect component for Tau = 24, $C_{W(24)}$, is computed using the surface wind derived from the FNWC P.E. sea-level pressure 24-hour prognosis.

(1) Speed

$$C_w = K\sqrt{W} \qquad (1)$$

where C_w = current speed in cm sec^{-1},

W = surface wind speed in m sec^{-1},

K = 4.2.

The constant K is adjusted to include mass transport by waves.

(2) Direction:

$A = 45.0 - 4.0\sqrt{W}$ for $0 \leq W \leq 25$ m sec^{-1}

$A = 0$ for $W > 25$ m sec^{-1}

A = amount the surface wind direction is rotated to the right to obtain current direction of the wind-effect vector.

(b) Thermal Effect Component, C_T

The thermal effect component, C_T, as computed from the surface and 600-ft temperature analyses, is used in the derivation of both the surface current analysis and 24-hour prognosis.

$$\overline{T} = K_1 T_0 + K_2 T_{600} \qquad (3)$$

where $\overline{T}$ = mean temperature of the surface to 600-ft layer,

T_0 = sea-surface temperature,

T_{600} = temperature at 600 ft,

K_1 = .585,

K_2 = $1 - K_1$.

Using $\overline{T}$, the thermal wind equation is applied to obtain the "permanent flow" component of the surface circulation.

$$u = -\frac{gz}{f\overline{T}}\frac{\partial \overline{T}}{\partial y} \tag{4}$$

$$v = \frac{gz}{f\overline{T}}\frac{\partial \overline{T}}{\partial x} \tag{5}$$

where u = current speed of the u component (parallel to I axis),

v = current speed of the v component (parallel to J axis),

z = 600 ft,

g = acceleration due to gravity,

f = coriolis parameter.

The horizontal temperature gradients in Equations (4) and (5) are found using the 4-point central difference approximation:

$$\left(\frac{\partial \overline{T}}{\partial x}\right)_{i,j} = K_3\left(\overline{T}_{i-2,j} - K_4\,\overline{T}_{i-1,j} + K_4\,\overline{T}_{i+1,j} - \overline{T}_{i+2,j}\right) \tag{6}$$

and similarly for $\frac{\partial \overline{T}}{\partial y}$

where $K_3 = 1/12$,

$K_4 = 8$

$$C_T = \sqrt{u^2 + v^2} \quad . \tag{7}$$

(c) The total surface current C is the resultant of combining C_w and C_T, vectorially:

$$C_{(0\ tau)} = C_{w(0)} + C_T \tag{8}$$

$$C_{(24\ tau)} = C_{w(24)} + C_T \quad . \tag{9}$$

(d) To obtain a nondivergent stream function, which is a single continuous field displaying both direction and speed, an analysis is made of the stream function, ψ, by solving the following by relaxation:

$$\nabla^2\psi = \frac{\partial v}{\partial x} - \frac{\partial u}{\partial y} \quad . \tag{10}$$

APPENDIX G

SYSTEMATIC ERRORS IN FNWC PRIMITIVE EQUATION MODEL PROGNOSES (APRIL 1973)

Systematic discrepancies/errors in the P.E. 500 mb and surface prognoses have been documented. These problem areas along with plans for implementing changes to overcome the errors are presented.

1. Phase-Speed

a. Error. It has been observed from inspection of the P.E. surface and 500 mb forecasts for periods 12 to 72 hours that the phase-speed of the shorter wavelength synoptic waves is less than that of the observed waves. This phase-speed error is more noticeable the shorter the wavelength and is not evident in the "long-waves" of the atmosphere as represented by the "SR-charts". Errors in phase-speed are one of the mathematical problems associated with using finite-difference equations to approximate differential equations. The usual formulations used in dynamic meteorology are 2nd-order finite difference schemes. Typical SD features have a phase-speed that is about 15% slower than real waves of the same wavelength. This spatial truncation error is believed to be the main cause of the phase-speed errors in the P.E. model. Long wave features, however, do not have any significant phase-speed error due to the mathematical formulation, and this is well verified by the lack of these errors in the P.E. model. An investigation covering this subject over the Pacific Ocean and North America seemed to verify the spatial truncation error for the Pacific, but there are other effects and errors present over North America. These extra errors must be associated with the interactions of the P.E. model and the underlying surface; i.e., mountains and heat exchange processes. A second study was conducted where the performance of the P.E. model was evaluated over a period of six months. One of the results noted was the slowness of the motion of synoptic waves.

b. Correction. Spatial truncation error is a function of the order of the finite difference scheme, and of the size of the grid mesh length used. Hence, two approaches are possible. The obvious is to reduce the mesh size. If the mesh size is reduced by 1/2, the error would be expected to drop to about 5% for a second order finite difference scheme and to about 1% with a fourth order scheme. Alternatively, for the same mesh size as used at present, a fourth order scheme should give about 6% error. The change in mesh size is costly in computing power since the computational time step must now be adjusted from its present ten minutes to five minutes, the number of points to be calculated increases by a factor of 4 and the memory requirement of the computer system is correspondingly increased. The net result is either eight times as long to run to a given forecast time or use a computer eight times as fast. Neither of these is possible in the present situation so that the alternate scheme has been attempted. This is to change the 2nd-order scheme to a 4th-order scheme in certain equations wherein the meteorological mode is affected or change the model everywhere to a 4th-order scheme wherein both meteorological and computational modes are affected. Both of these schemes were attempted in 1972 and gave nonmeteorological results in the tropics and sub-tropics and did not appear to produce consistent phase-speed error corrections in mid-latitudes. The matter has been held in abeyance until recently. Fourth-order schemes are again being tested in the model with some changes in the computing scheme. If a more consistent result is achieved then consideration will be given to using this change operationally. It is noted that using 4th-order schemes exacts a penalty. A partial 4th-order scheme decreases the time step by 17% and a complete 4th-order scheme by 33%, both resulting in a longer running operational model. Whether this can be tolerated has not been determined at present. FNWC is concurrently working on averaging of pressure gradient terms as has been done at NMC, in hopes of at least recovering the ten-minute time step.

2. Cyclogenesis and Precipitation

a. Error. The P.E. has always been considered to be among the best in forecasting rapid cyclogenesis especially over the western ocean areas. This skill is due, in part, to the complex precipitation mechanism in the model. The mechanism is composed of two effects; large-scale precipitation due to synoptic scale vertical motion and Arakawa type small-scale parameterized cumulus convection and precipitation. It is this latter type of mechanism that aids in producing the excellent cyclogenesis and

precipitation forecasts. Monthly mean charts show that the P.E. model has little net bias overall, but that certain areas show a consistent bias from month to month. One such area is Northern Eurasia where the surface forecasts at 24 and 48 hrs are consistently low. Another such biased area at 500 mb is that of the Himalayan plateau.

b. Correction. There are no tuning factors that can be adjusted per se to adjust the model for these effects. Certain physical constants, however, are not exactly known and can be modified in some cases to produce modified results. One way to adjust the deepening rate is to change the coefficient of drag, C_D, at the earth interface, but the effects are difficult to evaluate in single test runs. Operational forecasts of at least 30 model days or so should be required to check the net effect of a single such adjustment. Another method is to modify the amount of precipitation for a given amount of available convective energy. Again this effect is difficult to evaluate, and would require 30 model days of testing for each such adjustment. It is planned to modify the coefficient of drag formulation to represent the differences between land and sea in a better fashion until such time as the new planetary boundary layer modeling of this effect is completed.

3. Anti-cyclogenesis of Eastern ocean sub-tropical highs and cyclogenesis of mid and Western ocean sub-tropical lows

a. Error. The high pressure cells undergo excessive anti-cyclogenesis during the first twelve hours of a P.E. forecast and result in pressures that are about 4 mbs high. The principal effect is to tighten the gradient on the southern side of the highs such that the geostrophic winds are about 10 to 15 kts too high in the NE trade wind region. These excessive winds consistently generate too high waves/swell in the wave model and cause corresponding problems in OTSR operations. The lows undergo excessive cyclogenesis during the entire forecast period but usually during the first 36 to 42 hours. Kona lows are representative of this type of development. However, the forecast frequently fails and no low develops at all. A similar condition occurs in the Southern Caribbean. Both of these conditions generate excessive winds and resulting seas.

b. Correction. The cause of this effect has not been determined. It is believed to be associated with the artificial boundary that exists in the model between the areas wherein diabatic effects are calculated and not calculated. The boundary is presently set at 17.5°N LAT. It is believed that to the north of this boundary diabatic effects cause a net pressure increase in the sub-tropical highs (on a net decrease in the lows) while there is no such effect to the south. The result is a tightening of the gradient across this boundary. The sought for correction is to move the boundary sufficiently far southward that the net gradient increase will occur in a region of flat gradient or in the restoration boundaries of the model. This is being tested now. An alternate procedure is being tested wherein the surface forecast field is blended with the original analysis in the zone from 15° to 30° latitude. This results in a reversion to persistence for this region for the entire forecast period.

4. Thermal lows in Western continents

a. Error. The P.E. model frequently retrogrades thermal lows in these regions toward the West and SW resutling in too strong northerly winds over the adjacent ocean west of the low and weak winds on the coast. The resultant wave forecasts are also in error.

b. Correction. It is believed that two effects contribute to this problem. The present nominal mesh size of 381 km does not allow the proper specification of land/sea contrasts and effects. Secondly, terrain that is used is a smoothed version especially prepared for use in the P.E. model. The process of removing 2 and 3 mesh length features from the terrain field smears the terrain over the water areas and creates a shoreline different than the real one. Hence land/sea effects occur in unreal locations. The terrain effect can be minimized through very specialized treatment of the terrain field. Experiments are under way in this direction. As an interim measure, coastlines have been reestablished in their correct locations as far as the mesh size allows.

5. Excessive cyclogenesis in the Mediterranean Basis

a. Error. When the mean flow from 1000 to 500 mb is approximately at right angles to the east-west orientation of the Alps and Pyrenees mountains, excessive cyclogenesis frequently occurs in this area.

b. Correction. There is no correction readily available. The basic cause is due to the small width of these mountains and the inability to resolve this topography with the present grid dimensions. Parameterization of topographical sub-grid effects and reduction of grid size will eventually resolve this aspect of this problem.

6. Forecast skill relative to persistence

a. Error. The P.E. model RMS errors gradually increase with time but in a different manner than those due to assuming that persistence is the correct forecast. The result is that the P.E. model has its greatest skill relative to persistence at about 24 hours and thereafter slowly decreases. The P.E. model still has significant skill at 72 hours which is the limit to which forecasts are now produced operationally. Extrapolating the curves indicates that 96 hour (4 day) forecasts would still possess some operationally useable skill, and that the present limiting forecast might be about five days.

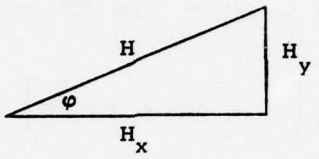
b. Correction. Improvement to longer periods of time depends on developing a global model to remove boundary effects, better initialization procedures to minimize model starting trauma, better physics at the interface and in the tropics, reduction of truncation errors by finer meshes and better computational procedures. All of these corrections are being investigated and as they prove feasible, they will be incorporated into the operational stream.

APPENDIX H
WAVE ANALYSIS AND PROGNOSIS
(GLOBAL BAND SINGULAR ADVECTIVE WIND-WAVE/SWELL MODEL)

The equations used in the Global Band Sea/Swell model will be described in flow-chart order of computation steps.

Propagation

The height and the direction in which waves are moving defines a vector.



H_x = $H \cos \varphi$

H_y = $H \sin \varphi$

$\bar{c}$ = mean speed of propagation in knots

= $\frac{gT}{4\pi} \approx 1.515\,T$, where T is period in seconds.

The advection equations are:

$$H_{x_i}^{(t+\Delta t)} = H_{x_i}^{(t)} \mp \frac{\bar{c}\,\Delta t}{d} \left[H_{x_i} - H_{x_{i\mp 1}} \right]^{(t)}$$

where $d = \Delta x$ or distance.

$$H_{y_j}^{(t+\Delta t)} = H_{y_j}^{(t)} \mp \frac{\bar{c}\,\Delta t}{d} \left[H_{y_j} - H_{y_{j\mp 1}} \right]^{(t)} .$$

$$H^{(t+\Delta t)} = \left[\left(H_x^{(t+\Delta t)} \right)^2 + \left(H_y^{(t+\Delta t)} \right)^2 \right]^{1/2} .$$

Dissipation

$$H_d = H_a \left\{ 1 - \frac{\Delta\varphi}{\pi} - \frac{\sin \Delta\varphi}{\pi} \right\} ,$$

where $\Delta\varphi = |\varphi_w - \varphi_a| \leq \pi$,

φ_w = current wind direction,

φ_a = direction of propagated waves,

H_d = wave height after dissipation, and

H_a = wave height after advection.

The fraction of the propagated energy retained is:

$$\frac{2}{\pi} \int_{-\frac{\pi}{2}+\frac{\Delta\varphi}{2}}^{\frac{\pi}{2}-\frac{\Delta\varphi}{2}} \cos^2 \theta d\theta =$$

$$\frac{1}{\pi}\left[\pi - \Delta\varphi + 2 \sin \frac{\Delta\varphi}{2} \cos \frac{\Delta\varphi}{2}\right]$$

$$= \frac{1}{\pi}\left[\pi - \Delta\varphi + \sin \Delta\varphi\right]$$

$$= 1 - \frac{\Delta\varphi}{\pi} + \frac{\sin \Delta\varphi}{\pi} \quad .$$

Growth

1. $$H_f = 7\left[\left(\frac{V}{19}\right)^2 - \left(\frac{V}{39}\right)^{3.3}\right] + 1 \quad ,$$

where H_f = fully developed height in feet, and

V = wind speed in knots.

2. If $$H_d \geq H_f \quad ,$$

wind waves have stopped growing:

$$H_g = H_d \quad .$$

3. If $$H_d < H_f \quad ,$$

wind waves are still growing:

$$H_g = H_d + \alpha\left(H_f - H_d\right)$$

where $0 < \alpha(V) \leq 1$, and

α = empirical coefficient.

Gross Error Check

$$H_{min} \leq H_{reported} \leq H_{max} ,$$

where

$$H_{max} = 7\left[\left(\frac{V}{19}\right)^2 - \left(\frac{V}{39}\right)^{3.3}\right] + 7.5$$

and

$$H_{min} = \frac{V}{4} - 2 \quad \text{for} \quad V \leq 40$$

or

$$H_{min} = .7\,V - 20 \quad \text{for} \quad V > 40 .$$

(H in feet, V in knots)

Test of Swell as Wind Wave

1. $|\varphi_{sw} - \varphi_{ww}| \leq 30°$

2. $H_{sw} > H_{ww}$

3. H_{sw} passes all G. E. C.

Controlling Swell Decay

1. Computational stability requires that

$$0 \leq \frac{\bar{c}\,\Delta t}{d} \leq 1 .$$

2. Ideally, $\frac{\bar{c}\,\Delta t}{d} = 1$ (no decay) .

3. Damping is actually a function (in this model) of:
   a. Speed of propagation
   b. Mesh length (75-150 naut. mi.)
   c. Main direction of propagation
   d. Geographical extent of swell

APPENDIX I

SEA-LEVEL PRESSURE ANALYSIS (FIB)

The Sea-Level Pressure Analysis at FNWC is done by the Fields by Information Blending (FIB) method. The FIB analysis technique is comprehensive, and can be applied to any scalar or vector field. The FIB formulations for Sea-Level Pressure analysis will be presented here in order of use in the model, as described in Section 4.1.

The Arbitrary ℓ,m Area Module

FIB/SLP

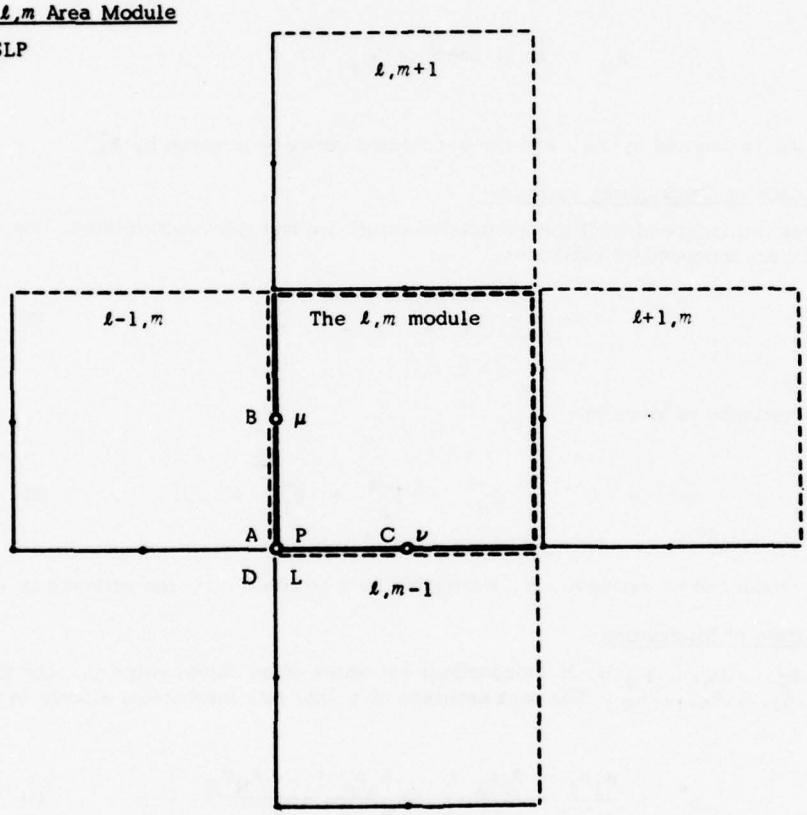


FIGURE I.1 The arbitrary ℓ,m area module (consisting of one corner point, two sides, and the interior area) and adjoining modules. Reference locations in the module are shown for the Sea-Level-Pressure parameter, $P_{\ell,m}$, and the finite-difference parameters:

$$\mu_{\ell,m} \Rightarrow P_{\ell,m+1} - P_{\ell,m} \; ; \; \nu_{\ell,m} \Rightarrow P_{\ell+1,m} - P_{\ell,m} \; ;$$

and $$L_{\ell,m} \Rightarrow P_{\ell+1,m} + P_{\ell,m+1} + P_{\ell-1,m} + P_{\ell,m-1} - 4\,P_{\ell,m}$$

The respective reliabilities of P, μ, ν, and L values are denoted by A, B, C and D; the reliability of a value is defined as the inverse of the error variance associated with the value.

Definitions and Rules

1. Weight or Reliability

Let p_n be an independent measurement of sea-level pressure. Let σ_n be the standard deviation associated with this measurement. The variance is σ_n^2. The weight or reliability of the information expressed by the estimate is defined as the inverse of the variance:

$$A_n \equiv 1/\sigma_n^2 \quad . \tag{1}$$

Let μ_m denote an estimate of the finite difference in pressure between two locations, m and $m+1$:

$$\mu_m \Rightarrow \text{an estimate of } p_{m+1} - p_m \quad . \tag{2}$$

The weight of μ_m is denoted by B_m, and the associated variance is given by B_m^{-1}.

2. Addition of Contributing Variances

Estimates are independent if the associated errors are mutually uncorrelated. For a linear combination of such independent estimates,

$$p = p_o \pm \mu_1 \pm \mu_2 \pm \ldots \quad , \tag{3}$$

the associated variance is given by

$$\sigma^2 \equiv A^{-1} = A_o^{-1} + B_1^{-1} + B_2^{-1} + \ldots \quad . \tag{4}$$

For the product of an estimate, p, multiplied by a constant, c, the variance is $c^2\sigma^2$.

3. Addition of Information

Let $p_1, p_2, \ldots p_n, \ldots p_N$ be N independent estimates of an object value p. Let the respective weights be $A_1, A_2, \ldots A_n, \ldots A_N$. The best estimate of p that this information affords is expressed by

$$p^* = \frac{A_1p_1 + A_2p_2 + \ldots A_np_n + \ldots A_Np_N}{A_1 + A_2 + \ldots A_n + \ldots A_N} \quad . \tag{5}$$

The weight is expressed by

$$A^* = A_1 + A_2 + \ldots A_n + \ldots A_N \quad . \tag{6}$$

This assimilation can be performed sequentially, saving only the accrued value and its growing weight. The result is independent of the order of assimilation.

4. Removal of Information

The contribution of a piece of information, p_n of weight A_n, which has already been assembled into a resultant, p^* of weight A^*, can be removed by subtraction:

$$p_B = \frac{A^* p^* - A_n p_n}{A^* - A_n} \tag{7}$$

$$A_B = A^* - A_n \quad . \tag{8}$$

The information, p_B of weight A_B, represents the independent background (i.e., verifying) information relative to the nth report which had been assembled into the resultant.

For a report that was withheld from the assembly, the total resultant, p^* of weight A^*, represents the independent background information:

$$p_B = p^* \quad , \quad A_B = A^* \quad . \tag{9}$$

The background information may be used to reevaluate or reject any piece of information.

5. First-Guess Field Preparation

1. Combination of Previous Analyses

Grid-point pressure values are first interpolated from the previous tropical analysis at each hemispheric grid point within the tropical grid (i.e., south of 60°N latitude). A weighted combination of the tropical interpolated and hemispheric values is made by the formula

$$p_o = wp_t + (1-w)\, p_h \tag{10}$$

where $w = 0.86 - \sin\varphi$, $(0 \leq w \leq 1)$,

φ is latitude,

p_h is the hemispheric grid point pressure value,

p_t is the interpolated tropical value, and

p_o is the resulting weighted value.

The formula gives a weight to the tropical value of zero at 60°N, 0.36 at 30°N, 0.86 at the equator and 1.0 from 8°S to the corners of the grid (19°S).

Use of the tropical analysis provides continuity with southern hemisphere data and, implicitly, with climatological information.

2. Prognostic Field

The FNWC P.E. surface pressure forecast is used, in combination with the previous analyses, above. The prognostic portion is weighted as a function of the sine of latitude so that in southern latitudes the extrapolated field carries more weight. The total weight of this field A_o increases from 0.001 at the north pole to 0.01 south of the equator.

6. Higher Derivative Fields

From the first-guess pressure field computed above, the first-guess finite difference (μ_o, ν_o) and the Laplacian (L_o) are calculated from the formulas in Fig. I.1. The weights are B_o, C_o, and D_o. B_o and C_o are computed as constant factors of D_o.

The second difference fields are computed from:

$$\hat{\mu}_{\ell,m} = p_{\ell,m+1} + p_{\ell,m-1} - 2p_{\ell,m} \quad , \tag{11}$$

$$\hat{\nu}_{\ell,m} = p_{\ell+1,m} + p_{\ell-1,m} - 2p_{\ell,m} \quad . \tag{12}$$

The second difference weights are denoted by $F_{\ell,m}$.

The cross difference is defined by the parameter

$$\gamma_{\ell,m} = p_{\ell+1,m+1} + p_{\ell,m} - p_{\ell+1,m} - p_{\ell,m+1} \quad , \tag{13}$$

The weight is $K_{\ell,m}$.

The Laplacian, second differences, and the cross difference are the spreading parameters.

7. Assembly of New Information

1. Pressure Reports

Pressure reports are extrapolated to the nearest grid point, which is found by rounding the exact i,j coordinates to the nearest integers. The extrapolation formula is

$$p_{\ell,m} = \left(p_o\right)_{\ell,m} + \left(p_n - p_o\right)_{i,j} \tag{14}$$

where $p_{\ell,m}$ is the extrapolated pressure at grid point (ℓ,m), $(p_o)_{\ell,m}$ is the guess value at the grid point, $(p_n)_{i,j}$ is the reported value at station location (i,j), and $(p_o)_{i,j}$ is the guess value interpolated at the station location using a 16-point operator.

The maximum allowable difference between the report and first guess increases with the magnitude of the gradients in the vicinity of the report and with latitude. The report is considered a gross error and rejected if

$$\left| p_n - p_o \right|_{\ell,m} > f_2 + f_3 \left| \overline{g} \right|_{\ell,m} + f_4 (1 - \cos\varphi) \quad , \tag{15}$$

where $\left| \overline{g} \right|_{\ell,m}$ is the mean absolute gradient in the surrounding grid points, φ is latitude ($\leq 60°$) and f_2, f_3 and f_4 are adjustable constants. In any area of strong gradients, north of 60°N latitude, the allowable tolerance may reach 30mb.

The reliability of a pressure report decreases with the magnitude of gradients in the vicinity of the report, with elevation, and with age. In terms of variance

$$\sigma_n^2 = f_5 + f_6 \overline{g^2}_{\ell,m} + f_7 E^2 + \left(f_8 + f_9 \overline{g^2}_{\ell,m}\right) H^2 \quad , \tag{16}$$

where σ_n^2 is the total variance of the pressure report, $\overline{g^2}_{\ell,m}$ is the mean square gradient surrounding the report, E is elevation, H is age and f_5 through f_9 are adjustable constants. The class of report is represented in f_5. The age term does not affect the intrinsic variance of a report, but does reduce its weight for assembly purposes. The weight, or reliability, of the report is $A_n = \sigma_n^{-2}$ where n refers to a single (unassembled) reliability. If several reports are received from the same station, their individual weights must be reduced since they are not independent information--their total weight should be A_n.

The assembled value of pressure at a grid point is a weighted mean of all data referred to the grid point, with each value contributing to the mean in accordance with its reliability. Such a weighted mean can be derived one report at a time, independent of assembly order, by

$$P_N = \left(P_{N-1} A_{N-1} + P_n A_n\right) / \left(A_{N-1} + A_n\right) \tag{17}$$

$$A_N = A_{N-1} + A_n \tag{18}$$

where p_n, A_n refer to a single report and P_N, A_N refer to the assembly of N reports.

2. Wind Reports

In order to use a report of wind direction and speed, conversion must first be made to components of pressure finite differences along the grid coordinates by an appropriate balance equation. The balance equation is written in vector form as

$$\mathbb{V} \cdot \nabla \mathbb{V} + f\,\mathbb{k} \times \mathbb{V} + \varkappa \mathbb{V} = f\,\mathbb{k} \times \mathbb{V}_g \tag{19}$$

where $\mathbb{V}_g$ is the geostrophic wind, $\mathbb{V}$ is the actual wind, $\mathbb{k}$ is the unit vertical vector, $\varkappa$ is a frictional parameter, and f is the coriolis parameter. Local accelerations of the wind are omitted. The frictional effect on the surface wind is contained in the $\varkappa$ term. In component form the geostrophic wind may be written as

$$\begin{aligned} u_g &= R\left(u + \frac{\varkappa}{f} v\right) + \frac{1}{f}\left[u\left(\frac{\partial v}{\partial x}\right)_{g,o} + v\left(\frac{\partial v}{\partial y}\right)_{g,o}\right] , \\ v_g &= R\left(v - \frac{\varkappa}{f} u\right) - \frac{1}{f}\left[u\left(\frac{\partial u}{\partial x}\right)_{g,o} + v\left(\frac{\partial u}{\partial y}\right)_{g,o}\right] , \end{aligned} \tag{20}$$

where the derivative subscripts refer to geostrophic wind components in the first-guess field (e.g., an analysis for the same time) and u,v are the reported winds in component form. Constant R has been added to increase the difference between the geostrophic and actual velocities without increasing the inflow angle. This empirically accounts for the fact that, due to vertical momentum transfer, the frictional force is not directed exactly opposite the surface wind but rather opposite a direction somewhere between the surface and free flow.

The $\varkappa$ term allows for variations in roughness. It can be shown from Eq. (20), assuming negligible curvature, that $\varkappa = f \cdot \tan \alpha$ where α is the inflow angle of the surface wind. The value of $\varkappa$ is set for an approximate inflow angle of 12° over the sea and 22° over land.

The derivative terms are computed as four separate fields using a 16-point operator. The values of the derivatives are then determined for each report by interpolation to exact station location.

The final pressure finite difference values, μ_n and ν_n, are computed by applying the geostrophic wind equation to the u_g and v_g components found above, and solving for pressure differences over 1 grid length in the m and ℓ grid directions, respectively.

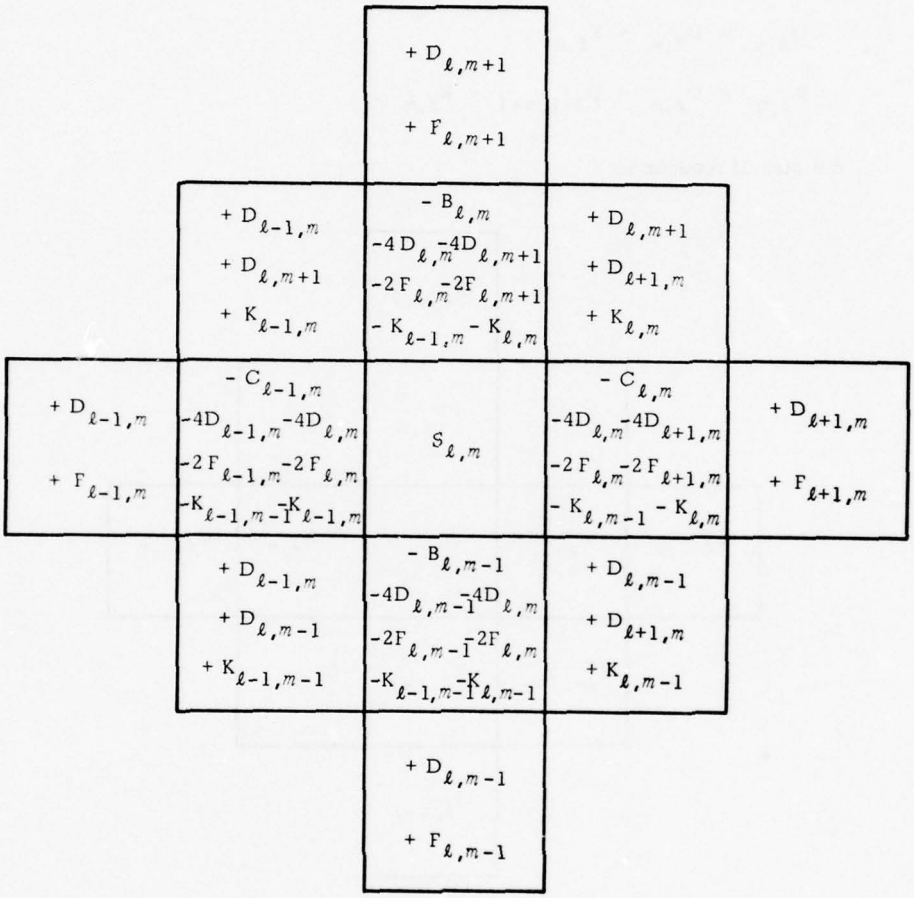
The variance of the wind report is

$$\sigma_n^2 = f_{10} \sin^2\varphi \left(\frac{1+\sin\varphi}{1.866}\right)^2 + f_6 \overline{g^2_{\ell,m}} + f_7 E^2 + \left(f_8 + f_9 \overline{g^2_{\ell,m}}\right) H^2 \quad (21)$$

where f_{10} is a class variance. The first term on the right is the "calm wind" variance. The $\sin^2\varphi$ portion is needed to convert from a wind variance to a variance in terms of pressure difference and the remainder of the term accounts for variation in grid spacing with latitude.

8. Blending for p*

When all data have been assembled into their respective fields, the program can blend the information into a best-fit p* field which minimizes the error functional. The requirement of minimizing the errors between the pressure field and its derivative fields at all grid points leads to the basic implicit blending equation. The implicit nature of the problem requires an iterative solution. Considerable computational simplification is possible by combining terms which are constant throughout the iteration or which are common multiples of the same p*. This leads to a forcing term which involves the starting fields only, and a sum term which concerns only p* at the grid point being solved. Other terms involve p* at surrounding grid points and can be grouped into a stencil operating on the p* field. The inclusion of second-difference and cross-difference fields requires additional terms. The total stencil is shown below:



The center box in the stencil refers to grid point (ℓ,m)--the box to the right of this contains all terms that are multiplied by p* one grid point to the right, or $p^*_{\ell+1,m}$, etc. The stencil is thus an operator on the p* field.

By transforming into the following fields:

$$X_{\ell,m} \equiv C_{\ell,m} + 4D_{\ell,m} + 4D_{\ell+1,m} + 2F_{\ell,m} + 2F_{\ell+1,m} + K_{\ell,m-1} + K_{\ell,m} ,$$

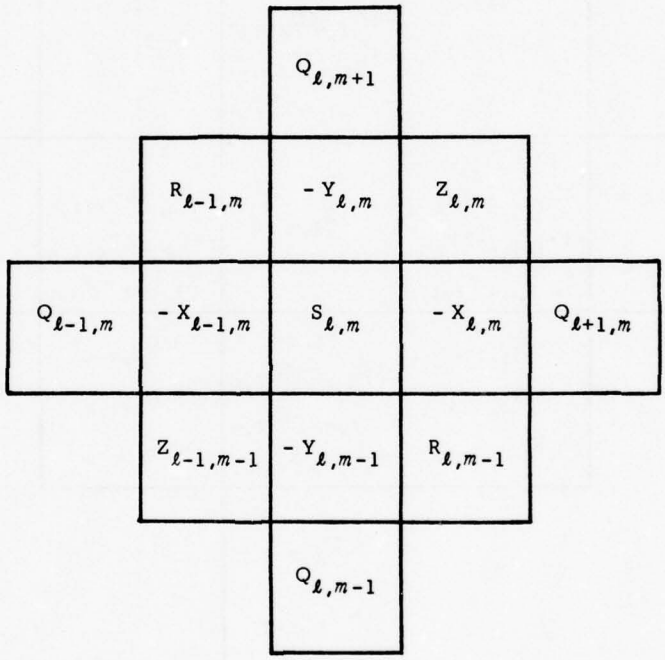
$$Y_{\ell,m} \equiv B_{\ell,m} + 4D_{\ell,m} + 4D_{\ell,m+1} + 2F_{\ell,m} + 2F_{\ell,m+1} + K_{\ell-1,m} + K_{\ell,m} ,$$

$$Z_{\ell,m} \equiv D_{\ell,m+1} + D_{\ell+1,m} + K_{\ell,m} ,$$

$$Q_{\ell,m} \equiv D_{\ell,m} + F_{\ell,m} ,$$

$$R_{\ell,m} \equiv D_{\ell,m} + D_{\ell+1,m+1} + K_{\ell,m} ,$$

the stencil reduces to



or
$$p^*_{\ell,m} = \Big[G_{\ell,m} + Q_{\ell,m+1}\left(p^*_{\ell,m+2}\right) + R_{\ell-1,m}\left(p^*_{\ell-1,m+1}\right) - Y_{\ell,m}\left(p^*_{\ell,m+1}\right) + Z_{\ell,m}\left(p^*_{\ell+1,m+1}\right) + Q_{\ell-1,m}\left(p^*_{\ell-2,m}\right) - X_{\ell-1,m}\left(p^*_{\ell-1,m}\right) - X_{\ell,m}\left(p^*_{\ell+1,m}\right) + Q_{\ell+1,m}\left(p^*_{\ell+2,m}\right) + Z_{\ell-1,m-1}\left(p^*_{\ell-1,m-1}\right) - Y_{\ell,m-1}\left(p^*_{\ell,m-1}\right) + R_{\ell,m-1}\left(p^*_{\ell+1,m-1}\right) + Q_{\ell,m-1}\left(p^*_{\ell,m-2}\right)\Big] / S_{\ell,m} \qquad (22)$$

The sum term is:

$$S_{\ell,m} = A_{\ell,m} + B_{\ell,m} + B_{\ell,m-1} + C_{\ell,m} + C_{\ell-1,m}$$
$$+ 16\,D_{\ell,m} + D_{\ell,m-1} + D_{\ell-1,m} + D_{\ell,m+1} + D_{\ell+1,m}$$
$$+ 8\,F_{\ell,m} + F_{\ell,m-1} + F_{\ell-1,m} + F_{\ell,m+1} + F_{\ell+1,m}$$
$$+ K_{\ell,m} + K_{\ell-1,m-1} + K_{\ell,m-1} + K_{\ell-1,m} \quad , \qquad (23)$$

and the forcing term is:

$$G_{\ell,m} = A_{\ell,m}\,p_{\ell,m} - B_{\ell,m}\,\mu_{\ell,m} + B_{\ell,m-1}\,\mu_{\ell,m-1} - C_{\ell,m}\,\nu_{\ell,m} + C_{\ell-1,m}\,\nu_{\ell-1,m}$$
$$-4D_{\ell,m}\,L_{\ell,m} + D_{\ell,m-1}\,L_{\ell,m-1} + D_{\ell-1,m}\,L_{\ell-1,m} + D_{\ell,m+1}\,L_{\ell,m+1} + D_{\ell+1,m}\,L_{\ell+1,m}$$
$$- 2F_{\ell,m}\,\hat{\mu}_{\ell,m} + F_{\ell,m-1}\,\hat{\mu}_{\ell,m-1} + F_{\ell,m+1}\,\hat{\mu}_{\ell,m+1}$$
$$- 2F_{\ell,m}\,\hat{\nu}_{\ell,m} + F_{\ell-1,m}\,\hat{\nu}_{\ell-1,m} + F_{\ell+1,m}\,\hat{\nu}_{\ell+1,m}$$
$$+ K_{\ell,m}\,\gamma_{\ell,m} + K_{\ell-1,m-1}\,\gamma_{\ell-1,m-1} - K_{\ell,m-1}\,\gamma_{\ell,m-1} - K_{\ell-1,m}\,\gamma_{\ell-1,m} \quad , \qquad (24)$$

where $\hat{\mu}$ and $\hat{\nu}$ are the second differences in the m and ℓ directions, and γ is the cross-difference. Thus, the blending operation requires eight 125x125 fields: X, Y, Z, Q, R, S, G and p*.

9. Computation of A*

The pressure reliabilities (A) assembled at each grid point represent only the reliability of the reports if they had no effect on each other, that is, if there were no blending or interaction between the grid points. The actual reliability of blended grid-point pressure values should always be greater than the assembled reliability to account for information propagated from surrounding grid points through gradient and higher-order information. For example, the reliability of a blended pressure value at a grid point with no assembled reports should be greater than the first-guess reliability if reports surround the grid point and if there is gradient knowledge.

The reliability field, A^*, to be associated with the field p^*, is the resultant of assembly and the highly non-linear blending of all weighted input information. It is dependent on all input weights but is completely independent of all input parameter values. The same reliability field would result if all input parameter values were zero--that is, if in Eq. (22) G is set identical to zero. This exact trivial solution of Eq. (22) is $p^* \equiv 0$. A perturbation technique is used to compute A^* at any one grid point by determining the change in the trivial solution which results from a change in the forcing term, G, at that grid point. At that grid point, G is changed from zero to $A_{\ell,m}\,p_{\ell,m} \neq 0$ but all other grid-point values of G are left at zero. The resulting new solution of the p^* field then yields

$$A^*_{\ell,m} = \frac{A_{\ell,m} p_{\ell,m}}{p^*_{\ell,m}} \quad . \tag{25}$$

Stated in words, if the assembled pressure change, $p_{\ell,m} \neq 0$, has small leverage and changes p^* only slightly from zero, then $p^*_{\ell,m}$ will be small and A^* will be much larger than A.

To obtain an exact solution of A^* it would be necessary at each grid point to re-solve for p^* over the entire field, given a fixed change of the one element (ℓ,m) in the forcing term. To keep the program computation time within reasonable limits, the re-solution is carried out only in the vicinity of the grid point (ℓ,m) as shown in Fig. I.2.

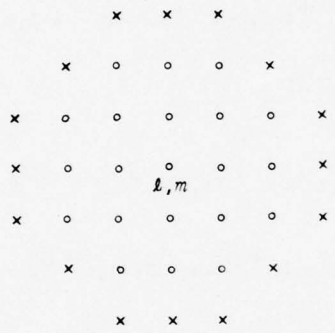


FIGURE I.2 Computational sub-area for $A^*_{\ell,m}$ indicated by (∘) grid points

Changes are made to p^* only at the (∘) points. At, and outside, the (×) points, no computation is performed when solving for A^* at grid point (ℓ,m). Holding p^* fixed at zero at the (×) points is the same as assuming infinite reliability at these points. The effect is to limit, somewhat, the change in $p^*_{\ell,m}$ and therefore overestimate A^*. This overestimation is noticeable only in data-sparse areas or when no information other than first-guess is found within the (×) points. In these situations, the computational area could be enlarged to include at least some minimum amount of assembled information. Computation of A^* extends to the grid boundaries. Points in the sub-area which are outside the grid do not affect the result since all weights extending across the boundaries have a value of zero.

The nine-row portions of the fields are sufficient for computing A^* along only one row, requiring 125 field exchanges. At each grid point (ℓ,m), p is changed in the forcing term only at (ℓ,m). Then p^* at all computation points is increased toward the expected result to speed convergence. The iteration for the modified p^* value is made through the area in a manner analagous to that used in the p^* blending.

(2)	5	3	1	(4)
1	4	2	5	3
5	3	1	4	2
4	2	5	3	1
(3)	1	4	2	(5)

FIGURE I.3 Subset labelling in the $A^*_{\ell,m}$ computational sub-area. Grid point (ℓ,m) is underlined.

In Fig. I.3, the #1 subset points are operated on first, then the #2 points, etc., through the #5 points. (The circled points are shown to complete the pattern only; no computations are made there.) This same pattern is repeated 4 times. Ordering within a subset is immaterial. In the last pass, the #5 point in the top row is skipped and a final computation is made at the center grid point (ℓ,m), underlined. (Note that the point skipped is not contained in the stencil for the center grid point.) $A^*_{\ell,m}$ may now be computed, knowing the $p_{\ell,m}$ applied to the forcing term, the $A_{\ell,m}$ value and $p^*_{\ell,m}$ computed.

No increase in the A^* computation area is attempted in data-sparse regions. It has been found that far-removed data have only a small effect on A^* which is nearly masked by the background reliability. This background reliability results from the higher-order derivatives which have small weight at individual grid points but which propagate over long distances.

The grid-point A^* values are needed in reevaluation which follows. In the first cycle of the program, A^* need be calculated only at data points, since the purpose of the first cycle is to evaluate the reports.

10. Reevaluation and Lateral Rejection

Knowledge of the blended pressure and resultant grid-point reliability enables the program to reevaluate, individually, any information that entered the analysis. By removing an individual datum value and its reliability from a grid point and comparing it with what remains, or the "background", the true reliability of the data may be quantitatively assessed.

Removal of a report from the blended fields is the exact reversal of assembly:

$$A_B = A^* - A_a \quad , \tag{27}$$

$$p_B = \left(A^* p^* - A_a p_n\right)/A_B \quad , \tag{28}$$

where p_n is the report that was assembled with weight A_a, and p_B is the background pressure, with weight A_B, that remains after removal of the report. The actual difference of these estimates is $p_n - p_B$ while the expected or standard difference is

$$\sigma_{n,B} = \left(A_n^{-1} + A_B^{-1}\right)^{1/2} \quad ,$$

where A_n is the true weight of the total report. (Expected difference must be based on true report weight; the assembled weight, A_a, is reduced from A_n when different values are reported from the same station, and when a report is off-time.) By squaring the actual and expected differences, the ratio may be expressed in terms of variance:

$$\lambda^2_{np} = \frac{A_B A_n}{A_B + A_n} \left(p_n - p_B\right)^2 \quad . \tag{29}$$

Some allowance may be made for disparity in position between p_n and p_B, accounting for the fact that reports occurring over a finite area must be expressed in a single grid-point value. This allowable disparity should be a function only of the gradient in the area of a grid point. If the λ^2 equation is

written in terms of blended values only, this allowance may be made by reducing the difference $(p_n - p^*)$ for a portion of the p* gradient. Substituting p* and A* in the λ^2_{np} equation:

$$\lambda^2_{np} = \frac{(A^* - A_a)A_n}{A^* - A_a + a_n}\left[p_n - \frac{A^* p^* - A_a p_n}{A^* - A_a}\right]^2 , \text{ or}$$

$$\lambda^2_{np} = \frac{A_n A^{*2}(p_n - p^*)^2}{(A^* - A_a + A_n)(A^* - A_a)} . \quad (30)$$

The mean square gradient per unit grid length around grid point (ℓ,m) is

$$\overline{g^2_{\ell,m}} = \left(\mu^{*2}_{\ell,m} + \mu^{*2}_{\ell,m-1} + \nu^{*2}_{\ell,m} + \nu^{*2}_{\ell-1,m}\right)/2 . \quad (31)$$

A reasonable position disparity to allow is the r.m.s. distance of a large population of reports from their respective grid points, or $(d^2/6)^{1/2}$, where d is the grid spacing. Then $\overline{g^2_{\ell,m}}$ should be weighted by the mean square distance in unit grid spacing, or 1/6.

The final equation for λ^2_{np} becomes

$$\lambda^2_{np} = \frac{A_n A^{*2}\left[(p_n - p^*)^2 - (\mu^2_{\ell,m} + \mu^2_{\ell,m-1} + \nu^2_{\ell,m} + \nu^2_{\ell-1,m})/12\right]}{(A^* - A_a + A_n)(A^* - A_a)} \geq 0. \quad (32)$$

The value of λ^2_{np} measures how accurate a pressure report actually is, as compared to its expected accuracy given by the reliability assigned to it. The median λ^2_{np} for all reports in the analysis should therefore be approximately 1.0, indicating a balance between reports with more error and reports with less error than expected. This offers a method for checking the assignment of class reliabilities to reports, which otherwise would be arbitrary.

The value of λ^2_{np} for a report can now be used for reevaluation. If $\lambda^2_{np} \leq 1$, the report is within its expected error and no change is made in its reliability. If $1 < \lambda^2_{np} < \lambda^2_{maxp}$, where λ^2_{maxp} is the maximum allowed λ^2 for a pressure report, the report is reevaluated by the formula

$$A_{nR} = \frac{2A_n}{1 + \lambda^2_{np}} \quad (33)$$

where R indicates reevaluation. Any report of $\lambda^2_{np} > \lambda^2_{maxp}$ is withheld from the final analysis cycle. Since this rejection is based on current information in the vicinity of the report, it may be termed a "lateral" reject as distinguished from the initial "gross error" reject.

Since blended difference reliabilities (B*, C*) are not produced, the reevaluation of wind reports must be done in a different manner. The expected variance of a wind report is approximately $1/B_n + \sigma_b^2$ where σ_b^2 is the variance added at the grid point for the balance approximation. (This is true only for a single wind report at a grid point since the balance variance is added only once, independent of the

number of reports.) The variance ratio for a wind report is

$$\lambda^2_{nw} = \frac{(\mu_n - \mu^*)^2 + (\nu_n - \nu^*)^2}{1/B_n + \sigma_b^2} \quad . \tag{34}$$

If $1 < \lambda^2_{nw} < \lambda^2_{maxw}$ the report is reevaluated:

$$B_{nR} = C_{nR} = \frac{1}{(1/B_n + \sigma_b^2)(1 + \lambda^2_{nw})/2 - \sigma_b^2} \quad . \tag{35}$$

The subtraction of σ_b^2 is necessary because it will be added back in the final assembly. As in the case of a pressure report, no change in reliability is made if $\lambda^2_{nw} \leq 1$ and the report is rejected if $\lambda^2_{nw} > \lambda^2_{maxw}$. A vector sum and difference ratio is also computed:

$$r = \frac{(\mu_n - \mu^*)^2 + (\nu_n - \nu^*)^2}{c + (\mu_n + \mu^*)^2 + (\nu_n + \nu^*)^2} \quad . \tag{36}$$

Using a value for c of 0.4, the report is rejected if $r > 0.5$. This test is most severe in light wind speed cases and causes rejection of many light or calm nighttime wind reports which occur as a result of high boundary layer stability. High elevation and valley reports, which are also nonrepresentative of the sea-level pressure gradient, are rejected by this test as well.

The relative merit of the separate first-guess fields and their derivatives can also be evaluated. In the case of the first-guess pressure, the ratio

$$F = \frac{(p_e - p^*)^2}{(p_e - p^*)^2 + (p_x - p^*)^2} \tag{37}$$

is computed where p_e is the prognostic field and p_x is the extrapolated field. The separate first guesses can now be reweighted to form the new first guess:

$$p_{oR} = Fp_x + (1 - F)\, p_e \quad . \tag{38}$$

The first-guess reliability, A_o, is not changed. The same procedure is applied to the first-guess difference and Laplacian fields. The new first-guess fields and the reevaluated data are saved for the reanalysis cycle.

APPENDIX J

GLOBAL BAND SURFACE PRESSURE AND WIND ANALYSIS

1. The correction applied at a grid point from observations affecting that grid point is given by

$$C_{\varphi}^{s} = \frac{\sum_{j=1}^{K} R_j \sum_{i=1}^{P} W_i \left(\varphi_{ob} - \varphi_g\right)_i}{\sum_{j=1}^{K} R_j P_j} , \qquad (1)$$

where C = Correction to be applied at a grid point,

s = scan or cycle number,

φ_{ob} = value of observation,

φ_g = value of guess field for scan(s) at the location of the observation,

W = weight function,

R = relative reliability of observation,

P = number of observations of relative reliability R_j affecting a grid point, and

K = number of classes of observation reliabilities.

In the above formulation, empirical knowledge concerning the relative goodness of specific classes of reports is incorporated through the use of K classes of relative reliability. Class distinctions with typical corresponding reliabilities are tabled below

Reliability weight and relative tolerance used in sea level pressure analysis

Type	Reliability Weight	Relative Tolerance
Weather Station Ship	4	2
Regular Ship	1	1
Island Station	2	1
Continental Station	1	1

Reliability for surface wind analysis

Type	Reliability Weight
Island Station	2
Regular Ship (Wind Estimated)	1
Regular Ship (Wind Measured)	2
Weather Station Ship	4

2. The weight function equation is as follows:

$$W = \frac{N^2 - A^2}{N^2 + A^2} \quad , \tag{2}$$

where

$$A^2 = \frac{D^2 B^2}{D^2 \sin^2\theta + B^2 \cos^2\theta} \quad , \tag{3}$$

$$B^2 = \left(MD\right)^2 \quad , \tag{4}$$

D = distance between observation and grid point,

M = 1.5 (empirical constant),

θ = angle between wind direction and radius vector from observation to grid point,

N = scan radius.

Prior to the application of this weight function in the sea level pressure analysis, the wind direction is turned 20° toward higher pressure over the oceans to account for the effects of surface friction.

3. The information density function used in the first scan is defined by

$$I = \frac{Wt}{\overline{W}} \tag{5}$$

where

$$Wt = \sum_{j=1}^{K} \sum_{i=1}^{P_j} W_i \quad ,$$

$\overline{W}$ = normalizing value

and the notation is the same as used in Eq. (1).

During subsequent cycles the scan radius in Eq. (2) is a function of the information density as follows:

$$N_s = N_{max} - I_{ob}\left(N_{max} - NM_s\right) : I_{ob} < 1 \quad , \tag{6}$$

$$N_s = NM_s : I_{ob} \geq 1 \quad , \tag{7}$$

where

N_{max} = maximum scan radius,

NM_s = nominal scan radius,

I = information density at location of observation.

For the second, third and fourth cycles the values chosen for NM and N_{max} are dependent on latitude. They are a maximum at the equator and decrease linearly with latitude to 30° N and 30° S. The table below lists the values of NM and N that best accommodate the various scales of motion over the globe.

Latitudinal variation of parameters used in calculation of scan radius

Cycle or Scan No.	Above 30°N and Below 30°S		Equator to 30°N Equator to 30°S	Equator (nm) (max)	
	NM(nm)	N_{max}(nm)	NM N_{max}	NM	N_{max}
2	300	600	Varies linearly with latitude	600	900
3	200	600	"	300	900
4	100	600	"	150	900

4. Tolerances for rejection of erroneous observations are based on the Root Mean Square Error (RMSE) of the observations and guess field for that cycle. The RMSE is computed for selected latitude bands and the tolerances are equal to these values multiplied by empirical constants. The constants currently used are shown in the table below. Also listed are the limiting values for each tolerance. The most suitable values for the empirical constants are very difficult to determine since factors such as seasonal variability and the various meteorological scales represented on the globe must be considered. Consequently, these parameters are undergoing evaluation, and are subject to change.

Empirical constants used to obtain reject-accept tolerances and reject-accept tolerance limits

Latitude Bands	Empirical Constant	Maximum Tolerance (mb)
60°N - 90°N	3.0	20
45°N - 60°N	3.0	20
30°N - 45°N	3.0	20
15°N - 30°N	3.0	10
15°S - 15°N	3.0	5
30°S - 15°S	3.0	10
45°S - 30°S	3.0	20
60°S - 45°S	3.0	20
90°S - 60° S	3.0	20

5. The calculation of RMSE is done as follows:

$$\text{RMSE} = \left(\frac{\sum \left(P_f - P_o \right)^2}{\sum \left(\frac{1}{m} \right)^2} \right)^{1/2} , \qquad (8)$$

where P_o = observed pressure,

P_f = pressure of analyzed field at the location of the observation

with the sum taken over all observations.

4. Tolerances for rejection of erroneous observations are based on the Root Mean Square Error (RMSE) of the observations and guess field for that cycle. The RMSE is computed for selected latitude bands and the tolerances are equal to these values multiplied by empirical constants. The constants currently used are shown in the table below. Also listed are the limiting values for each tolerance. The most suitable values for the empirical constants are very difficult to determine since factors such as seasonal variability and the various meteorological scales represented on the global band must be considered. Consequently, these parameters are undergoing evaluation, and are subject to change.

Empirical constants used to obtain reject-accept tolerances and reject-accept tolerance limits

Latitude Bands	Empirical Constant	Maximum Tolerance (mb)
45°N - 60°N	3.0	20
30°N - 45°N	3.0	20
15°N - 30°N	3.0	10
15° S - 15°N	2.0	5
30° S - 15° S	3.0	10
41° S - 30° S	4.0	20

Numerical Variational Analysis Equations

1. The horizontal momentum equations used as dynamical constraints in the analysis scheme are:

$$\frac{\partial u}{\partial t} + \mathbb{V} \cdot \nabla u - fv = -\frac{1}{\rho}\frac{\partial p}{\partial x} + \frac{1}{\rho}\frac{\partial \tau_x}{\partial z} \qquad (1)$$

$$\frac{\partial v}{\partial t} + \mathbb{V} \cdot \nabla v + fu = -\frac{1}{\rho}\frac{\partial p}{\partial y} + \frac{1}{\rho}\frac{\partial \tau_y}{\partial z} \qquad (2)$$

where t : time

x : east-west coordinate (positive eastward)

y : north-south coordinate (positive northward)

z : vertical coordinate (positive upwards)

$\mathbb{V}$: $u\hat{i} + v\hat{j}$: horizontal velocity

$\hat{i}$: unit vector along positive x

$\hat{j}$: unit vector along positive y

p : pressure

ρ : density ($= 1.22\ \text{kg-m}^{-3}$)

f : coriolis parameter

$\vec{\tau}$: $\tau_x \hat{i} + \tau_y \hat{j}$: stress

$\nabla( )$: $\frac{\partial ( )}{\partial x}\hat{i} + \frac{\partial ( )}{\partial y}\hat{j}$: gradient operator.

2. The frictional effects are derived from:

$$\frac{1}{\rho}\frac{\partial \vec{\tau}}{\partial z} = - \varkappa (u\hat{i} + v\hat{j}) \tag{3}$$

where $\varkappa$ is assumed constant (10^{-1} hr^{-1}) and is found by assuming the following scale values: (1) $|\mathbb{V}|$ = 20 kt, (2) $C_D = 2.5 \times 10^{-3}$, (3) $\rho/\bar{\rho} = 1$, and (4) H - 0.5 n mi.

3. The analysis couples observations (input analysis) and dynamics through the minimization of the following functional:

$$I = \iint_S \left\{ \begin{array}{l} \tilde{\alpha}(u-\tilde{u})^2 + \tilde{\alpha}(v-\tilde{v})^2 + \tilde{\beta}(p-\tilde{p})^2 \\ \\ + \left[\alpha\left(\frac{\partial u}{\partial t}\right)^2 + \alpha\left(\frac{\partial v}{\partial t}\right)^2 \right] \end{array} \right\} dS \tag{4}$$

where $(\tilde{\ })$ indicates the conventional analysis and where the surface integral extends over the entire analysis region, S. This formulation is called the timewise localized version of NVA (Sasaki, 1970)*. The first set of bracketed terms forces the analysis toward the input fields in direct proportion to the "observational" weights on wind and pressure, $\tilde{\alpha}$ and $\tilde{\beta}$, respectively. The second set of terms brings the dynamics into the analysis and controls the degree of steadiness in direct proportion to the "dynamic" weight α.

These weights are specified beforehand and are not determined as a result of the variational operations. They are a function of space; and the observational weights, $\tilde{\alpha}$ and $\tilde{\beta}$, reflect the confidence in the input fields. It is natural to vary these weights as a function of the number of accepted observations that contributed to the analysis at a particular point. Accordingly, data density is used to determine these observational weights.

It is convenient to specify the weights $\tilde{\alpha}$ and $\tilde{\beta}$ in terms of the desired variance between input fields and NVA fields. By analogy, the weight α can be specified in terms of the variance of acceleration which would be found from (1) and (2). Using this concept, the weights are given by:

$$\tilde{\alpha} = \frac{1}{\sigma_w} \quad , \quad \tilde{\beta} = \frac{1}{\sigma_p} \quad , \quad \alpha = \frac{1}{\sigma_t} \tag{5}$$

where σ_w is the variance between NVA and conventional analysis of wind, σ_p the variance between NVA pressure and input pressure, and σ_t is the variance of acceleration as calculated by (1) and (2). In accord with the previous statement, variances σ_w and σ_p should decrease with an increase of data density.

4. In order to directly incorporate the assumptions on parameterization of friction and the special handling of the nonlinear terms, the momentum equations are rewritten:

$$\frac{\partial u}{\partial t} + \tilde{\mathbb{V}} \cdot \nabla \tilde{u} - fv = - \frac{1}{\rho}\frac{\partial p}{\partial x} - \varkappa u \quad , \tag{6}$$

$$\frac{\partial v}{\partial t} + \tilde{\mathbb{V}} \cdot \nabla \tilde{v} + fu = - \frac{1}{\rho}\frac{\partial p}{\partial y} - \varkappa v \quad . \tag{7}$$

*Sasaki, Y., 1970; "Some basic formalisms in numerical variational analysis, Mon. Wea. Rev., 98, 875-883.

5. The Euler Equations. Using the modified momentum equations (6) and (7) as the dynamic constraints, and substituting into $\delta I = 0$, obtained from minimizing (4) by substituting

$$\frac{\partial u}{\partial t} \quad \text{and} \quad \frac{\partial v}{\partial t}$$

from (1) and (2) into (4), leads to the following relation:

$$0 = \iint_S (U\delta u + V\delta v + P\delta p \quad ds \qquad (8)$$

$$+ \text{ boundary terms}$$

where δu, δv, and δp are the variations of the two velocity components and the pressure, respectively. This form of the integral relation is obtained by using integration by parts, the standard procedure in the calculus of variations. The expressions U, V, and P are partial differential equations involving u, v, and p; however, they are free from any terms involving δu, δv, or δp.

6. Since the variations of U, V, and P are independent, the solution to (8) reduces to

$$U = 0 \quad , \quad V = 0 \quad , \quad P = 0 \quad . \qquad (9)$$

These are the Euler equations for our particular variational formulation and the differential expressions are as follows:

$$U = \left\{ \begin{array}{l} \tilde{\alpha}(u-\tilde{u}) + f^2 \alpha u + \frac{\alpha f}{\rho}\frac{\partial p}{\partial y} + \frac{\alpha \varkappa}{\rho}\frac{\partial p}{\partial x} \\ + \varkappa^2 \alpha u + \alpha \varkappa \tilde{A} + \alpha f \tilde{B} \end{array} \right\} = 0 \qquad (10)$$

$$V = \left\{ \begin{array}{l} \tilde{\alpha}(v-\tilde{v}) + f^2 \alpha v - \frac{\alpha f}{\rho}\frac{\partial p}{\partial x} + \frac{\alpha \varkappa}{\rho}\frac{\partial p}{\partial y} \\ + \varkappa^2 \alpha v - \alpha f \tilde{A} + \alpha \varkappa \tilde{B} \end{array} \right\} = 0 \qquad (11)$$

$$P = \left\{ \begin{array}{l} \tilde{\beta}(p-\tilde{p}) + \frac{\partial}{\partial x}\left(\frac{f\alpha v}{\rho}\right) - \frac{\partial}{\partial y}\left(\frac{f\alpha u}{\rho}\right) \\ - \frac{1}{\rho^2}\frac{\partial}{\partial x}\left(\alpha \frac{\partial p}{\partial x}\right) - \frac{1}{\rho^2}\frac{\partial}{\partial y}\left(\alpha \frac{\partial p}{\partial y}\right) \\ - \frac{1}{\rho}\frac{\partial}{\partial x}(\varkappa \alpha u) - \frac{1}{\rho}\frac{\partial}{\partial y}(\varkappa \alpha v) \\ - \frac{1}{\rho}\frac{\partial}{\partial x}(\alpha \tilde{A}) - \frac{1}{\rho}\frac{\partial}{\partial y}(\alpha \tilde{B}) \end{array} \right\} = 0 \qquad (12)$$

where

$$\tilde{A} = \tilde{W} \cdot \nabla \tilde{u} \qquad (13)$$

$$\tilde{B} = \tilde{W} \cdot \nabla \tilde{v} \quad . \qquad (14)$$

Equations (10) and (11) can be solved for u and v as functions of p, respectively. These expressions are then substituted into (12) to get the following elliptic equation (Helmholtz type) for p:

$$\nabla \cdot (r \nabla p) - \rho^2 \tilde{\beta} p = \left\{ \begin{array}{l} - \rho^2 \tilde{\beta} \tilde{p} + \rho \nabla \times (f r \tilde{\mathbb{V}}) \\ - \rho \nabla \cdot (\varkappa r \tilde{\mathbb{V}}) - \rho \nabla \cdot (r \mathbb{C}) \end{array} \right\} \tag{15}$$

where vector products have been used for ease of notation and the following symbols were introduced:

$$r = \frac{\alpha \tilde{\alpha}}{\tilde{\alpha} + \alpha \left(f^2 + \varkappa^2 \right)} = \frac{\alpha}{1 + \frac{\alpha}{\tilde{\alpha}} \left(f^2 + \varkappa^2 \right)} \tag{16}$$

$$\mathbb{C} = \tilde{A} \hat{i} + \tilde{B} \hat{j} \quad . \tag{17}$$

Once the solution for (15) is found, it is then a simple algebraic problem to substitute this solution into (10) and (11) to obtain u and v.

APPENDIX K

UPPER-AIR ANALYSIS

The Atmospheric Mass-Structure Model

The Upper Air Analysis System at FNWC is based on a modelling of the atmospheric mass structure that incorporates the hydrostatic-equation and gas-law approximations. The independent vertical coordinate is pressure, and the model is defined by eight layers:

1000-775, 775-600, 600-450, 450-350,

350-275, 275-225, 225-175, 175-0mb.

Each of these layers has a static stability, σ, that varies horizontally and in time, but does not vary with pressure within each layer segment of the column structure.

Static stability, defined in terms of the virtual potential temperature θ_v, is

$$\sigma \equiv - R p_o^{-\varkappa} p^{1+\varkappa} \partial\theta_v/\partial p \qquad (1)$$

where p_o is a reference pressure (1000 mb), R is the gas constant for dry air, θ_v is the virtual potential temperature, and $\varkappa \equiv R/C_p$ where C_p is the specific heat at constant pressure. The pressure independence of σ in a column segment makes the virtual temperature, T_v, linear in $p^{\varkappa}$.

The mass structure of a column is uniquely defined by the eight values of σ together with the 1000-mb height value and a temperature parameter of either the 1000- to 500-mb or 1000- to 300-mb thickness.

The interfaces defining the layers were selected to give the most stable non-singular square-matrix (i.e., all linear) transformation with the heights of ten standard pressure levels. This set of heights is defined by the vector $\underset{\sim}{z}$, made up of the height values for ten levels:

1000, 850, 700, 500, 400, 300, 250, 200, 150, and 100 mb.

The transformation matrix for obtaining $\underset{\sim}{\sigma}$ from $\underset{\sim}{z}$ is defined by $\underset{\approx}{D}$:

$$\underset{\sim}{\sigma} = \underset{\approx}{D}\,\underset{\sim}{z} \qquad (2)$$

It is used to transform the $\underset{\sim}{z}$ vector determined by an atmospheric sounding (radiosonde) into the corresponding $\underset{\sim}{\sigma}$ vector. The mass-structure analysis is expressible by the fields of $\underset{\sim}{\sigma}$; the height fields are recovered by the inversion of the σ vector of Eq. (2):

$$\underset{\sim}{z} = \underset{\approx}{D}^{-1}\,\underset{\sim}{\sigma} \quad . \qquad (3)$$

The virtual temperatures at the ten standard levels are defined by the vector $\underset{\sim}{T}$:

$$\underset{\sim}{T}_v = \langle T_a , T_b , T_c \ldots T_j \rangle \quad . \qquad (4)$$

This vector is determined from $\underset{\sim}{z}$ by the singular transformation matrix $\underset{\approx}{Q}$:

$$\underset{\sim}{T}_v = \underset{\approx}{Q}\,\underset{\sim}{z} \quad . \tag{5}$$

The seven layer-interface levels are defined as follows:

775, 600, 450, 350, 275, 225, 175 mb.

The virtual temperature and heights of these seven levels are defined by the fourteen-component vector, $\underset{\sim}{F}$:

$$\underset{\sim}{F} = \langle T_k , T_1 \ldots T_q , z_k , z_1 \ldots z_q \rangle \quad . \tag{6}$$

This vector is determined from $\underset{\sim}{z}$ by the transformation matrix $\underset{\approx}{S}$:

$$\underset{\sim}{F} = \underset{\approx}{S}\,\underset{\sim}{z} \quad . \tag{7}$$

The virtual temperature, T_v, for any pressure level, p, as obtained by Eq. (5) for standard levels and Eq. (7) for interface levels, may be converted to the density, ρ, by the gas-law approximation:

$$\rho = \frac{p}{RT_v} \quad . \tag{8}$$

The pressure dependencies within a layer are as follows: For virtual temperature,

$$T = T_1 + \frac{p^{\varkappa} - p_1^{\varkappa}}{p_u^{\varkappa} - p_1^{\varkappa}} \left(T_u - T_1 \right) \tag{9}$$

where subscript 1 denotes the lower interface, and subscript u the upper interface, of the layer. This transforms into density by Eq. (8). For height, integrate the hydrostatic equation:

$$z = z_1 - \frac{R}{g} \int_{p_1}^{p_u} T_v \frac{dp}{p} \quad , \tag{10}$$

which integrates to

$$z = N_* + M_* p^{\varkappa} - \sigma (g\varkappa)^{-1} \ln p \quad . \tag{11}$$

The constants N_* and M_* are evaluated at the interfaces.

The determination of the density for any specified pressure level reduces to a linear combination of the components of $\underset{\sim}{z}$, and involves solution of an implicit transcendental equation. The model was obviously not designed to facilitate this route. Such determinations are simplified, in violation of the model, to interpolation schemes between the interface and standard level specifications.

APPENDIX L

PRIMITIVE EQUATION MODEL

1. The governing differential equations of the P.E. model are shown below, first in continuous form, then in finite difference form.

a. Momentum Equation in the E-W direction

$$\frac{\partial \pi u}{\partial t} = -m^2 \left\{ \frac{\partial}{\partial x}\left(\frac{uu\pi}{m}\right) + \frac{\partial}{\partial y}\left(\frac{uv\pi}{m}\right) \right\} + \pi \frac{\partial (wu)}{\partial \sigma}$$

$$+ \pi vf - m \left\{ \frac{\partial \Phi}{\partial x} + RT \frac{\partial \pi}{\partial x} \right\} + D_u + F_x \quad , \tag{1}$$

$$(\pi u)_*^{n+1} = (\pi u)_*^{n-1} + 2\Delta t \left\{ \left[-\mathbf{l}(u)_* + (f\pi v)_* - \left(\frac{\Delta \Phi}{\Delta x}\right)_* \right]^n \right.$$

$$\left. - F_x^{n-1} + K \frac{m_{ij}^2}{d^2} \left(\nabla^2 D_u\right)_*^{n-1} \right\} \quad , \tag{2}$$

where u,v = x,y components of velocity true on the earth,

π = underlying terrain pressure,

t = time,

m = map factor,

w = vertical velocity variable,

σ = vertical coordinate,

f = coriolis parameter,

Φ = latitude,

R = gas constant for air,

T = temperature,

D = lateral diffusion,

F = surface stress

$*$ = denotes the point (i,j,k),

superscripts denote time level,

$\mathbf{l}$ = finite difference advective operator defined in Eq. (7),

Δ = the centered time and space difference operator,

∇^2 = the finite difference Laplacian defined in Eq. (7), and

d = grid mesh size.

b. Momentum Equation in the N-S direction

$$\frac{\partial \pi v}{\partial t} = -m^2 \left\{ \frac{\partial}{\partial x}\left(\frac{uv\pi}{m}\right) + \frac{\partial}{\partial y}\left(\frac{vv\pi}{m}\right)\right\} + \pi \frac{\partial wv}{\partial \sigma}$$

$$- \pi uf - m\left\{\pi \frac{\partial \Phi}{\partial y} + RT\frac{\partial \pi}{\partial y}\right\} + D_v + F_y \qquad (3)$$

$$(\pi v)_*^{n+1} = (\pi v)_*^{n-1} + 2\Delta t \left\{\left[-\mathbf{L}(v)_* - (f\pi u)_* - \left(\frac{\Delta \Phi}{\Delta y}\right)_*\right]^n\right.$$

$$\left. - F_y^{n-1} + K\frac{m_{ij}^2}{d^2}\left(\nabla^2 D_v\right)_*^{n-1}\right\} \qquad (4)$$

c. Thermodynamic Energy Equation

$$\frac{\partial \pi T}{\partial t} = -m^2\left\{\frac{\partial}{\partial x}\left(\frac{\pi uT}{m}\right) + \frac{\partial}{\partial y}\left(\frac{\pi vT}{m}\right)\right\} + \pi\frac{\partial (wT)}{\partial \sigma} + H\pi$$

$$+ D_T + \frac{RT}{c_p\sigma}\left\{-w\pi + \sigma\left[\frac{\partial \pi}{\partial t} + m\left(u\frac{\partial \pi}{\partial x} + v\frac{\partial \pi}{\partial y}\right)\right]\right\} \qquad (5)$$

$$(\pi T)_*^{n+1} = (\pi T)_*^{n-1} + 2\Delta t\left\{-\mathbf{L}(T)_* + \frac{RT_*}{\sigma_K C_p}\right.$$

$$\left[-\frac{\pi_{ij}}{2}\left(w_K + w_{K-1}\right)_{ij} + \sigma_K\left(\frac{\partial \pi}{\partial t}\right)_{ij} + \frac{\sigma_K m_{ij}}{2d}\left(\mathbb{W}_* \cdot \Delta \pi\right)\right]^n$$

$$\left. + \frac{Km_{ij}^2}{d^2}\nabla^2\left(D_T\right)_*^{n-1} + H_*\pi_{ij}^{n-1}\right\} \qquad (6)$$

with $w \equiv -d\sigma/dt$, the vertical motion.

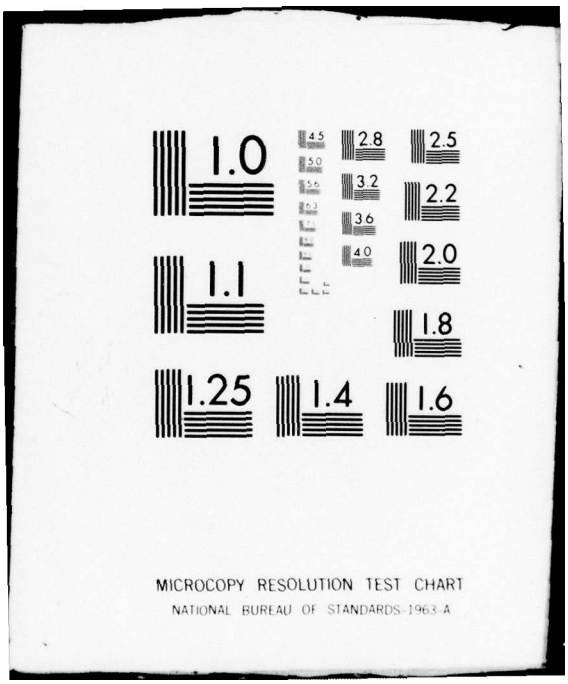
AD-A065 511 NAVAL WEATHER SERVICE COMMAND WASHINGTON D C F/G 4/2
U.S. NAVAL WEATHER SERVICE NUMERICAL ENVIRONMENTAL PRODUCTS MAN--ETC(U)
FEB 79 E T HARDING

UNCLASSIFIED NAVAIR-50-16-522-REV NL

4 OF 4
AD
A065511



END
DATE
FILMED
5-79
DDC


1.0
1.1
1.25
1.4
1.6
1.8
2.0
2.2
2.5
2.8
3.2
3.6
4.0
4.5
5.0
5.6
6.3
MICROCOPY RESOLUTION TEST CHART
NATIONAL BUREAU OF STANDARDS-1963-A

The advective operator and the Laplacian are defined,

$$\mathbf{L}(\psi)_* \equiv \frac{m_{ij}^2}{4d}\left[\left\{\left(\alpha_{i+1}+\alpha_i\right)\left(\psi_{i+1}+\psi_i\right) - \left(\alpha_{i-1}+\alpha_i\right)\left(\psi_{i-1}+\psi_i\right)\right\}_{jk} + \left\{\left(\beta_{j+1}+\beta_j\right)\left(\psi_{j+1}+\psi_i\right) - \left(\beta_{j-1}+\beta_j\right)\left(\psi_{j-1}+\psi_j\right)\right\}_{ik}\right] + \frac{\pi_{ij}}{.4}\left[w_K\left(\psi_{K+1}+\psi_K\right) - w_{K-1}\left(\psi_K+\psi_{K-1}\right)\right]_{ij} \tag{7}$$

$$\nabla^2(\psi)_* \equiv \left(\psi_{i+ij} + \psi_{i-ij} + \psi_{ij+1} + \psi_{ij-1} - 4\psi_{ij}\right) \tag{8}$$

d. Continuity Equation

$$\frac{\partial \pi}{\partial t} = -m^2\left\{\frac{\partial}{\partial x}\left(\frac{u\pi}{m}\right) + \frac{\partial}{\partial y}\left(\frac{v\pi}{m}\right)\right\} + \pi\frac{\partial w}{\partial \sigma} \tag{9}$$

$$w_{ijK+1} = w_* - \frac{.2}{\pi_{ij}}\left\{\left(\frac{\partial \pi}{\partial t}\right)_{ij} + \frac{m_{ij}^2}{2d}\left[\left(\alpha_{i+1}-\alpha_{i-1}\right)_{jk} + \left(\beta_{j+1}-\beta_{j-1}\right)_{iK}\right]\right\} \tag{10}$$

e. Moisture Conservation Equation

$$\frac{\partial e\pi}{\partial t} = -m^2\left\{\frac{\partial}{\partial x}\left(\frac{\pi u e}{m}\right) + \frac{\partial}{\partial y}\left(\frac{\pi v e}{m}\right)\right\} + \frac{\pi\partial(we)}{\partial\sigma} + Q\pi + D_e \tag{11}$$

where Q = moisture source/sink term.

$$(\pi e)_*^{n+1} = (\pi e)_*^{n-1} + 2\Delta t\left\{-\mathbf{L}(e)_*^n + Q_*\pi_{ij}^{n-1} + K\frac{m_{ij}^2}{d^2}\nabla^2\left(D_e\right)_*^{n-1}\right\} \tag{12}$$

f. Hydrostatic Equation

$$\frac{\partial \Phi}{\partial \sigma} = - \frac{RT}{\sigma} \tag{13}$$

The hydrostatic equation is given at the lowest level by

$$\Phi_* = \Phi_{TERRAIN} - RT_* \ln (0.9) \tag{14}$$

and for subsequent levels,

$$\Phi_{KH} = \Phi_K - R \ln \left(\frac{\sigma_{K+1}}{\sigma_K} \right) \left[\frac{T_K \ln \left(\frac{\sigma_K}{\pi} \right) + T_{K+1} \ln \left(\frac{\sigma_{K+1}}{\pi} \right)}{\ln \sigma_K + \ln \sigma_{K+1} - 2 \ln \pi} \right] . \tag{15}$$

The lower boundary pressure is computed from

$$\pi_{ij}^{n+1} = \pi_{ij}^{n-1} + 2\Delta t \left(\frac{\partial \pi}{\partial t} \right)_{ij}^{n} \tag{16}$$

where, for the entire column, the local change is evaluated as:

$$\left(\frac{\partial \pi}{\partial t} \right)_{ij}^{n} = - \sum_{K=1}^{5} .1 \frac{m_{ij}^2}{d} \left(\alpha_{i+1jK} - \alpha_{i-1jK} + \beta_{ij+1K} - \beta_{ij-1K} \right)^n \tag{17}$$

where, for notational convenience, we define the quantities

$$\alpha \equiv \frac{u\pi}{m} \tag{18}$$

and

$$\beta \equiv \frac{v\pi}{m} . \tag{19}$$

2. Heating and Moisture Source Terms

The heating can be written

$$H = H_{sw} + H_{Lw} + H_c + H_\Gamma \tag{20}$$

where H_{sw} refers to the heating due to absorption of short wave solar radiation, H_{Lw}, the heating due to absorption of terrestrial infra-red radiation, H_c, the heating resulting from the condensation of water vapor and H_Γ, the heating due to sensible heat transfer from the surface.

a. Solar Radiation

The incoming solar radiation at the top of the model atmosphere is given by:

$$S = S_0 \cos \mu \tag{21}$$

where μ is a function of time of day, latitude and season.

The heating of the atmosphere is dependent on the vertical distribution of moisture above each grid point. For the radiation calculations the model carries a simple form of middle cloud which is assumed to exist between $\sigma = .4$ and $.8$. Use of Smagorinsky's empirical formula for midd'e cloud,

$$CL = 2.0\left[\frac{e}{e_s}\right]_{.7} - .7 \tag{22}$$

gives the amount of cloudiness in terms of the relative humidity at $\sigma = .7$. Limits of 1.0 and 0.0 are set on the range of values given from Equation (22).

The absorption of incoming solar radiation for the upper layer ($\sigma = 0$ to $\sigma = .6$) is given by,

$$A_{(2)} = \left\{(1 - CL)\,\mathfrak{I}_1 + CL\,(1-\alpha_c)\,\mathfrak{I}_2\right\} .349S \tag{23}$$

for the lower layer ($\sigma = .6$ to $\sigma = 1.0$),

$$A_{(1)} = \left\{(1 - CL)\,\mathfrak{I}_3 + CL\,(1-\alpha_c)\,\mathfrak{I}_4\right\} .349S \tag{24}$$

where
$$\mathfrak{I}_1 = .271\left[pw(3)\,\frac{S_o}{S}\right]^{.303}$$

$$\mathfrak{I}_2 = .271\left[1.66\left(\frac{pw(c)}{2} + pw(3)\right)\right]^{.303}$$

$$\mathfrak{I}_3 = .271\left[(pw(3) + pw(2) + pw(1))\,\frac{S_o}{S}\right]^{.303} - \mathfrak{I}_1 \tag{25}$$

$$\mathfrak{I}_4 = .271\left[1.66\;(pw(c) + pw(3) + pw(2) + pw(1))\right]^{.313} - \mathfrak{I}_2$$

and where the precipitable water (pw) is given by,

$$pw = \frac{1}{g}\int_o^P q\,dp \quad . \tag{26}$$

PW(c) is the amount of liquid water assumed to be present in the cloud. This is arbitrarily set at 75% of the calculated precipitable water in the column.

The cloud's albedo, α_c, is set at .5. Finally, the smount of solar radiation which reaches the surface is needed as this will be used in the calculation of sensible heating over the land areas. This is given by

$$S_g = \left[1 - \alpha_g\right]\left\{(1-CL)\left[.349S - A_{(2)} - A_{(1)} + \frac{.651S(1-\alpha_S)}{1 - \alpha_S\alpha_g}\right]\right.$$

$$\left. + CL\left[\frac{.349S\left((1-\alpha_S)-(1-\alpha_c)(\mathfrak{I}_1+\mathfrak{I}_2)\right)}{1 - \alpha_c\alpha_g} + \frac{1-\alpha_{Sc}}{1-\alpha_{Sc}\alpha_g}\;.651S\right]\right\} . \tag{27}$$

In Equation (27) α_g, the ground surface albedo, is given as a function of latitude over the sea and as a function of snow cover over the land, α_S is albedo of clear sky and α_{Sc} the albedo of cloudy sky. The snow cover is assumed to be a function of the mean monthly temperature.

b. Terrestrial Radiation

The infra-red fluxes at $\sigma = .2$, $\sigma = .6$ and $\sigma = 1.0$, are computed by

$$F_{1.0} = F^*_{1.0} + St\,(T_g^4 - T_S^4) \tag{28}$$

$$F_{0.6} = F^*_{0.6} + \frac{0.8(1-CL)\,(F_{1.0} - F^*_{1.0})}{1 + 1.75(pw(1) + pw(2))^{.416}} \tag{29}$$

$$F_{0.2} = F^*_{0.2} + \frac{0.8(1-CL)(F_{1.0} - F^*_{1.0})}{1 + 1.75(pw(1) + pw(2)) + pw(3)^{.416}} \cdot \tag{30}$$

$F^*_{1.0}$, $F^*_{0.6}$ and $F^*_{0.2}$ are the fluxes computed assuming the surface temperature is given by a downward extrapolated temperature (T_s). The factor 0.8 is an empirical correction to account for the effect of CO_2.

In Equation (28), T_g is given over the oceans from the operational sea-surface analyses, over the land areas it is given from the solution of a heat balance equation to be explained in the section on sensible heat transfer and evaporation.

The approximate fluxes, F^*, are computed by

$$F^*_{1.0} = St\left\{(1-CL)\left[-T_S^4 + T_{.8}^4\,\varphi(X1) + T_{.3}^4\,(\varphi(X2) - \varphi(X1))\right] + CL\left[T_{.8}^4 - T_S^4 + (T_{.9}^4 - T_{.8}^4)\,\varphi(X4)\right]\right\} \tag{31}$$

$$F^*_{0.6} = St\left\{(1-CL)\left[-T_S^4 + (T_S^4 - T_{.8}^4)\,\varphi(X1) + T_{.3}^4\,\varphi(X3)\right]\right\} \tag{32}$$

$$F^*_{0.2} = St\left\{(1-CL)\left[-T_S^4 + (T_S^4 - T_{.8}^4)\,(\varphi(X2) - \varphi(X3)) + (T_S^4 - T_{.3}^4)\,\varphi(X3)\right] + CL\left[-T_{.4}^4\right]\right\} \tag{33}$$

where

$$\varphi(XN) = .0105\,(XN)^2 + .1675\,(XW) + .542 \tag{34}$$

and

$$\begin{aligned} X1 &= \text{Log}_{10}\,(PW(1) + PW(2)) \\ X2 &= \text{Log}_{10}\,(PW(1) + PW(2) + PW(3)) \\ X3 &= \text{Log}_{10}\,(PW(3)) \\ X4 &= \text{Log}_{10}\,(PW(1)) \end{aligned} \tag{35}$$

and for these calculations PW (Equation (26)) is modified to

$$PW = \frac{1}{g} \int_{o}^{P} .622\, \frac{e}{p} \left(\frac{p}{1000}\right)^{.85} \left(\frac{273}{T}\right)^{.5} dp \tag{36}$$

Finally, to convert to a heating rate,

$$H_{LW\,(2)} = -\,(F_{1.0} - F_{0.6})\, \frac{g\Delta t}{\pi C_p \Delta_p} \quad (^\circ C/hr) \tag{37}$$

$$H_{LW\,(1)} = -\,(F_{0.6} - F_{0.2})\, \frac{g\Delta t}{\pi C_p \Delta_p} \quad (^\circ C/hr) \tag{38}$$

since the fluxes are computed in cgs units.

c. Sensible Heating and Evaporation

Sinsible heating is computed as a function of the difference of the surface temperature (T_g) and the temperature of the air near the surface (T_x). Similarly, evaporation is computed as a function of the saturation moisture at the surface (q_s) and the moisture near the surface (q_x). Difficulty arises in the model as near-surface temperature, wind or moisture are not carried. To surmount this difficulty the air near the surface is assumed to be a very thin boundary layer which does not absorb or store a significant amount of heat or moisture. The fluxes of sensible heat and moisture are therefore the same through the top and the bottom of this thin boundary layer. Generally for heat transfer an equation of the form

$$\Gamma = -\,K_H \frac{\Delta\theta}{\Delta Z} \tag{39}$$

is used where θ is potential temperature. Equation (39) is modified to

$$\Gamma = \rho_{1.0} C_p \frac{K^*}{\left[1 + \dfrac{a^*(\theta_{.9} - \theta_S)}{(Z_{.9} - Z_{1.0})}\right]} \left\{ \gamma_c - \frac{(\theta_{.9} - \theta_x)}{(Z_{.9} - Z_{1.0})} \right\} \tag{40}$$

In Equation (40) the expression for K_H is allowed to vary with the stability of the lowest level. K^*, a^* and γ_c are empirical constants. γ_c allows for a somewhat more realistic variation of Γ between day and night. The subscript S refers to the value of a parameter extrapolated to the surface from the levels $\sigma = .9$ and $\sigma = .7$.

The sensible heat flux through the bottom of the boundary layer is given by the equation,

$$H_\Gamma = \rho_{1.0} C_p C_d V_s \left(T_g - T_x\right) \tag{41}$$

where for this computation

$$V_s = .7 \left| W_s \right| + G_u \quad , \tag{42}$$

where G_u, the gustiness factor, is 2.2 m/sec.

From Equations (40) and (41), T_x can be obtained, given T_g.

Over the land areas T_g must be computed from a surface heat balance equation,

$$\left(1 + \frac{1}{r}\right) H_\Gamma - S_{tg} + F_{1.0} = 0 \quad , \tag{43}$$

in which only the heat storage has been neglected. A Bowen ratio, r, is determined by

$$r = 9.6 \, (\mathrm{SIN}\varphi)^2 - 7.93 \, (\mathrm{SIN}\varphi) + 2.0 \tag{44}$$

where a minimum value of .2 for $\sin\varphi$ is enforced. This leads to problems over low-latitude deserts. Equation (43) is modified over ice covered ocean to

$$\left(1 + \frac{1}{r}\right) H_\Gamma - S_{tg} + F_{1.0} = B\left(T_w - T_g\right) \quad , \tag{45}$$

where B is an ice conduction coefficient and $T_w = 271.2^\circ C$.

Evaporation over the ice-free ocean is determined in a similar manner to the heat flux. The equation resulting is

$$E = \frac{\rho_{1.0} C_p V_s}{1 + \dfrac{\pi C_p V_s}{10_g \rho_{1.0}} \left\{ \dfrac{K^*}{1 + \dfrac{a^*(\theta_{.9} - \theta_{.7})\pi}{10_c \rho_{1.0}}} \right\}} (q_{sg} - q_x) \tag{46}$$

with the approximate relation

$$q_{sg} = .622 \, e^{\left(AE - BE/T_g\right)/\pi} - e^{\left(AE - BE/T_g\right)} \quad , \tag{47}$$

with AE = 21.656, BE = 5418.

d. Heating Resulting from Condensation

The computed release of latent heat is based on the assumptions that for synoptic scale motion the atmosphere is not in a supersaturated state or that it is not hydrostatically unstable.

To satisfy the first of these, the solution of the equation

$$C_p\left(T_{new} - T_{old}\right) = L\left(q_{old} - q_{new}\right) \tag{48}$$

is involved.

If the computation is for the lowest level of the model and if supersaturation exists (q_{old}), then some amount of water must be condensed in order to reduce the amount of water vapor to saturation (q_{new}). At the same time the temperature will rise (from T_{old} to T_{new}). This process is modified slightly for the second and third level. At these levels the possibility of evaporating any precipitated water into the next lower level and letting rain fall to the ground only if the next lower layer thus becomes saturated is checked.

The enforcement of a convective adjustment on the model is divided into two parts, a moist convective adjustment and a dry convective adjustment.

Three types of moist convection are considered. The first type is that occurring between sigma levels 0.5 and 0.7, the second type is that occurring among sigma levels 0.9, 0.7, and 0.5, and the third type is that occurring in sigma levels 0.9 and 0.7. Precipitation may result from types 1 and 2 but not from type 3.

Two parameters used to indicate which type may occur are the energy parameters,

$$h = C_pT + gZ + Lq \tag{49}$$

and

$$E_n + C_pT + gZ + L_{qs} \quad . \tag{50}$$

E_n is constant along a moist pseudoadiabot and $(C_pT + gZ)$ is constant along a dry adiabat. Thus comparison of h and E_n for various levels allows for a sufficient test of conditional instability.

Type 1 convection will occue if

$$h_2 > E_{n3} \quad . \tag{51}$$

If $E_{n2} \approx E_{n3}$ a moist adiabatic lapse rate would exist between levels 2 and 3 since $h_2 < E_{n2}$ inequality (Eq. (51)) implies that a conditionally unstable lapse rate exists. Furthermore, Eq. (51) can be rewritten

$$q_2 > \left(E_{n3} - C_pT_2 - gZ_2\right)/L \quad . \tag{52}$$

Type 2 convection will occur if

$$E_{n3} > h_2 \, , \, h_1 > E_{n3} \quad . \tag{53}$$

Conditional instability does not exist here between levels 2 and 3 but does exist between levels 1 and 3.

Finally type 3 convection will occur if,

$$E_{n3} > h_1 > E_{n2} \quad . \tag{54}$$

Levels 1 and 2 are conditionally unstable, levels 2 and 3 are not.

The procedure now is to write down equations describing the budget for the moisture and the potential temperature for each type of convection. Before this can be done, the energy budget for the lower part of the cloud is considered, neglecting any accumulated storage of energy within the cloud.

Using type 2 as an example, when $\eta > 1$ entrainment exists and the parameter E_n in the clouds, E_{nc}, is given by a mixing of h_1 and h_2 in the lower part of the clouds when $\eta > 1$,

$$E_{nc} = h_2 + \frac{1}{\eta}\left(h_1 - h_2\right) \tag{55}$$

since h is approximately conserved with respect to an air parcel. At level three,

$$E_{nc} = C_pT_{c3} + gZ_3 + Lq_s\left(T_{c3}\right) \tag{56}$$

whereas for the environmental air,

$$E_{n3} = C_pT_3 + gZ_3 + Lq_s\left(T_3\right) \quad . \tag{57}$$

Therefore,

$$T_{c3} - T_3 = \frac{1}{1 + \frac{L}{C_p}\left(\frac{\partial q_s}{\partial T}\right)_3} \left\{ \frac{E_{nc} - E_{n3}}{C_p} \right\} \quad . \tag{58}$$

For type 1 and 3 convection E_{nc} is given by h_2 and h_1 respectively. From the Equation (58) one can obtain approximately

$$q_{c3} - q_{s3} = \frac{\gamma_3}{1 + \gamma_3} \left\{ \frac{E_{nc} - E_{n3}}{L} \right\} \tag{59}$$

where

$$\gamma_3 \equiv \frac{L}{C_p} \left(\frac{\partial q_s}{\partial T}\right)_3 \quad . \tag{60}$$

For types 1 and 2 the convective terms in the moisture and potential temperature budget can be written in flux form,

$$\frac{\Delta p_3}{g} \frac{\partial q_3}{\partial t} = \eta C \left\{ q_{S3} + \frac{\gamma_3}{1+\gamma_3} \left(\frac{E_{nc} - E_{n3}}{L} \right) - \frac{q_3 + q_2}{2} \right\} \tag{61}$$

$$\frac{\Delta p_2}{g} \frac{\partial q_2}{\partial t} = \eta C \left\{ \frac{q_3 - q_2}{2} + \frac{1}{\eta} \left(\frac{q_2 - q_1}{2} \right) \right\} \tag{62}$$

$$\frac{\Delta p_1}{g} \frac{\partial q_1}{\partial t} = C \left[\frac{q_2 - q_1}{2} \right] \quad \text{(Type 2 only)} \tag{63}$$

$$\frac{\Delta p_3}{g} \frac{\partial \textcircled{H}_3}{\partial t} = \eta C \left[\frac{E_{nc} - E_{n3}}{1 + \gamma_3} + \frac{\textcircled{H}_3 - \textcircled{H}_2}{2} \right] \tag{64}$$

$$\frac{\Delta p_2}{g} \frac{\partial \textcircled{H}_2}{\partial t} = \eta C \left[\frac{\textcircled{H}_3 - \textcircled{H}_2}{2} + \frac{1}{\eta} \left(\frac{\textcircled{H}_2 - \textcircled{H}_1}{2} \right) \right] \tag{65}$$

$$\frac{\Delta p_1}{g} \frac{\partial \textcircled{H}_1}{\partial t} = C \left[\frac{\textcircled{H}_2 - \textcircled{H}_1}{2} \right] \quad \text{(Type 2 only)} \tag{66}$$

and for type 3 convection,

$$\frac{\Delta p_2}{g}\frac{\partial q_2}{\partial t} = C\left(\frac{q_1 - q_2}{2}\right) = -\frac{\Delta p_1}{g}\frac{\partial q_1}{\partial t} \tag{67}$$

$$\frac{\Delta p_2}{g}\frac{\partial \textcircled{H}_2}{\partial t} = C\left(\frac{\textcircled{H}_1 - \textcircled{H}_2}{2}\right) = -\frac{\Delta p_1}{g}\frac{\partial \textcircled{H}_1}{\partial t} \tag{68}$$

where $\textcircled{H} \equiv C_pT + gZ$.

For type 1 convection it can be shown by manipulation of the above equations,

$$\eta C = \frac{\Delta p}{g\tau}\,\frac{1+\gamma_3}{2+\gamma_3}\,\frac{(h_2 - E_{n3})}{\left[\left(h_2 - E_{n3}\right) + \left(\frac{1+\gamma_3}{2}\right)\left(\textcircled{H}_3 - \textcircled{H}_2\right)\right]} \tag{69}$$

where τ is the time scale for the convective process (1 hour is used).

For type 2 convection a value of 1°C was used for $(T_{C3} - T_3)$, though tests with values as low as .1°C give nearly the same result. Therefore from Equations (55) and (58),

$$\eta = \left(h_1 - h_2\right)/\left(E_{n3} + C_p\left(1+\gamma_3\right) - h_2\right) \tag{70}$$

and it can be shown that,

$$C = \frac{\Delta p}{g\tau}\,\frac{\left(h_1 - E_{n3}\right)}{\left[\eta\left(1+\gamma_3\right)\left(C_p + \frac{\textcircled{H}_3 + \textcircled{H}_2}{2}\right) + \left(\frac{h_1 + h_2}{2}\right)\right]} \tag{71}$$

For the type 3 convection one can obtain,

$$C = \frac{1}{\tau}\,\frac{\left(h_1 - E_2\right)}{\left[\left(\frac{2-\gamma_2}{2}\right)\textcircled{H}_1 - \textcircled{H}_2 - L\left(\frac{q_1 - q_2}{2}\right)\right]} \tag{72}$$

Finally for the dry convective adjustment the vertical lapse rate of potential temperature is checked to assure that it be not allowed to become negative. If it does, it must be adjusted in such a manner that the mean potential temperature in the vertical is conserved.

3. Boundary Conditions

The restoration boundary technique used in the FNWC P.E. model was devised by the modellers, and is used in no other P.E. models. The technique is described below and illustrated on the accompanying figure.

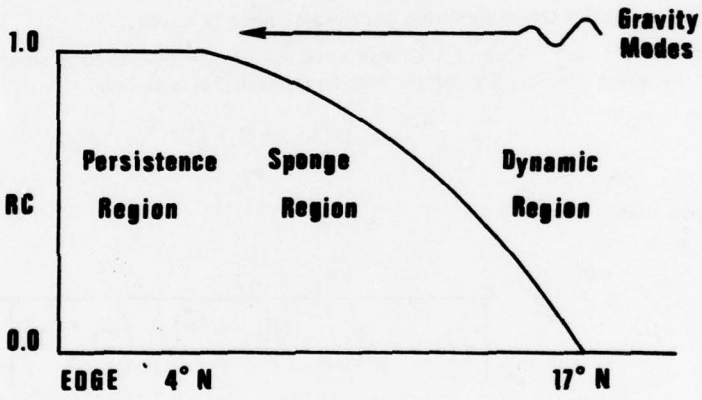
A field of restoration coefficients which vary continuously from unity (at and south of 4 North) to zero (at and north of 17 North) is computed and saved. At the end of each ten-minute time step the new values (just obtained) of all forecast variables are restored back toward their values at the previous time step (in the region south of 17 North) according to the amount specified by the field of restoration coefficients. The net effect of this procedure is to produce a fully dynamic forecast north of 17 North,

a persistence forecast south of 4 North, with a blend in between. The mathematical-physical effect of the technique is that the blend region acts as an energy "sponge" for outwardly propagating inertio-gravity oscillations. The initial fluxes on the grid square boundary are preserved. No restructuring of the tropics is necessary. These boundaries have been used routinely for integrations to three days with no perceptible difficulties in the products.

CONSTANT FLUX, RESTORATION BOUNDARIES

1. **Save initial values of winds, temperatures.**

2. **Compute restoration coefficients (RC).**



3. **After integration, restore variables 'RC' amount toward initial values.**

CONSTANT FLUX, RESTORATION BOUNDARIES. The values of the variables obtained in each time step are returned toward their previous values, in the latitudes indicated, an amount indicated by the field of restoration coefficients.

4. Pertinent Reference

Anyone who has read to this point must have more than a passing interest in P.E. models. Professor G. J. Haltiner's (US Naval Postgraduate School) new book "Numerical Weather Prediction" (Reference 4 of Section 4.8) is an excellent reference for further study. Sections 9.4, 10.4, 11.0, 13.7, and the Appendix of the book are pertinent to the FNWC P.E. model.

APPENDIX M

SCALE AND PATTERN SEPARATION MODEL

The Scale and Pattern Separation program is designed for application to atmospheric mass-structure parameters and their inherent scales: disturbance, long wave, and planetary vortex. The separation of such a parameter, denoted by Φ, may be expressed by

$$\Phi = \Phi_{SD} + \Phi_{SR} \quad , \quad \text{and} \tag{1}$$

$$\Phi = \Phi_{SD} + \Phi_{SL} + \Phi_{SV} \quad . \tag{2}$$

Equation (1) indicates separation into disturbance, SD, and large-scale or residual, SR, components. Equation (2) indicates the additional separation of the large scale into long-wave, SL, and planetary-vortex, SV, components. The separation scales (i.e., cuts) for these components may be specified by values of the linear degree-of-smoothing parameter α; this smoothing parameter enters into basic formulations. The one cut of Eq. (1) is defined as α_R and the further cut of Eq. (2) is defined as α_V.

Formulation

Let Φ be the arbitrary object field. We make Φ dependent on a degree-of-smoothing parameter, α, by the process formulation:

$$\partial\Phi/\partial\alpha = \delta s_*^2 \nabla^2 \Phi \quad . \tag{3}$$

With the grid-length dimension, δs_*, in the formulation, α is non-dimensional. Equation (3), together with

$$\Phi(\alpha) = \Phi \quad \text{for} \quad \alpha = 0 \quad , \tag{4}$$

defines the dependency $\Phi(\alpha)$. The formulation may also be expressed in integral form:

$$\Phi(\alpha) = \Phi + \int_0^\alpha \delta s_*^2 \nabla^2 \Phi \, d\alpha \quad . \tag{5}$$

The operational Beta program produces third-degree-steepness scale separation. The residual component is accordingly given by

$$\Phi_{SR} = 3\Phi(\alpha_R) - 3\Phi(2\alpha_R) + \Phi(3\alpha_R) \quad . \tag{6}$$

Its determination requires the integration of Eq. (5) to degree-of-smoothing amounts α_R, $2\alpha_R$ and $3\alpha_R$. The planetary-vortex component is given by

$$\Phi_{SV} = 3\Phi(\alpha_V) - 3\Phi(2\alpha_V) + \Phi(3\alpha_V) \quad , \tag{7}$$

requiring further integration of Eq. (5) out to a maximum of $3\alpha_V$.

Numerical Analogues

As numerical analogue for the operator $\delta s_*^2 \nabla^2$ the numerical operator is expressed by

$$m^2 \nabla^2 \tag{8}$$

where ∇^2 denotes the minimal five-point stencil (a minus four with four adjoining plus ones) for the Laplacian, and

$$m = \delta s_* / \delta s \tag{9}$$

is the map factor which is unity at 60°N. This analogue neglects the gradient of m; this is generally permissible provided the field of Φ has enough variance.

The field of Φ is numerically represented by the vector $\underset{\sim}{\Phi}$; each element of the column is a grid-point value taken in some selected order. As partial analogue for Eq. (3) we choose

$$\partial \underset{\sim}{\Phi} / \partial \alpha = \underset{\approx}{F}\,\underset{\approx}{L}\,\underset{\sim}{\Phi} \tag{10}$$

where $\underset{\approx}{L}$ is the matrix equivalent of ∇^2 and $\underset{\approx}{F}$ is the map-factor matrix. The map-factor matrix has zero for all elements except for the main diagonal which has the values of m^2.

The numerical analogue of Eq. (3), or Eq. (5), is complete with the choice of a centered implicit scheme:

$$\underset{\sim}{\Phi}(\alpha + \delta\alpha) = \underset{\sim}{\Phi}(\alpha) + \frac{\delta\alpha}{2}\,\underset{\approx}{F}\,\underset{\approx}{L}\left[\underset{\sim}{\Phi}(\alpha + \delta\alpha) + \underset{\sim}{\Phi}(\alpha)\right] \quad . \tag{11}$$

The application of Eq. (11) involves a matrix inversion in order to achieve an incremental advance $\delta\alpha$. Express the equation by

$$\underset{\approx}{M}\,\underset{\sim}{\Phi} = \underset{\sim}{d} \tag{12}$$

where

$$\underset{\sim}{\Phi} \equiv \underset{\sim}{\Phi}(\alpha + \delta\alpha) \tag{13}$$

$$\underset{\approx}{M} \equiv \underset{\approx}{D}\left(\underset{\approx}{I} - \frac{\delta\alpha}{2}\,\underset{\approx}{F}\,\underset{\approx}{L}\right) \tag{14}$$

$$\underset{\sim}{d} \equiv \underset{\approx}{D}\left(\underset{\approx}{I} + \frac{\delta\alpha}{2}\,\underset{\approx}{F}\,\underset{\approx}{L}\right)\Phi(\alpha) \tag{15}$$

The matrix $\underset{\approx}{D}$ is one in which only the main-diagonal elements are non-zero; it appears as a factor in order to make all main-diagonal elements of $\underset{\approx}{M}$ equal to minus one. It is convenient to invert $\underset{\approx}{M}$ by the method of successive overrelaxation which is an iterative method of successive approximations of Φ.

Expand the matrix $\underset{\approx}{M}$ into

$$\underset{\approx}{M} = \underset{\approx}{A} + \underset{\approx}{B} - \underset{\approx}{I} \tag{16}$$

where $\underset{\approx}{A}$ has non-zero elements only above the main diagonal, $\underset{\approx}{B}$ has non-zero elements only below the main diagonal, and $\underset{\approx}{I}$ is the identity matrix. The method of successive overrelaxation may be expressed by

$$\underset{\sim}{\Phi}^{(r+1)} = \underset{\sim}{\Phi}^{(r)} + \omega\,\underset{\sim}{R}^{(r+1/2)} \tag{17}$$

where the residual is defined by

$$\underset{\sim}{R}^{(r+1/2)} = \underset{\approx}{B}\,\underset{\sim}{\Phi}^{(r+1)} + \underset{\approx}{A}\,\underset{\sim}{\Phi}^{(r)} - \underset{\sim}{\Phi}^{(r)} - \underset{\sim}{d} \tag{18}$$

and ω is known as the relaxation factor. We begin the iterations with $\underset{\sim}{\Phi}^{(0)} = \underset{\sim}{\Phi}(\alpha)$. N iterations are performed as determined by the required accuracy.

The best relaxation factor is given by

$$\omega = 1 + \left[\frac{\bar{q}^{\,2}}{1 + \left(1 - \bar{q}^{\,2}\right)^{1/2}}\right]^2 \tag{19}$$

where

$$\bar{q} \approx \frac{2\,\delta\alpha}{2\,\delta\alpha + 1} \tag{20}$$

The number of iterations required for adequate accuracy is

$$N \geq \frac{\ln 0.02}{\ln(\omega - 1)} \tag{21}$$

APPENDIX O

SEA-SURFACE TEMPERATURE ANALYSIS (FIB)

1. Introduction

The analysis scheme requires a first-guess field, T_G, the adjunct independent reliability, A_G, and first-guess gradients and associated reliabilities, μ^*, B^*, ν^*, C^*. The initialization phase, 2-6 below, is directed toward development of these fields.

Formulas used in the SSTFIB field computations are discussed in order of Flow of Operations. The basic ℓ,m module is shown in Figure O.1. Once explained, symbol meaning will not be repeated; refer to preceding equations as necessary. Adjustable parameters in the formulas that follow are designated by underlined symbols.

2. First-Guess Temperature Field

The preceding analysis, $T^*_{-\tau}$, is tended toward climatology, T_C, to improve its prediction value. T_C is computed for each analysis time as a weighted mean, with the current month having a weight of 1/2 and the preceding and following months having a combined weight of 1/2. In month M,

$$T_c = \frac{1}{2}\left(T_M + \left(1 - \frac{h}{H}\right) \cdot T_{M-1} - \frac{h}{H} \cdot T_{M+1}\right) \qquad (1)$$

where h is the hour of the month, H is total hours in the month, and T_C is the interpolated climatological temperature for the analysis time.

The first-guess temperature field, T_G, comes from the combination

$$T_G = (1-F) \cdot T^*_{-\tau} + F \cdot T_C \quad , \qquad (2)$$

where F is the proportional weight assigned to climatology. F is reduced in areas of strong gradients of T_C, where major anomalies might be expected, by

$$F = \frac{\underline{\sigma_c^2} \cdot F_{max}}{\underline{\sigma_c^2} + \underline{f_1}\left(\mu^2_{\ell,m} + \nu^2_{\ell,m} + \mu^2_{\ell,m-1} + \nu^2_{\ell-1,m}\right)_C} \quad , \qquad (3)$$

where σ_c^2 = variance of climatology,

f_1 = adjustable parameter, and

μ and ν = climatological gradients.

3. First-Guess Gradient Fields

To decay small-scale anomalies caused by sporadic reports in data-sparse areas, the climatic anomaly is very lightly smoothed to yield the base field, T_B, from which the first-guess gradients, μ^* and ν^* are obtained as single differences

$$T_B = \left(T_G - T_c\right)_{\text{SMOOTHED}} + T_c \quad . \tag{4}$$

4. Reliability of First-Guess Temperature Field

At each grid point the variance of the preceding analysis, $\sigma^{*2}_{-\tau}$, is augmented by the variance caused by local processes, σ^2_{loc}, and from advection, σ^2_{adv}:

$$\sigma^{*2}_G = \sigma^{*2}_{-\tau} + \sigma^2_{\text{loc}} + \sigma^2_{\text{adv}} \quad , \tag{5}$$

where σ^{*2}_G is the variance of the first-guess field. The last term is gradient-dependent, its value estimated by the mean gradient surrounding the point:

$$\sigma^2_{\text{adv}} = f_2 \cdot \frac{1}{4}\left(\mu^2_{\ell,m} + \mu^2_{\ell,m-1} + \nu^2_{\ell,m} + \nu^2_{\ell-1,m}\right)_{-\tau} \quad , \tag{6}$$

where f_2 is the mean grid-length displacement in τ hours. In order to recover the reliability, A_G, of the first-guess field, the ratio of the variances of the independent information and the blended information is assumed to be unchanged during the variance growth process:

$$\frac{\sigma^2_G}{\sigma^{*2}_G} = \frac{\sigma^2_{-\tau}}{\sigma^{*2}_{-\tau}} \quad . \tag{7}$$

Eliminating σ^{*2}_G in Eq. (5) yields the desired first-guess reliability

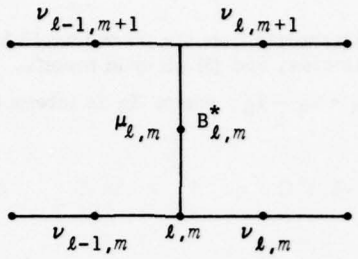
$$A_G = A_{-\tau}\left[1 + A^*_{-\tau}\left(\sigma^2_{\text{loc}} + \sigma^2_{\text{adv}}\right)\right]^{-1} \quad . \tag{8}$$

5. First-Guess Gradient Reliability

The error variance of μ^* is composed of local and advective components. The latter can be further divided into translational and rotational components. This can be expressed by

$$\left(B^*_{\ell,m}\right)^{-1} = \sigma^2_{\text{BC}} + f_3\,\mu^2_{\ell,m} + f_4\,\overline{\nu^2_{\ell,m}} \quad , \tag{9}$$

where the terms on the right side represent local, translational, and rotational components respectively. $\overline{\nu^2_{\ell,m}}$ is defined as the mean square of the four surrounding ν's as shown in the figure below.



Evaluation of $B^*_{\ell,m}$. The grid point is shown by ℓ,m. The The μ and ν values are shown at the midpoints of their respective influence areas.

Similarly,

$$\left(C^*_{\ell,m}\right)^{-1} = \underline{\sigma^2_{BC}} + \underline{f_3}\,\nu^2_{\ell,m} + \underline{f_4}^2\,\overline{\mu^2_{\ell,m}} \quad . \tag{10}$$

6. The Analysis Field

T_B (3, above) is the chosen base field. The object difference field, $\mathfrak{J}$, is defined by

$$\mathfrak{J} = T - T_B \quad . \tag{11}$$

The first-guess difference field, $\mathfrak{J}_o$, is given by

$$\mathfrak{J}_o = T_G - T_B \quad . \tag{12}$$

The weight field of $\mathfrak{J}_o$ is that of T_G, namely A_G. Observations (subscripted n) are transformed into difference values:

$$\mathfrak{J}_n = T_n - T_B \text{, with weight } A_n \quad , \tag{13}$$

where T_B is interpolated to station location.

Upon completion of the analysis field, the product field, T^*, is recovered:

$$T^* = \mathfrak{J}^* + T_B \tag{14}$$

where superscript * indicates that the field is the result of a blending operation.

7. Data Preparation

All ship and bathythermograph reports from the preceding 12 hours are screened to eliminate (1) reports not containing SST, (2) duplicates, and (3) off-grid reports.

Then, T_n is converted to $\mathfrak{T}_n = T_n - T_B$, where T_B is interpolated to station location. The report is withheld if

$$T_n < -2.1°C \quad , \quad T_n > 34°C \qquad \text{or}$$

$$\mathfrak{T}_n > \underline{\delta T} + f_5 \left(\mu^2_{\ell,m} + \mu^2_{\ell,m-1} + \nu^2_{\ell,m} + \nu^2_{\ell-1,m} \right)^{1/2}_c$$

as determined at the nearest grid point.

Report reliabilities are assigned. The reliability is a function of the contributing variances

$\underline{\sigma^2_o}$ for class of report

$\underline{\sigma^2_2}$ for age of report

$\underline{\sigma^2_3}$ for station location uncertainty

$\underline{\sigma^2_4}$ for uncertainty in extrapolation to nearest grid point.

Since magnitude of the latter two increases with gradient, they are combined:

$$\sigma^2_1 = \sigma^2_3 + \sigma^2_4 = \underline{f_6} \cdot \frac{1}{2} \left(\mu^2 + \nu^2 \right)_B \qquad (15)$$

where μ^2 and ν^2 are those nearest the observation and $\underline{f_6}$ is a function of the average position displacement of the grid point.

The variance due to age is composed of local and advective components and is

$$\sigma^2_2 = \delta t \left[\underline{f_7} + \frac{1}{2} \cdot \underline{f_8} \left(\mu^2 + \nu^2 \right)_B \right] \qquad (16)$$

where δt is age of the report in hours.

Report reliability is then

$$A_n = \left(\underline{\sigma^2_o} + \sigma^2_1 + \sigma^2_2 \right)^{-1} \qquad (17)$$

The final step is to reduce report weights for quasi-duplication. This is necessary when there are a number of nonidentical observations from the same reporting platform (e.g., 3 hourlies from a station ship). Weights are reduced so that the combined reliability relates to that for a single report.

8. Assembly

Each report that has passed the initial gross error checks and passes a land/sea check is assembled at the nearest grid point. The report $\mathcal{J}_n$, A_n is added to the accrued information (initially $\mathcal{J}_o$, A_o) to produce the new resultant

$$\mathcal{J}_N = \frac{A_n \mathcal{J}_n + A_{N-1} \mathcal{J}_{N-1}}{A_N} \quad , \tag{18}$$

$$A_N = A_n + A_{N-1} \quad , \tag{19}$$

where N refers to the stage of the assembly and n to the single report.

9. Blending for $\mathcal{J}^*$

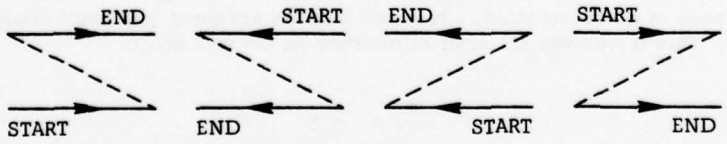
The blending equation for $\mathcal{J}^*$ is

$$\begin{aligned} \mathcal{J}^*_{\ell,m} = S^{-1}_{\ell,m} \Big[& A_{\ell,m,N} \mathcal{T}_{\ell,m,N} \\ & + \Big\{ B_{\ell,m} \mathcal{J}^*_{\ell,m+1} + C_{\ell,m} \mathcal{J}^*_{\ell+1,m} \\ & + B_{\ell,m-1} \mathcal{J}^*_{\ell,m-1} + C_{\ell-1,m} \mathcal{J}^*_{\ell-1,m} \Big\} \Big] \end{aligned} \quad , \tag{20}$$

where

$$S_{\ell,m} \equiv A_{\ell,m} + B^*_{\ell,m} + C^*_{\ell,m} + B^*_{\ell,m-1} + C^*_{\ell-1,m} \quad . \tag{21}$$

The method of solution is iterative; successive approximations for $\mathcal{J}^*$ are substituted on the right-hand side as they are calculated for each module. The ordering for each pass follows the sequence:



The initial guess value for $\mathcal{J}^*_{\ell,m}$ is $\mathcal{J}_{\ell,m,N}$, where N refers to the final assembled value.

10. Solution for A^*

In terms of $\mathfrak{I}$,

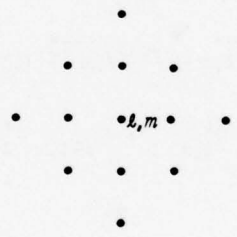
$$A^*_{\ell,m} = A_{\ell,m}\,\delta\mathfrak{I}_{\ell,m}/\delta\mathfrak{I}^*_{\ell,m} \quad . \tag{22}$$

The method requires the specification of $\delta\mathfrak{I}_{\ell,m}$ and recomputation of $\mathfrak{I}^*_{\ell,m}$. If we set $\delta\mathfrak{I}_{\ell,m} = A^{-1}_{\ell,m}$ then

$$A^*_{\ell,m} = \delta\mathfrak{I}^{*\,-1}_{\ell,m} = \left(\mathfrak{I}^*_{\text{mod}} - \mathfrak{I}^*\right)^{-1}_{\ell,m} \quad , \tag{23}$$

where $\mathfrak{I}^*_{\text{mod}}$ refers to the recomputed $\mathfrak{I}^*$.

After testing various subsets for the $\mathfrak{I}^*_{\text{mod}}$ blending, the 13-point diamond shown below was selected as a balance between adequacy and economy. Convergence is expedited by increasing $\mathfrak{I}^*_{ij}$ by an amount proportional to $A_{\ell,m}$ throughout the subset. (Note that ℓ,m refers to the center point of the subset while i,j are dummies for the subset.) The iterations are performed in an ordered sequence designed for rapid convergence.



A^* Computation Grid

11. Second Gross Error Check and Reevaluation

After the first analysis of $\mathfrak{I}^*$ and determination of A^*, an additional gross error check is made on each observation and, for each accepted report, the reliability, A_n, is reevaluated.

The influence of an observation is removed from its assigned grid point resulting in background values T_b, A_b. This represents all other information at the grid point:

$$A_b = A^* - A_{np} \quad , \tag{24}$$

$$\mathfrak{I}_b = \frac{A^*\mathfrak{I}^* - A_{np}\mathfrak{I}_n}{A_b} \quad , \tag{25}$$

where A_{np} is assembled weight; i.e., reduced for quasi-duplication.

$\mathcal{J}_n$, A_n and $\mathcal{J}_b$, A_b are mutually independent and the variance of $\mathcal{J}_b - \mathcal{J}_n$ is

$$\sigma_o^2 = \sigma_b^2 + \sigma_n^2 = \frac{A_b + A_n}{A_b A_n} \quad . \tag{26}$$

Note that the class weight is used above since a class variance is being determined; A_{np} is used only to determine background values.

A measure of the actual difference in terms of the standard difference is given by

$$\lambda \equiv \frac{\mathcal{J}_b - \mathcal{J}_n}{\sigma_o} \qquad \text{and} \tag{27}$$

$$\lambda^2 = \frac{A_n A_b}{A_n + A_b} \left(\mathcal{J}_b - \mathcal{J}_n\right)^2 \quad . \tag{28}$$

If $\lambda^2 > \lambda^2_{\underline{max}}$ the report is rejected.

If $\lambda^2 < \lambda_{\underline{max}}$ the reliability is reevaluated by

$$A_{nR} = \frac{2 A_n}{1 + \lambda^2} \tag{29}$$

with the requirement $A_{nR} \leq A_{nj}$; i.e., no increase in reliability is allowed simply on the basis of an actual difference smaller than the standard difference.

By a similar analysis, λ^2 for the first-guess reliability, A_G, is found to be

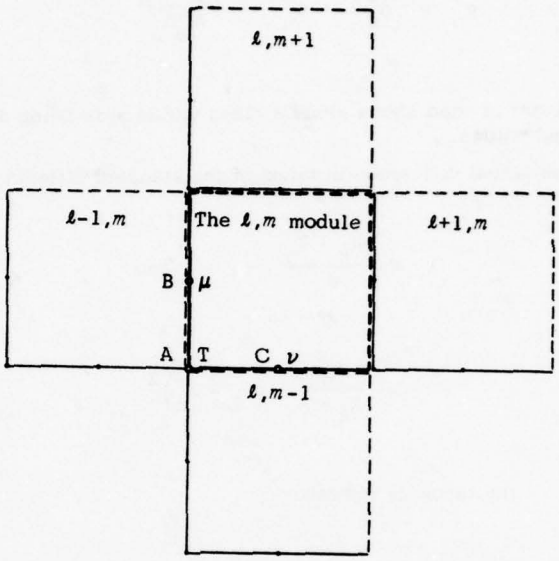
$$\lambda^2 = \frac{A^* A_G}{A^* - A_G} \left(\mathcal{J}^* - \mathcal{J}_G\right)^2 \quad , \tag{30}$$

and

$$A_{GR} = \frac{2 A_G}{1 + \lambda^2} \tag{31}$$

with the requirement $A_{GR} \leq A_G$.

FIB/SST



The arbitrary ℓ,m area module (consisting of one corner point, two sides, and the interior area) and adjoining modules. Reference locations in the module are shown for the Sea-Surface Temperature parameter, $T_{\ell,m}$, and the finite-difference parameters:

$$\mu_{\ell,m} = T_{\ell,m+1} - T_{\ell,m} \quad \text{and} \quad \nu_{\ell,m} = T_{\ell+1,m} - T_{\ell,m}$$

The respective reliabilities of T, μ, ν values are denoted by A, B, and C; the reliability of a value is defined as the inverse of the error variance associated with the value.

FIGURE O.1

APPENDIX P
SINGULAR SEA/SWELL MODEL

Equations used in the Sea/Swell model will be discussed below in the same order that they are used in the program computation.

1. Geostrophic Wind Equation on a Geopotential Surface

$$\mathbf{k} \times \mathbb{W}_g = -\frac{1}{f\rho} \nabla_z p \tag{1}$$

where z = 0, since operations are at the surface,

$\mathbf{k}$ = vertical unit vector,

$\mathbb{W}_g$ = geostrophic wind,

f = coriolis parameter, and

ρ = density.

2. Computation of $\partial p/\partial x$ and $\partial p/\partial y$ Gradients

To achieve maximum pressure gradient continuity, the gradient is computed by a fourth order equation

$$\frac{\partial p}{\partial X} = \frac{1}{12}\left(p_{n-2} - 8p_{n-1} + 8p_{n+1} - p_{n+2}\right) \tag{2}$$

where X is the horizontal coordinate (x or y) and n refers to the applicable grid coordinate (i or j). The appropriate map factor and other constants must be applied.

3. Curvature Correction to Wind

$$V_G = \sqrt{u^2 + v^2} \tag{3}$$

where V_G = geostrophic wind velocity, u and v = components of the geostrophic wind.

$$R = \frac{V_G^3}{u\left[\frac{\partial v}{\partial t} + u\frac{\partial v}{\partial x} + v\frac{\partial v}{\partial y}\right] - v\left[\frac{\partial u}{\partial t} + u\frac{\partial u}{\partial x} + v\frac{\partial u}{\partial y}\right]} \tag{4}$$

where R = radius of curvature of trajectory,

$$V_{gr} = \frac{Rf}{2}\left(\sqrt{1 + \frac{4V_G}{Rf}} - 1\right), \tag{5}$$

where V_{gr} = gradient wind speed, and

f = coriolis parameter.

4. Corrected Surface Wind Speed and Direction

$$V_c = |\mathbb{W}_{gr}| \left(k_1 - k_2 \mathbb{W}_{gr} \cdot \nabla T - k_3 T\right) \quad , \quad \text{and} \tag{6}$$

$$\theta = \theta_g - k_4 - k_5 \sin\left(\frac{k_6 \pi}{2} \mathbb{W}_{gr} \cdot \nabla T\right) - k_7 T \quad , \tag{7}$$

where $\mathbb{W}_{gr}$ = gradient wind vector,

V_c = corrected surface wind speed,

θ_g = the gradient wind direction.

θ = corrected surface wind direction,

T = sea surface temperature, and

k's = are empirical constants.

5. Weighted Winds (a duration substitute)

Winds in the Sea/Swell model are weighted toward the current time by

$$\bar{u}_t = a u_t + (1 - a)\, \bar{u}_{t-\Delta t} \quad , \quad \text{and} \tag{8}$$

$$\bar{v}_t = a v_t + (1 - a)\, \bar{v}_{t-\Delta t} \tag{9}$$

where u, v are the wind components at output time and $\bar{u}$, $\bar{v}$ are the time weighted components used to generate waves.

Weighted wind components are carried forward from previous analyses. In the twice-daily synoptic runs, Δt = 12 hrs and a = 0.7 which results in a weighting of 70% for current winds, 21% of 12-hr-old, 6.3% for 24-hr-old, etc.

6. Generation of Wind Waves

The equation relating wave height and wind speed is

$$H_{w\ 1/3} = 7\left[\left(\frac{\bar{V}}{10}\right)^2 - \left(\frac{\bar{V}}{20}\right)^{3.3}\right] + 1 \tag{10}$$

where $H_{w\ 1/3}$ = average height of highest 1/3 waves in feet, and

V = weighted wind speed in meters per second.

The average period of wind waves varies linearly with wind speed, by the expression

$$P_w = \frac{\bar{V}}{2} + 2 \quad ,$$

where P_w = average period in seconds.

A fetch correction is applied in regions of offshore flow. The correction is proportional to the wind speed and the upwind distance to land or ice. 100% development occurs in distance

$$D(\text{naut. miles}) = 2V(0.4V-1) = 0.8V^2 - 2V \qquad V(\text{m/sec}) \tag{11}$$

$$V_f = 1.25\ (1 + \sqrt{1 + 0.8D}) \tag{12}$$

where V_f is highest velocity for which full development can occur at D.

7. Decay, Period, and Speed of Swell

Swell is decayed along great-circle paths by the equations

$$H_s(t) = H_w \left[(1+a) - a \log_{10}(t+10)\right] \quad \text{and} \tag{13}$$

$$P_s(t) = P_w \left[(1-b) + b \log_{10}(t+10)\right] , \tag{14}$$

where $H_s(t)$ and $P_s(t)$ are the swell height and period, respectively, after t hours of decay from initial wave height and period H_w and P_w.

The speed at which swell moves is half the phase velocity, or

$$u = \frac{g}{4\pi} P_w \tag{15}$$

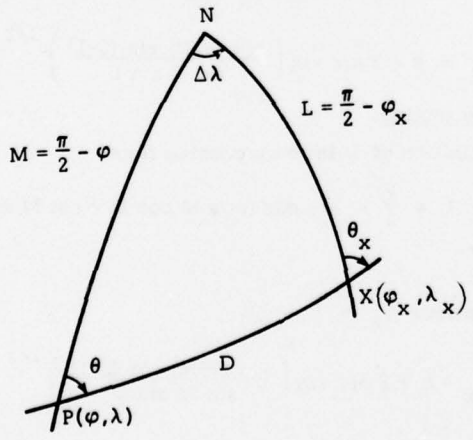
with a resultant travel distance,

$$D \approx 1.5\, t\, P_w \tag{16}$$

where D is in nautical miles and t is in hours.

8. Swell Movement on a Great-Circle Path

The method by which swell is moved on a great-circle path may be described as follows. The initial location (latitude and longitude), geographic direction of movement and distance of movement are given information. Position and direction of movement at the end of travel is required. The figure below shows the problem in terms of a spherical triangle with its vertex at the North Pole. Sides D, L, and M are great circles, as required in a spherical triangle. L and M are also the λ and λ_x meridians. D is the specified great-circle path.



Spherical triangle representation of great-circle problem.

Definitions are as follows:

θ - starting direction, towards (45° is towards northeast) (If $\theta > 180°$, θ is transformed to $360° - \theta$ and $\Delta\lambda$ is considered negative.)

D - travel distance (radians) ($D_{radians} = D_{naut.mi.}/3437.87$)

M - distance to pole of starting point (radians)

L - distance to pole of terminal point (radians)

N - North Pole

P - starting point (lat = φ, long = λ)

X - terminal point (lat = φ_x, long = λ_x)

$\Delta\lambda$ - change in longitude

θ_x - terminal direction (towards)

By the law of cosines for spherical triangles:

$$\cos L = \cos M \cos D + \sin M \sin D \cos \theta \tag{17}$$

Let

$$S \equiv (M + D + L)/2$$

Then the half angle sine formula gives:

$$\sin \frac{\Delta\lambda}{2} = \left[\frac{\sin (S-M) \sin (S-L)}{\sin M \sin L}\right]^{1/2}$$

Transforming:

$$\Delta\lambda = 2 \arcsin \left(\frac{\sin (S-M) \sin (S-L)}{\sin M \sin L}\right)^{1/2} \tag{18}$$

The half angle sine formula for the complement of θ_x leads to:

$$\theta_x = \pi - 2 \arcsin \left(\frac{\sin (S-D) \sin (S-L)}{\sin D \sin L}\right)^{1/2}$$

which is the required terminal direction.

From Eq. (17) and the definition of L in the preceding figure

$$\varphi_x = \frac{\pi}{2} - L = \frac{\pi}{2} - \arccos (\cos M \cos D + \sin M \sin D \cos \theta) \tag{19}$$

which is the final latitude.

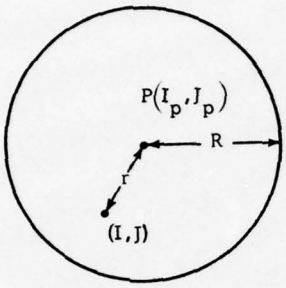
From Eq. (18) and the relation: $\lambda_x = \lambda + \Delta\lambda$,

$$\lambda_x = \lambda + 2 \arcsin \left(\frac{\sin (S-M) \sin (S-L)}{\sin M \sin L}\right)^{1/2} \tag{20}$$

which represents the final longitude.

9. Spreading the Swell

Once the end position of a great circle segment has been computed by the above method, the swell height is spread to surrounding grid point location (I,J) in accordance with the following figure and discussion.



Schematic representation of terminal swell point P, circle of radius R (see test) and an arbitrary grid point (I,J)

Definitions are:

P - exact location of terminal point (fractional I,J)

r - distance from P to grid point (integer I,J) in mesh lengths

R - radius of circle = KD

where D is distance (mesh lengths) swell has traveled from origin, and

K = 1.0 if swell age is 12 hrs

K = 0.7 if swell age is 24 hrs

K = 0.4 if swell age is 36 hrs

K = 0.3 if swell age ≧ 48 hrs

The swell height at any point (I,J) surrounding P for which $r < R$ is

$$H_s(I,J) = H_s(P)\,\frac{R^2 - r^2}{R^2} \quad . \tag{21}$$

where

$$r = \left[\left(I_P - I\right)^2 + J_P - J^2\right]^{1/2} \text{ (mesh lengths)} \quad . \tag{22}$$

10. Combined Height

The combined height is defined as

$$H_C = \left(H_w^{\,2} + H_s^{\,2}\right)^{1/2} \quad . \tag{23}$$

VIII GLOSSARY

GLOSSARY

Words included in this glossary are selected from those appearing without definition in the Products Manual. Words undefined in the text but defined in the AMS Glossary of Meteorology are not included here except in a few cases where a less technical definition might be helpful.

AFTERNOON EFFECT: See Transient Thermocline.

ALGORITHM: A statement of the step-by-step procedure for solving complex problems by simple steps. An unambiguous set of directions specifying a sequence of operations designed to solve a particular type of problem. OTSR, for example, forecasts routes using the Global Constrained Minimum-Time Route (GMTR) algorithm. The algorithm tells what input data to use, what computations to make, and the order in which computations are to be made.

ALPHANUMERIC: For alphabetic-numeric. A set of characters including letters, numerals, and special symbols. A teletype weather report is an alphanumeric message.

AMBIENT: Ambient means surrounding on all sides. Ambient temperature means the temperature of the air surrounding the thermometer. Ambient noise means the noise from all sides that reaches a listening device--noise from ships, waves, animal life, etc.

ANCILLARY EQUIPMENT: Same as Peripheral Equipment.

ASSEMBLY: The gathering and weighting of information at grid points prior to a computer analysis. Reports are combined with first-guess information, after passing a Gross Error Check. A weight or reliability is assigned to each piece of information to establish how much it will count in the assembly.

BIT: Binary digit. One of the characters of a two-valued or binary number system.

BLENDING: Synonymous with analyzing--called this because many pieces of data are "blended" into one analysis.

BOGUS REPORT: A "made up" report inserted into a data field so as to influence a portion of an analysis in some desired direction. In a surface pressure analysis, for example, the first pass might come out with a low pressure center that doesn't look deep enough--either from history or from other evidence like satellite pictures or from late reports of some kind. The Command Duty Officer or Environmental Watch Officer corrects by making up a report with appropriate pressure for a selected position. This bogus report goes into the next analysis pass as though it were a real report, and forces the analysis to be modified in the trouble spot.

BYTE: A small group of adjacent binary digits (bits), such as 4, 6, or 8 bits, that form a unit of information. A 6-bit byte might be used to specify a letter of the alphabet.

CONVERGENCE ZONES (Acoustical): Zones near the ocean surface where sound rays are focused through the effects of refraction. High sound intensities occur in convergence zones--good for submarine detection. Convergence zones typically occur at 30-35 mile intervals down-range from the sound source, with gains of 10-15 decibels in the zone.

COVARIANCE: A measure of the tendency of two values to vary in the same way. In numerical analysis, spatial covariance is an expression of how strongly the change at a grid point affects an adjacent grid point.

DERIVATIVE: When one variable is dependent upon another, the derivative measures the instantaneous rate of change of the first variable with respect to the second. For example, the distance a moving object travels increases with time. The speed of travel represents the change of distance with time, and is a derivative.

DERIVATIVE, PARTIAL: A partial derivative is like an ordinary derivative for the case where there are many variables and one or more are held constant. For example, the vertical pressure gradient is a partial derivative that measures the rate of change with height; but the horizontal coordinates, x and y, are kept fixed when computing this derivative.

DIFFERENTIAL EQUATION: An equation containing one or more derivatives.

DISCRETE: Separate and distinct, discontinuous. Values of 2.0, 2.3, 2.6, 2.8, and 3.0 are discrete values as opposed to saying any value between 2 and 3.

DYNAMICAL FORECASTING: Same as numerical forecasting.

EMPIRICAL: A system or scheme based on observational or factual information rather than theoretical knowledge. The equations used to forecast growth of wind waves are based on thousands of wave height observations taken under rigidly selected and prescribed conditions. Some of the old weather proverbs are good examples of empirically developed forecasting tools. "When the sun is in its house (halo), it will rain soon." The old-timers observed many cases of rain following a halo, and set up the rule, not knowing that the halo came from refraction of light through the ice crystals of a cirrostratus layer and that cirrostratus are often the first sign of an approaching warm front.

FINITE: Limited, restricted, bounded. Used in "a finite distance" as meaning a limited, defined distance. A finite number of grid points would mean a limited or certain number of grid points.

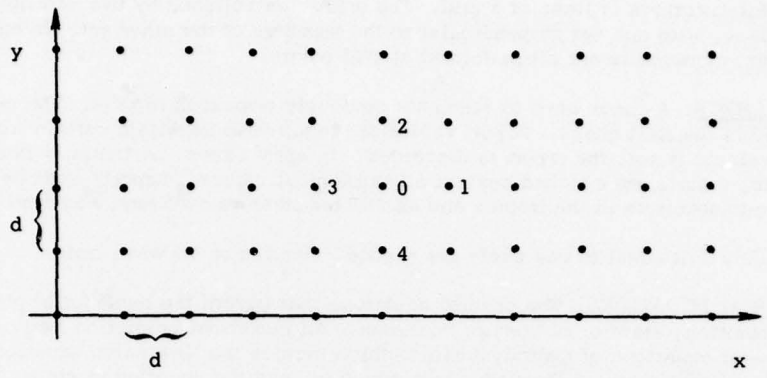
FINITE DIFFERENCE METHOD: The finite difference method is a purely numerical method for solving differential equations. The general hydrodynamical equations are nonlinear, and not solvable by exact analytic methods. Only the finite difference method will do the job.

The method consists of:

1. Representing the distribution of each dependent variable (viz., pressure or temperature) by its values at a finite number of regularly spaced points (grid points).
2. Replacing the derivative of each variable by the corresponding ratio of finite increments--i.e., the difference between the values of the variable at adjacent grid points divided by the distance.
3. Solving the system of finite difference equations. In general, the solution of a finite difference equation more and more closely approaches the solution of the corresponding differential equations as the grid interval is made smaller and smaller.

As a simple illustration of the finite-difference method, consider the finite difference equivalent of $(\partial p/\partial x)$. (This is the same method used for computing the geostrophic wind components from height gradients.)

Begin by considering the values of p at discrete points spaced a distance d apart in the x-direction, as shown in the figure.



Grid for Finite-Difference Solution

The point at which $(\partial p/\partial x)$ is to be computed is arbitrarily labeled "zero", and the points immediately to the right, above, to the left, and below are labeled 1, 2, 3, and 4 respectively. The values of p at those points will be denoted by corresponding subscripts. Now, by definition, $(\partial p/\partial x)$ at the point "zero" is the value toward which $[(p_1 - p_3)/2d]$ tends as d becomes infinitesimally small. That is,

$$\frac{\partial p}{\partial x} = \lim_{d \to \epsilon} \frac{p_1 - p_3}{2d} \quad , \quad (\epsilon = 0)$$

The essence of the finite-difference method is that the equation above is very nearly correct even if ϵ is finite, provided it is fairly small in comparison with the distance between adjacent maxima and minima of p. Subject to this proviso, $(\partial p/\partial x)$ is approximately

$$\frac{\partial p}{\partial x} \approx \frac{p_1 - p_3}{2d} \quad \text{(for small d)}$$

Similarly, if the gridpoints are spaced a distance d apart in the y direction,

$$\frac{\partial p}{\partial y} \approx \frac{p_2 - p_4}{2d}$$

By following the same general procedure, the time derivative of any quantity may be expressed in terms of its values at successive and closely spaced instants in time.

FIRST GUESS: An estimate of what an analysis will be without considering current data. The first guess provides continuity into data-sparse areas, gives an estimate of the shape of the field, and is a base for testing the credibility of synoptic reports.

FORMULATE: As used in the Products Manual, to describe or define a problem mathematically. The equations (formulations) are used in a computer program or model to solve the problem.

GRID POINT: Intersections of lines of a grid. The grid is established by two parallel sets of lines in the same plane, with one set perpendicular to the members of the other set. In environmental models, computer calculations are all performed at grid points.

GROSS ERROR CHECK: A check used to eliminate obviously erroneous reports. The most frequently used standard is the first guess. Report values are required to be within certain limits of the first-guess values; if not, the report is discarded. In some cases, particularly in oceanographic analysis, reports are matched against climatological values. Reports must be realistic. A freezing temperature in the tropics and an SST temperature over land would be thrown out.

HERTZ: Frequency unit equal to one cycle per second. Applies to all wave motion.

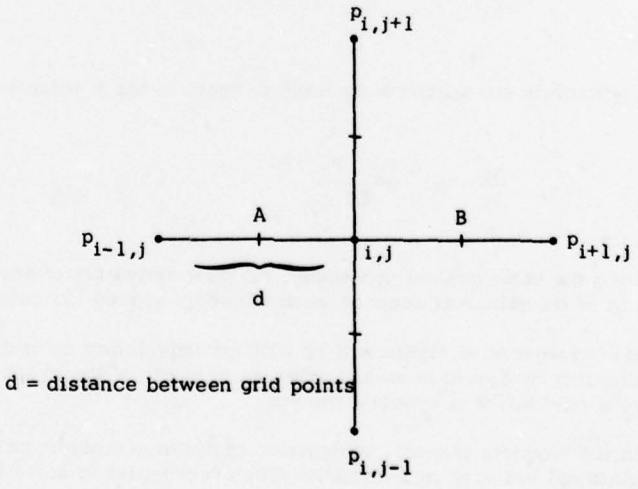
HYDRODYNAMICAL EQUATIONS: The general equations that govern the behavior of all fluids, irrespective of composition, state of motion, or container. All numerical prediction methods are derived from the general equations of hydrodynamics, which include the Newtonian equations of motion, the equation of continuity, a thermodynamic equation, and the equation of state.

INHERENT: Structural or involved in the constitution or essential character of something. A built-in characteristic. The inherent error in a class of observations means that these observations will always fluctuate about a true value because of some built-in flaw in the observation system or people who observe.

INPUT: As a noun, input refers to data to be processed or operated upon by the computer. As a verb, input is the process of transferring data from external storage to internal storage of a computer.

ITERATE: Used in mathematics for "repeat". Repeated execution of a series of steps. A simple example would be to extract the square roots of a series of numbers. The formula for extracting the square root doesn't change; it is used over and over. The iterative process is usually repeated until some mathematical condition is satisfied, as in the relaxation process.

LAPLACIAN: The Laplacian is an elliptic partial differential equation, $\nabla^2 \varphi = 0$, where φ is a scalar function of position and ∇^2 is the Laplacian operator. The Laplacian is a measure of the curvature or rate of change of the gradient of the field.



$\frac{\partial p}{\partial x}$ is the rate of change or gradient along the x axis. The centered finite difference approximation at A is given by

$$\left(\frac{\partial p}{\partial x}\right)_A = \frac{p_{i,j} - p_{i-1,j}}{d} \quad . \qquad (1)$$

At B:

$$\frac{\partial p}{\partial x} = \frac{p_{i+1,j} - p_{i,j}}{d} \quad . \qquad (2)$$

The second derivative, which gives the rate of change of the gradient, is given by

$$\left(\frac{\partial^2 p}{\partial x^2}\right)_{i,j} = \frac{\left(\frac{\partial p}{\partial x}\right)_B - \left(\frac{\partial p}{\partial x}\right)_A}{d^2} \quad , \qquad (3)$$

or, from (1) and (2) above

$$\left(\frac{\partial^2 p}{\partial x^2}\right)_{i,j} = \frac{p_{i+1,j} + p_{i-1,j} - 2\,p_{i,j}}{d^2} \quad . \qquad (4)$$

Doing the same steps in the y direction:

$$\left(\frac{\partial^2 p}{\partial y^2}\right)_{i,j} = \frac{p_{i,j+1} + p_{i,j-1} - 2\,p_{i,j}}{d^2} \quad . \qquad (5)$$

Combining (4) and (5) gives the two-dimensional Laplacian

$$\left(\frac{\partial^2 p}{\partial x^2}\right)_{i,j} + \left(\frac{\partial^2 p}{\partial y^2}\right)_{i,j} = \frac{p_{i+1,j} + p_{i-1,j} + p_{i,j+1} + p_{i,j-1} - 4\,p_{i,j}}{d^2} \quad . \qquad (6)$$

LATERAL ERROR CHECK: A method of checking reports against neighboring reports. The assumption made is, for example, that if there are five reports, of which four agree quite well and one doesn't, the non-agreeing report must be wrong and is thrown out of the analysis. The checking method is usually to remove each report from the analysis and compare the report with the remaining background. The difference between the reported data and the background value is compared against a prescribed tolerance.

LINEAR INTERPOLATION: In the Products Manual, linear interpolation most frequently refers to interpolation between grid points. The interpolation is done on a straight line between points, and the values change linearly, as though being picked off from the straight-line plot of a linear equation. If grid point values are 1020 and 1010, the value at midpoint along a straight line between grid points would be 1015.

MICROSECOND: A millionth of a second.

NANOSECOND: One-billionth of a second. 10^{-9} sec.

NORMALIZE: As used in the Products Manual, normalize means: To divide a field or array of values (e.g., temperature) by some standard value, such as the mean, so that the new scaled values are approximately equal to one. If several hundred temperature values, ranging from 67 to 91, had a mean of 80, all values would be divided by 80. This scales the mean to 1; other values would fluctuate within a narrow range on either side of 1.

NUMERICAL FORECASTING: The prediction of meteorological parameters by numerical solution of the hydrodynamic equations governing atmospheric motions. The governing equations are the Newtonian equations of motion, the equation of continuity, first law of thermodynamics, and the equation of state.

OUTPUT: Data that have been processed by a computer; or the process of transferring data from internal to external storage of a computer or to its peripheral equipment.

PARAMETER: Used throughout the Products Manual in the loose sense of standing for almost any quantity or element. In this way, analyzing the parameters just means analyzing the variables concerned--maybe pressure and temperature. Strictly speaking, a parameter is any quantity of a problem that is not an independent variable. It is a variable that is assigned a constant value for a specific purpose or process or equation.

PARAMETERIZATION: Representing physical effects in a dynamic model in terms of selected parameters rather than determining the effects directly as a result of the dynamics of the model. An example is parameterization of atmospheric humidity using cloudiness and temperature. Cloudiness and relative humidity are strongly correlated. Satellites measure cloudiness, so this parameter is used to derive relative humidity. Specific humidity is a function of cloudiness and temperature, and can be obtained from these two satellite-measured parameters. Having relative humidity and specific humidity, there are many possible applications, such as computations of precipitable water, water budget studies, fog forecasting, and in models of the general circulation.

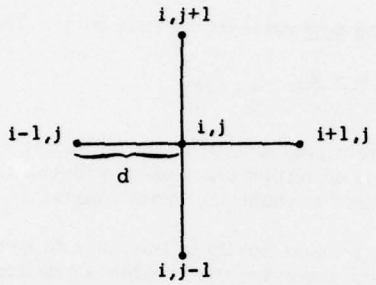
PERIPHERAL EQUIPMENT: All the devices associated with a data-processing system other than the Central Processing Unit (CPU). Peripheral equipment is the means of communication between a computer and the outside world. Peripheral equipment includes such things as magnetic tape units, disc storage units, printers, sorters, card readers, analog-digital converters, and typewriters.

READ IN: To move data from an external device to an internal device. For example, a set of climatological values might be stored on disc or tape. These values are moved from disc or tape to a computer storage position--computer memory--from where they can be used in the active program at the appropriate point in the calculations.

RELAXATION: A numerical method for solving differential equations.

An example is the familiar one of finding temperature distribution on the surface of a slab, given temperatures at the perimeter. The problem requires solution of the Laplacian, a partial differential equation:

$$\frac{\partial^2 T}{\partial x^2} + \frac{\partial^2 T}{\partial y^2} = 0$$



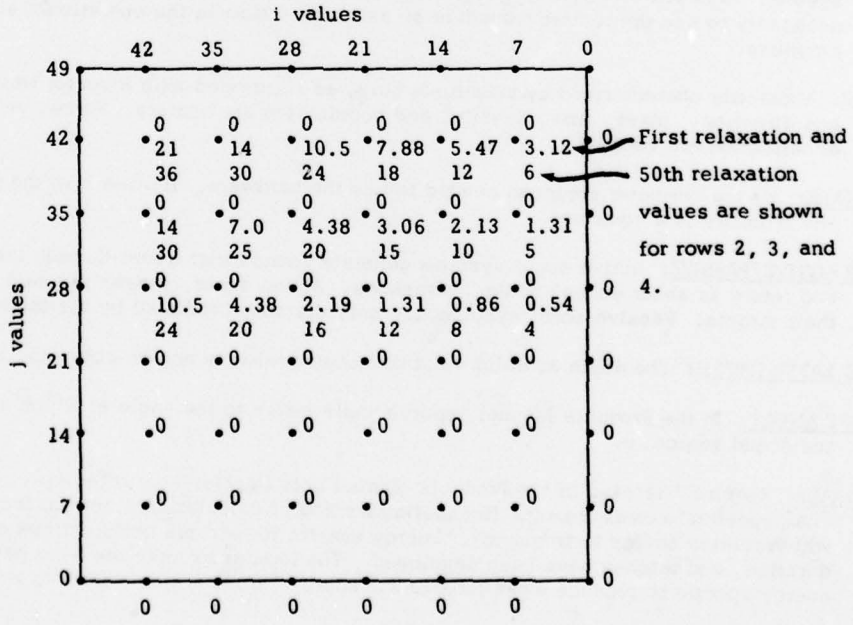
Grid points are identified by the i,j method. The Laplacian becomes:

$$\frac{T_{i,j+1}+T_{i+1,j}+T_{i,j-1}+T_{i-1,j}-4T_{i,j}}{d^2} = 0$$

To simplify the arithmetic assume that d, the distance from grid point to grid point, is a unit distance. Then, solving for $T_{i,j}$, the equation becomes:

$$T_{i,j} = \frac{T_{i,j+1} + T_{i+1,j} + T_{i,j-1} + T_{i-1,j}}{4}$$

This says that the temperature at point i,j is the average of the temperatures at the four nearest grid points, which is a realistic and sensible assumption for this temperature distribution case.



The temperatures along the perimeter are known, and do not change during the calculations. The interior points are the unknowns, all zero to start with. Calculations start with the top left interior point and proceed point by point along the first row, then go to the second row, and continue this way until the first approximation is determined for all grid points. This is one "relaxation" of the relaxation process.

The first point would give:

$$\frac{42 + 0 + 0 + 42}{4} = 21 \quad .$$

The adjacent point is calculated, using the new value at the first point. This gives:

$$\frac{35 + 0 + 0 + 21}{4} = 14 \quad .$$

Relaxations over the whole grid are repeated until exact grid-point values are reached. This is indicated when relaxations produce no further changes in grid-point values. In the example problem, 50 relaxations are required to reach the exact values.

RELIABILITY: In the Products Manual, reliability is used mostly in reference to measurements of some parameter. Reliability is a statistical term involving the standard deviation of the errors associated with measurement of some unknown quantity. The worth of a measurement is defined by its reliability. A high reliability signifies a measurement close to the truth--a dependable measurement.

RESOLUTION: How well a set of measurements tells the true story of a particular condition. For instance, how accurately an upper-air sounding describes the actual pressure, temperature, and humidity with height. A measurement always does some averaging over time and space. The smaller the time and space interval the higher the resolution.

RESTART: Restarting means to start a program over, either at the beginning or at some planned points within the program. Restarting is most frequently required because of trouble in the computer system. In cases of very long programs, such as the P.E. or Prop Loss, it is sometimes necessary to use the restart procedure so as to make time in the operational schedule for shorter programs.

SCALAR: A quantity characterized by magnitude only, as contrasted with a vector which has magnitude and direction. Mass, time, density, and coordinates are scalars. Force, velocity, and acceleration are vectors.

SOFTWARE: All the computer programs needed to use the hardware. Hardware is the physical machinery and circuitry of a computer.

SONAR ACTIVE/PASSIVE: Active sonar systems generate sounds that travel through the sea to the target and return as sonar echoes to the hydrophone. Active sonar systems are said to "echo-range" on their targets. Passive sonar systems use only the sound radiated by the target.

SONIC LAYER DEPTH: The depth at which maximum sound velocity occurs above the thermocline.

SOURCE ANGLE: In the Products Manual, source angle refers to the angle at which a sound ray leaves the sound source.

SPECTRAL: "Spectral" is used in the Products Manual only in reference to the spectral sea-swell models. The "spectral" comes from the forecasting method of calculating a sea surface energy spectrum which relates energy to frequency. Energy spectra for various combinations of wind speeds, duration, and fetches have been developed. The forecaster uses the wind parameters and the energy spectra to produce wave forecasts. Energy values are converted to wave heights.

SYNOPTIC: In the Products Manual, the word "synoptic" is used only in its specialized sense of using data obtained simultaneously over a wide area for the purpose of presenting a comprehensive, nearly-instantaneous picture of the state of the atmosphere or oceans. The true meaning of synoptic is just in the sense of pertaining to or providing an overall view.

TRANSIENT THERMOCLINE: A thermocline is a layer in the ocean in which temperature decreases with depth. Generally there is a seasonal and a main thermocline. Transient thermoclines sometimes form within the mixed layer from heating or wind action. These transients are short-lived and of small temperature magnitude ($< 1^{\circ}C$). The most common transient thermoclines form from daytime heating of the surface waters--a phenomenon known in acoustic circles as the "afternoon effect". These transients disappear at night as the sea surface cools. Surface-ship sonar efficiency is strongly affected by these transients.

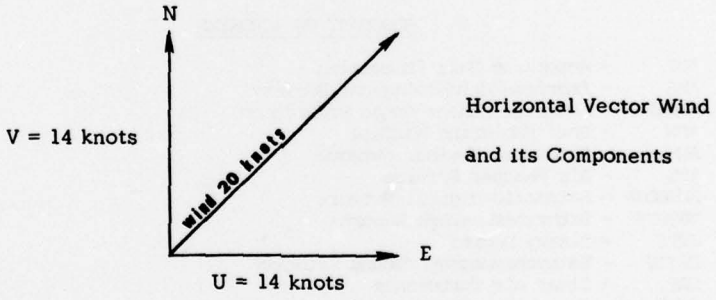
TUNING: Used in the Products Manual in the sense of tuning a model or program. The equations used in a program often contain adjustable empirical constants. If we have

$$k_A A + k_B B + k_C C = D \quad ,$$

and we know what D should be, the constants, k , can be adjusted experimentally until the equation gives the best answer. In programs of any complexity, the tuning may take several months. Sometimes it may take a year, with the final result that the constants are not really constant, but may need changing every month or every season.

The adjustable constants are purely empirical and are not to be confused with unchangeable constants of the "gravity force" sort. The old term "J factor" is not too bad a title for the adjustable constants.

U,V: Used to describe components or velocity of the wind where U is in x direction or from the west, and V is in the y direction or from the south. With a southwest wind of 20 knots, U = 14 knots, V = 14 knots.



VARIANCE: A measure of variability or spread of possible values of a random variable around its average value. For example, in dropping bombs, it is important to know, in general, how close to the target the shells land. With a series of observations of some parameter, the way the values cluster around the "true" value is valuable information. Just computing the average deviation value gives no information--because of plus and minus values cancelling, the result would be zero. This points to use of absolute values or their squares, and for computational simplicity the squares are used. A simple sample is:

Temp Values	Deviation	Deviations^2
69	-3	9
72	0	0
73	+1	1
71	-1	1
75	+3	9
360	0	20

Mean 72

4 = variance (average of the square of the deviations)

$\sqrt{4}$ = 2 = standard deviation

The unit of the variance is (temperature)^2. To convert to temperature units, the square root of the variance is taken. This is called the standard deviation. Variance is generally used in theoretical statistics and the standard deviation is applied. At FNWC, the principal use of variance is in determining reliability or worth of observations. Reliability = 1/variance.

WEAX: Route Weather Forecasts (WEAX) provide a synoptic weather picture and tailored 24-hour forecasts along a projected ship's track. Forecasts are updated every twelve hours. WEAX service must be requested by the ships.

WEIGHTING: Assigning relative degrees of importance to values of a variable, to establish statistical reliability. In analysis systems, weighting is usually done by complex mathematical procedures, but it can be as simple as saying that a wind observation from an ocean station vessel will count for twice as much as an observation from a nearby merchant ship. Golfers in a tournament are weighted by their handicaps.

GLOSSARY OF ACRONYMS

ADP - Automatic Data Processing
AMS - American Meteorological Society
ASRAP - Acoustic Sensor Range Prediction
ASW - Anti Submarine Warfare
AWN - Automated Weather Network
AWS - Air Weather Service
AUTODIN - Automatic Digital Network
BATHYS - Bathythermograph Reports
BITS - Binary Digits
BT/SV - Bathythermograph/Sound Velocity
CAT - Clear Air Turbulence
CCAT - Convective Clear Air Turbulence
CCU - Convective Cumulus
DR - Dead Reckoning
EPRF - Environmental Prediction Research Facility
FIB - Fields by Information Blending
FIBSLP - Fields by Information Blending Sea Level Pressure
FLAPS - Field Identifier (Field, Length, Area, Projection, Source)

FNWC - Fleet Numerical Weather Central
FORTRAN - Computer Language (Formula Translation)
FTER - Fog Terrain Level (Parameter Input)
FWC - Fleet Weather Central
FWF - Fleet Weather Facility
GEC - Gross Error Check
GEM - General Environmental Message
GGζ - Gradient of the Gradient of a Dummy Variable, ζ
HATRACK - Hurricane and Typhoon Tracking
HN - Hydrodynamical Numerical Model
HWD - Horizontal Weather Depiction
LMW - Level of Maximum Wind
MODHATR - Operational Version of MOHATT
MOHATT - Modified Hurricane and Typhoon Tracking
MLD - Mixed Layer Depth
NATTC - Naval Air Technical Training Command
NEDN - Naval Environmental Data Network
NEDS - Naval Environmental Data System
NEPRF - Naval Environmental Prediction Research Facility
NEWS - Naval Environmental Watch System
NHC - National Hurricane Center
NMC - National Meteorological Center
NVA - Numerical Variational Analysis
NWSED - Naval Weather Service Environmental Detachment
OPCON - Operations Control Center
OPNAV - Office of Chief of Naval Operations
OSD - Ocean State Depiction
OTSR - Optimum Track Ship Routing
PBL - Planetary Boundary Layer
P.E. - Primitive Equation
PI - Panofsky Index
POTMLD - Potential Mixed Layer Depth
PVA - Positive Vorticity Advection
RADFO - Radiological Fallout
RATT - Radio Teletype
RH - Relative Humidity
Ri - Richardson Number
RMS - Root-Mean-Square
RMSE - Root-Mean-Square Error
SAR - Search and Rescue
SCM - Successive Correction Method
SD - Small Scale Disturbance Pattern
SES - Surface Effect Ship
SHARPS - Ship-Helicopter Acoustic Range Prediction System
SIRS - Satellite Infrared Spectometer
SL - Large Scale Disturbance Pattern
SLP - Sea Level Pressure
SOWM - Spectral Ocean Wave Model
SR - Residual Field
SST - Sea Surface Temperature
SUBRAP - Submarine Range Prediction
SV - Planetary Vortex
SWEAT - Severe Weather Threat
SWOP - Stereo Wave Observation Program
TAU - Time Increment
TYRACK - Typhoon Tracking
WEAX - In Route Weather
WMO - World Meteorological Organization
ZOOM - Field Expansion